CHARACTERIZING MATERIAL PERFORMANCE FOR DESIGN OF HIGH-PRESSURE HIGH-TEMPERATURE (HPHT) EQUIPMENT IN ACCORDANCE WITH API RP 6HP PRACTICES

Prepared for:

Mineral Management Service
MMS Contract No.: M07PC13016
Herndon, Virginia 20170

Prepared by:

Mohr Engineering Division
A Division of Stress Engineering Services, Inc.
13602 Westland East Blvd
Houston, Texas 77041

7 March 2008

Characterizing Material Performance for Design of High-Pressure High-Temperature (HPHT) Equipment in Accordance with API RP 6HP Practices

Prepared for:
Minerals Management Service
MMS Contract No.: M07PC13016
Herndon, Virginia 20170

Mohr Project No.: 172883

7 March 2008

Prepared by: _____
Kenneth Young, P.E.

Reviewed by: _____
Paul Kovach, P.E.

MOHR ENGINEERING DIVISION
a division of STRESS ENGINEERING SERVICES, INC.

Limitations of this Report

The scope of this report is limited to the matters expressly covered. This report is prepared for the sole benefit of MMS. In preparing this report, Mohr Engineering Division of Stress Engineering Services (Stress) has relied on information provided by MMS. Stress has made no independent investigation as to the accuracy or completeness of such information and has assumed that such information was accurate and complete. Further, Stress is not able to direct or control the operation or maintenance of the client's equipment or processes.

All recommendations, findings and conclusions stated in this report are based on facts and circumstances as they existed at the time that this report was prepared. A change in any fact or circumstance on which this report is based may adversely affect the recommendations, findings, and conclusions expressed in this report.

NO IMPLIED WARRANTY OF MERCHANTABILITY OR FITNESS FOR A PARTICULAR PURPOSE SHALL APPLY. MOHR ENGINEERING DIVISION OF STRESS ENGINEERING SERVICES MAKES NO REPRESENTATION OR WARRANTY THAT IMPLEMENTATION OR USE OF THE RECOMMENDATIONS, FINDINGS, OR CONCLUSIONS OF THIS REPORT WILL RESULT IN COMPLIANCE WITH APPLICABLE LAWS OR PERFECT RESULTS.

Table of Contents

Executive Summary ..... **v**

1 Introduction **1**

2 Background **1**

3 Objectives **2**

4 Scope of Work **2**

5 Results **3**

5.1 Properties of Forged Materials 3
5.2 Tension Test Results 6
5.3 Charpy V-Notch Toughness Measurements 14
5.4 Fracture Toughness 21
5.5 Fatigue Crack Growth Rate 29

6 Conclusions **37**

7 References **38**

Annex A Material Specifications
Annex A.1 Test Sample Material Specifications
Annex A.2 Material Certificates

Annex B Reference Drawings

Annex C Test Procedures
Annex C.1 Tension Test
Annex C.2 Charpy V-Notch Tests
Annex C.3 Fracture Toughness
Annex C.4 Fatigue Crack Growth Rate

Annex D Results from Tension Tests
Annex D.1 Lab Tension Test Data
Annex D.2 Tension Test Data Analysis

Annex E Results from Charpy V-notch Tests
Annex E.1 Lab Charpy Test Data
Annex E.2 Charpy Data Analysis

Annex F Results from Fracture Toughness Tests
Annex F.1 Lab Toughness Test Data
Annex F.2 Toughness Data Analysis

Annex G Results from Fatigue Crack Growth Rate Tests
Annex G.1 Lab Crack Growth Rate Test Data
Annex G.2 Crack Growth Rate Data Analysis

List of Tables

Table 1: Chemical Composition of Blocks by Weight Percent of Material 4
Table 2: Mechanical Properties (from Original Material Test Reports) 4
Table 3: Impact Properties (from Original Material Test Reports) 5
Table 4: Tension Test Results 6
Table 5: Summary of Weibull Analysis of Tension Data 7
Table 6: Linearization of Weibull Tension Data 10
Table 7: Modulus of Elasticity vs. Temperature 13
Table 8: Charpy V-Notch Test Results 15
Table 9: Charpy Impact Results Converted to Fracture Toughness at -20°F 17
Table 10: Summary of Weibull Analysis of Charpy Data at -20°F 20
Table 11: Fracture Toughness Test Results 24
Table 12: Equivalent Plane Strain Fracture Toughness 26
Table 13: Weibull Summary – Fracture Toughness 28
Table 14: Published Crack Growth Rate Factors – Air 32
Table 15: Published Crack Growth Rate Factors – Seawater 35

List of Figures

Figure 1: Forged Blocks used for Materials Characterization Tests 4
Figure 2: Specimen Sectioning from Forged Block 5
Figure 3: CDF of Yield Strength 8
Figure 4: PDF of Yield Strength 8
Figure 5: CDF for Tensile Strength 9
Figure 6: PDF for Tensile Strength 9
Figure 7: Material Strength with Temperature 10
Figure 8: Yield Strength Reduction (comparing AWHEM and SES/MMS test data) 11
Figure 9: Change in Elongation with Temperature 12
Figure 10: Change in Reduction of Area with Temperature 12
Figure 11: Change in Modulus of Elasticity with Temperature 13
Figure 12: Charpy V-Notch Specimen Orientation 14
Figure 13: Charpy V-notch Specimen Geometry (from ASTM E 23) 14
Figure 14: Charpy V-Notch Absorbed Energy with Temperature 16
Figure 15: CDF for Charpy V-Notch Results 18
Figure 16: PDF for Charpy V-Notch Results 18
Figure 17: CDF for Fracture Toughness from Charpy Data 19
Figure 18: PDF for Fracture Toughness from Charpy Data 19
Figure 19: Schematic of Compact Tension Specimen (from ASTM E 1820) 21
Figure 20: Example R-Curve 22
Figure 21: Compact Tension Specimen Orientation 23
Figure 22: CDF for Fracture Toughness Results 27
Figure 23: PDF for Fracture Toughness Results 27
Figure 24: Fatigue Crack Growth Rate Specimen (from ASTM E 647) 30
Figure 25: Plot of FCGR Data in Air 31
Figure 26: Plot of FCGR Data – Walker Equation 33
Figure 27: Plot of FCGR in Seawater with Cathodic Protection 34
Figure 28: Plot of FCGR in H_2S Environment 36
Figure 29: Combined FCGR Curves 37

Executive Summary

The Minerals Management Service (MMS) contracted Mohr Engineering Division of Stress Engineering Services (Stress) to conduct a materials performance characterization test program focused on high-pressure high-temperature (HPHT) equipment in accordance with American Petroleum Institute (API) Recommended Practice 6HP (API RP 6HP). API is developing this new recommended practice that prescribes design and design verification methodology for HPHT equipment. This API document is largely based on the ASME Boiler and Pressure Vessel Code, Section VIII, Division 3 (ASME VIII-3). The methodology of ASME Div 3 calls for evaluating pressure integrity of high-pressure equipment and evaluating service life of equipment through fatigue and fracture-mechanics analyses.

The objective of this materials characterization program was to obtain material properties necessary for performing design verification analyses of HPHT equipment in accordance with API RP 6HP methodology, and specifically focused on 2¼ Cr – 1 Mo quenched and tempered low-alloy steel. Testing was to follow ASTM standards where applicable and to document supplemental procedural information as needed. Testing consisted of:

- Tensile properties as a function of elevated temperature
- Charpy V-notch toughness properties
- Fracture toughness properties
- Fatigue crack growth rate properties

Three separate heats of forged material were obtained for the test program. The material was an 85-ksi specified minimum yield strength (SMYS) forging of 2¼ Cr – 1 Mo material that is typically used in the manufacture of high-pressure drilling equipment. This material meets the requirements of NACE MR0175/ISO 15156.

The protocol for this test program was to measure tensile properties for the subject steel up to 350°F. Therefore, tension testing was conducted in accordance with ASTM E 8 and E 21 at 75°F, 200°F, and 350°F. The resulting Weibull B_{50} values from these tension tests are shown in Table ES-1.

Table ES-1. Summary of Weibull Analysis of Tension Data

Test Temp °F	No. of Specimens	Yield Strength ksi	Tensile Strength ksi	Elongation %	ROA %	Modulus 10^6 psi
75	6	89.11	106.1	22.3	72.6	30.97
200	6	84.87	100.4	21.0	71.9	29.80
350	6	82.25	97.30	19.3	71.6	29.69

The Association of Wellhead Equipment Manufacturers (AWHEM) recently completed a similar project for API 6A on various low-alloy steels, one of which included a 75-ksi version of the same material under study here. Their project included five heats of 75-ksi material, with specimens sent to three different test labs. Tests were also conducted at 350°F and 450°F. AWHEM reported a yield strength reduction factor at 350°F of 0.91. In the present study, a strength reduction factor at 350°F of 0.92 was observed for both yield strength and tensile strength. However, based on the larger sample size and broader temperature range of the AWHEM data, a strength reduction factor of 0.91 for 350°F is recommended.

Within the present study, a good correlation of material modulus was observed with data published in ASME Section II Part D for 2¼ Cr – 1 Mo material, which provides a smooth curve fit over the temperature range of -325°F to 1400°F. Therefore, it is recommended that the ASME data (Table ES-2) be used for modulus.

Table ES-2. Modulus of Elasticity vs. Temperature

Temperature, °F	70	200	300	350	400	450
Modulus, 10^6 psi	30.6	29.9	29.4	29.1	28.8	28.55

Charpy V-notch impact testing was conducted in accordance with ASTM E 23 over a temperature range of -75°F to +75°F. Based on test data, the Charpy impact data yielded values at -20°F that are on the upper shelf of the temperature transition curve. Twelve specimens from the three heats of material were tested at -20°F (because -20°F is the minimum metal design temperature for most HPHT equipment).

An equivalent plane strain fracture toughness value, K_{IC}, was calculated for each of these 12 test specimens based on Charpy V-notch impact energy test results at -20°F. The correlation equation used for calculating fracture toughness was as specified in API 579 and ASME VIII-3 for upper shelf toughness:

$$\left(\frac{K_{IC}}{S_y}\right)^2 = 5 \times \left(\frac{CVN}{S_y} - 0.05\right)$$

The Weibull B_{50} and B_1 values from the tests at -20°F are shown in Table ES-3.

Table ES-3. Summary of Weibull Analysis of Charpy Data at -20°F

Weibull	Charpy Impact Energy ft-lb	Percent Shear %	Lateral Expansion mil	Equiv Fracture Toughness ksi·√in.
B_{50}	116.3	85.7	74.4	222.5
B_1	60.4	55.5	45.2	162.1

API 579 states that Charpy impact tests can be used to provide a qualitative indication of a material's fracture toughness, but cannot be used directly to provide an indication of toughness for use in a fitness-for-service assessment.

Plane strain fracture toughness testing was also conducted in accordance with ASTM E 1820. All specimens were 1-inch thick compact tension specimens from each of the three heats of material. Two specimens from each heat of material were tested in each of three environments, for a total of 18 specimens. All testing employed a slow loading rate of 0.008 mm/min. The three test environments were:

1. Air environment at 75°F
2. Soaked in simulated seawater at 75°F as defined in ASTM D 1141 with cathodic protection at a level of -1100 mV for a minimum of 5 days and immediately tested in air at ambient temperature
3. Soaked in a mild H_2S solution at 75°F for a minimum of 5 days and immediately tested in air at ambient temperature
    a. The gas mixture was comprised of 7% H_2S and the balance nitrogen.
    b. A buffered solution chemistry of 5.00% by weight sodium chloride and 0.40% by weight sodium acetate in deionized water.
    c. pH of the test solution before saturation was adjusted to 4.0 using hydrochloric acid.
    d. Bubble rate of H_2S gas through the solution was 10 ml/min.

Cracked tip opening displacement (CTOD) values and J-integral values obtained from each test were converted to an equivalent plane strain fracture toughness, K_{IC}. The correlation equation to convert J-integral toughness data to an equivalent K_{IC} is specified in both ASME VIII-3 and API 579:

$$K_{IC} = \sqrt{\frac{E \cdot J_C}{1 - \nu^2}}$$

The correlation equation to convert CTOD toughness data to K_{IC} is an approximate plane strain fracture toughness and varies depending on which standard is referenced. The correlation equations specified in ASME and API 579, respectively, are:

$$K_{IC} = \sqrt{E \cdot \sigma_y \cdot \delta_C}$$

$$K_{IC} = \sqrt{\frac{1.4 \cdot E \cdot \sigma_{flow} \cdot \delta_C}{1 - \nu^2}}$$

Based on strength properties of this material, equivalent fracture toughness using the ASME correlation equation for CTOD data is approximately 23% lower than that from the API 579 correlation. In addition,

this API 579 correlation for CTOD data is approximately 10% below the value obtained from the J-integral correlation.

BS 7910 states that it is not intended that CTOD toughness data be transformed to an equivalent K_{IC}.

Table ES-4 lists the Weibull B_{50} and B_1 values for K_{IC}.

Table ES-4. Weibull Values for Equivalent Plane Strain Fracture Toughness (K_{IC})

Environment	Weibull Analysis	CTOD			J-Integral		
		Test Data	Equivalent Fracture Toughness, K_{IC}		Test Data	Equivalent Fracture Toughness, K_{IC}	
		mm	ASME ksi·√in	API 579 ksi·√in	N/mm	ASME ksi·√in	API 579 ksi·√in
Air	B_{50}	0.229	156	202	263	225	225
	B_1	0.201	139	182	215	203	203
Seawater w/ CP	B_{50}	0.179	138	179	209	199	199
	B_1	0.102	103	134	127	156	156
H_2S	B_{50}	0.008	31	39	12	48	48
	B_1	0.001	9	11	3	24	24

The fracture toughness data presented for the material soaked in an H_2S environment is presented for information only and should not be used for design purposes.

Fatigue crack growth rate testing was conducted in the spirit of ASTM E 647. All specimens were 0.25-inch thick compact tension specimens from the three heats of material. Testing was done in the same three environments specified for the fracture toughness testing.

The test protocol was designed to grow the crack while maintaining a constant load ratio, R, with an increasing ΔK. Tests in the air environment were run at two different R ratios (R = 0.1 and R = 0.5) at a frequency of 20 Hz. Tests in the seawater environment with cathodic protection were run at R = 0.1 at a frequency of 1 Hz. Tests in the H_2S environment were run at R = 0.1 at a frequency of 0.33 Hz. All tests were at lab room temperature.

Curve fitting of the air environment fatigue crack growth rate, FCGR, results in a slope of the Paris equation of 2.989, which is between the 3.26 specified by ASME Div 3 and the 2.88 specified by API 579. The position of data is slightly below both the ASME curve and the API 579 curve. The lower section (ΔK < 9.07 ksi·√inch) of the API 579 Paris equation appears to be non-conservative. Therefore, the Walker equation recommended for design purposes in air is defined as:

$$da/dN \cdot \frac{inch}{cycle} = 3.45 \times 10^{-10} \cdot \left(\frac{\Delta K \cdot ksi \cdot \sqrt{inch}}{(1-R)^{1-0.828}} \right)^{2.989}$$

The Paris equation defined by BS 7910 appears to be the upper bound for the steel in a marine environment with cathodic protection. However, due to the scatter in the data from this series of tests, additional testing may be needed to characterize the material performance for design purposes. The Paris equation in the seawater with cathodic protection is defined as:

$$da/dN \cdot \frac{inch}{cycle} = 3.12 \times 10^{-7} \cdot \left(\Delta K \cdot ksi \cdot \sqrt{inch} \right)^{1.4}$$

The fatigue crack growth rate testing in a sour H_2S environment resulted in significant scatter of the data and is reported for information only. The data is not to be used for design purposes.

1 Introduction

The Minerals Management Service (MMS) contracted Mohr Engineering Division of Stress Engineering Services (SES) to design and perform a test program to measure and characterize materials performance for high-pressure high-temperature (HPHT) equipment in accordance with American Petroleum Institute Recommended Practice 6HP (API RP 6HP). The scope of work was to encompass a material testing program to enable operators to safely produce oil and gas from HPHT reservoirs. Completion of the program will ultimately support more widespread development of HPHT reserves by providing designers with some of the essential material properties needed to perform design verification analyses of HPHT equipment in accordance with API RP 6HP.

2 Background

The Gulf of Mexico (GoM) is reported to contain substantial undeveloped oil and gas reserves in HPHT reservoirs. The industry believes that these more challenging environments represent the future of petroleum production in the GoM and that they will form a significant proportion of future additions to USA domestic reserves, if these HPHT fields can be produced safely and economically. Safe development of these reserves requires equipment such as wellheads, trees, and blowout preventers that are manufactured and certified for use in HPHT environments. Much of the required equipment is not now commonly available. Moreover, development of this essential equipment is predicted to require several years at the current pace of technological evolution.

To aid the industry in these developments, API is drafting a new recommended practice, API RP 6HP, that addresses design and design-verification methodology for HPHT drilling and completion equipment. It is largely based on the ASME Boiler and Pressure Vessel Code, Section VIII, Division 3 (ASME VIII-3), which was published in 1997 to address the design and verification of pressure vessels rated for high-pressure service. ASME VIII-3 methodology accounts for anticipated failure modes of high-pressure equipment as well as reduced material properties, which are expected in environments with extreme pressures and temperatures. It evaluates service life of the equipment through fatigue and fracture-mechanics analyses.

Design of equipment in accordance with API RP 6HP requires designers to understand materials behavior and to utilize material properties measured at HPHT conditions. Much of the essential data is not currently available, even for materials commonly used in the oil patch, such as low-alloy steels and some corrosion-resistant alloys (CRAs). Thus, the materials testing program undertaken here was designed to provide engineers and designers with material property data needed to design equipment in accordance with API RP 6HP and to expedite development and production of HPHT reserves in the USA.

The API RP 6HP Steering Committee has charged a Work Group to prepare a materials testing protocol to support API RP 6HP design verification methodology. As such, the Work Group is to define test

environments, test methods, and testing standards for qualification of candidate materials for HPHT drilling, completion, and production working environments. Thus, it is expected that the protocol developed by this API Work Group will largely establish the rules for future HPHT materials qualification.

The level of technical and financial resources required to carry out the essential materials testing under HPHT conditions is immense. Therefore, it is unlikely that any single organization will invest significantly in this process without assurance that other organizations will share the burden. However, individual organizations are more likely to invest once the process gains momentum within the industry. Furthermore, manufacturers and testing authorities are likely to invest in expanding their facilities and capabilities as the demand for HPHT materials and qualification testing becomes more widespread.

Based on the strategic need to catalyze this process within the industry, MMS provided limited funding for testing the most common materials of construction (2¼ Cr – 1 Mo low-alloy steel). It is expected that this initial program will serve as the foundation for an ongoing joint-industry project that will leverage funding from operators, service companies, and manufacturers of HPHT equipment. This will accelerate first oil from domestic HPHT reserves by several years.

3 Objectives

Strategic objectives of this project include:

1. Support technology developed by the API RP 6HP standard by characterizing, through testing, material properties necessary to perform design verification analyses of HPHT equipment
2. Qualify selected low-alloy steels to determine their suitability for use in manufacturing HPHT drilling and completion equipment
3. Document results of the materials characterization
4. Recommend specific improvements for existing and new technologies that are suitable for testing and evaluating materials for HPHT applications

4 Scope of Work

The scope of work of this testing program includes:

1. Procure representative examples of low-alloy steel forgings like those commonly used to manufacture wellheads, trees, BOP bodies, etc. Forgings will be ordered from multiple manufacturers or from multiple heats using a common purchase specification. The primary material of interest for this work is 2¼ Cr – 1 Mo quenched and tempered low-alloy steel with specified minimum yield strength (SMYS) of 85 ksi and maximum hardness of HRc 22 in compliance with NACE MR0175/ISO 15156-2.

2. Heat-treat and machine the forgings into coupon blanks suitable for preparation of test specimens. Serialize the coupons to maintain traceability back to the original heat of steel.
3. Contract with one or more commercial machine shops to prepare test specimens from the coupons. Detailed drawings of specimen layout within the coupons will be supplied to each machine shop to maintain traceability of each specimen to its original location within the serialized coupons.
4. Contract with one or more recognized testing authorities to conduct the tests specified below under item 5. Laboratories selected for this test work must have extensive experience as well as acceptable safety records related to the required tests.
5. The following ASTM standard tests will be conducted:
    a. Room temperature and elevated temperature (350°F) tension tests in accordance with ASTM E 8 and ASTM E 21, respectively.
    b. Fracture toughness tests including:
        i. Charpy V-notch impact toughness in accordance with ASTM E 23. This test verifies that the temperature at which the material starts to become brittle is below the equipment minimum design operating temperature.
        ii. Plane strain fracture toughness in accordance with ASTM E 1820. This test evaluates the maximum stress intensity that results in unstable crack propagation within the material.
    c. Fatigue crack growth rate (*da/dN*) tests in accordance with ASTM E 647. Fatigue testing in corrosive environments presents multiple technical challenges, but is necessary to fully apply the design-verification methodology of API RP 6HP. Thus, tests will be conducted in air, simulated seawater, and a mild H_2S solution to quantify the effects of these environments on fatigue crack growth rate.
6. Analyze test results and assemble the data in a format suitable for design-analysis applications in accordance with API RP 6HP.

5 Results

5.1 Properties of Forged Materials

For this material characterization testing program, three forged and heat-treated blocks were obtained from Hydril from different heats of material, but all from the same material specification. They were randomly selected from Qualification Test Coupons (QTC) supplied by Ellwood City Forge for blowout preventer (BOP) type products. The blocks measured 8 x 8 x 9 in. (20.3 x 20.3 x 22.9 cm) in accordance with the material specification detailed below and in Annex A.1. The forged blocks as received are shown in Figure 1.

Figure 1: Forged Blocks used for Materials Characterization Tests

Material certificates for each of the blocks are presented in Annex A.2. The original material test report data are listed in Table 1 for the chemical composition, Table 2 for mechanical properties, and Table 3 for impact properties. The Charpy V-Notch testing was done at a lower temperature (-75°F), but the values still met the requirements for -20°F.

Table 1: Chemical Composition of Blocks by Weight Percent of Material (from Original MTRs)

Heat	C	Mn	P	S	Si	Ni	Cr	Mo	Al	V	Cu	Ti
HT1	0.15	0.55	0.010	0.007	0.28	0.14	2.27	1.02	0.035	0.011	0.21	0.0033
HT2	0.14	0.53	0.013	0.008	0.28	0.10	2.26	1.00	0.030	0.008	0.16	0.0026
HT3	0.13	0.56	0.012	0.007	0.26	0.08	2.30	1.00	0.027	0.009	0.14	0.0023

Table 2: Mechanical Properties (from Original MTRs)

Heat	Test Loc	Yield Strength psi	Tensile Strength	Elongation %	RA %	Hardness BHN
HT1	Long	93,155	110,362	25	73	228
HT2	Long	88,746	105,706	22	71	217
HT3	Long	85,000	101,610	24	73	217

Table 3: Impact Properties (from Original MTRs)

Heat	Test Loc	Test Temp	Impact ft-lb	Shear %	Lateral Expansion
HT1	Trans	-75°F	37 38 25	5 5 5	0.025 0.026 0.017
HT2	Long	-75°F	72 39 26	30 10 10	0.053 0.027 0.020
HT3	Trans	-75°F	79 91 54	40 50 10	0.056 0.061 0.037

The material specification requires the amount of hot work to be sufficient to result in a wrought structure throughout the entire cross-section of the forging, and for the minimum forging reduction ratio be 3 to 1 throughout the block. The material test reports indicated that the reduction ratio for these three forgings was 5.1 to 1.

The forged and heat-treated blocks were sawed into test blanks for material testing (Figure 2) and detailed in accordance with the drawing in Annex B. The intent was to obtain material specimens within the ¼T envelope of the forged blocks. In addition, the test samples were intended to be transverse-orientation specimens (with the 9-inch dimension defined as the longitudinal orientation). The two mutually perpendicular 8-inch dimensions of the test blocks were indistinguishable, so both could be identified as T (long transverse axis of the forging).

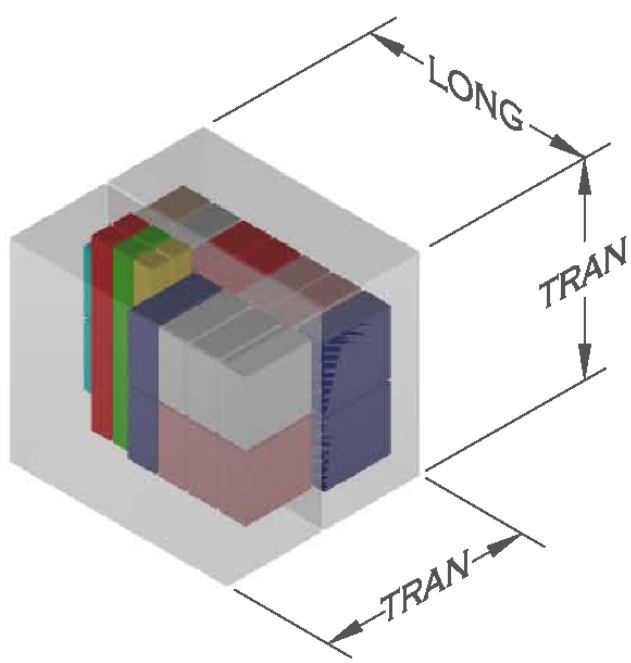

Figure 2: Specimen Sectioning from Forged Block

5.2 Tension Test Results

The program's tension specimens were tested by Westmoreland Mechanical Testing & Research, Inc. in Youngstown, Pennsylvania. The test specimens were transverse specimens and within ¼T of the forged blocks. The specimens were prescribed to be 0.505-inch diameter per ASTM E 8. Unfortunately, the test lab machined some of the blanks too short to fabricate 0.505-inch specimens and have the proper gauge length for elevated temperature testing. Therefore, some specimens were turned down to make standard 0.357-inch diameter specimens. Specimen sizes and test results are listed in Table 4. All tension testing was conducted in accordance with ASTM E 8 or E 21, and the test protocol specified in Annex C.1. Tensile test certificates are included in Annex D.1.

Table 4: Tension Test Results

Specimen ID	Test Temperature	Specimen Diameter	Yield Strength	Tensile Strength	Elongation	Reduction of Area	Modulus
	°F	inch	ksi	ksi	%	%	10^6 psi
1-01-T-1	75	0.357	89.5	107.4	23	71	29.0
1-01-T-2		0.505	89.1	106.4	22	71	31.7
2-01-T-1		0.357	91.7	108.9	22	70	30.7
2-01-T-2		0.505	91.9	108.5	22	71	32.2
3-01-T-1		0.357	83.3	100.2	24	76	29.0
3-01-T-2		0.505	87.0	103.1	23	74	32.3
1-02-T-1	200	0.357	84.9	100.8	20.5	68	28.8
1-02-T-2		0.357	84.9	101.2	21.5	69	28.9
2-02-T-1		0.505	87.0	102.3	20.5	71.5	27.3
2-02-T-2		0.505	88.8	104.2	20	71	31.9
3-02-T-1		0.357	79.7	94.4	22	75.5	28.1
3-02-T-2		0.505	82.5	97.3	21.5	74.5	32.7
1-03-T-1	350	0.357	81.5	97.4	20	71	28.9
1-03-T-2		0.357	81.1	97.3	20	71	27.8
2-03-T-1		0.357	85.3	100.7	20	73	28.9
2-03-T-2		0.505	85.1	100.4	19.5	69	31.2
3-03-T-1		0.357	80.8	93.4	17	73.5	28.3
3-03-T-2		0.505	77.9	92.4	19	70.5	32.1

A Weibull analysis was performed to model the distribution of these material property data at each temperature. The Weibull distribution model is applicable to systems or components which fail when the

weakest component or link in the system fails. This makes it popular for analysis of the strength distribution of materials.

Results from the Weibull analysis are summarized in Table 5, which lists η, β, B_{50} and B_2 values for each of the material properties. The η (eta) value represents the characteristic life, i.e., the life at which 63.2% of the population will have failed. β (beta) represents the slope of the Weibull curve. B_{50} is the value that 50% of the specimens should statistically fall below, and B_2 is the value that 2% of the specimens should fall below. All tensile data from this relatively small population of samples are greater than this minimum B_2 value. Therefore, to obtain higher confidence in the true B_2 value, a larger sample size should be used.

Table 5: Summary of Weibull Analysis of Tension Data

Lognormal Analysis Parameter	Test Temp °F	Sample Size	Yield Strength ksi	Tensile Strength ksi	Elong %	ROA %	Modulus 10^6 psi
η (Weibull characteristic life)	75	6	90.23	107.3	22.76	73.17	31.47
	200	6	85.99	101.7	21.27	72.89	30.49
	350	6	83.19	98.47	19.63	72.11	30.22
β (Weibull slope)	75	6	29.32	33.19	16.39	39.86	22.73
	200	6	27.80	29.83	30.93	26.70	16.02
	300	6	32.31	30.79	19.14	47.48	20.48
B_{50}	75	6	89.11	106.1	22.26	72.60	30.97
	200	6	84.87	100.4	21.02	71.89	29.80
	350	6	82.25	97.30	19.26	71.55	29.69
B_2	75	6	78.98	95.41	17.94	66.44	26.51
	200	6	74.73	89.21	18.75	62.98	23.90
	300	6	73.72	86.75	16.01	66.42	24.98

The Weibull distribution analysis of yield strength data showing the cumulative distribution function (CDF), i.e., the statistical percent of failure, is shown in Figure 3. The probability density function (PDF), the histogram of the data, is shown in Figure 4. Each curve represents data for a different temperature. Data from Weibull distribution analysis for each of the material properties at each temperature are presented in Annex D.2.

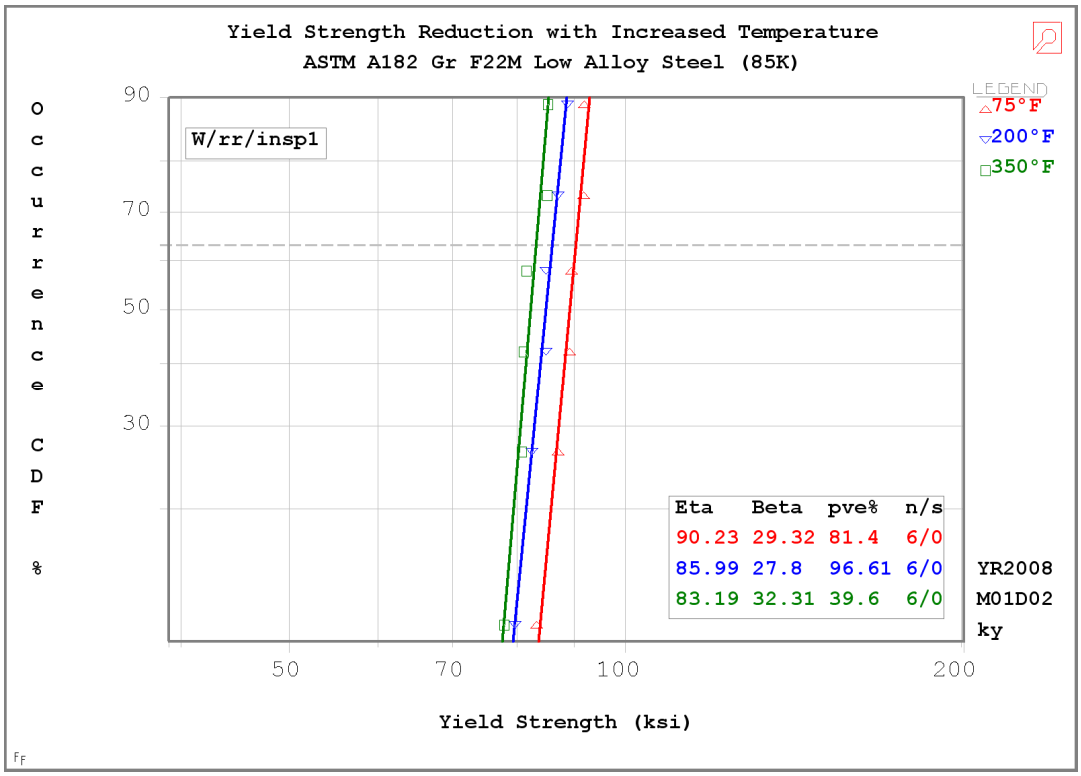

Figure 3: CDF of Yield Strength

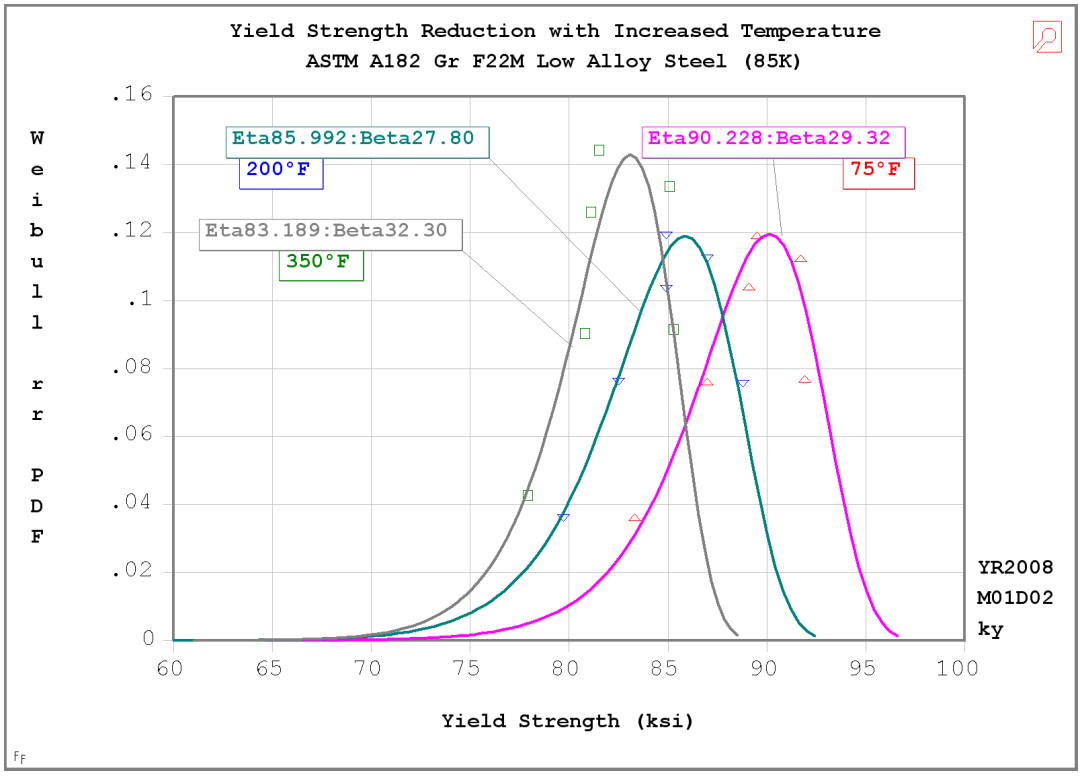

Figure 4: PDF of Yield Strength

Figure 5 shows the CDF plot for the tensile strength test data; Figure 6 shows the PDF plot.

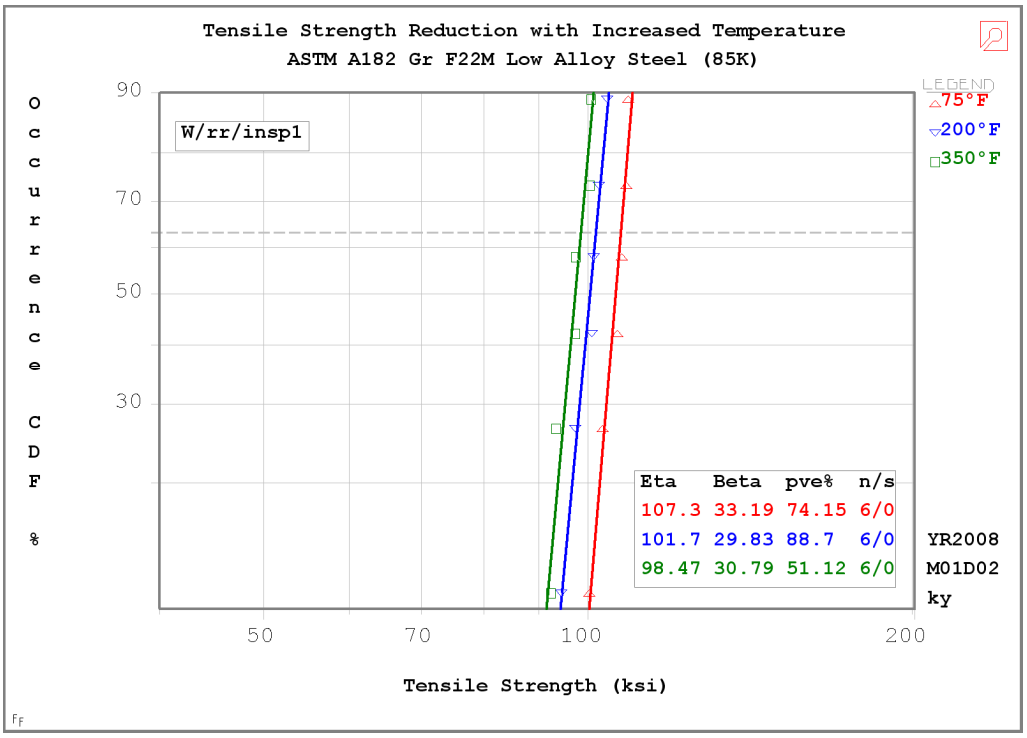

Figure 5: CDF for Tensile Strength

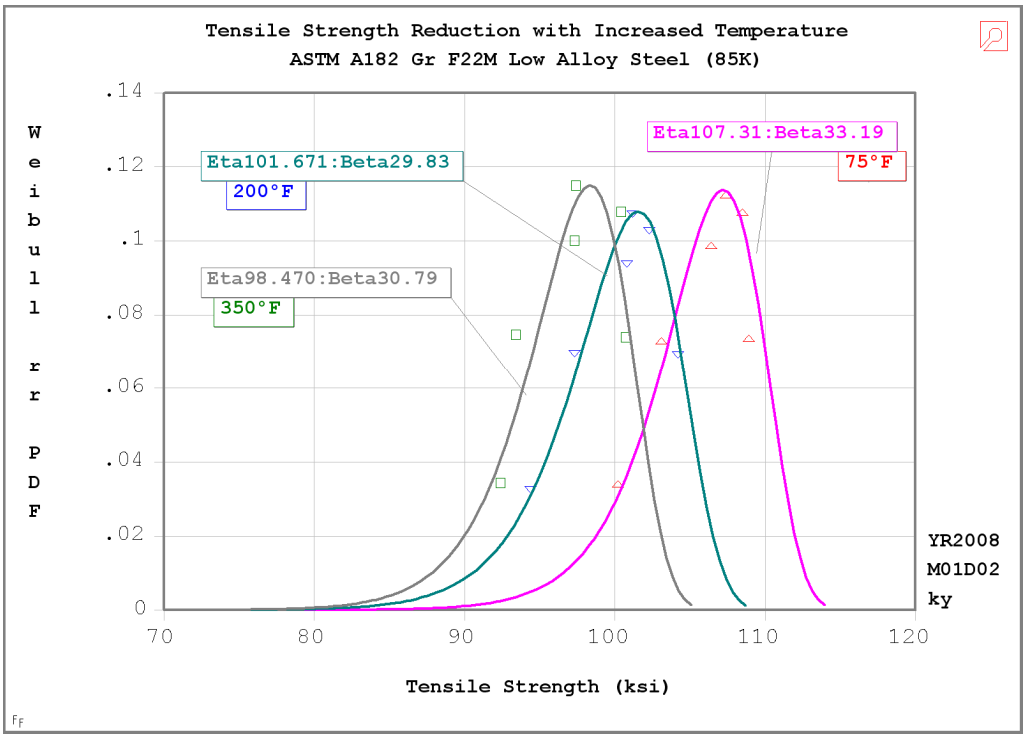

Figure 6: PDF for Tensile Strength

Least-squares linear approximations of the B_{50} and B_2 yield-strength and tensile-strength data were then calculated. Results are listed in Table 6 and shown graphically in Figure 7 along with the raw data. Analysis of the data showed that yield and tensile strength of this material at 350°F is about 92% of the strength at 75°F.

Table 6: Linearization of Weibull Tension Data

Test Temperature °F	Yield Strength, ksi			Tensile Strength, ksi		
	B_{50}	B_2	Linearized Strength Derating Factor	B_{50}	B_2	Linearized Strength Derating Factor
75	88.70	78.31	1.00	105.48	94.60	1.00
200	85.62	75.97	0.952	101.53	90.72	0.963
350	81.91	73.16	0.923	96.79	86.06	0.918

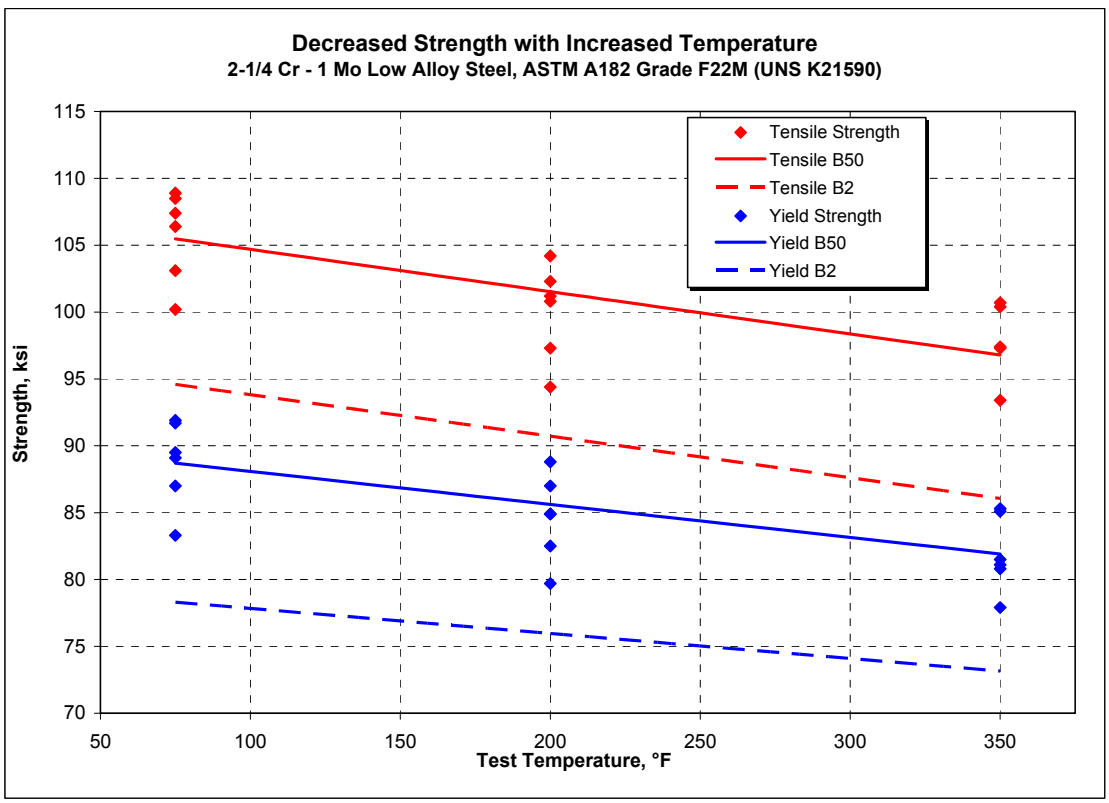

Figure 7: Material Strength with Temperature

AWHEM recently completed a similar test program for API 6A on materials that included 2¼ Cr – 1 Mo and other low-alloy steels. Their test program consisted of 75-ksi material from a 5-inch equivalent round (ER) bar or prolongation. They used five heats of material and sent samples to three test labs. This provided 15 samples at each of four temperatures—75°F, 300°F, 350°F, and 450°F.

The effect of temperature on strength from the SES test program was compared to data from the AWHEM materials test project for the 2¼ Cr – 1 Mo material (Figure 8). AWHEM reported a strength reduction for this material to 91% at 350°F and 89% at 450°F. Comparison of these two data sets showed good agreement in the trend of strength reduction with increased temperature. Since the AWHEM data set is larger and over a greater temperature range, a reduction factor to 91% of yield strength at 350°F as compared to room temperature is recommended for use in API RP 6HP.

The forged blocks used for material testing should probably have been post-weld heat treated, PWHT, prior to specimen preparation and testing. This may have resulted in a closer representation of the material strength properties for design purposes. If the equipment receives a PWHT during the manufacturing process after welding, the strength properties may be affected.

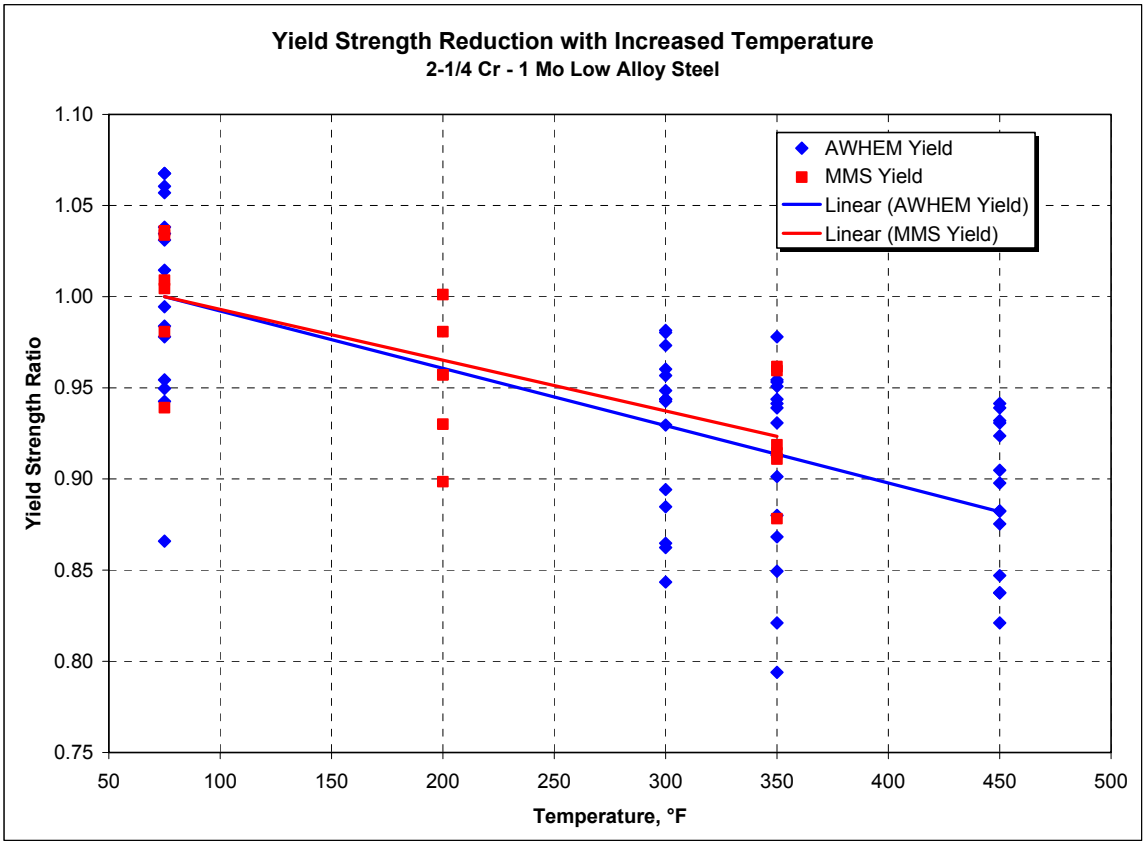

Figure 8: Yield Strength Reduction (comparing AWHEM and SES/MMS test data)

In addition to tensile strength, elongation, reduction of area, and modulus data were also recorded. Figure 9 shows the decrease in elongation at failure as temperature is increased. Figure 10 shows the change in reduction of area as a function of test temperature.

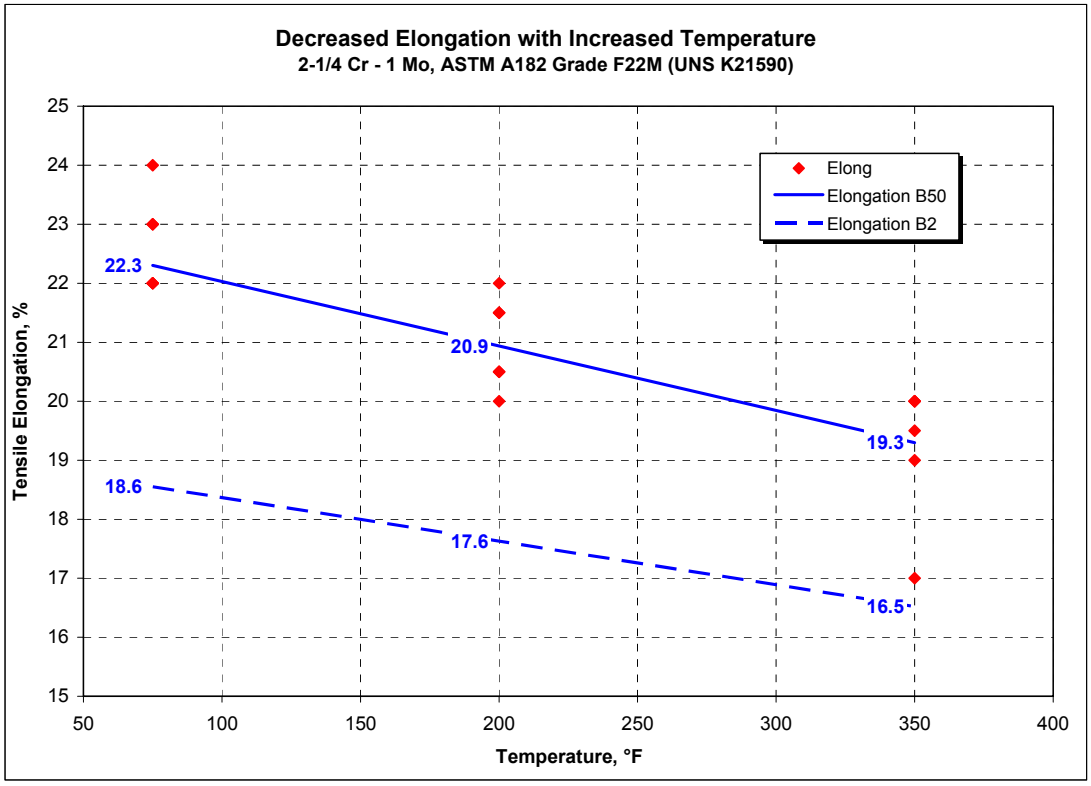

Figure 9: Change in Elongation with Temperature

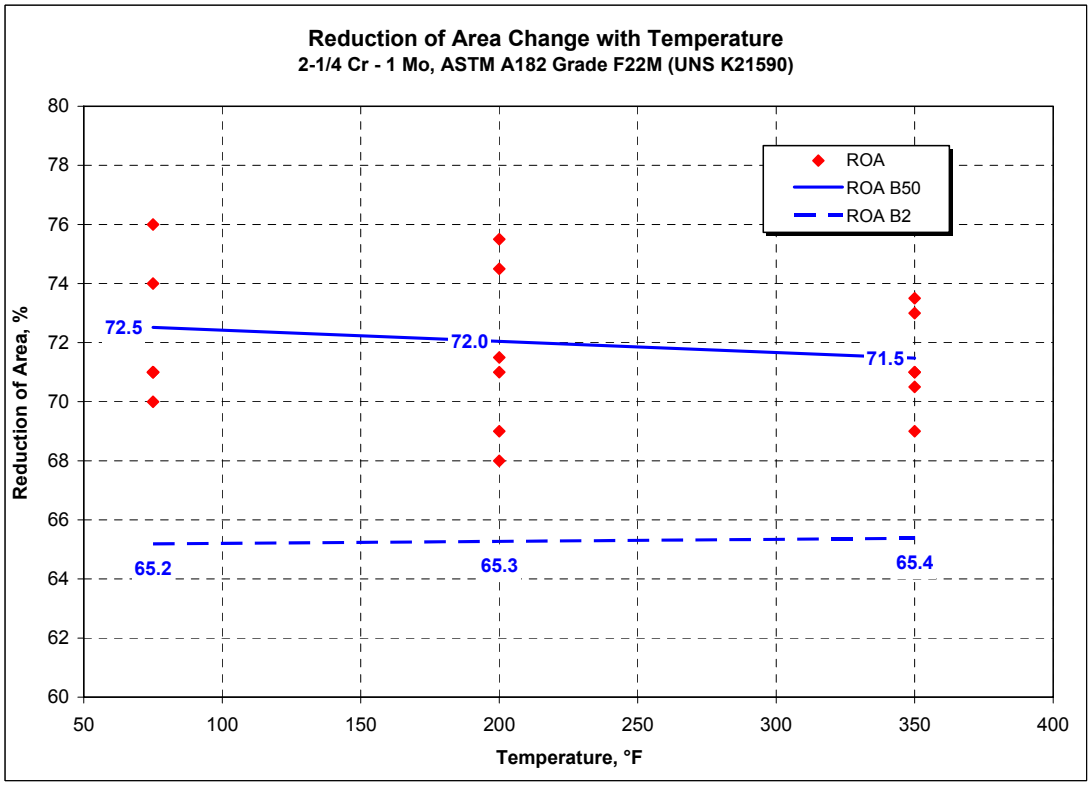

Figure 10: Change in Reduction of Area with Temperature

Figure 11 summarizes the impact of temperature on modulus of elasticity for 2¼ Cr – 1 Mo material. The solid (blue) line represents data from ASME Section II Part D tables over the temperature range of -325°F to 1400°F. The red triangles represent the B_{50} values for the three sets of specimens measured during this test program. The measured data are very close to the ASME data. However, the ASME results are derived from a much larger data set and over a larger temperature range. It is recommended that the ASME data for modulus be used in the analysis of this material. The ASME modulus is 30.6 x 10^6 psi at 75°F and 29.1 x 10^6 psi at 350°F. ASME modulus data are summarized in Table 7.

The full report from Westmoreland on the tension testing at temperature is included in Annex D.

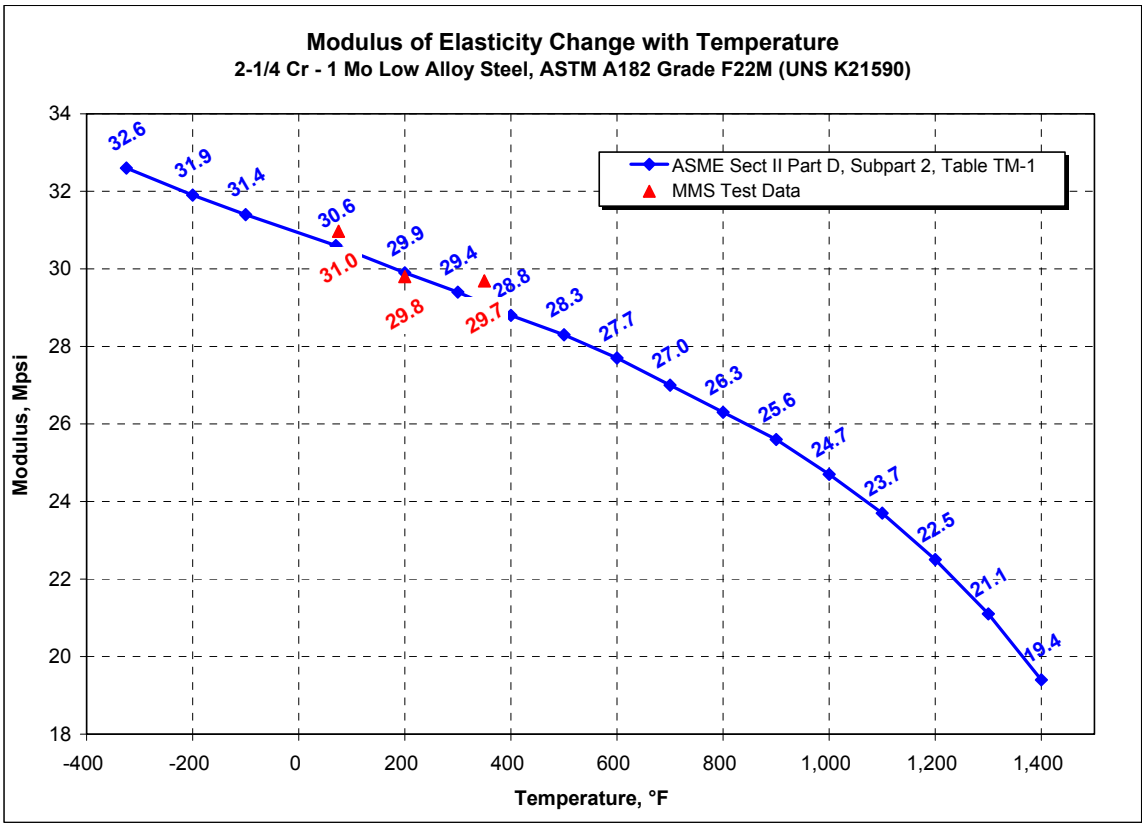

Figure 11: Change in Modulus of Elasticity with Temperature

Table 7: Modulus of Elasticity vs. Temperature

Temperature, °F		70	200	300	350	400	450
Modulus 10^6 psi	ASME	30.6	29.9	29.4	29.1	28.8	28.55
	SES	31.0	29.8		29.7		

5.3 Charpy V-Notch Toughness Measurements

Charpy V-notch toughness tests were performed by Bryan Laboratory, Inc. in Houston, Texas. As prescribed in ASTM E 23, the toughness specimens were machined as 10 x 10 mm (0.39 x 0.39 in.) full-size transverse samples. Figure 12 shows the orientation of the Charpy V-notch specimen within the forged block. Figure 13, extracted from ASTM E 23, illustrates the configuration of the full size CVN impact specimens as tested.

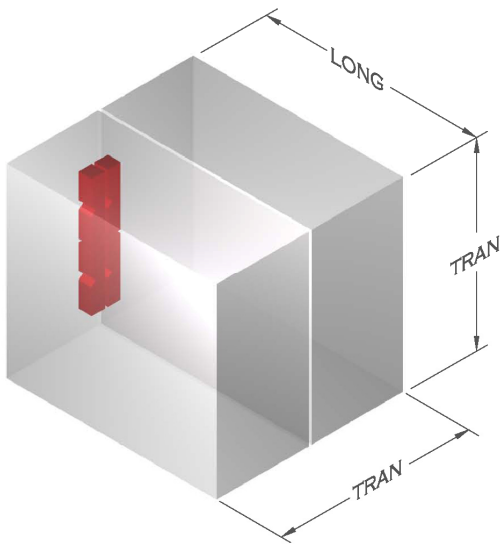

Figure 12: Charpy V-Notch Specimen Orientation

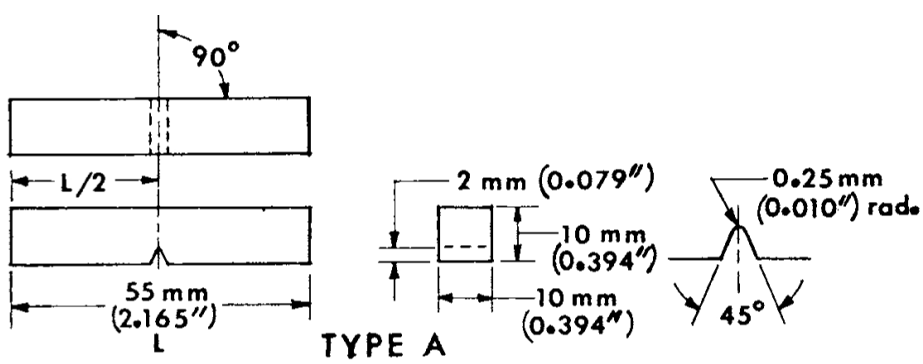

Figure 13: Charpy V-notch Specimen Geometry (from ASTM E 23)

Twelve specimens were initially tested at -20°F. Additional specimens were tested at various temperatures ranging from -75°F to +75°F (Table 8). The Charpy V-notch test certificates are included in Annex E.1.

Table 8: Charpy V-Notch Test Results

Test Temperature °F	Forging	Specimen	Absorbed Energy ft-lb	Percent Shear %	Lateral Expansion mil
75°	1	10-3	120	100	73
	2	10-4	130	100	75
	3	10-7	130	100	76
40°	1	10-3	124	100	78
	2	10-3	122	100	79
	3	10-3	140	100	84
10°	1	10-2	117	75	72
	2	10-2	128	100	82
	3	10-2	148	100	82
-20°	1	04-1	85	66	58
		04-2	98	80	66
		04-3	100	85	66
		04-4	98	80	62
	2	04-1	123	100	76
		04-2	121	100	74
		04-3	102	75	66
		04-4	124	100	83
	3	04-1	145	100	86
		04-2	140	100	84
		04-3	144	100	89
		04-4	108	80	71
-50°	1	10-4	27	25	22
	2	10-4	63	30	44
	3	10-4	90	50	60
-75°	1	10-1	26	20	19
	2	10-1	42	15	29
	3	10-1	64	20	44

The Charpy V-notch impact energy data were plotted against test temperature (Figure 14). The plot shows that the data for -20°F are on the upper shelf, even though there is increased scatter at -20°F as compared to higher temperatures.

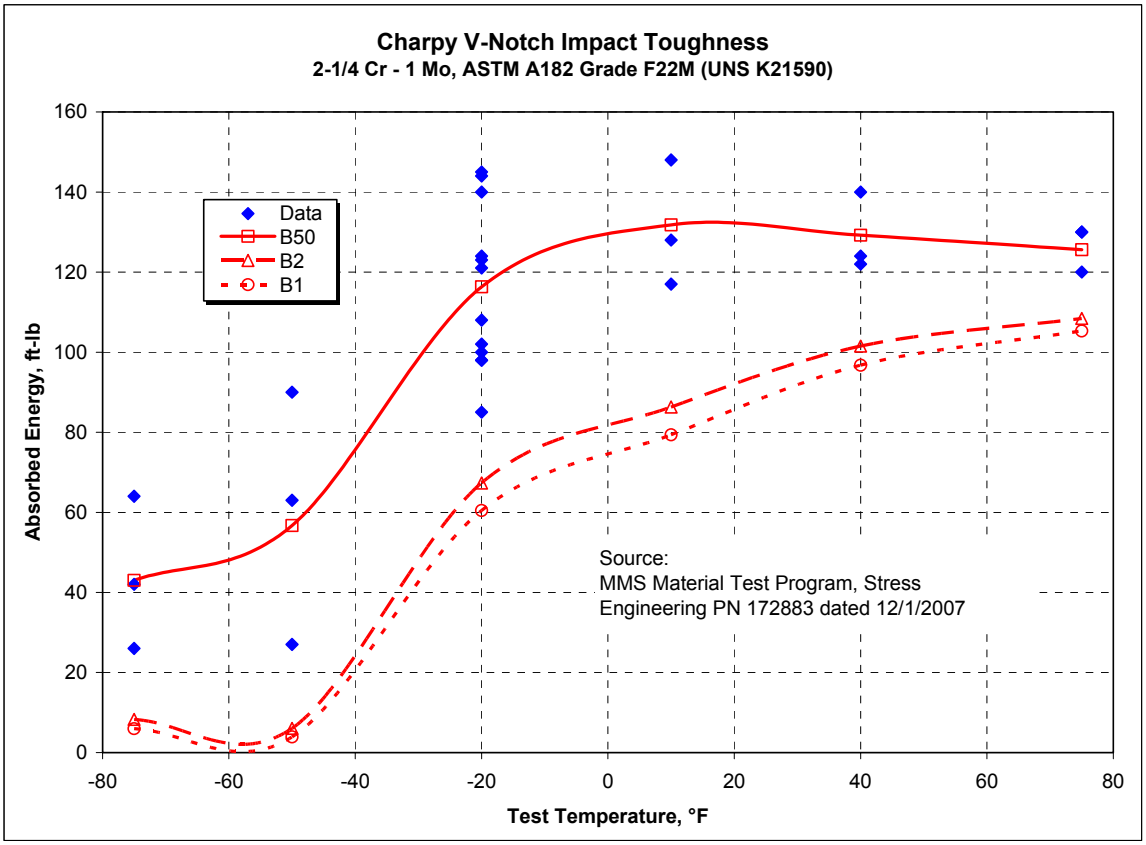

Figure 14: Charpy V-Notch Absorbed Energy with Temperature

Fracture toughness is a measure of a material's ability to resist crack propagation and fracture. API 579 states that Charpy impact tests can be used to provide a qualitative indication of fracture toughness. However, results from these tests should not be used directly for material toughness as part of a Fitness-for-Service assessment.

The equivalent fracture toughness for this material was calculated based on the Charpy impact data using Equation 1. Since the minimum design metal temperature is -20°F, Charpy V-notch impact energy data at -20°F were then paired with 75°F yield-strength data (see Table 4). Yield-strength data at 75°F were used to error on the conservative side of the fracture toughness conversion. From these data, equivalent plane strain fracture toughness, K_{IC}, was calculated (Table 9) per the conversion equation specified in ASME Section VIII Division 3 Appendix D Section D-600. (The same conversion equation is specified in API 579 F.4.5.2.)

$$\left(\frac{K_{IC}}{S_y}\right)^2 = 5 \times \left(\frac{CVN}{S_y} - 0.05\right) \qquad \text{(Eq 1)}$$

Table 9: Charpy Impact Results Converted to Fracture Toughness at -20°F

Specimen ID	Charpy Impact CVN	Yield Strength S_Y	Equivalent Fracture Toughness K_{IC}
	ft-lb	ksi	ksi·√in
1-1	85	89.3	190
1-2	98		204
1-3	100		207
1-4	98		204
2-1	123	91.8	233
2-2	121		231
2-3	102		211
2-4	124		234
3-1	145	85.1	245
3-2	140		240
3-3	144		244
3-4	108		210

A Weibull distribution analysis was performed using the Charpy impact data and equivalent fracture toughness data. Figure 15 and Figure 16 show the probability of failure plot and the probability density plot for the Charpy impact data. Figure 17 and Figure 18 show the probability of failure plot and the probability density plot for the equivalent plane strain fracture toughness data.

The Weibull distribution analysis report data for the Charpy V-notch data is presented in Annex E.2.

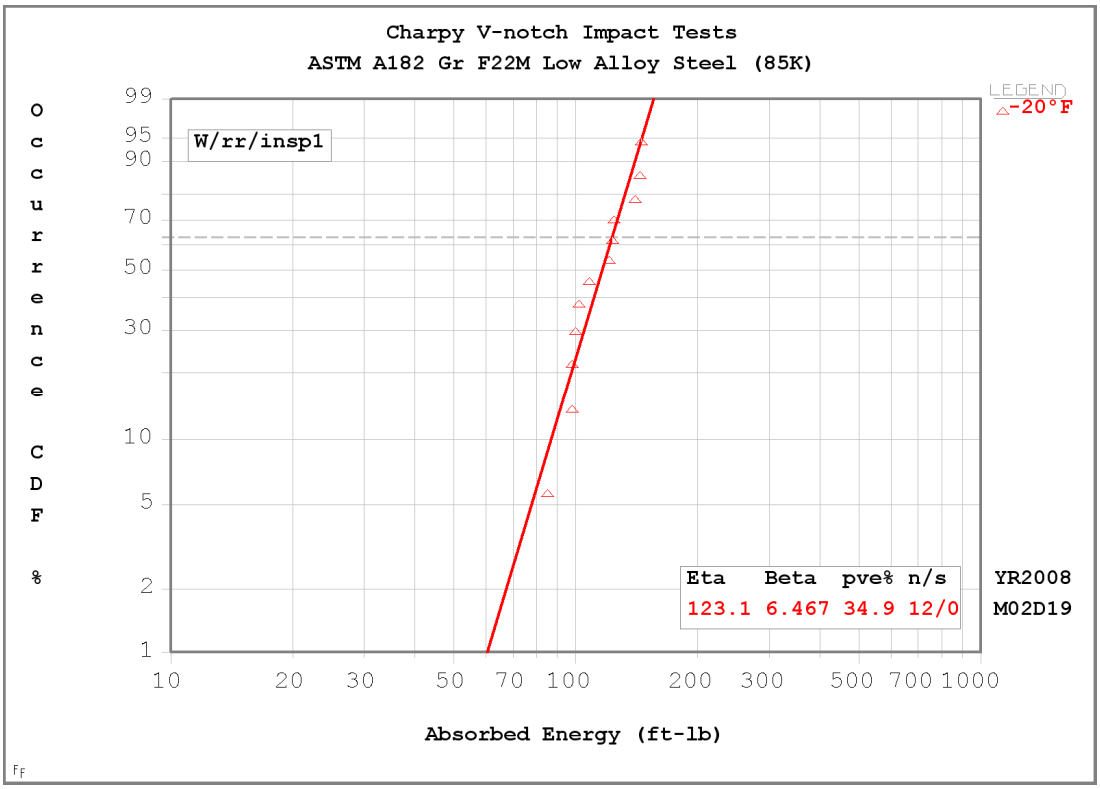

Figure 15: CDF for Charpy V-Notch Results

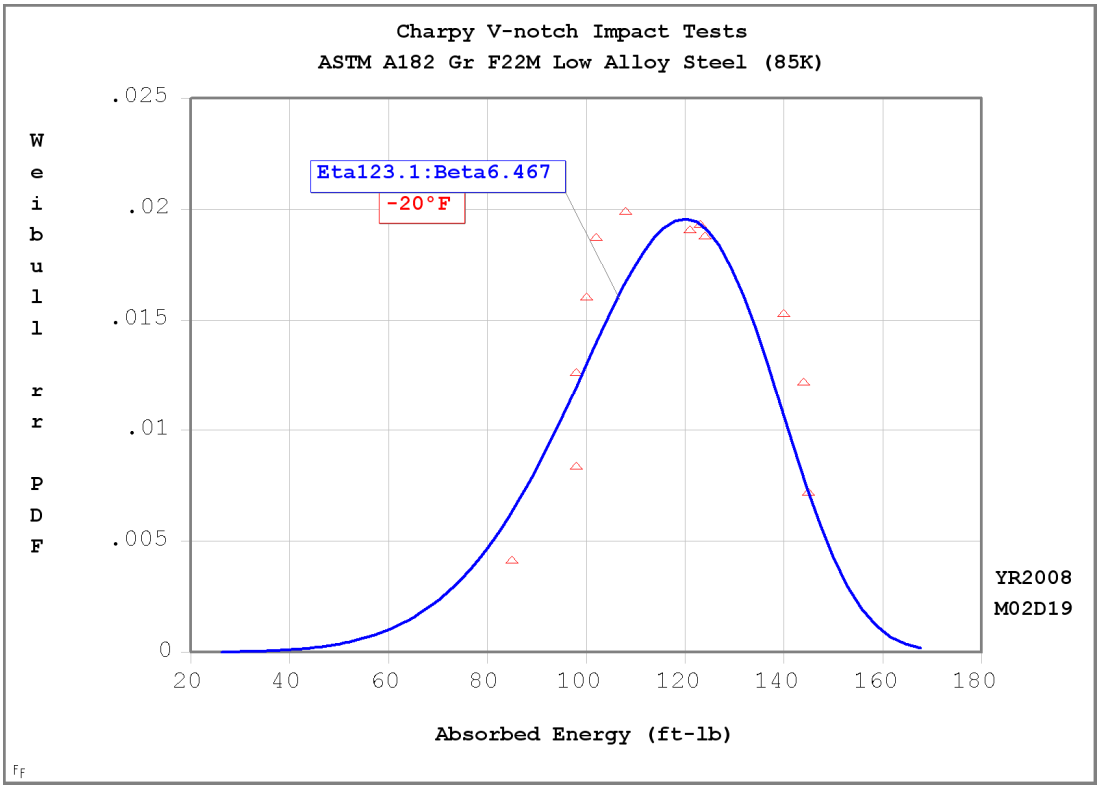

Figure 16: PDF for Charpy V-Notch Results

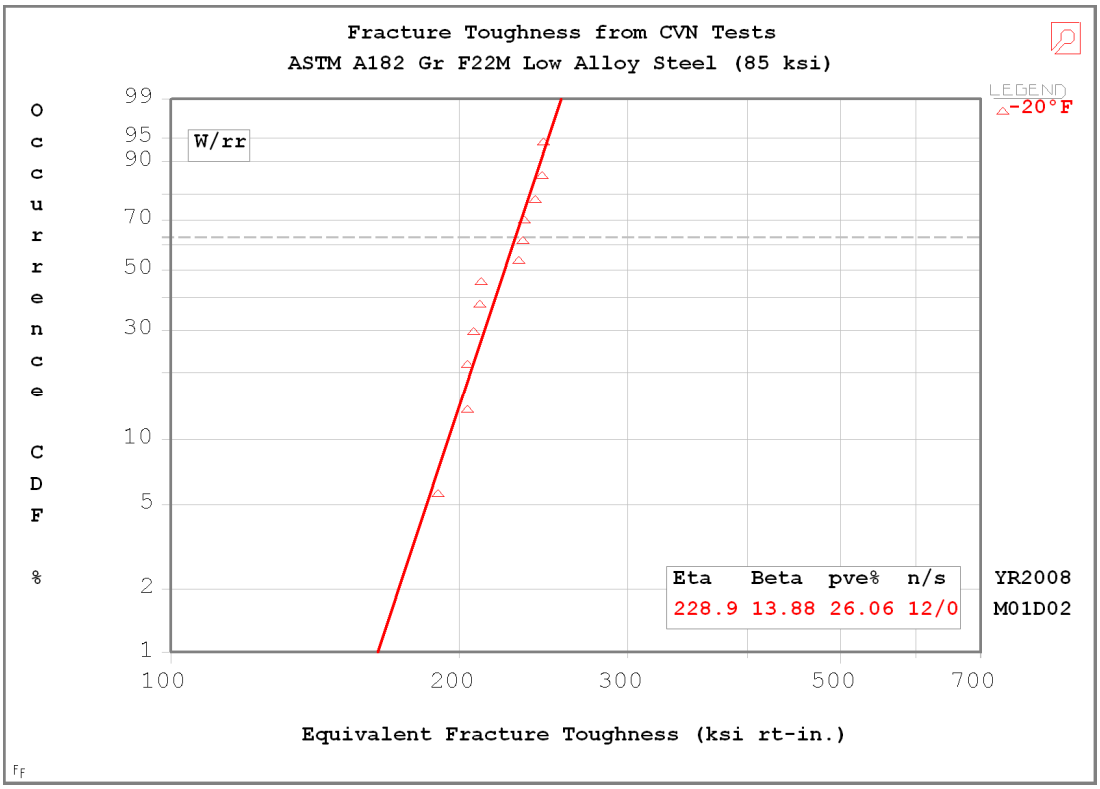

Figure 17: CDF for Fracture Toughness from Charpy Data

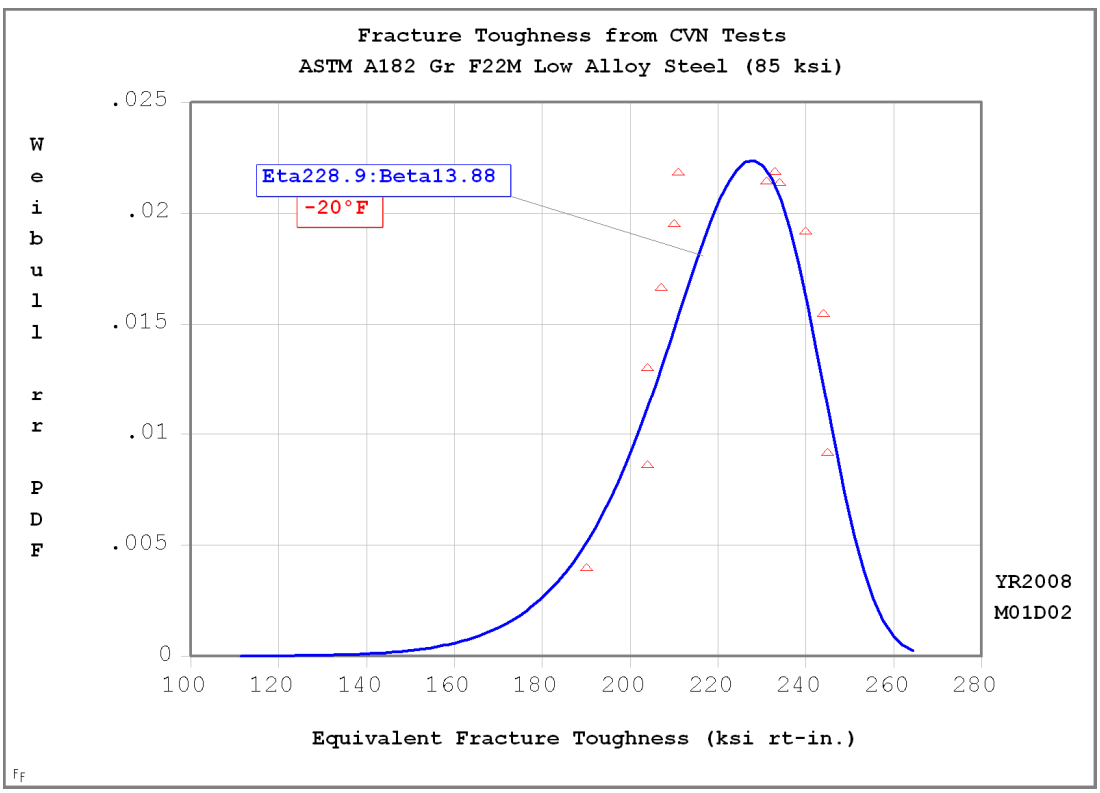

Figure 18: PDF for Fracture Toughness from Charpy Data

Based on the Weibull analysis, the B_{50} value for Charpy V-notch absorbed energy is 116 ft-lb and the B_1 value is 60 ft-lb at -20°F (Table 10). This is based on a sample size of 12 specimens from three different heats. Analysis of equivalent plane strain fracture toughness yields a B_{50} of 223 ksi·√in. and a B_1 of 162 ksi·√in. at -20°F. Weibull analysis of equivalent plane strain fracture toughness based on CVN data results in a coefficient of variation of 8.8%. This distribution is shown in Figure 18.

The complete report from Bryan Labs on the Charpy V-notch tests is included in Annex E.

Table 10: Summary of Weibull Analysis of Charpy Data at -20°F

Weibull Analysis Parameter	Sample Size	Absorbed Energy ft-lb	Percent Shear %	Lateral Expansion mil	Equivalent Fracture Toughness ksi·√in
η	12	123.1	89.00	77.71	228.7
β	12	6.467	9.738	8.474	13.36
B_{50}	12	116.3	85.71	74.42	222.5
B_1	12	60.44	55.49	45.15	162.1

Analysis of this series of ASTM Charpy V-notch impact tests led to the following observations for this material:

- Based on the Charpy impact toughness versus temperature plot over temperatures of -75°F to +75°F, the material toughness at -20°F is on the upper shelf.
- The Weibull B_{50} Charpy impact toughness of this material at -20°F is 116 ft-lb. This results in a calculated equivalent plane strain fracture toughness, K_{IC}, value of 223 ksi·√in. A temperature of -20°F was chosen because it is the default minimum design metal temperature specified by most API equipment specifications, such as API Specification 6A.
- The Weibull B_1 Charpy impact toughness at -20°F drops to 60.4 ft-lb due to variation in the measurements at -20°F (COV = 18%).
- The B_1 values for impact toughness and lateral expansion from this series of tests are approximately three times the minimum values required as specified in API Specification 6A.
- API 579 states that Charpy impact tests can be used to provide a qualitative indication of a material's fracture toughness. However, results from these tests cannot be used directly to provide an indication of toughness for use in a fitness-for-service assessment.

5.4 Fracture Toughness

Material specimens for measuring plane strain fracture toughness were tested by Bodycote Testing Group in Houston, Texas. Test specimens consisted of 1-inch thick compact tension [C(T)] specimens per ASTM E 1820 (Figure 19).

The full report from Bodycote Testing Group is included in Annex F.

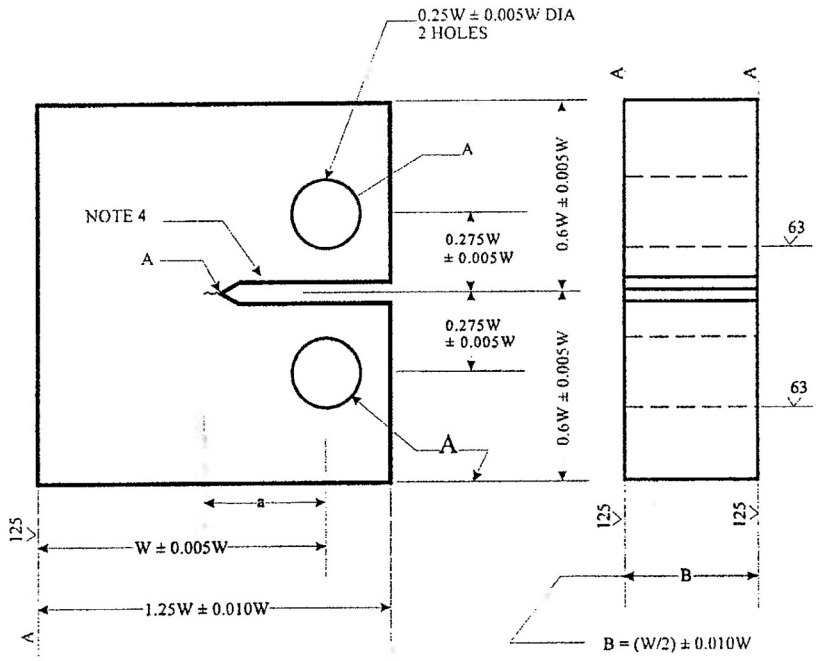

NOTE 1—A surfaces shall be perpendicular and parallel as applicable to within 0.002 *W* TIR.
NOTE 2—The intersection of the crack starter notch tips with the two specimen surfaces shall be equally distant from the top and bottom edges of the specimen within 0.005 W.
NOTE 3—Integral or attachable knife edges for clip gage attachment to the crack mouth may be used.
NOTE 4—For starter-notch and fatigue-crack configuration see Fig. 7.

FIG. A2.2 Compact Specimen for K_{Ic} Testing

Figure 19: Schematic of Compact Tension Specimen (from ASTM E 1820)

ASTM E 1820 provides requirements and recommendations for three types of specimens for fracture toughness testing: single-edge bend [SE(B)], compact tension [C(T)], and disk-shaped compact [DC(T)]. Specimen dimensional requirements vary according to the fracture toughness analysis applied. The guidelines are established through consideration of material toughness, material flow strength, and the individual qualification requirements of the toughness value with respect to the specific values sought. For the present case, the value sought was plane strain fracture toughness applicable to thick-walled pressure vessels. Correspondingly, a 1-inch thick specimen design was selected. The specimens also included side grooves as defined in Section 7.5 of ASTM E 1820.

The objective of fracture toughness testing of C(T) specimens was to load a fatigue-precracked specimen to induce either (or both):

- Unstable crack extension, including significant "pop-in" (referred to as "fracture instability" in ASTM E 1820)
- Stable crack extension, referred to as "stable tearing" in ASTM E 1820

Fracture instability results in a single value of fracture toughness determined at the point of instability. Stable tearing results in a continuous relationship between fracture toughness and crack extension (an R-curve) from which significant point values may be determined (Figure 20).

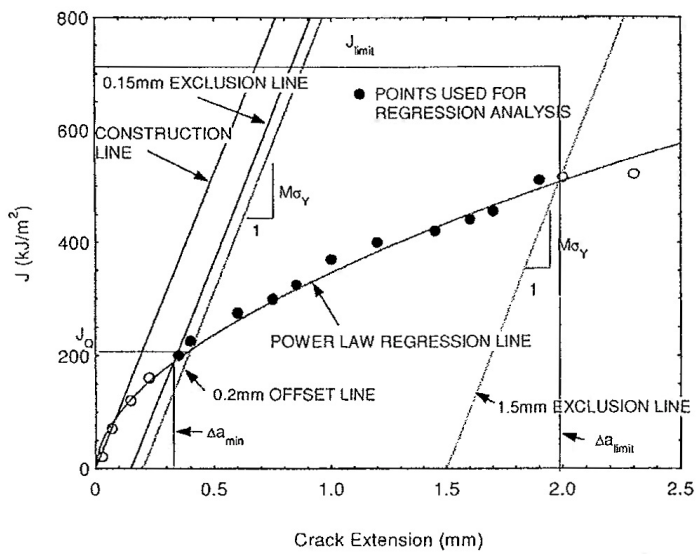

Figure 20: Example R-Curve

ASTM E 1820 describes two alternative procedures for measuring crack extension. This test program utilized the resistance-curve procedure, which uses an elastic unloading procedure to obtain a J- or CTOD-based resistance curve from a single specimen. Crack size is measured from compliance and verified by post-test optical measurements.

Specimens were extracted from three different forged blocks with a transverse (T-T) orientation (Figure 21). There were 19 total specimens, six from each forging plus one extra from forging no. 2. These specimens were then divided into three groups of six specimens each (two specimens from each forging). The extra specimen from forging 2 was used as an initial control and was tested in air at standard loading rates. The remaining 18 specimens were tested at slow loading rates. The slowest rate permissible by ASTM E 1820 is to reach maximum load within three minutes. The initial control sample was loaded at a rate of 0.66 mm/min, which resulted in a load time of just less than three minutes. The objective of this test program was to obtain the minimum level of material response and determine the lowest level of toughness value without any amplification from dynamics. Therefore, the other 18 test specimens were tested at a load rate more than 50 times slower.

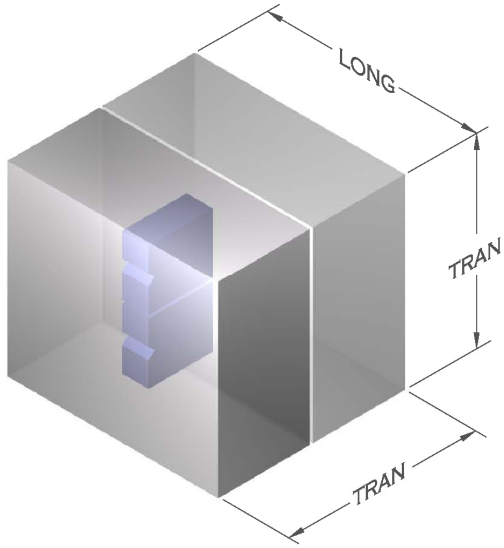

Figure 21: Compact Tension Specimen Orientation

Each group of six specimens was exposed to a different environment prior to testing:

1. Lab air at 75°F
2. Simulated seawater at 75°F as defined in ASTM D 1141 with cathodic protection at a level of -1100 mV
3. Mild H_2S solution at 75°F. The solution is defined as a gas mixture of 7% H_2S and the balance nitrogen. A buffered solution chemistry of 5.00% by weight sodium chloride and 0.40% by weight sodium acetate in deionized water. pH of the test solution before saturation was adjusted to 4.0 using hydrochloric acid. Bubble rate of the H_2S gas through the solution was 10 ml/min.

The mild H_2S solution was as defined by the API Sour Resource Group for C-110 casing testing. The mild H_2S data are provided for information only and are not intended for design analysis.

After precracking per the ASTM standard, the specimens were charged in the environment for a minimum of five days. Each specimen was then removed from the environment and immediately tested in lab air. The specimens were tested in air due to equipment limitations—it was not possible to expose the test equipment clip gages to the special environments.

The initial control specimen was tested in air at a load rate of 0.66 mm/min (0.026 in/min) with a partial unloading/reloading rate of 300 N/sec (67 lb/sec). The other 18 specimens were loaded at a slow load rate of 0.008 mm/min (3.1×10^{-4} in/min) with a partial unloading/reloading rate of 150 N/sec (34 lb/sec). Results from the fracture toughness testing are summarized in Table 11, which lists toughness value at the 0.2-mm offset in accordance with ASTM E 1820 along with toughness at the maximum load.

Table 11: Fracture Toughness Test Results

Sample No.	Environment	Loading Rate	CTOD		J-Integral	
			0.2-mm offset	max load	0.2-mm offset load	max load
		mm/min	mm	mm	N/mm	N/mm
2-07-T-1	Air	0.66	0.430	0.430	506	506
1-05-T-1	Air	0.008	0.218	0.218	245	245
1-05-T-2			0.227	0.244	271	272
2-05-T-1			0.223	0.271	260	295
2-05-T-2			0.238	0.261	256	285
3-05-T-1			0.228	0.298	253	323
3-05-T-2			0.237	0.310	285	344
1-05-T-1	Seawater with cathodic protection	0.008	0.187	0.231	220	252
1-05-T-2			0.193	0.287	230	313
2-05-T-1			0.133	0.244	166	262
2-05-T-2			0.199	0.250	230	270
3-05-T-1			0.168	0.352	184	346
3-05-T-2			0.181	0.304	219	330
1-06-T-1	H_2S solution	0.008	0.013	0.066	16.9	74
1-06-T-2			0.017	0.066	9.6	72
2-06-T-1			0.013	0.063	17.1	72
2-06-T-2			0.005	0.066	6.4	74
3-06-T-1			0.016	0.081	13.6	88
3-06-T-2			0.003	0.086	11.5	100

The correlation between the J-integral value and equivalent plane strain fracture toughness, K_{IC}, is defined in ASTM E 1820. The same correlation equation is referenced in API 579, BS 7910 and ASME Section VIII, Division 3, Appendix D and defined as follows:

$$K_{IC} = \sqrt{\frac{E \cdot J_C}{1 - \nu^2}} \qquad \text{(Eq 2)}$$

where:

K_{IC} = Equivalent plane strain fracture toughness

E = Young's modulus

J_C = Critical J-Integral value

ν = Poisson's ratio

The correlation between cracked tip opening displacement (CTOD), δ_C, to an approximate plane strain fracture toughness varies depending on the reference used. API 579, ASME Section VIII Division 3, and Barsom Rolfe all have similar (but different) correlation equations. BS 7910 states that it is not intended that CTOD toughness data be transformed to an equivalent K_{IC}.

API 579 defines the correlation from CTOD to an approximate plane strain fracture toughness as follows:

$$K_{IC} = \sqrt{\frac{1.4 \cdot E \cdot \sigma_{flow} \cdot \delta_C}{1 - \nu^2}} \qquad \text{(Eq 3)}$$

where:

σ_{flow} = Flow stress

δ_C = Critical CTOD value

ASME Section VIII, Division 3, Appendix D defines the correlation from CTOD, δ_C, to an equivalent plane strain fracture toughness, K_{IC}, as follows.

$$K_{IC} = \sqrt{E \cdot \sigma_y \cdot \delta_C} \qquad \text{(Eq 4)}$$

where:

σ_y = Yield strength

Barsom Rolfe defines the correlation from CTOD to an equivalent plane strain fracture toughness as follows:

$$K_{IC} = \sqrt{1.7 \cdot E \cdot \sigma_{flow} \cdot \delta_C} \qquad \text{(Eq 5)}$$

Results from these equivalent fracture toughness calculations are listed in Table 12. Based on these values for K_{IC}, a Weibull analysis indicated that the coefficient of variation (COV) of the six specimens in air is only 3.0%. The COV for the six specimens soaked in the seawater environment is 7.1%, and the COV for the six specimens soaked in H_2S solution is 19.3%. The Weibull cumulative distribution function (CDF) and probability density function (PDF) histograms from these three data sets are shown in Figure 22 and Figure 23.

Table 12: Equivalent Plane Strain Fracture Toughness

Sample No	Environment	Loading Rate	Equivalent Plane Strain Fracture Toughness *(K_{IC})* ksi·√in.			
			From CTOD			From J-integral
		mm/min	ASME (Eq. 4)	API 579 (Eq. 3)	Barson Rolfe (Eq. 5)	API 579 (Eq. 2)
2-07-T-1	Air	0.66	218	283	297	312
1-05-T-1	Air	0.008	153	199	209	217
1-05-T-2			156	203	214	228
2-05-T-1			157	204	214	223
2-05-T-2			162	210	221	222
3-05-T-1			153	199	209	220
3-05-T-2			156	203	213	234
1-05-T-1	Seawater with cathodic protection	0.008	142	184	194	205
1-05-T-2			144	187	197	210
2-05-T-1			121	157	165	179
2-05-T-2			148	192	202	210
3-05-T-1			131	171	179	188
3-05-T-2			136	177	186	205
1-06-T-1	H_2S solution	0.008	37	49	51	57
1-06-T-2			27	36	38	43
2-06-T-1			38	49	52	57
2-06-T-2			24	30	32	35
3-06-T-1			41	53	55	51
3-06-T-2			18	23	24	47

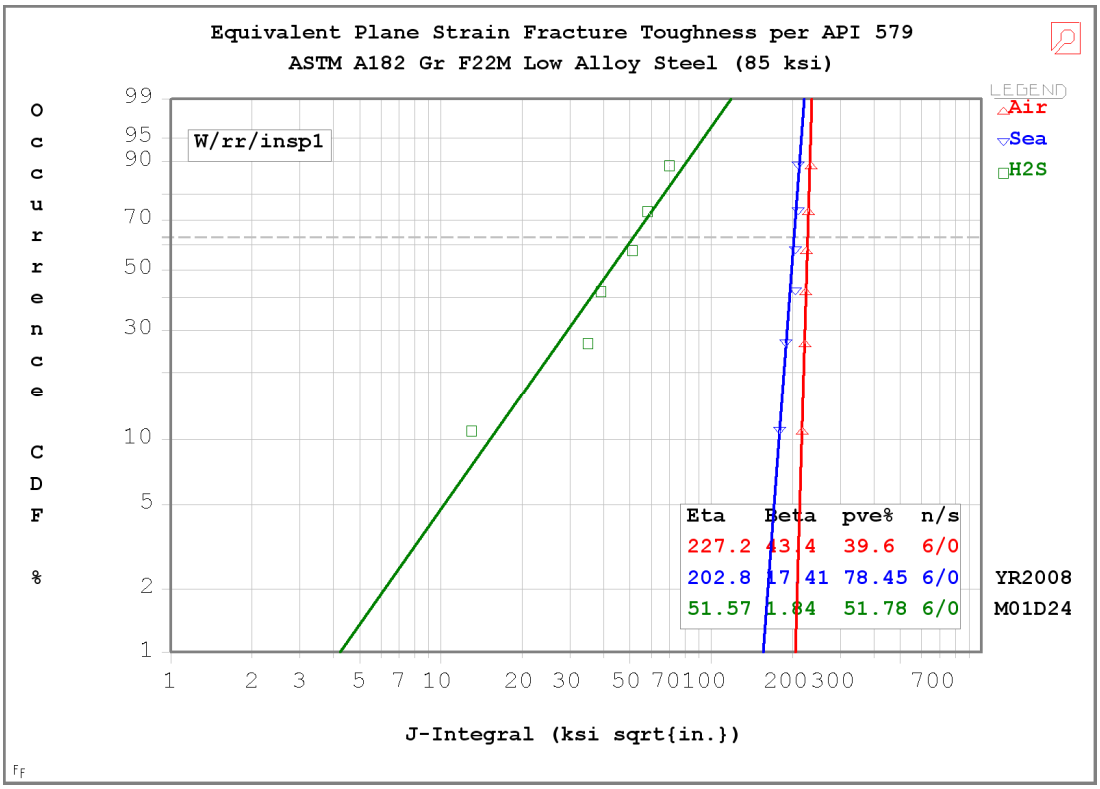

Figure 22: CDF for Fracture Toughness Results

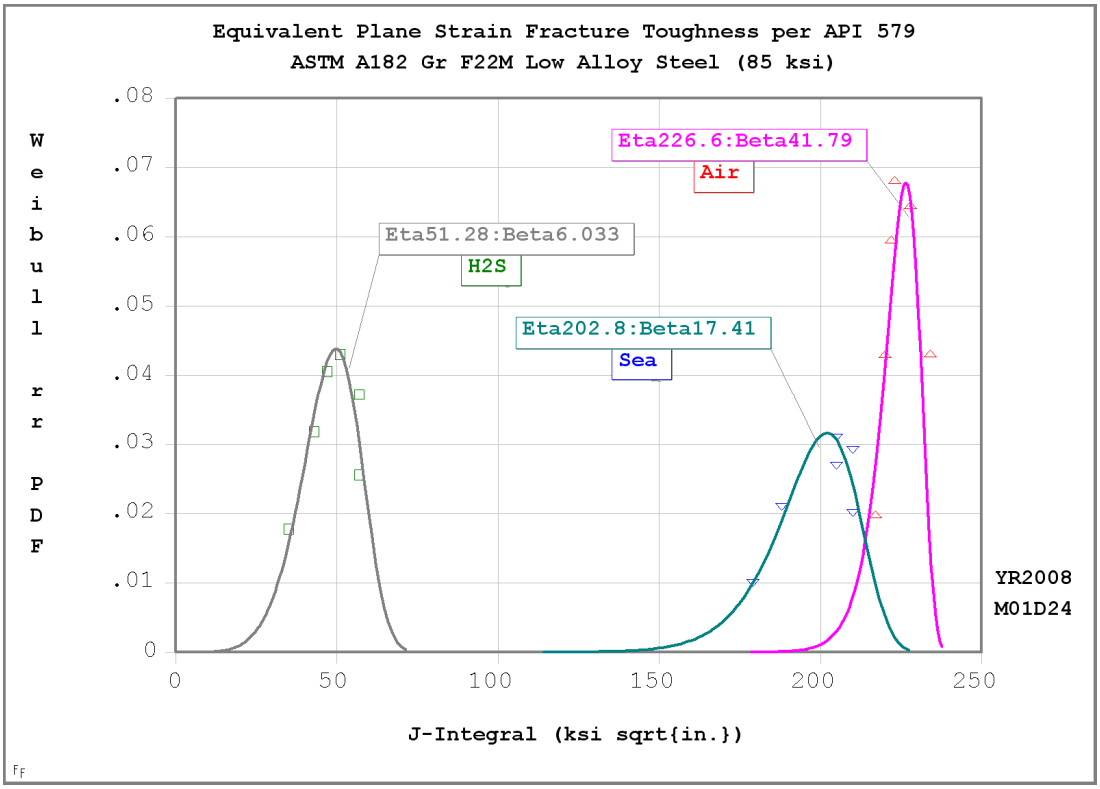

Figure 23: PDF for Fracture Toughness Results

Table 12 compares equivalent plane strain fracture toughness using the four defined conversion equations and the toughness values at the 0.2 mm offset load listed in Table 11. Table 13 presents an overall summary of the Weibull analysis for the equivalent fracture toughness correlations for the three data sets (air, seawater, and H_2S).

Table 13: Weibull Summary – Fracture Toughness

Weibull Distribution Value	Environment	Equivalent Plane Strain Fracture Toughness ksi·√in.				
		From CVN	From CTOD			From J-Integral
		API 579	ASME	API 579	Barson Rolfe	API 579
η (characteristic life)	Air, -20°F	228.7				
	Air, 75°F		157.2	204.3	215.1	226.6
	Seawater, 75°F		141.5	183.8	193.4	202.8
	H_2S, 75°F		34.35	43.15	46.86	51.28
β (Weibull slope)	Air, -20°F	13.36				
	Air, 75°F		37.39	39.69	41.00	41.79
	Seawater, 75°F		14.47	14.64	14.37	17.41
	H_2S, 75°F		3.36	3.39	3.30	6.03
B_{50}	Air, -20°F	223				
	Air, 75°F		156	202	213	225
	Seawater, 75°F		138	179	189	199
	H_2S, 75°F		31	39	42	48
B_1	Air, -20°F	162				
	Air, 75°F		139	182	192	203
	Seawater, 75°F		103	134	140	156
	H_2S, 75°F		9	11	12	24

The full report by Bodycote on the fracture toughness testing is included in Annex F.1. The Weibull analysis reports for fracture toughness data are included in Annex F.2.

Based on this series of ASTM fracture toughness tests, the following observations were noted for this material:

- The Charpy V-notch impact toughness and the equivalent plane strain fracture toughness, K_{IC}, has considerable more scatter in the data as compared to CTOD and J-integral data.

- The ASME fracture-toughness correlation for CTOD data is the most conservative of the correlations—it results in the lowest fracture toughness value.
- The correlation for estimating fracture toughness from CTOD data varies depending on the reference used.
- BS 7910 states that it is not intended that CTOD toughness data be transformed to an equivalent K_{IC}.
- The correlations for fracture toughness from J-integral data are the same from each of the referenced standards.
- Equivalent fracture toughness from CTOD data is slightly more conservative than that calculated from J-integral data.
- Equivalent fracture toughness for the specimens soaked in seawater showed a mean reduction in fracture toughness of approximately 12% as compared to the air environment.
- Fracture toughness for the specimens soaked in H_2S solution was very low. In addition, the measurements had significantly more variation than those from the other environments. Based on low values and variability of the data, performance data from the H_2S environmental fracture toughness testing should not be used for design purposes.

5.5 Fatigue Crack Growth Rate

A series of tests for measuring fatigue crack growth rate was performed by Southwest Research Institute in San Antonio, Texas. Test specimens were 0.25-inch thick compact tension specimens [C(T)] per ASTM E 647 (Figure 24). Specimens were tested in air, seawater with cathodic protection, and in H_2S. The full report from Southwest Research Institute is included in Annex G.1.

The objective of these tests was to determine the fatigue crack growth rate, *da/dN*, expressed as a function of crack-tip stress-intensity factor range, ΔK, which characterizes a material's resistance to stable crack extension under cyclic loading.

The primary application for the material being investigated was large valve-body forgings, such as choke and kill valves and BOP bodies. The primary load mechanism for this type of equipment is pressure cycling usually at or near the same high pressure for each cycle. After each pressure cycle, the pressure is normally reduced to zero or to the hydrostatic (internal or external) pressure difference for subsea applications. Consequently, these tests were designed to grow the crack while maintaining a constant load ratio, R. Tests in an air environment were run at two different load ratios ($R = 0.1$ and $R = 0.5$). The test protocol used an increasing ΔK at a frequency of 20 Hz. All testing was conducted at ambient temperature.

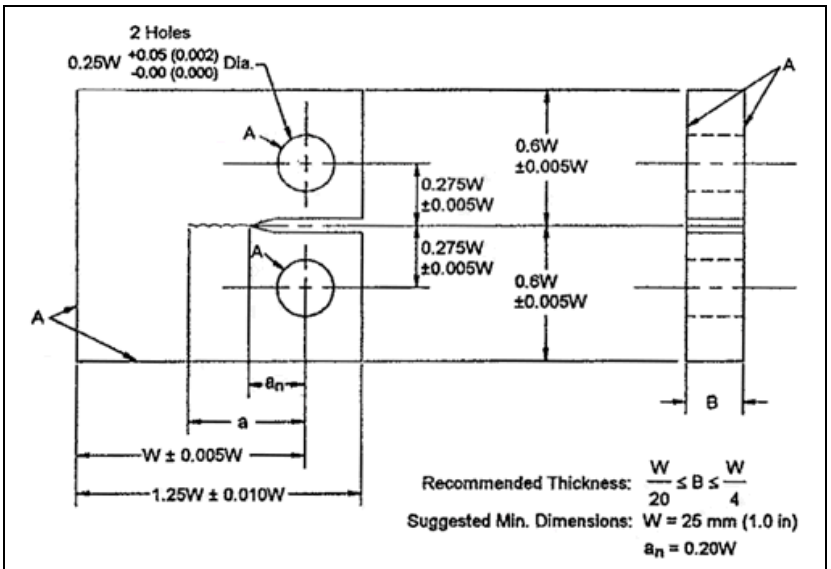

NOTE 1—Dimensions are in millimetres (inches).

NOTE 2—*A*-surfaces shall be perpendicular and parallel as applicable to within ±0.002 *W*, TIR.

NOTE 3—The intersection of the tips of the machined notch (a_n) with the specimen faces shall be equally distant from the top and bottom edges of the specimen to within 0.005 *W*.

NOTE 4—Surface finish, including holes, shall be 0.8 (32) or better.

Figure 24: Fatigue Crack Growth Rate Specimen (from ASTM E 647)

The lab air specimens were well behaved through a ΔK range from approximately 3 ksi·√inch to approximately 60 ksi·√inch. The crack growth rate data was very linear and exhibited a variance less than expected for low alloy steels. Figure 25 is a plot of the crack growth rate data in air for both low and medium load ratio tests.

Preparation of the test specimens included fatigue compression precracking, which is a deviation from the procedure in the current version of ASTM E 647, but being considered for future revisions. This method appears to provide the advantage of obtaining the crack growth rate data in the linear region of the *da/dN* versus ΔK curve at lower ΔK values. The evidence of a threshold ΔK value in Figure 25 is not readily apparent. This raises questions about the significance of the threshold value – does it truly exist as a response of the material or is it a function of the load history applied to the material.

Over the years, a number of relationships have been developed to represent the linear region of the *da/dN* versus ΔK fatigue crack growth rate curve. The simplest and most common of these equations is the Paris equation:

$$da/dN = C \cdot (\Delta K)^n \qquad \text{(Eq 6)}$$

where C and n are empirical parameters determined from a curve fit to the test data. This model is referenced in most standards, such as API 579. The Paris equation constants from noted references are listed in Table 14.

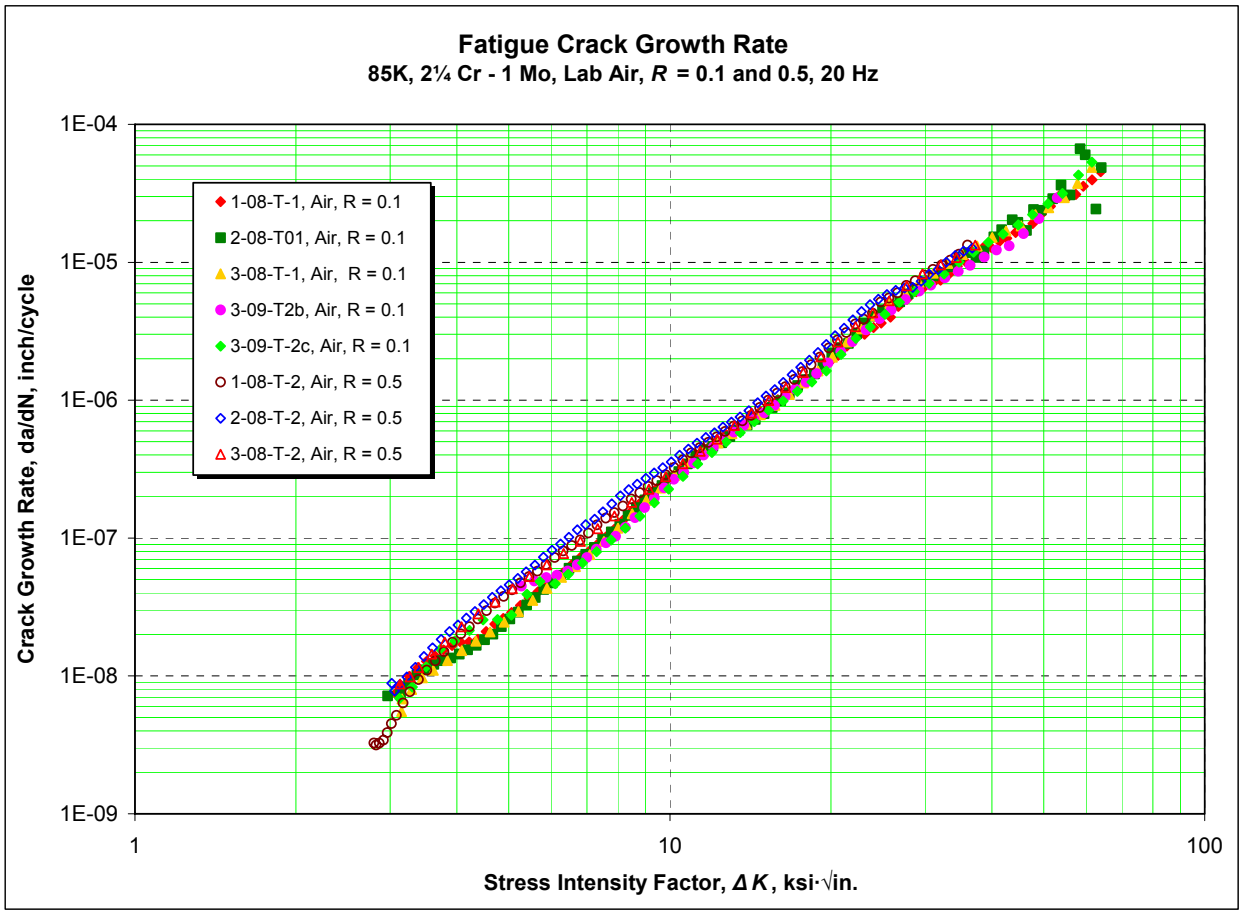

Figure 25: Plot of FCGR Data in Air

Curve fitting of the air data results in a Paris equation slope of n = 2.958 for the five sets of data at R = 0.1 and n = 3.019 for the three sets of data at R = 0.5. Note that the slope of this data is between the slope listed from ASME VIII-3 and the slope from API 579 as noted in Table 14.

Table 14: Published Crack Growth Rate Factors – Air

Reference	Material	Environment	C in./cyc / (ksi·√in.)^n	n
ASME Div 3 Table KD-430 $R = 0$	High strength low alloy steels, Sy > 90 ksi	Air	1.95×10^{-10}	3.26
API 579 Table F.12 $R < 0.5$	Steels, Sy ≤ 101.5 ksi (upper stage of curve $\Delta K > 9.07$ ksi·√in.)	Air or other non-aggressive environments at temperatures up to 212°F	4.29×10^{-10}	2.88
BS 7910 Table 4 $R < 0.5$	Steels, Sy ≤ 101.5 ksi (upper stage of curve $\Delta K > 10$ ksi·√in.)	Air or other non-aggressive environments at temperatures up to 212°F	4.29×10^{-10} (3.98×10^{-13} mm/cyc / MPa·√mm)	2.88

The Walker equation is a linear model that incorporates the mean stress effects through the use of the load ratio, R, where $R = \sigma_{min} / \sigma_{max}$ or K_{min} / K_{max}.

$$da/dN = C \cdot \left(\frac{\Delta K}{(1-R)^{1-m}} \right)^n \qquad \text{(Eq 7)}$$

where C, n, and m are again empirical parameters determined from a curve fit to test data. This curve fitting requires test data at multiple load ratios. We obtained test data at $R = 0.1$ and at $R = 0.5$ during this series of tests. Doing a curve fit analysis for this data for the two load ratio groups using the Walker equations results in the relationship as shown.

$$da/dN \cdot \frac{inch}{cycle} = 2.349 \times 10^{-10} \cdot \left(\frac{\Delta K \cdot ksi \cdot \sqrt{inch}}{(1-R)^{1-0.828}} \right)^{2.989} \qquad \text{(Eq 8)}$$

Comparing the Equation 8 curve to the ASME VIII-3 and API 579 curves, we find that both curves are shifted upwards slightly from the Equation 8 curve. This results in the ASME VIII-3 and API 579 curves resulting in a more conservative design prediction. Shifting Equation 8 upwards to equate with the ASME VIII-3 equation at a $\Delta K = 10$ ksi·√inch would result in Equation 9.

$$da/dN \cdot \frac{inch}{cycle} = 3.45 \times 10^{-10} \cdot \left(\frac{\Delta K \cdot ksi \cdot \sqrt{inch}}{(1-R)^{1-0.828}} \right)^{2.989} \qquad \text{(Eq 9)}$$

A plot of the air data and Equation 9 are shown in Figure 26. This curve fit takes into account the load ratio, *R*, as required in ASME VIII-3 and is a conservative fit for the crack growth rate of this material. Equation 9 is represented in Figure 26 with the two load ratios (*R* = 0.1 and *R* = 0.5) as blue lines.

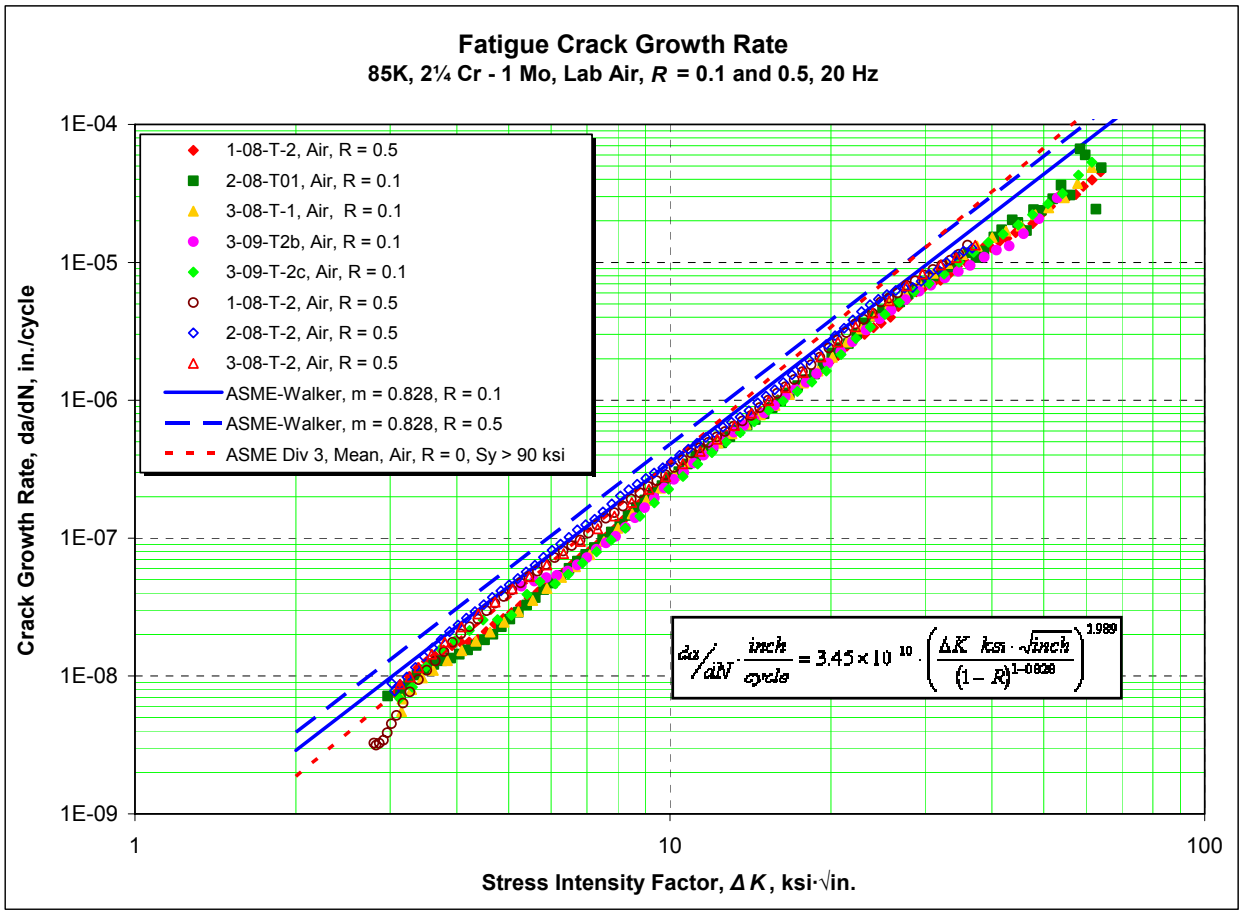

Figure 26: Plot of FCGR Data – Walker Equation

In addition to the air data, fatigue crack growth rate tests were done on three specimens in a seawater environment with cathodic protection and three specimens in an H_2S environment. Results from the H_2S tests were intended for information only and not to be used for design purposes. The H_2S environment was identical to that used in fracture toughness testing and is described in Section 5.4.

The fatigue crack growth rate test results in seawater are shown in Figure 27. The specimens were compression precracked, as was done for the lab air test specimens. The crack growth rate testing of the seawater specimens were initially started in lab air below a ΔK of 7.5 ksi·√inch and cycled at 20 Hz. Beyond this point, the seawater with cathodic protection was added with a soak period of 24 hours prior

to continuing the crack growth rate cycling. The cycling in the seawater environment was done at a rate of 1 Hz.

As shown in the plot of the test data in Figure 27, the testing proved difficult with the crack growth arresting in two of the three specimens (specimens 1-09-T-2 and 3-09-T-1). There was also significantly more scatter in this data than was seen in the air data. However, the test results from this series of tests are generally below the seawater design curve listed in BS 7910, illustrated in Figure 27 and listed in Table 15.

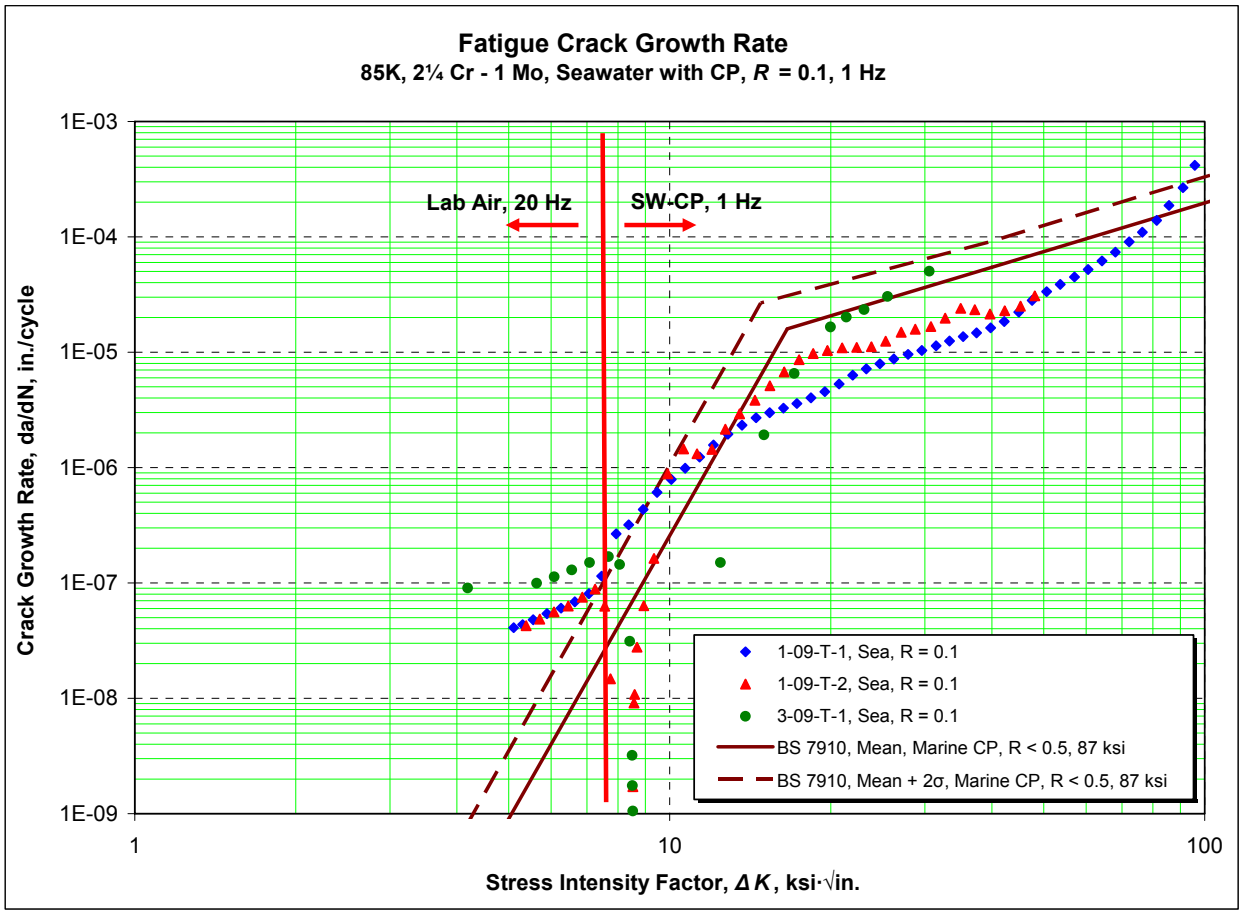

Figure 27: Plot of FCGR in Seawater with Cathodic Protection

Table 15: Published Crack Growth Rate Factors – Seawater

Reference	Material	Environment	C in./cyc / (ksi·√in.)^n	n
BS 7910 Table 5 $R < 0.5$	Steels, Sy ≤ 87 ksi (upper stage of mean curve)	Marine environment with cathodic protection at -1100 mV (Ag/AgCl)	3.12×10^{-7} (9.24×10^{-8} mm/cyc / MPa·√mm)	1.4
	Steels, Sy ≤ 87 ksi (upper stage of mean + 2SD curve)		5.23×10^{-7} (1.02×10^{-7} mm/cyc / MPa·√mm)	1.4

The fatigue crack growth rate test results for the H_2S environment are shown in Figure 28. As noted on the chart, the specimens were initially cycled below ΔK of 7.5 ksi·√inch in lab air at 20 Hz. Above this level the seawater with cathodic protection was introduced and cycled at 1 Hz until reaching 10 ksi·√inch. At this level the H_2S solution was introduced and cycled at 0.33 Hz. While the three results are similar from 10 to approximately 14 ksi·√inch, above 14 ksi·√inch, there is significant scatter. These data are presented for information only and is not to be used for design purposes.

Figure 29 shows the combined FCGR results for the tests in air, seawater with cathodic protection, and H_2S environments. From this chart we can see that the crack growth rate initially increases faster after being introduced into the more aggressive environments. However, after a point the crack growth rate diminishes and eventually approaches the growth rate of the tests in air.

Based on this series of fatigue crack growth rate tests, the following observations were noted for this material:

- Compression precracking is a viable process for preparing C(T) specimens for fatigue crack growth rate testing. This method permits obtaining crack growth rate data at lower ΔK values.
- The in-air tests showed relatively small scatter. This allowed usage of the Paris Law equation to be defined including the dependence on the load ratio, R.
- The slope of the Paris equation curve fit of the air data is between the ASME VIII-3 and the API 579 curves.
- The ASME VIII-3 Paris equation curve for steel in air is slightly conservative.
- The FCGR in air with $R = 0.5$ is about 1.35 times higher than at $R = 0.1$.
- The lower section (ΔK < 9.07 ksi·√in) of the Paris curve for steel in air, as defined in API 579, appears to be non-conservative.
- The tests in seawater show a fair amount of scatter and test-to-test variability with a greater chance of crack arresting after introduction into the environment. The reason for this is not fully understood, but may be partially attributed to the low R-ratio of the tests.

- The test in seawater with cathodic protection showed more scatter, but generally were consistent with published crack growth curves from BS 7910.
- Performance data for fatigue crack growth rate in a seawater environment appears to be attainable from testing. However, more research is needed to better understand the variables which affect the crack growth rate performance.
- The crack growth rate in the more aggressive environment of H_2S shows an increased growth rate over the seawater environment data, but seamed to plateau at near the same ΔK level.
- Fatigue crack growth rate data in a H_2S environment and the essential variables affecting performance are not well understood. Therefore, the data is presented for information only and not to be used for design purposes.

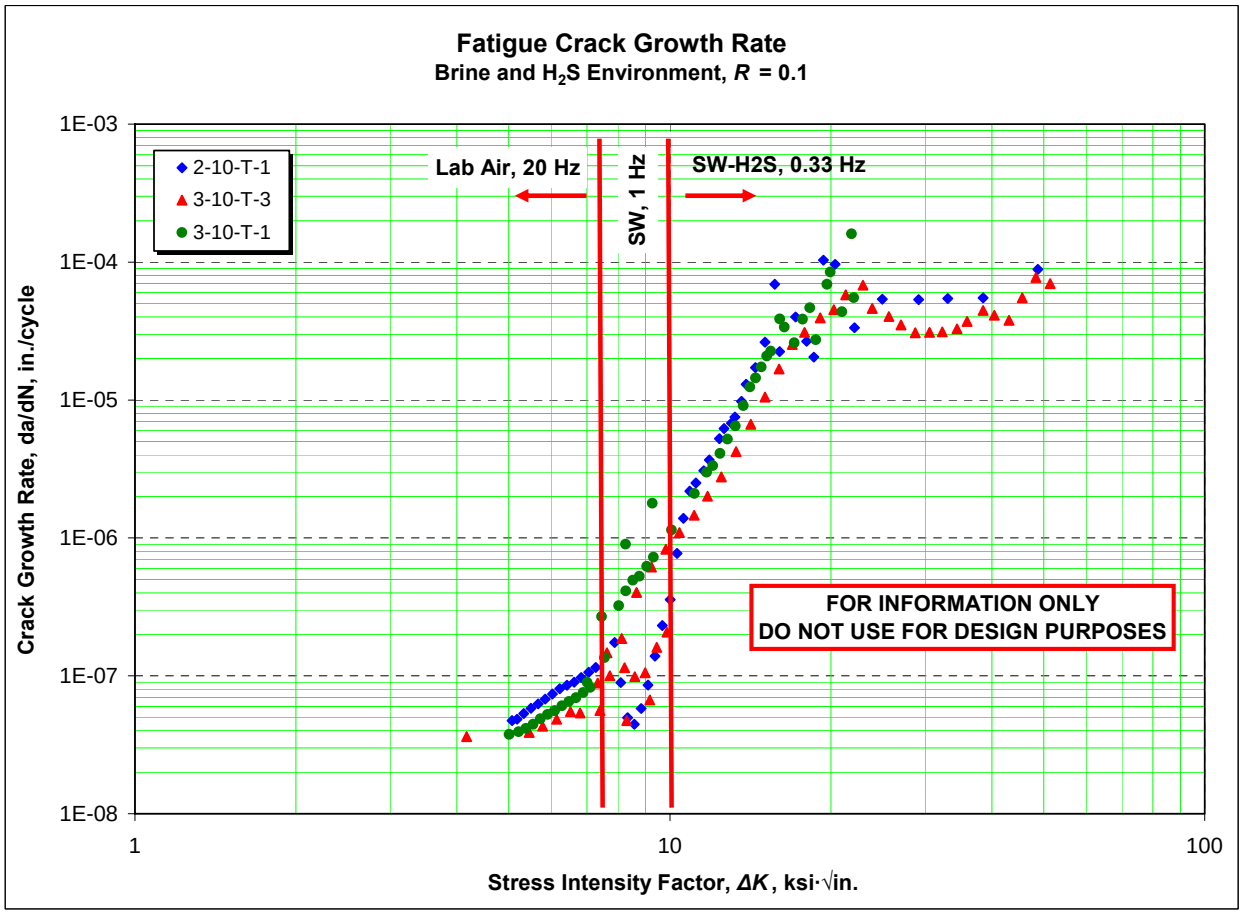

Figure 28: Plot of FCGR in H_2S Environment

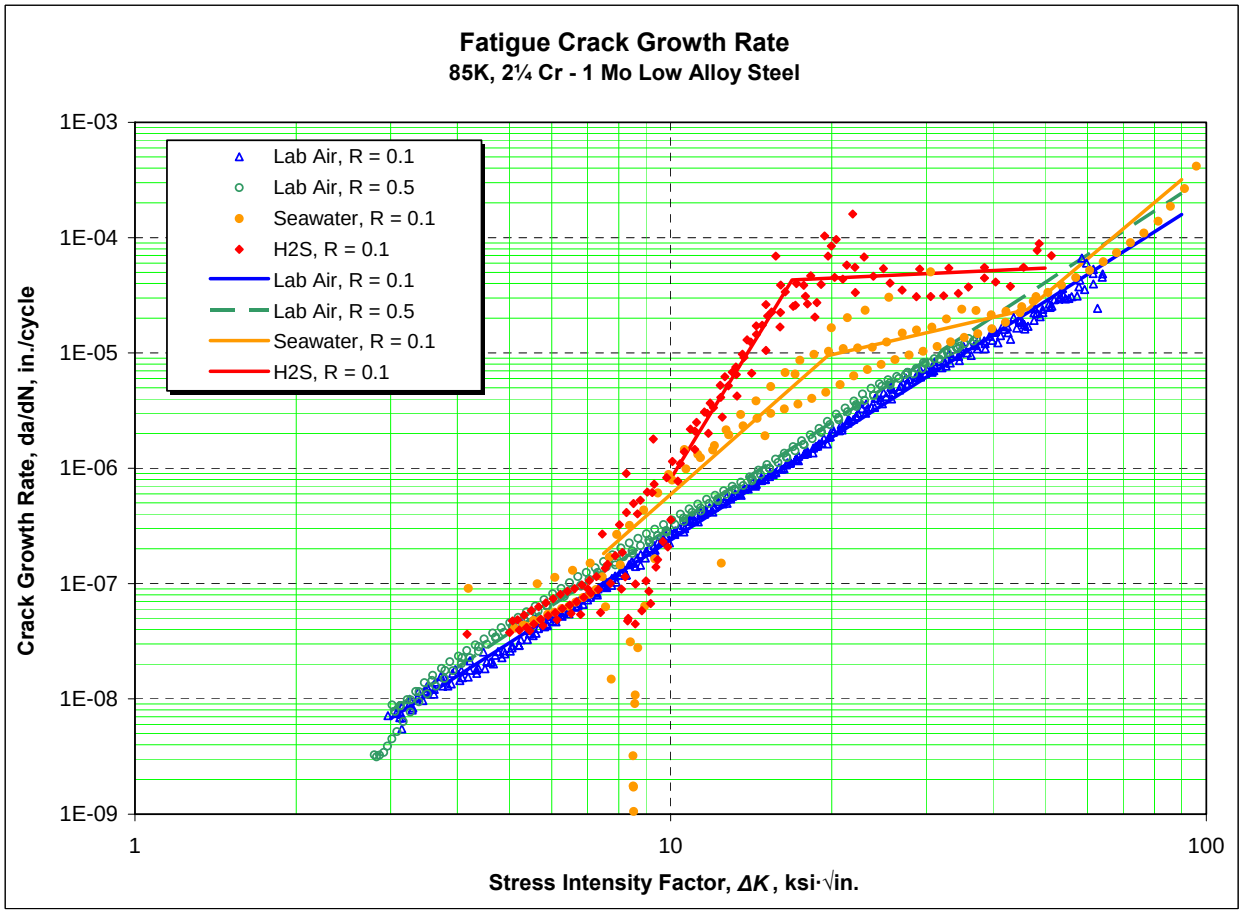

Figure 29: Combined FCGR Curves

6 Conclusions

1. Forged blocks used for material testing should probably be post-weld heat treated, PWHT, prior to specimen preparation and testing. This may result in a closer representation of the material strength properties due to PWHT requirements after welding during the manufacturing process.
2. The AWHEM recommendation for strength reduction factor of 0.91 for 350°F for 2¼ Cr – 1 Mo material should be applied.
3. Values for the modulus of elasticity as a function of temperature as defined in ASME Section II Part D should be used for design purposes.
4. Fracture toughness and fatigue crack growth rate data in an H_2S environment are provided for information only and should not be used for equipment design.

5. The equivalent plane strain fracture toughness tests in air resulted in a mean value, B_{50}, of 225 ksi·√inch and a lower bound, B_1, value of 203 ksi·√inch.
6. The equivalent plane strain fracture toughness tests in seawater with cathodic protection resulted in a mean value, B_{50}, of 199 ksi·√inch and a lower bound, B_1, value of 156 ksi·√inch.

7 References

1. API RP 6HP, *Recommended Practice for Equipment with Pressure Rating Greater Than 15,000 psi*, Draft 5, API, Washington, DC, June 2006.
2. API Specification 6A, *Specification for Wellhead and Christmas Tree Equipment*, 19th Edition, API, Washington, DC, July 2004.
3. API Specification 16A, *Specification for Drill Through Equipment*, 3rd Edition, API, Washington, DC, June 2004.
4. API 579-1/ASME FFS-1, *Fitness for Service*, 2nd Edition, API, Washington, DC, June 2007.
5. API SC6 Minutes of Meeting from Standardization Conference, API, Washington, DC, June 2006.
6. ASME Boiler & Pressure Vessel Code, Section VIII, Division 3, *Alternative Rules for Construction of High Pressure Vessels*, ASME, New York, New York, 2007.
7. ASTM A 182, *Standard Specification for Forged or Rolled Alloy and Stainless Steel Pipe Flanges, Forged Fittings, and Valves and Parts for High-Temperature Service*, 2006.
8. ASTM A 370, *Standard Test Methods and Definitions for Mechanical Testing of Steel Products*, 2006.
9. ASTM D 1141, *Standard Practice for the Preparation of Substitute Ocean Water*, 2003.
10. ASTM E 21, *Standard Test Methods for Elevated Temperature Tension Tests of Metallic Materials*, 2003.
11. ASTM E 23, *Standard Test Methods of Notched Bar Impact Testing of Metallic Materials*, 2006.
12. ASTM E 647, *Standard Test Method for Measurement of Fatigue Crack Growth Rates*, 2005.
13. ASTM E 1820, *Standard Test Method for Measurement of Fracture Toughness*, 2006.
14. ASTM E 1823, *Standard Terminology Relating to Fatigue and Fracture Testing*, 1996 (Reapproved 2002).
15. Abernethy, R.B., *The New Weibull Handbook*, 5th Edition, 2004.
16. Anderson, T.L., *Fracture Mechanics: Fundamentals and Applications*, 2nd Edition, CRC Press LLC, Boca Raton, Florida, 1995.

17. Barsom, J.M. and Rolfe, S.T., *Fracture and Fatigue Control in Structures: Application of Fracture Mechanics*, 3rd Edition, American Society for Testing and Materials, West Conshochocken, PA, 1999.

18. BS 7910, *Guide to Methods for Assessing the Acceptability of Flaws in Metallic Structures*, 2005.

19. Todinov, Michael, *Reliability and Risk Models: Setting Reliability Requirements*, John Wiley & Sons, 2005.

20. NACE MR0175 / ISO 15156-1, *Petroleum and natural gas industries – Materials for use in H2S-containing Environments in Oil and Gas Production – Part 1: General Principles for Selection of Cracking-Resistant Materials*, 1st Edition, NACE International, Houston, Texas, 2001.

21. NACE MR0175 / ISO 15156-2, *Petroleum and natural gas industries – Materials for use in H_2S-containing Environments in Oil and Gas Production – Part 2: Cracking-Resistant Carbon and Low Alloy Steels, and the Use of Cast Irons*, 1st Edition, NACE International, Houston, Texas, 2003.

Annex A. Material Specifications

Annex A.1 Test Sample Material Specifications

Material Specification for Forged ASTM A 182 Grade F22M (UNS K21590) Material

The forged material for this test program shall be forged and shall meet or exceed all of the requirements of ASTM A 182 Grade F22 and API Specification 16A.

The forged and heat-treated coupons for this test program shall be 8.00 inch x 8.00 inch x 9.00 inch.

The chemical composition shall be:

Range	C	Mn	P	S	Si	Cu	Ni	Cr	Mo	V	Al
Min	0.10	0.30						2.00	0.87		
Max	0.15	0.60	0.025	0.025	0.50	0.35	0.25	2.50	1.13	0.03	0.04

The amount of hot work shall be sufficient to result in a wrought structure throughout the entire cross-section of the forged bar with a minimum forging reduction ratio of 3 to 1.

The forgings shall be normalized, water-quenched, and tempered to result in the following mechanical properties. The test temperature for the Charpy V-Notch may use -75°F, but the minimum values shall remain the same.

Yield Strength	Tensile Strength	Elongation	Reduction of Area	Hardness	Charpy V-Notch Impact Energy		
min, ksi	min, ksi	min, %	min, %	HBN	ft-lb	Lat Exp	Temp
85.0	100.0	18	35	217-237	20/15	20 mils	-20°F

Annex A.2. Material Certificates

Ellwood City Forge
Ellwood City,PA

Block #1

Sold To:	Hydril Company LP 3300 N Sam Houston Pwky East Houston, TX 77032	**Date:** **P.O.#:** **Job #:**	11/16/06 1105464 F1227
Grade and Description:	F22 BODY PREFORM - R. MILL & BORE	**Specification:** **Drawing #:**	HEMPS 2.580-10 REV. B5 COND. X-85K, DWG & PO NOTES QP1000003-01 REV. B5 BOM ME-3130900 REV C2 ME-3130900 REV C2 PART NO ME-3130900

Job #	Piece #	Heat/ Ingot #	Ingot Size	Ingot Weight	Product Size	Shipped Weight
F1227	02	R4102-1				

CHEMICAL ANALYSIS

Heat #	C ✓	Mn ✓	P ✓	S ✓	Si ✓	Ni ✓	Cr ✓	Mo ✓	Al ✓	V ✓	Cu	Hppm	Ti
R4102	.15	.55	.010	.007	.28	.14	2.27	1.02	.035	.011	.21	1.5	.0033

TENSILE TEST RESULTS: TENSILE TEST DIA. .505" **BRINELL RESULTS**

TENSILE TESTS TAKEN FROM QTC N2341 02 8 X 8 X 9 OBTAINED FROM F1227 02

Piece #	Test Loc	Yield Strength .2% offset	Tensile Strength	Elong in 2"	R A %	BRINELL
02	LONG	93,155 ✓	110,362 ✓	25 ✓	73 ✓	BHN ON PC 226-222-227-236
						BHN ON TENSILE 228
						BHN ON QTC 237-236

IMPACT RESULTS: TEST SIZE: 10mm x 10mm

Piece#	Test Loc	Test Temp	Ft lbs.	%Shear	Lateral Expansion
02	TRANS	✓ -75 F	37 38 25	5 5 5	.025 .026 .017

MELT METHOD: ELECTRIC FURNACE VACUUM DEGASSED LADLE REFINED,CALCUIM TREATED MELTED TO FINE GRAIN PRACTICE
HEAT TREATED IN FURNACES CERTIFIED TO MIL-H-6875 F
HEAT TREATMENT OF PROD. PART.:LOAD 62805A HEAT TO 1750°F 12 HRS MIN NORM. LOAD 62839A HEAT TO 1750°F 8 HRS MIN WATER ✓
QUENCH, LOAD 62839B TEMPER 1215°F 7 HOURS ✓
WATER QUENCH TEMP. WAS 70°F AT START AND 98°F AT END OF QUENCH ✓
HEAT TREATMENT OF QTC N2341 02 LOAD 62412A HEAT TO 1750°F 5 HRS MIN NORM.LOAD 62445A HEAT TO 1750°F 5 HRS MIN WATER QUENCH,LOAD 62445B TEMPER 1215°F 5 HRS
WATER QUENCH TEMP WAS 62°F AT START AND 73°F AT END OF QUENCH
HEAT TREATMENT OF QTC N2342 02 LOAD 62421A HEAT TO 1750°F 5 HRS MIN NORM.LOAD 62458A HEAT TO 1750°F 5 HRS MIN WATER QUENCH ,LOAD 62458BTEMPER 1215°F 5 HRS
WATER QUENCH TEMP WAS 62°F AT START AND 70°F AT END OF QUENCH
NO WELDING PERFORMED ON MATERIAL FORGE REDUCTION: 5.1 TO 1
CAPABILITY OF FINISH PARTS PER MPT DWG NOTE 12(HEMPS 10.202-05 REV F & AMEND. E CODE VI W/SUPPL. 1 REV NC) AND LIQUID PENETRANT SPEC HEMPS 10.302-05 CODE V REV G,SONIC PER HEMPS 10.501 SUPL 6 REV NC AMEND A
CAPABLE OF MEETING LIQUID PENETRANT OF "RAM COMPARTMENT" BORES ONLY PER HEMPS 10.302 REV M(1/8" NAX FLAW) AT FINISH SIZE

HYDRIL COMPANY LP
Q.C. Receiving Inspection
Ht# S/N M2420
P/N ME-3130900 Rev. C1
Vendor Ellwood City Forge
P.O.# 1105464 Qty 1
Date 11-30-06 HBN 233

HTC 7

Signed: Kathy Carsale
Certification Clerk

SCANNED NOV 30 2006

-1

Ellwood City Forge
Ellwood City,PA

Block #2

Sold To:	Hydril Company LP 3300 N Sam Houston Pwky East Houston, TX 77032	**Date:** **P.O.#:** **Job #:**	10/06/06 1105463 F1226
Grade and Description:	F22 BODY PREFORM - R. MILL & BORE	**Specification:** **Drawing #:**	HEMPS 2.580-10 REV. B5 COND. X-85K, DWG & PO NOTES QP1000003-01 REV. B5 BOM ME-3130900 REV C1 ME-3130900 REV C1 PART NO ME-3130900 REV C1

Job #	Piece #	Heat/ Ingot #	Ingot Size	Ingot Weight	Product Size	Shipped Weight
F1226	02	R3317-1				

CHEMICAL ANALYSIS

Heat #	C ✓	Mn✓	P ✓	S ✓	Si ✓	Ni ✓	Cr ✓	Mo ✓	Al✓	V ✓	Cu✓	Hppm	Ti
R3317	.14	.53	.013	.008	.28	.10	2.26	1.00	.030	.008	.16	1.0	.0026

TENSILE TEST RESULTS: TENSILE TEST DIA. .505" **BRINELL RESULTS**

TENSILE TESTS TAKEN FROM QTC N2339 02 8 X 8 X 9 OBTAINED FROM F1226 02

Piece #	Test Loc	Yield Strength .2% offset	Tensile Strength	Elong in 2"	R A %	BRINELL
02	LONG	✓ 88,746	✓ 105,706	✓ 22	✓ 71	BHN ON PC 235-237-237-231
						BHN ON TENSILE 217
						BHN ON QTC 221-222

IMPACT RESULTS: TEST SIZE: 10mm x 10mm

Piece#	Test Loc	Test Temp	Ft lbs.	%Shear	Lateral Expansion
02	LONG	✓ -75 F	72 39 26	30 10 10	.053 .027 .020

MELT METHOD: ELECTRIC FURNACE VACUUM DEGASSED LADLE REFINED,CALCUIM TREATED MELTED TO FINE GRAIN PRACTICE
HEAT TREATED IN FURNACES CERTIFIED TO MIL-H-6875 F
HEAT TREATMENT OF PROD. PART.:LOAD 62101A HEAT TO 1750°F 8 HOURS MIN NORM. LOAD 62113A HEAT TO 1750°F 14 HOURS MIN WATER QUENCH, LOAD 62113BTEMPER 1215°F 7 HOURS
WATER QUENCH TEMP. WAS 72 °F AT START AND 95 °F AT END OF QUENCH
HEAT TREATMENT OF QTC N2339 02: LOAD 61530A HEAT TO 1750°F 5 HOURS MIN NORM.LOAD 61558A HEAT TO 1750°F 5 HRS MIN WATER QUENCH,LOAD 61558B TEMPER 1215°F 5 HOURS ✓
WATER QUENCH TEMP WAS 75°F AT START AND 86°F AT END OF QUENCH ✓
HEAT TREATMENT OF QTC N2340 02: LOAD61546A HEAT TO 1750°F 5 HOURS MIN NORM.LOAD 61578A HEAT TO 1750°F 5 HOURS MIN WATER QUENCH ,LOAD 61578BTEMPER 1215°F 5 HOURS
WATER QUENCH TEMP WAS 74°F AT START AND 88°F AT END OF QUENCH
NO WELDING PERFORMED ON MATERIAL FORGE REDUCTION: 5.1 TO 1
CAPABILITY OF FINISH PARTS PER MPT DWG NOTE 12(HEMPS 10.202-06 REV F & AMEND. E CODE VI W/SUPPL. 1 REV NC) AND LIQUID PENETRANT SPEC HEMPS 10.302-05 CODE V REV G,SONIC PER HEMPS 10.501 SUPL 6 REV NC AMEND A
CAPABLE OF MEETING LIQUID PENETRANT OF "RAM COMPARTMENT" BORES ONLY PER HEMPS 10.302 REV M(1/8" NAX FLAW) AT FINISH SIZE

HYDRIL COMPANY LP
Q.C. Receiving Inspection
Ht# - S/N M2216
P/N ME-3130900 Rev. C1
Vendor Ellwood City Forge
P.O.# 1105463 Qty 1
Date 10-12-06 MBN 229

Signed: Kathy Carsele
Certification Clerk

HTC 7

SCANNED OCT 13 2006

Ellwood City Forge
Ellwood City,PA

Block #3

Sold To:	Hydril Company LP 3300 N Sam Houston Pwky East Houston, TX 77032	**Date:** **P.O.#:** **Job #:**	10/19/06 1105464 F1227
Grade and Description:	F22 BODY PREFORM - R. MILL & BORE	**Specification:** **Drawing #:**	HEMPS 2.580-10 REV. B5 COND. X-85K, DWG & PO NOTES QP1000003-01 REV. B5 BOM ME-3130900 REV C1 ME-3130900 REV C1 PART NO ME-3130900 REV C1

Job #	Piece #	Heat/ Ingot #	Ingot Size	Ingot Weight	Product Size	Shipped Weight
F1227	01	R3663-1			DRA 11686	

CHEMICAL ANALYSIS

Heat #	C ✓	Mn ✓	P ✓	S ✓	Si ✓	Ni ✓	Cr ✓	Mo ✓	Al ✓	V ✓	Cu ✓	Hppm	Ti ✓
R3663	.13	.56	.012	.007	.26	.08	2.30	1.00	.027	.009	.14	1.1	.0023

TENSILE TEST RESULTS: TENSILE TEST DIA. .505" **BRINELL RESULTS**

TENSILE TESTS TAKEN FROM QTC N2341 01 8 X 8 X 9 OBTAINED FROM F1227 01

Piece #	Test Loc	Yield Strength .2% offset	Tensile Strength	Elong in 2"	R A %	BRINELL
01	LONG	✓ 85,000	✓ 101.61	✓ 24	✓ 73	BHN ON PC 217-218-222-225
						BHN ON TENSILE 217
						BHN ON QTC 217-218

IMPACT RESULTS: TEST SIZE: 10mm x 10mm

Piece#	Test Loc	Test Temp	Ft lbs.	%Shear	Lateral Expansion
01	TRANS	✓ -75 F	79 91 54	40 50 10	.056 .061 .037

MELT METHOD: ELECTRIC FURNACE VACUUM DEGASSED LADLE REFINED,CALCUIM TREATED MELTED TO FINE GRAIN PRACTICE
HEAT TREATED IN FURNACES CERTIFIED TO MIL-H-6875 F
HEAT TREATMENT OF PROD. PART.:LOAD 62223A HEAT TO 1750°F 10 HRS MIN NORM. LOAD 62251A HEAT TO 1750°F 10 HRS MIN WATER QUENCH, LOAD 62251B TEMPER 1215°F 7 HOURS
WATER QUENCH TEMP. WAS 63°F AT START AND 88°F AT END OF QUENCH
HEAT TREATMENT OF QTC N2341 01 LOAD 61901A HEAT TO 1750°F 5 HRS MIN NORM.LOAD 62059A HEAT TO 1750°F 5 HRS MIN WATER QUENCH,LOAD 62059B TEMPER 1215°F 5 HRS
WATER QUENCH TEMP WAS 65°F AT START AND 76°F AT END OF QUENCH
HEAT TREATMENT OF QTC N2342 01 LOAD 61890A HEAT TO 1750°F 5 HRS MIN NORM.LOAD 61917A HEAT TO 1750°F 5 HRS MIN WATER QUENCH ,LOAD 61917BTEMPER 1215°F 5 HRS
WATER QUENCH TEMP WAS 63°F AT START AND 74°F AT END OF QUENCH
NO WELDING PERFORMED ON MATERIAL FORGE REDUCTION: 5.1 TO 1
CAPABILITY OF FINISH PARTS PER MPT DWG NOTE 12(HEMPS 10.202-06 REV F & AMEND. E CODE VI W/SUPPL. 1 REV NC) AND LIQUID PENETRANT SPEC HEMPS 10.302-05 CODE V REV G,SONIC PER HEMPS 10.501 SUPL 6 REV NC AMEND A
CAPABLE OF MEETING LIQUID PENETRANT OF "RAM COMPARTMENT" BORES ONLY PER HEMPS 10.302 REV M(1/8" NAX FLAW) AT FINISH SIZE

HYDRIL COMPANY LP
Q.C. Receiving Inspection
Ht# S/N M 2281
P/N ME-3130900 Rev.C1
Vendor Ellwood City Forge
P.O.# 1105464 Qty 1
Date 10-27-06 MBN 223

HTC 7

Signed: Kathy Carsile
Certification Clerk

SCANNED OCT 2 6 2006

Annex B. Reference Drawings

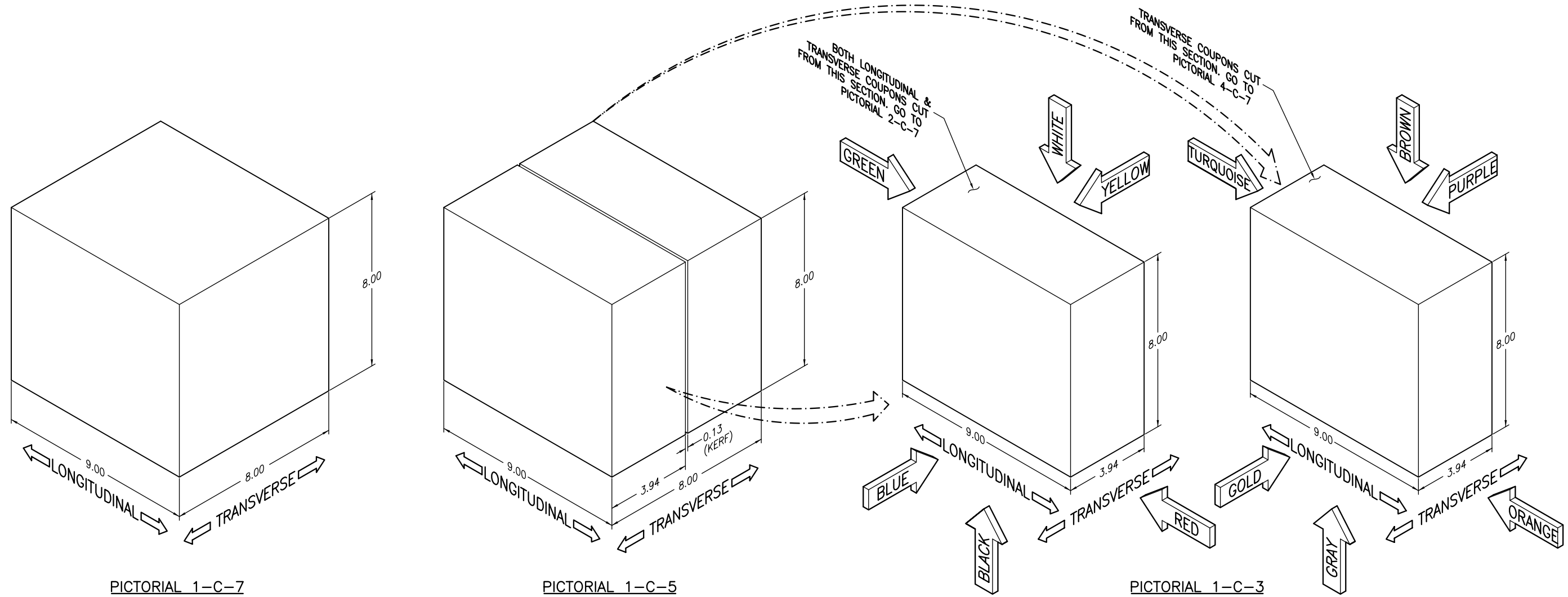

PICTORIAL 1-C-7

STEP ONE (1)

PICTORIAL 1-C-5

STEP TWO (2)

PICTORIAL 1-C-3

STEP THREE (3)

1

NOTES

1. **IT IS VERY IMPORTANT FOR THE FABRICATOR TO PAINT AFTER EACH STEP AS DEPICTED IN PICTORIALS.** THE COLORS HELP MAINTAIN ORIENTATION OF COUPONS (LIKE NORTH, SOUTH, EAST AND WEST). COLORS WILL BE REPAINTED ON SURFACES TO MAINTAIN ORIENTATION OF COUPON UNTIL STAMPED. FABRICATOR MAY PAINT ENTIRE SURFACE OR USE PAINT DABS.

2. STAMP OR ETCH COUPON AS SHOWN. EXPLANATION OF MARKINGS:

EXAMPLE: 1-06-T-02

- 1-06 — ITEM FROM CHART (ON SHEET 6)
- T — TRANSVERSE OR LONGITUDINAL
- 02 — NUMBER OF COUPON

1: BASE MATERIAL, BLOCK 1
2: BASE MATERIAL, BLOCK 2
3: BASE MATERIAL, BLOCK 3

IN THIS EXAMPLE, THE COUPON WOULD FROM BASE MATERIAL BLOCK 1, IS ITEM 6 FROM THE CHART ON SHEET 6, (WHICH MAKES IT 1.13 x 2.75 x 2.75 LG.) IT IS A TRANSVERSE SAMPLE AND IS THE 2 COUPON OF 5.

3. THE LAST DIGIT OF THE STAMPINGS IS THE NUMBER OF COUPON. FOR EXAMPLE ON THE CHART ON SHEET 2, ITEM 6, REQUIRES 5 TRANSVERSE COUPONS. IN THE CASE OF THESE TRANSVERSE COUPONS, MADE FROM BASE MATERIAL, BLOCK 1, THEIR MARKINGS WOULD BE AS SUCH:

1-06-T-01
1-06-T-02
1-06-T-03
1-06-T-04
1-06-T-05

4. QUANTITIES IN CHART ON SHT. 6, REFLECT TESTING FOR ONE (1) SPECIMEN.
THERE ARE THREE SPECIMENS TO BE TESTED.

EACH TO HAVE DIFFERENT HEAT TREAT AS FOLLOWS:
BASE MATERIAL BLOCK 1 : M2420
BASE MATERIAL BLOCK 2 : M2216
BASE MATERIAL BLOCK 3 : M2281

1 5. IT IS SUGGESTED THAT THE FABRICATOR MAKE A TRIAL CUT ON AN ALUMINUM OR WOODEN SAMPLE, PRIOR TO CUTTING THE ACTUAL COUPON.

REV.	DESCRIPTION	DATE	BY	CHK BY
1	SHT. 1 ADDED NOTE 5, MODIFIED SHT. 3	03/05/07		
0	ISSUED FOR MANUFACTURE	02/23/07		

MOHR

TOLERANCES UNLESS OTHERWISE SPECIFIED:
0.X = ±0.030
0.XX = ±0.015
0.XXX = ±0.005
FRACTIONS = ±1/16
ANGLES = ±1/2°
BREAK CORNERS = 0.03 x 45° MAX.
INTERNAL RADII = R0.03 MAX.
CONCENTRICITY = 0.005
SURFACE FINISH = XXX
DIMENSIONS ARE IN INCHES

DESCRIPTION
MMS MATERIAL TESTING
ASTM A 182 GR. F22M
(2 1/4 Cr-1 Mo)
COUPON BLANK

MATERIAL/STRENGTH
85 ksi MSYS

THIS DRAWING IS THE PROPERTY OF MOHR ENGINEERING DIVISION. IT MAY NOT BE USED WITH THE EXPRESS WRITTEN PERMISSION FROM MOHR.

DRAWN BY JHP	DATE 01/24/07	SCALE 2:1
CHECKED BY JCS	DATE 01/25/07	REV 1
APPROVED BY KY	DATE 02/02/07	

DWG. NO. KY172883-01 SHT. 1 OF 6

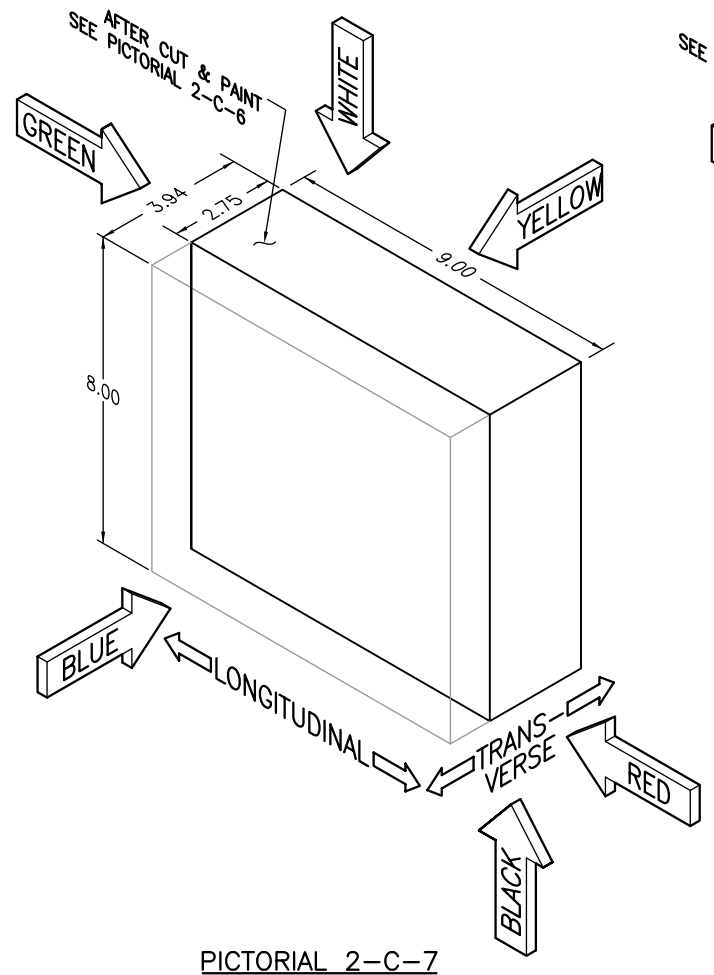

PICTORIAL 2-C-7

STEP FOUR (4)
REF. 1-D-4

1

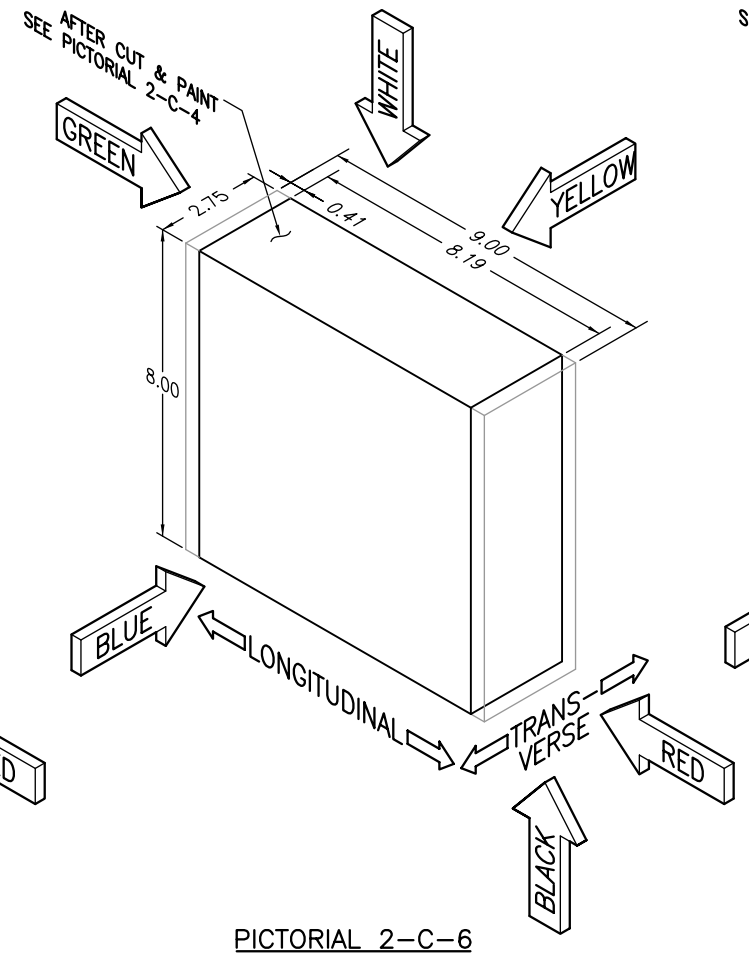

PICTORIAL 2-C-6

STEP FIVE (5)
REF. 2-D-8

1

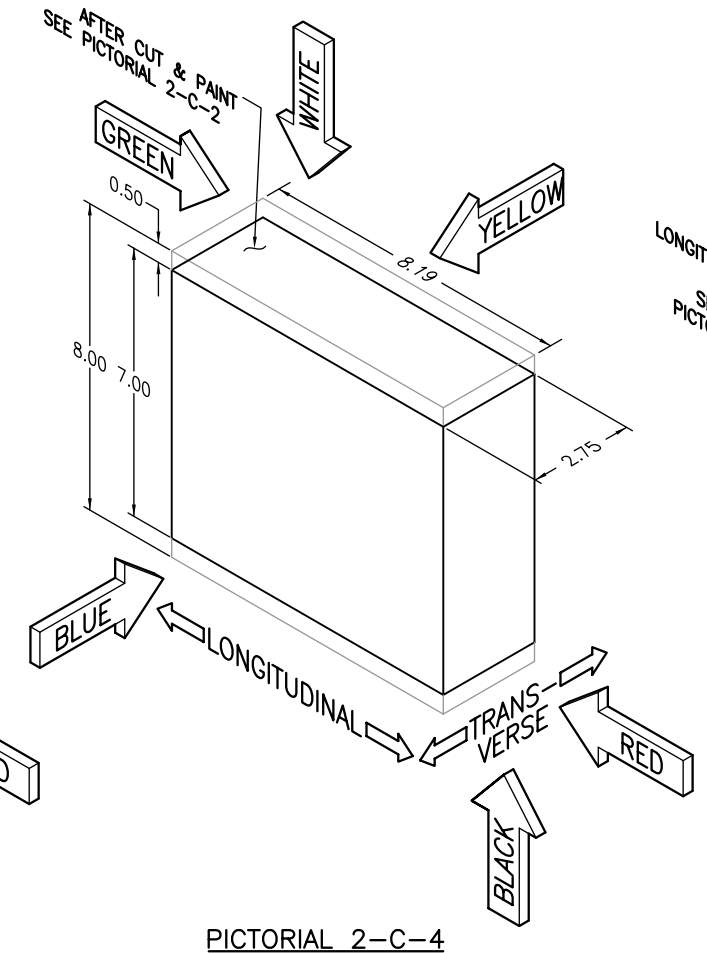

PICTORIAL 2-C-4

STEP SIX (6)
REF. 2-D-6

1

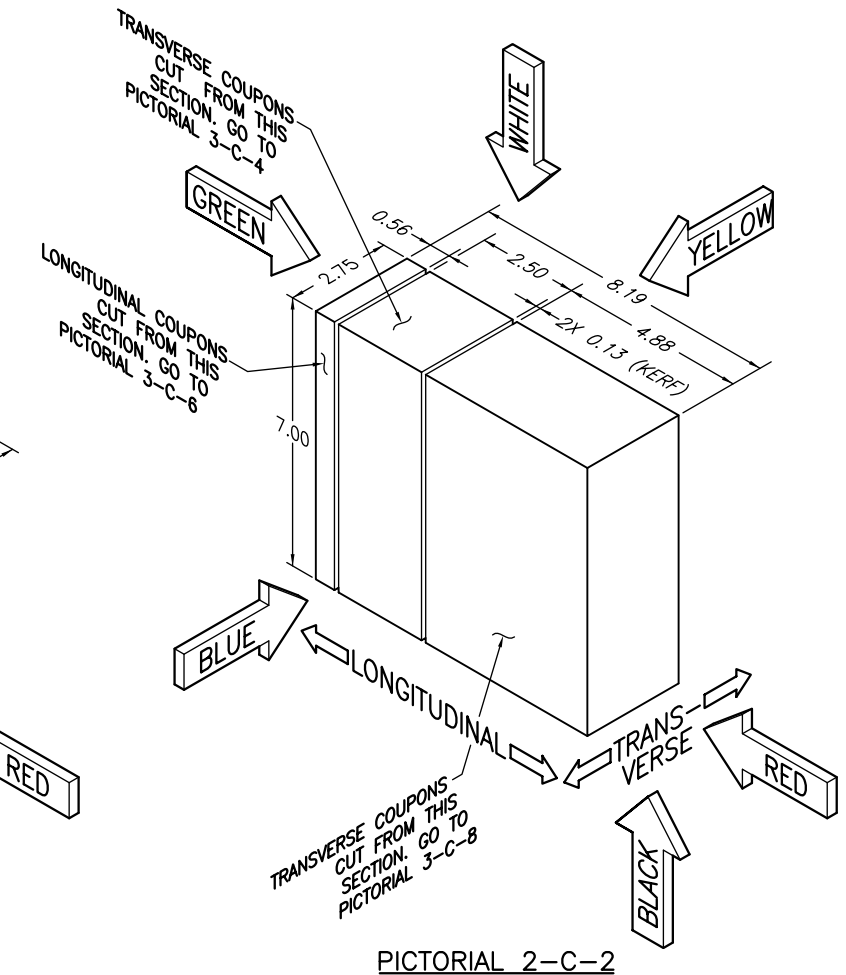

PICTORIAL 2-C-2

STEP STEP SEVEN (7)
REF. 2-D-4

1

REV.	DESCRIPTION	DATE	BY	CHK BY
1	MOD. SHT. 1 & 3	03/05/07		
0	ISSUED FOR MANUFACTURE	02/23/07		

MOHR

TOLERANCES
UNLESS OTHERWISE SPECIFIED:

0.X = ±0.030
0.XX = ±0.015
0.XXX = ±0.005
FRACTIONS = ±1/16
ANGLES = ±1/2°
BREAK CORNERS = 0.03 x 45° MAX.
INTERNAL RADII = R0.03 MAX.
CONCENTRICITY = 0.005
SURFACE FINISH = XXX
DIMENSIONS ARE IN INCHES

DESCRIPTION

MMS MATERIAL TESTING
ASTM A 182 GR. F22M
(2 1/4 Cr-1 Mo)
COUPON BLANK

MATERIAL/STRENGTH
85 ksi MSYS

THIS DRAWING IS THE PROPERTY OF MOHR ENGINEERING DIVISION. IT MAY NOT BE USED WITH THE EXPRESS WRITTEN PERMISSION FROM MOHR.

DRAWN BY	DATE	SCALE
JHP	01/24/07	2:1
CHECKED BY	DATE	REV
JCS	01/25/07	1
APPROVED BY	DATE	
KY	02/02/07	

DWG. NO.
KY172883-01 SHT. 2 OF 6

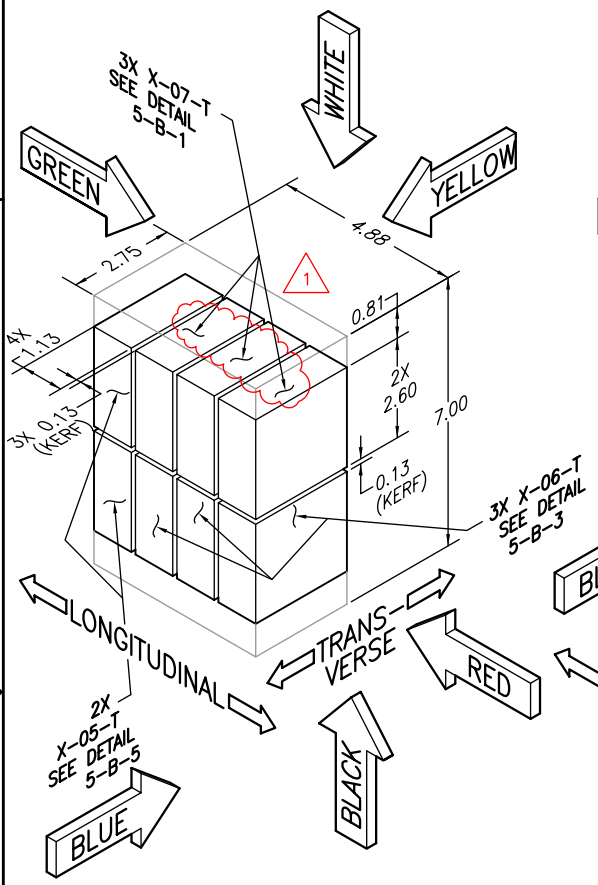

PICTORIAL 3-C-8

STEP EIGHT (8)
REF. 2-B-2

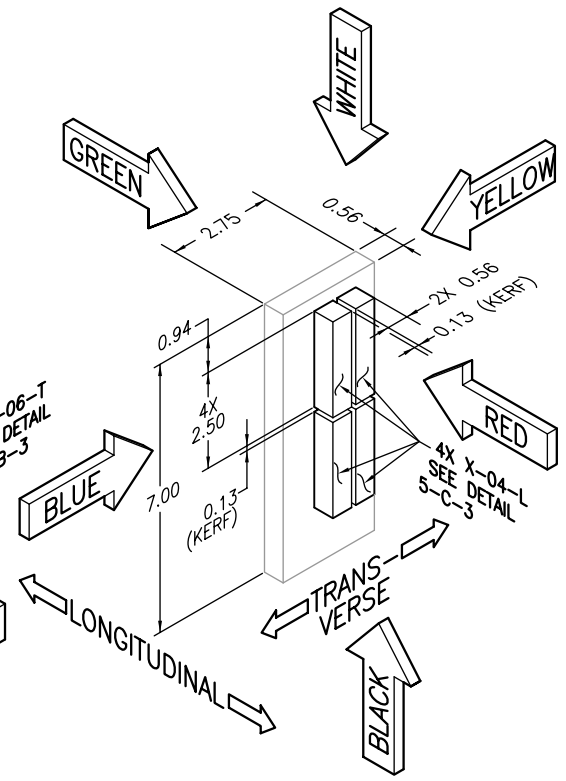

PICTORIAL 3-C-6

STEP NINE (9)
REF. 2-C-3

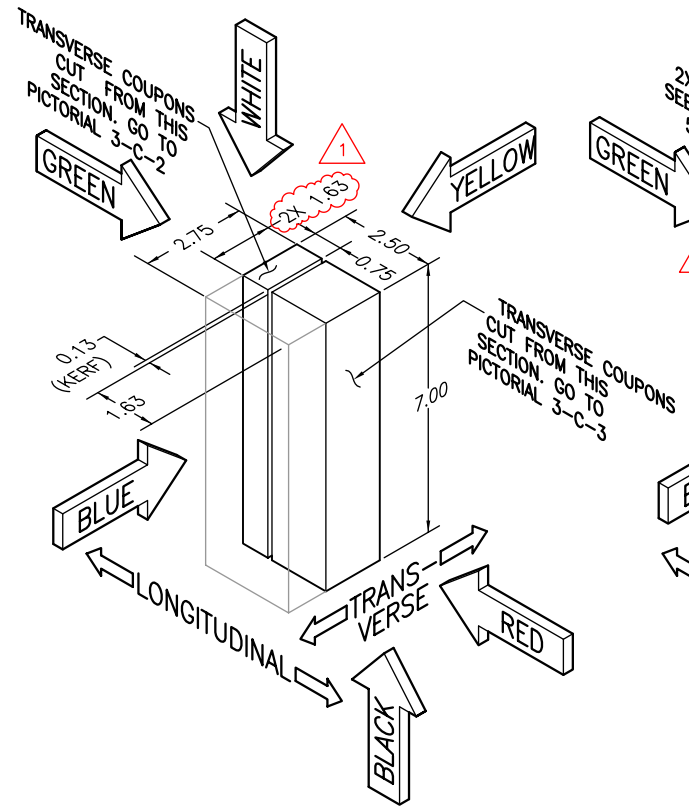

PICTORIAL 3-C-4

STEP TEN (10)
REF. 2-D-3

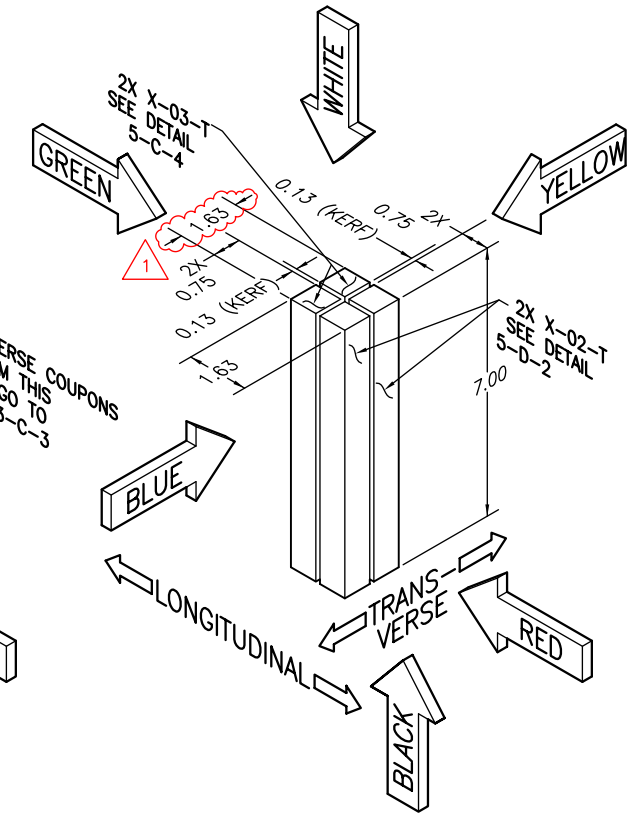

PICTORIAL 3-C-3

STEP ELEVEN (11)
REF. 3-C-4

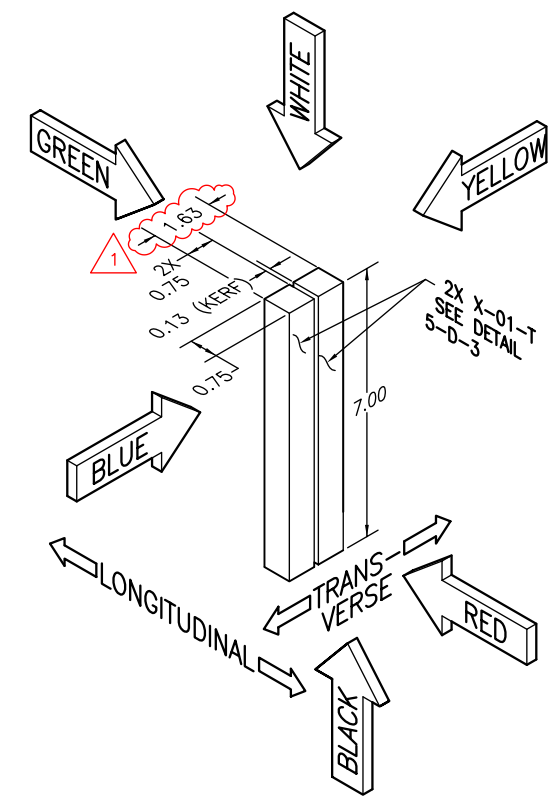

PICTORIAL 3-C-2

STEP TWELVE (12)
REF. 3-D-5

REV.	DESCRIPTION	DATE	BY	CHK BY
1	WAS 0.56 IS 1.63, WAS 2.75 IS 1.63, MOD.	03/05/07		
	PICTORIAL 3-C-8			
0	ISSUED FOR MANUFACTURE	02/23/07		

MOHR

TOLERANCES
UNLESS OTHERWISE SPECIFIED:

0.X = ±0.030
0.XX = ±0.015
0.XXX = ±0.005
FRACTIONS = ±1/16
ANGLES = ±1/2°
BREAK CORNERS = 0.03 x 45° MAX.
INTERNAL RADII = R0.03 MAX.
CONCENTRICITY = 0.005
SURFACE FINISH = XXX
DIMENSIONS ARE IN INCHES

DESCRIPTION

MMS MATERIAL TESTING
ASTM A 182 GR. F22M
(2 1/4 Cr-1 Mo)
COUPON BLANK

MATERIAL/STRENGTH
85 ksi MSYS

THIS DRAWING IS THE PROPERTY OF
MOHR ENGINEERING DIVISION.
IT MAY NOT BE USED WITH THE EXPRESS
WRITTEN PERMISSION FROM MOHR.

DRAWN BY	DATE	SCALE
JHP	01/24/07	2:1
CHECKED BY JCS	DATE 01/25/07	REV 1
APPROVED BY KY	DATE 02/02/07	

DWG. NO.
KY172883-01 SHT. 3 OF 6

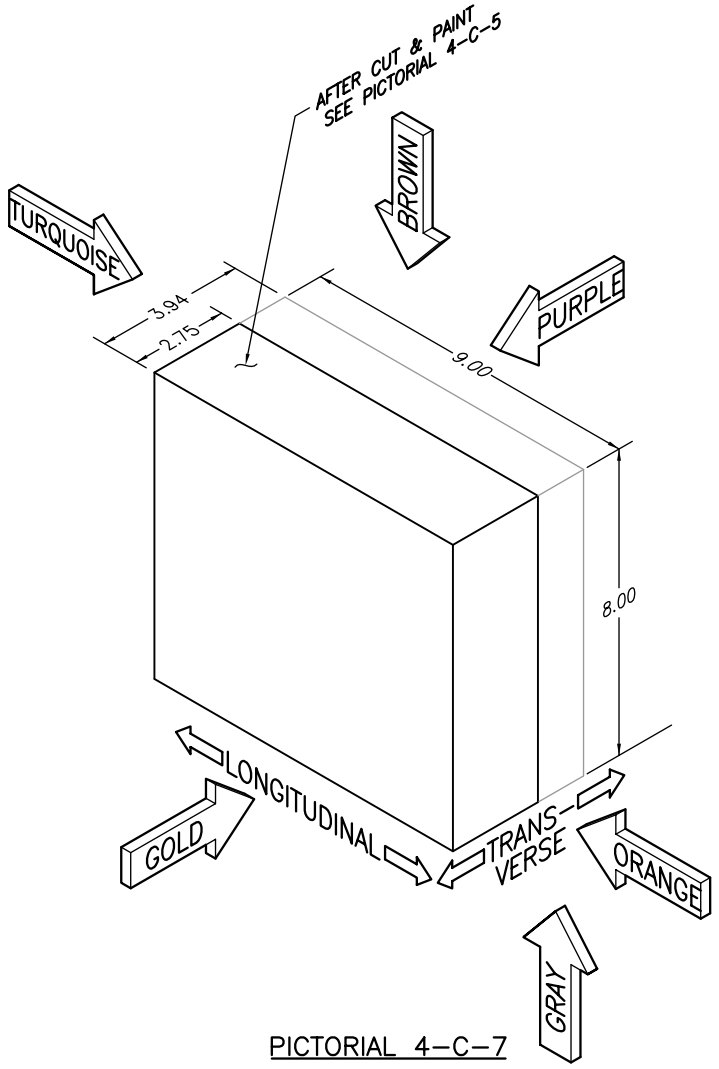

PICTORIAL 4-C-7

STEP THIRTEEN (13)
REF. 1-D-2

1

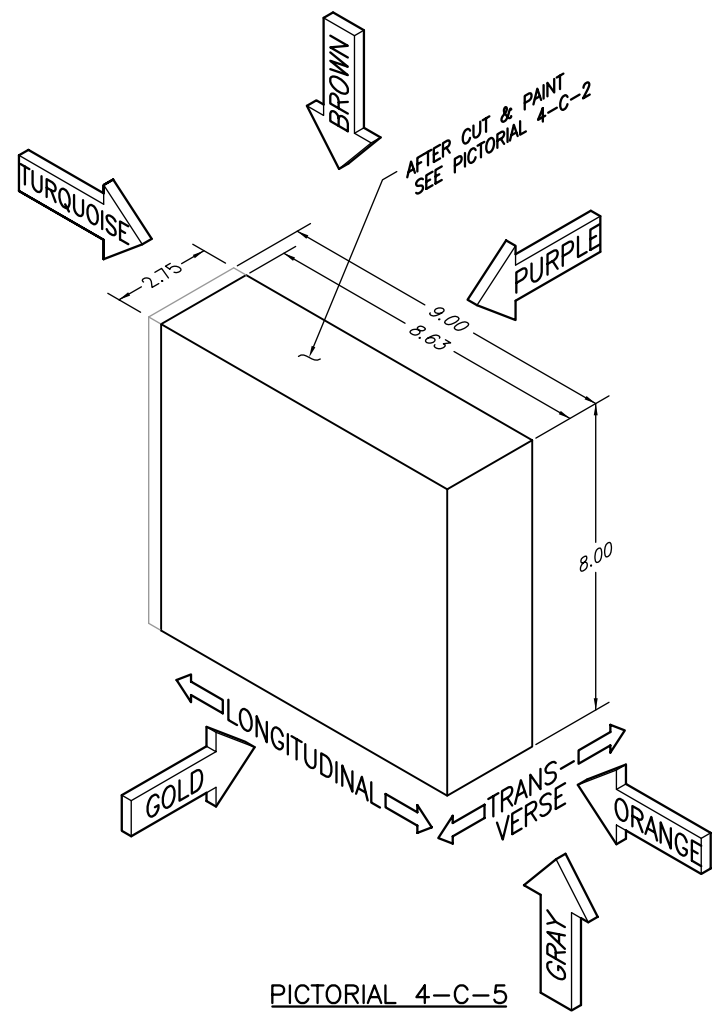

PICTORIAL 4-C-5

STEP FOURTEEN (14)
REF. 4-D-7

1

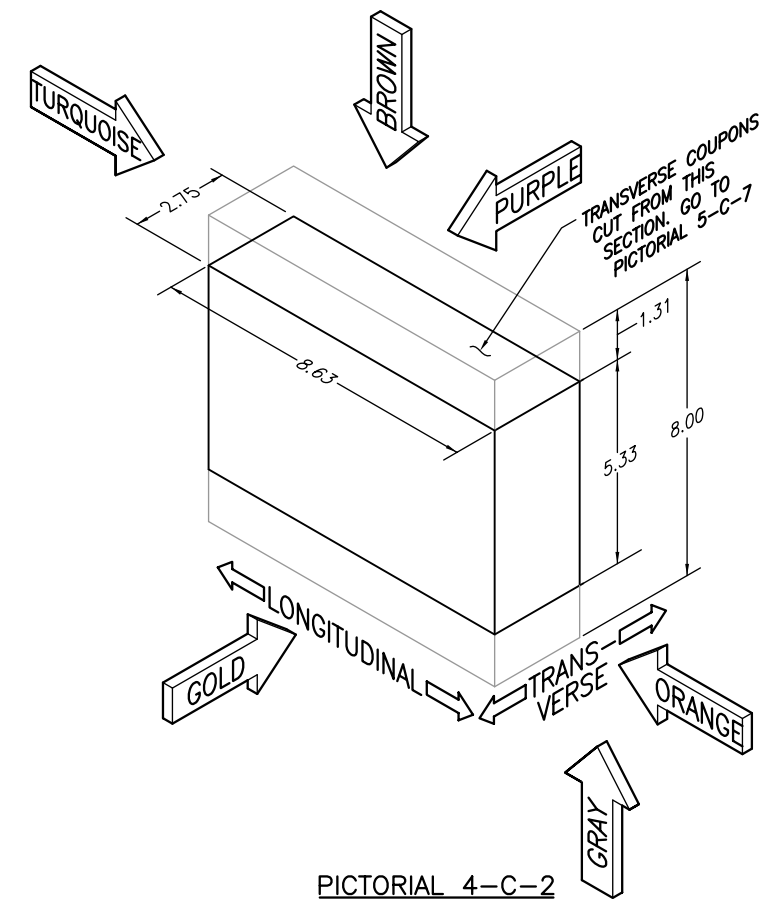

PICTORIAL 4-C-2

STEP FIFTEEN (15)
REF. 4-D-5

1

REV.	DESCRIPTION	DATE	BY	CHK BY
1	MOD. SHT. 1 & 3	03/05/07		
0	ISSUED FOR MANUFACTURE	02/23/07		

MOHR

TOLERANCES
UNLESS OTHERWISE SPECIFIED:

0.X = ±0.030
0.XX = ±0.015
0.XXX = ±0.005
FRACTIONS = ±1/16
ANGLES = ±1/2°
BREAK CORNERS = 0.03 x 45° MAX.
INTERNAL RADII = R0.03 MAX.
CONCENTRICITY = 0.005
SURFACE FINISH = XXX
DIMENSIONS ARE IN INCHES

DESCRIPTION

MMS MATERIAL TESTING
ASTM A 182 GR. F22M
(2 1/4 Cr-1 Mo)
COUPON BLANK

MATERIAL/STRENGTH
85 ksi MSYS

THIS DRAWING IS THE PROPERTY OF
MOHR ENGINEERING DIVISION.
IT MAY NOT BE USED WITH THE EXPRESS
WRITTEN PERMISSION FROM MOHR.

DRAWN BY	DATE	SCALE
JHP	01/24/07	2:1
CHECKED BY	DATE	REV
JCS	01/25/07	1
APPROVED BY	DATE	
KY	02/02/07	

DWG. NO.
KY172883-01 SHT. 4 OF 6

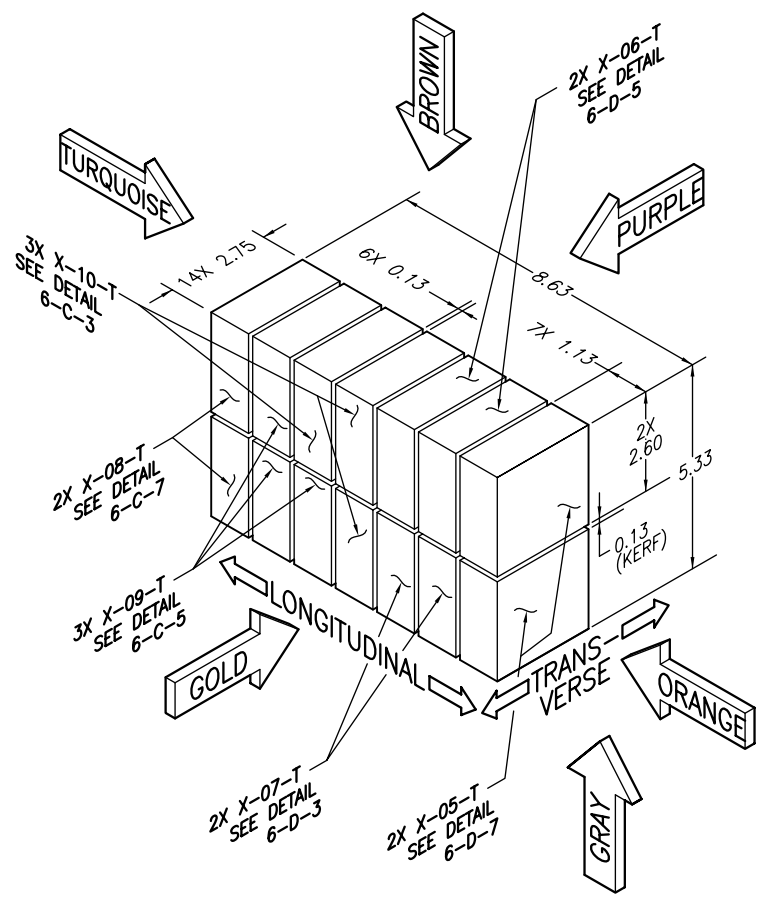

PICTORIAL 5-C-7

STEP SIXTEEN (16)
REF. 4-C-2

1

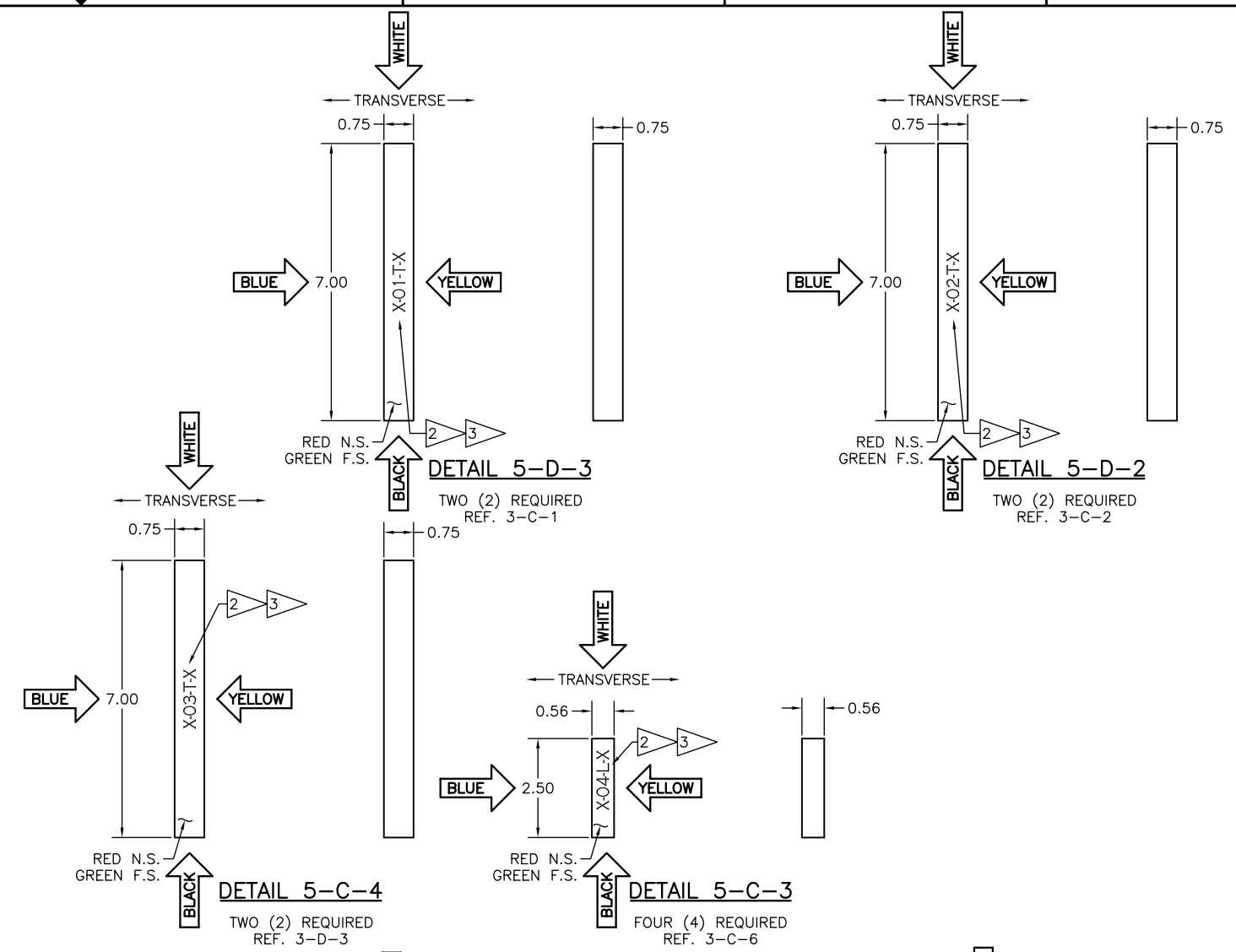

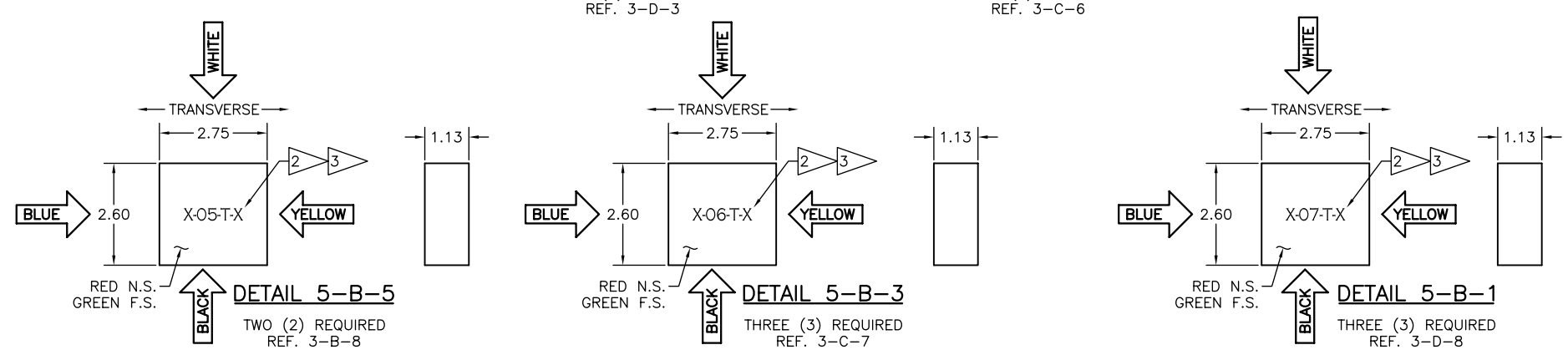

REV.	DESCRIPTION	DATE	BY	CHK BY
1	MOD. SHT. 1 & 3	03/05/07		
0	ISSUED FOR MANUFACTURE	02/23/07		

MOHR

TOLERANCES
UNLESS OTHERWISE SPECIFIED:

0.X = ±0.030
0.XX = ±0.015
0.XXX = ±0.005
FRACTIONS = ±1/16
ANGLES = ±1/2°
BREAK CORNERS = 0.03 x 45° MAX.
INTERNAL RADII = R0.03 MAX.
CONCENTRICITY = 0.005
SURFACE FINISH = XXX
DIMENSIONS ARE IN INCHES

DESCRIPTION

MMS MATERIAL TESTING
ASTM A 182 GR. F22M
(2 1/4 Cr-1 Mo)
COUPON BLANK

MATERIAL/STRENGTH
85 ksi MSYS

THIS DRAWING IS THE PROPERTY OF MOHR ENGINEERING DIVISION. IT MAY NOT BE USED WITH THE EXPRESS WRITTEN PERMISSION FROM MOHR.

DRAWN BY	DATE	SCALE
JHP	01/24/07	2:1
CHECKED BY JCS	DATE 01/25/07	REV 1
APPROVED BY KY	DATE 02/02/07	

DWG. NO. KY172883-01 SHT. 5 OF 6

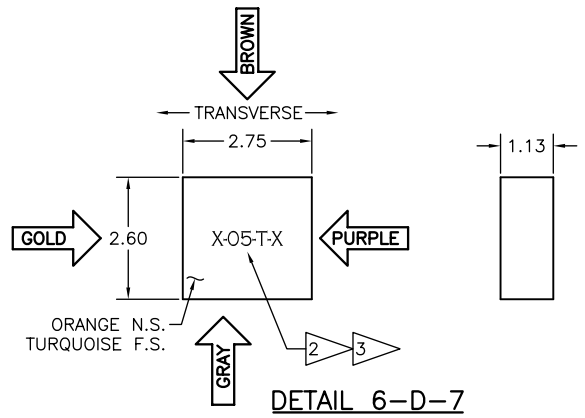

DETAIL 6–D–7

TWO (2) REQUIRED
REF. 5–B–7

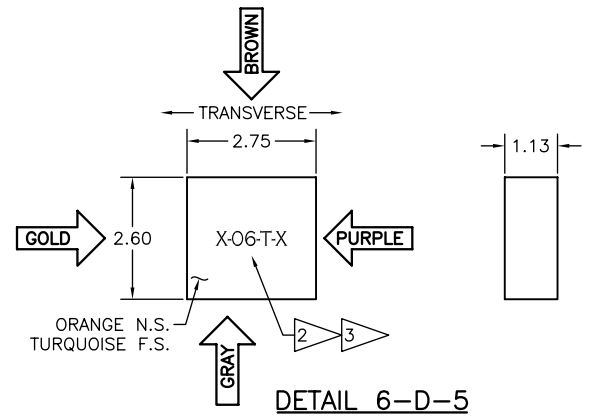

DETAIL 6–D–5

TWO (2) REQUIRED
REF. 5–D–7

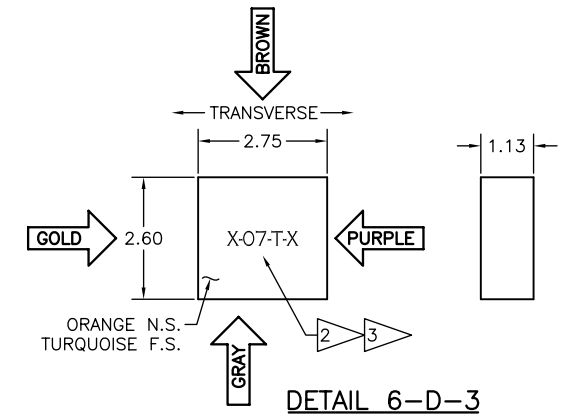

DETAIL 6–D–3

TWO (2) REQUIRED
REF. 5–B–8

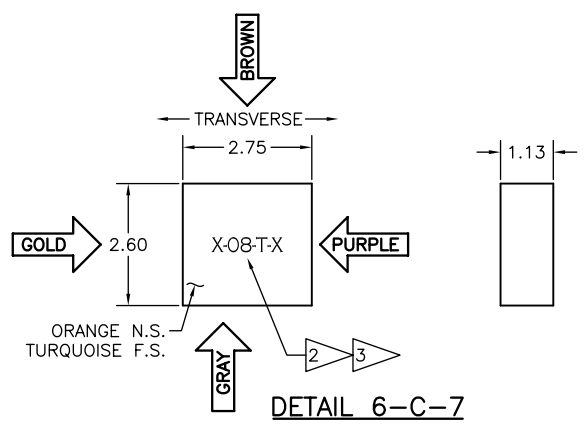

DETAIL 6–C–7

TWO (2) REQUIRED
REF. 5–C–8

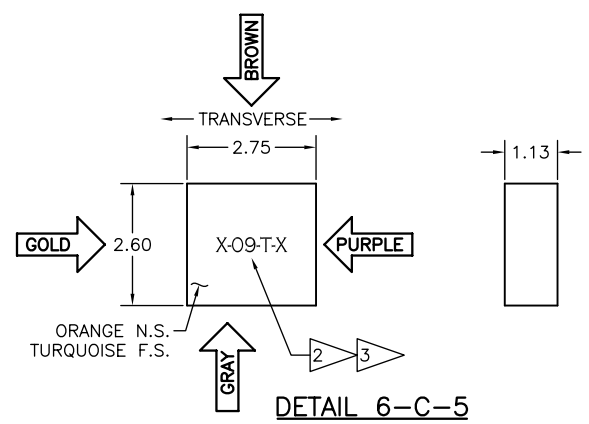

DETAIL 6–C–5

THREE (3) REQUIRED
REF. 5–B–8

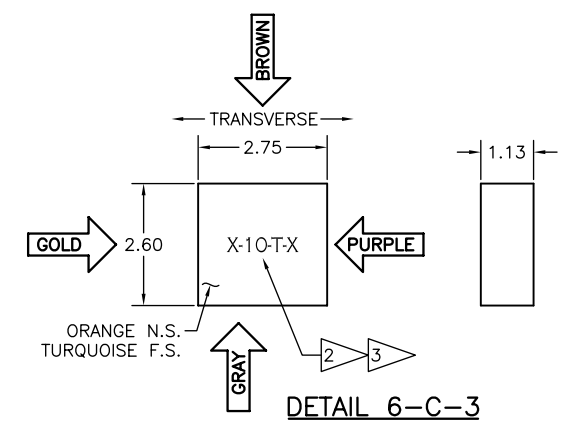

DETAIL 6–C–3

THREE (3) REQUIRED
REF. 5–C–8

MMS MATERIAL TESTING PROGRAM 4

		ITEM: 01–T	ITEM: 02–T	ITEM: 03–T	ITEM: 04–L	ITEM: 05–T	ITEM: 06–T	ITEM: 07–T	ITEM: 08–T	ITEM: 09–T	ITEM: 10–T
	TEST	TENSILE	TENSILE AT TEMPERATURE	TENSILE AT TEMPERATURE	TOUGHNESS CHARPY	TOUGHNESS C/T	TOUGHNESS C/T	TOUGHNESS C/T	CRACK GROWTH RATE C/T	CRACK GROWTH RATE C/T	CRACK GROWTH RATE C/T
	STANDARD	ASTM A 370	ASTM E 21	ASTM E 21	ASTM E 23	ASTM E 1820	ASTM E 1820	ASTM E 1820	ASTM E 647	ASTM E 647	ASTM E 647
	ENVIR FLUID	AIR	AIR	AIR	AIR	AIR	MILD SOUR	AGGRESSIVE SOUR	AIR	MILD SOUR	AGGRESSIVE SOUR
	ENVIR TEMP – F°	73	200	350	–20	–20	–20	–20	73	73	73
FINISH SPECIMEN	W	0.63	0.63	0.63	0.394	2.40	2.40	2.40	2.40	2.40	2.40
	H	0.63	0.63	0.63	0.394	2.50	2.50	2.50	2.50	2.50	2.50
	L	6.00	6.00	6.00	2.165	1.00	1.00	1.00	1.00	1.00	1.00
COUPON BLANK	W	0.75	0.75	0.75	0.56	2.60	2.60	2.60	2.60	2.60	2.60
	H	0.75	0.75	0.75	0.56	2.75	2.75	2.75	2.75	2.75	2.75
	L	7.00	7.00	7.00	2.50	1.13	1.13	1.13	1.13	1.13	1.13
	DETAIL	5–D–3	5–D–2	5–C–3	5–C–2	5–B–5 & 6–D–7	5–B–3 & 6–D–5	5–B–1 & 6–D–3	6–C–7	6–C–5	6–C–3
QUANTITY PER BLOCK											
		2	2	2	4	4	5	5	2	3	3

MOHR

TOLERANCES
UNLESS OTHERWISE SPECIFIED:

0.X = ±0.030
0.XX = ±0.015
0.XXX = ±0.005
FRACTIONS = ±1/16
ANGLES = ±1/2°
BREAK CORNERS = 0.03 x 45° MAX.
INTERNAL RADII = R0.03 MAX.
CONCENTRICITY = 0.005
SURFACE FINISH = XXX
DIMENSIONS ARE IN INCHES

REV.	DESCRIPTION	DATE	BY	CHK BY
1	MOD. SHT. 1 & 3	03/05/07		
0	ISSUED FOR MANUFACTURE	02/23/07		

DESCRIPTION
MMS MATERIAL TESTING
ASTM A 182 GR. F22M
(2 1/4 Cr–1 Mo)
COUPON BLANK

THIS DRAWING IS THE PROPERTY OF MOHR ENGINEERING DIVISION. IT MAY NOT BE USED WITH THE EXPRESS WRITTEN PERMISSION FROM MOHR.

DRAWN BY	DATE	SCALE
JHP	01/24/07	2:1
CHECKED BY JCS	DATE 01/25/07	REV 1
APPROVED BY KY	DATE 02/02/07	

MATERIAL/STRENGTH
85 ksi MSYS

DWG. NO.
KY172883–01 SHT. 6 OF 6

Annex C. Test Procedures

Annex C.1 Tension Test

1. Tension test specimens are ASTM A 182 Grade F22M material (85 ksi) extracted from an 8 x 8 x 9-inch forged block. Test blanks are 0.75 x 0.75 x 7.00-inch sawed blanks extracted from the forged test blocks per Mohr drawing KY172883-01. All test blanks are within ¼T of the forged block and have an orientation in the transverse direction (based on 9.0 inch being the longitudinal dimension).
2. Traceability of the test specimens shall be retained throughout testing and reporting. The traceability identification information of the test specimens is per the table below:

Test Temperature	Specimen Identification
75°F	1-01-T-1
	1-01-T-2
	2-01-T-1
	2-01-T-2
	3-01-T-1
	3-01-T-2
200°F	1-02-T-1
	1-02-T-2
	2-02-T-1
	2-02-T-2
	3-02-T-1
	3-02-T-2
350°F	1-03-T-1
	1-03-T-2
	2-03-T-1
	2-03-T-2
	3-03-T-1
	3-03-T-2

3. The test lab shall machine the blanks as standard 0.500-inch round tension specimens per ASTM E 8. The gage length shall be 2.00 inch minimum for room temperature samples and 3.00 inch minimum for elevated temperature samples.
4. A Brinell hardness test shall be performed in accordance with ASTM E 10 on each test specimen prior to tension testing.

5. Tension testing at room temperature shall be in accordance with ASTM E 8. Reporting shall be in accordance with ASTM E 8.
6. Tension testing at elevated temperature shall be in accordance with ASTM E 21. Reporting shall be in accordance with ASTM E 21.
7. Load/deflection data shall be recorded electronically and supplied in a format compatible with Microsoft Excel.
8. All data noted in the reporting section of the ASTM standards shall be reported for each specimen.

Annex C.2 Charpy V-Notch Tests

1. Charpy test specimens shall be ASTM A 182 Grade F22M material (85 ksi) extracted from an 8 x 8 x 9-inch forged block. Test blanks are 0.56 x 0.56 x 2.50 inch sawed blanks extracted from the forged test blocks per Mohr drawing KY172883-01. All samples are within ¼T of the forged block and have a crack plane orientation in the transverse direction (based on the 9.0 inch direction being the longitudinal direction) as defined by ASTM E 1823.
2. Traceability of the test specimens shall be retained throughout testing and reporting.
3. All Charpy samples shall be notched on the "BLUE" side. Specimens should have a transverse orientation and notched as shown by the "S-T" designation in Figure A2.3 of ASTM E 1823.
4. Impact testing shall be in accordance with ASTM E 23 at -75°F, -50°F, -20°F, 10°F, 40°F, and 75°F test temperature.

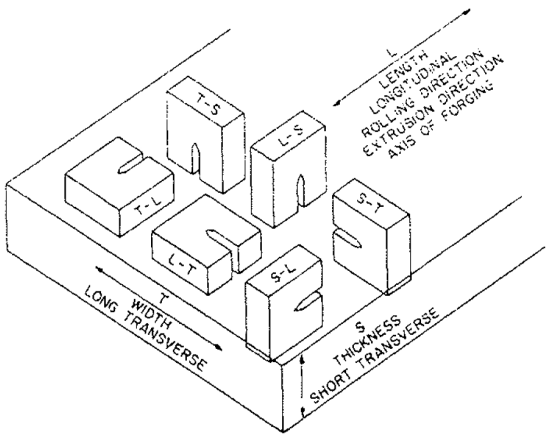

FIG. A2.3 Crack Plane Orientation Code for Rectangular Sections

Annex C.3 Fracture Toughness

1. Fracture toughness test specimens shall be ASTM A 182 Grade F22M material (85 ksi) extracted from an 8 x 8 x 9-inch forged block. The test blanks are 2.60 x 2.75 x 1.13-inch sawed blanks extracted from the forged test blocks per Mohr drawing KY172883-01. All specimens shall be within ¼T of the forged block and have a crack plane orientation in the transverse direction (based on the 9.0 inch direction being the longitudinal direction) as defined by ASTM E 1823.
2. Traceability of the test specimens shall be retained throughout testing and reporting. (See table on next page.)
3. All test blanks shall be machined as standard compact tension test specimens with a 1.00-inch base dimension per ASTM E 1820 and notched on the "gold" side (opposite the "purple" side) or "yellow side" (opposite the "blue" side). Specimens should have a transverse orientation and notched as shown by the "S-T" designation in Figure A2.3 of ASTM E 1823.

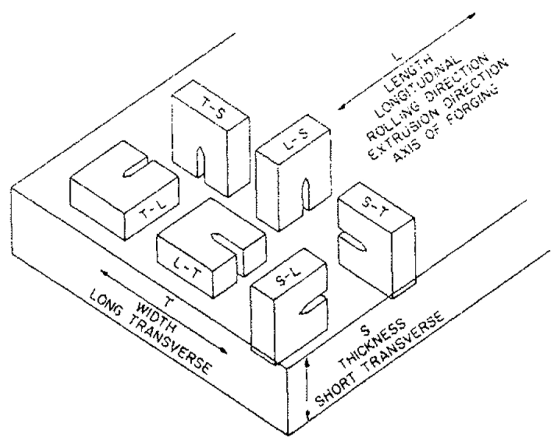

FIG. A2.3 Crack Plane Orientation Code for Rectangular Sections

4. Plane strain fracture toughness shall be determined by testing in accordance with ASTM E 1820 using the resistance curve (R-curve) procedure and the following parameters:
    a. The objective is to obtain values for K_{IC}, J_{IC}, and CTOD (δ_{IC}).
    b. Test temperature for all samples shall be 75°F.
    c. The test environment shall be
        i. Air
        ii. Seawater as defined in ASTM D 1141 with cathodic protection at -1100 mV
        iii. A mild H_2S solution, defined as a gas mixture of 7% H_2S and the balance nitrogen. A buffered solution chemistry of 5.00% by weight sodium chloride and 0.40% by weight sodium acetate in deionized water. The test solution pH before H2S saturation shall be adjusted to 4.0 using hydrochloric acid.
    d. Environmental specimens shall be charged in the environment for one week prior to testing. Testing shall occur immediately after the soak period.
    e. Specimens shall be loaded to 90% of the pre-crack load at a rate of 150 N/sec (33.7 lb/sec). Above this load, a slow strain rate of 0.008 mm/min (3.1 x 10^{-4} in/min) shall be

used. Incremental unloading and reloading to the previous level can be at a higher load rate of 150 N/sec.

5. Reporting shall be in accordance with ASTM E 1820.
6. All test specimens shall be returned to Mohr.

Serial Number	Drawing Blank Detail	Color of Notched Side	Color Opposite Notched Side	Test Environment
1-05-T-1	5-B-5	Yellow	Blue	Air
1-05-T-2	5-B-5	Yellow	Blue	Air
1-05-T-1	6-D-7	Gold	Purple	Seawater
1-05-T-2	6-D-7	Gold	Purple	Seawater
1-06-T-1	6-D-5	Gold	Purple	Mild H_2S
1-06-T-2	6-D-5	Gold	Purple	Mild H_2S
2-05-T-1	5-B-5	Yellow	Blue	Air
2-05-T-2	5-B-5	Yellow	Blue	Air
2-05-T-1	6-D-7	Gold	Purple	Seawater
2-05-T-2	6-D-7	Gold	Purple	Seawater
2-06-T-1	6-D-5	Gold	Purple	Mild H_2S
2-06-T-2	6-D-5	Gold	Purple	Mild H_2S
3-05-T-1	5-B-5	Yellow	Blue	Air
3-05-T-2	5-B-5	Yellow	Blue	Air
3-05-T-1	6-D-7	Gold	Purple	Seawater
3-05-T-2	6-D-7	Gold	Purple	Seawater
3-06-T-1	6-D-5	Gold	Purple	Mild H_2S
3-06-T-2	6-D-5	Gold	Purple	Mild H_2S

Annex C.4 Fatigue Crack Growth Rate

1. Fracture crack growth rate test specimens shall be ASTM A 182 Grade F22M material (85 ksi) extracted from an 8 x 8 x 9-inch forged block. The test blanks shall be 2.60 x 2.75 x 1.13-inch sawed blanks extracted from the forged test blocks per Mohr drawing KY172883-01. All samples shall be within ¼T of the forged block and have a crack plane orientation in the transverse direction (based on the 9.0 inch side being the longitudinal direction) as defined by ASTM E 1823.
2. Traceability of the test blanks shall be retained throughout testing and reporting.
3. All test blanks shall be machined as standard compact tension test specimens with a 0.25-inch base dimension per ASTM E 647 and notched on the "gold" side (opposite the "purple" side). Specimens shall have a transverse orientation and notched as shown by the "S-T" designation in Figure A2.3 of ASTM E 1823.

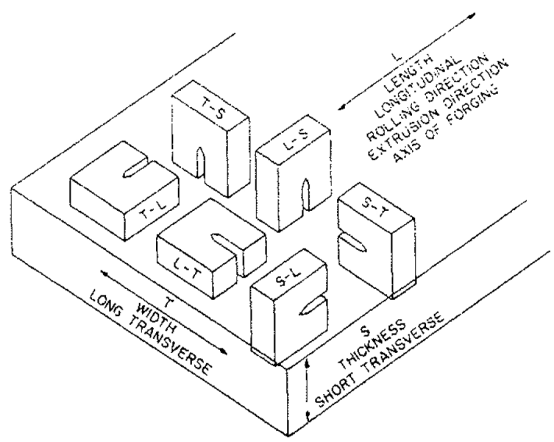

FIG. A2.3 Crack Plane Orientation Code for Rectangular Sections

4. The test environments for fatigue crack growth rate testing shall be:
   a. Lab air
   b. Simulated seawater per ASTM D 1141 with cathodic protection at -1100 mV
   c. A mild H_2S solution, defined as a gas mixture of 7% H_2S and the balance nitrogen. A buffered solution chemistry of 5.00% by weight sodium chloride and 0.40% by weight sodium acetate in deionized water. Test solution pH before H_2S saturation shall be adjusted to 4.0 using hydrochloric acid.
5. Fatigue crack growth rate, *da/dN*, shall be determined in accordance with ASTM E 6476 using the following parameters:
   a. Test temperature for all specimens shall be 75°F.
   b. Compression precracking shall be used for specimen preparation for the fatigue crack growth rate, FCGR, testing.
   c. The *K*-increasing procedure shall be used for all specimens.
   d. Load ratio, *R*, shall be held constant during testing of each specimen. The value of *R* shall be as specified in the table below for the specific test project.
   e. Test cycle frequency shall be 20 Hz in air, 1 Hz in seawater, and 1/3 Hz in H_2S environment.

f. All tests shall start with a low initial ΔK. Cycling shall continue at an increasing ΔK while maintaining a constant R ratio until crack growth rate becomes non-linear with respect to ΔK, or fracture occurs.

6. Reporting shall be in accordance with ASTM E 647.

7. All test specimens shall be returned to Mohr.

Serial Number	Drawing Detail (Reference)	Test Environment	R Ratio
1-08-T-1	6-C-7	Air	0.1
1-08-T-2	6-C-7	Air	0.5
2-08-T-1	6-C-7	Air	0.1
2-08-T-2	6-C-7	Air	0.5
3-08-T-1	6-C-7	Air	0.1
3-08-T-2	6-C-7	Air	0.5
1-09-T-1	6-C-5	Seawater	0.1
2-09-T-1	6-C-5	Seawater	0.1
3-09-T-1	6-C-5	Seawater	0.1
1-10-T-1	6-C-3	Mild H_2S	0.1
2-10-T-1	6-C-3	Mild H_2S	0.1
3-10-T-1	6-C-3	Mild H_2S	0.1

Annex D. Results from Tension Tests

Annex D.1. Lab Tension Test Data

Westmoreland Mechanical Testing & Research, Inc.
P.O. Box 388
Westmoreland Drive
Youngstown, Pa. 15696-0388 U.S.A.
Telephone: 724-537-3131 Fax: 724-537-3151
Website: www.wmtr.com
WMT&R is a technical leader in the material testing industry.

ACCREDITED
TESTING CERT 621-01 & 621-02

Accredited Nadcap Materials Testing Laboratory

May 22, 2007

CERTIFICATION

WMT&R Report No. 7-29300
P.O. No. 72883-YOK-20070417
WMT&R Quote No. QN270777

Stress Engineering Services Inc.
13800 Westfair East Drive
Houston, TX 77041-1101

Attention: Kenneth Young

Subject: All processes, performed upon the material as received, were conducted at WMT&R, Inc. in accordance with the WMT&R Quality Assurance Manual, Rev. 9, dated 4/1/2000.
The following tests were performed on this order: HARDNESS and TENSILE

HARDNESS - ASTM E10-07

REQUIREMENT: None

ACTUAL:

Sample ID	Result	Test Log No.	Disposition
1-01-T-01	229 HBW	F42615	Report
2-01-T-01	230 HBW	F42616	Report
3-01-T-01	217 HBW	F42617	Report
1-02-T-01	229 HBW	F42618	Report
1-02-T-02	229 HBW	F42619	Report
2-02-T-01	229 HBW	F42620	Report
3-02-T-01	217 HBW	F42621	Report
1-03-T-01	229 HBW	F42622	Report
1-03-T-02	228 HBW	F42623	Report
2-03-T-01	230 HBW	F42624	Report
3-01-T-01	228 HBW	F42625	Report

Roy E. Starr\Matt Wojton
____ Technical Services Manager____ Tensile Supervisor May 22, 2007

KNOWINGLY OR WILLFULLY FALSIFYING OR CONCEALING A MATERIAL FACT ON THIS FORM OR MAKING FALSE, FICTITIOUS OR FRAUDULENT STATEMENTS OR REPRESENTATIONS HEREIN COULD CONSTITUTE A FELONY PUNISHABLE UNDER FEDERAL STATUTES. THIS CERTIFICATE OR REPORT SHALL NOT BE REPRODUCED EXCEPT IN FULL, WITHOUT THE WRITTEN APPROVAL OF WMTR, INC.

Westmoreland Mechanical Testing & Research, Inc.
P.O. Box 388
Westmoreland Drive
Youngstown, Pa. 15696-0388 U.S.A.
Telephone: 724-537-3131 Fax: 724-537-3151
Website: www.wmtr.com
WMT&R is a technical leader in the material testing industry.

ACCREDITED
TESTING CERT 621-01 & 621-02

Accredited Nadcap Materials Testing Laboratory

May 22, 2007

CERTIFICATION

WMT&R Report No. 7-29300
P.O. No. 72883-YOK-20070417

Stress Engineering Services Inc.

TENSILE RESULTS: ASTM E21-05
SOAK TIME: 30 Minutes
SPEED OF TESTING: 0.005 in./in./min., 0.05 in./min./in.
MATERIAL: CrMo **DISPOSITION: Report**

Specimen ID	TestLog Number	Temp. °F	UTS ksi	0.2% YS ksi	Elong %	RA %	Modulus Msi	Ult. Load lbf	0.2% YLD. lbf	Orig. Dia. (in.)	Final Dia. (in.)	4D Orig GL (in.)	4D Final GL (in.)	Orig. Area (sq. in.)	Machine Number	A\U\R
1-02-T-01	F42607	200	100.8	84.9	20.5	68.0	28.8	10030	8451	0.3560	0.2011	1.40	1.69	0.09953822	M14	R
1-02-T-02	F42608	200	101.2	84.9	21.5	69.0	28.9	10060	8440	0.3558	0.1978	1.40	1.70	0.09942641	M14	R
2-02-T-01	F42609	200	102.3	87.0	20.5	71.5	27.3	10220	8698	0.3567	0.1904	1.40	1.69	0.09993005	M14	R
3-02-T-01	F42610	200	94.4	79.7	22.0	75.5	28.1	9455	7984	0.3572	0.1768	1.40	1.71	0.10021040	M14	R
2-02-T-02	F50764	200	104.2	88.8	20.0	71.0	31.9	20920	17832	0.5056	0.2715	2.00	2.40	0.20077240	M13	R
3-02-T-02	F50765	200	97.3	82.5	21.5	74.5	32.7	19580	16610	0.5062	0.2548	2.00	2.43	0.20124920	M13	R

A\U\R: A=ACCEPTABLE, U=UNACCEPTABLE, R=REPORT

TENSILE RESULTS: ASTM E21-05
SOAK TIME: 30 Minutes
SPEED OF TESTING: 0.005 in./in./min., 0.05 in./min./in.
MATERIAL: CrMo **DISPOSITION: Report**

Specimen ID	TestLog Number	Temp. °F	UTS ksi	0.2% YS ksi	Elong %	RA %	Modulus Msi	Codes	Ult. Load lbf	0.2% YLD. lbf	Orig. Dia. (in.)	Final Dia. (in.)	4D Orig GL (in.)	4D Final GL (in.)	Orig. Area (sq. in.)	Machine Number	A\U\R
1-03-T-01	F42611	350	97.4	81.5	20.0	71.0	28.9	---	9718	8140	0.3565	0.1912	1.40	1.68	0.09981802	M14	R
1-03-T-02	F42612	350	97.3	81.1	20.0	71.0	27.8	---	9691	8081	0.3561	0.1915	1.40	1.68	0.09959415	M14	R
2-03-T-01	F42613	350	100.7	85.3	20.0	73.0	28.9	---	10030	8505	0.3562	0.1859	1.40	1.68	0.09965009	M14	R
3-03-T-01	F42614	350	93.4	80.8	17.0	73.5	28.3	D	9181	7946	0.3538	0.1813	1.40	1.64	0.09831178	M14	R
2-03-T02	F50766	350	100.4	85.1	19.5	69.0	31.2	---	20150	17070	0.5054	0.2805	2.00	2.39	0.20061359	M13	R
3-03-T-02	F50767	350	92.4	77.9	19.0	70.5	32.1	---	18630	15710	0.5066	0.2753	2.00	2.38	0.20156738	M13	R

A\U\R: A=ACCEPTABLE, U=UNACCEPTABLE, R=REPORT

Roy E. Starr\Matt Wojton
____ Technical Services Manager____ Tensile Supervisor May 22, 2007

KNOWINGLY OR WILLFULLY FALSIFYING OR CONCEALING A MATERIAL FACT ON THIS FORM OR MAKING FALSE, FICTITIOUS OR FRAUDULENT STATEMENTS OR REPRESENTATIONS HEREIN COULD CONSTITUTE A FELONY PUNISHABLE UNDER FEDERAL STATUTES. THIS CERTIFICATE OR REPORT SHALL NOT BE REPRODUCED EXCEPT IN FULL, WITHOUT THE WRITTEN APPROVAL OF WMTR, INC.

Westmoreland Mechanical Testing & Research, Inc.
P.O. Box 388
Westmoreland Drive
Youngstown, Pa. 15696-0388 U.S.A.
Telephone: 724-537-3131 Fax: 724-537-3151
Website: www.wmtr.com
WMT&R is a technical leader in the material testing industry.

ACCREDITED
TESTING CERT 621-01 & 621-02

Accredited Nadcap Materials Testing Laboratory

May 22, 2007

CERTIFICATION

WMT&R Report No. 7-29300
P.O. No. 72883-YOK-20070417

Stress Engineering Services Inc.

TENSILE RESULTS: ASTM E8-04
SPEED OF TESTING: 0.005 in./in./min., 0.05 in./min./in.
MATERIAL: CrMo

DISPOSITION: Report

Specimen ID	TestLog Number	Temp.	UTS ksi	0.2% YS ksi	Elong %	RA %	Modulus Msi	Codes	Ult. Load lbf	0.2% YLD. lbf	Orig. Dia. (in.)	Final Dia. (in.)	4D Orig GL (in.)	4D Final GL (in.)	Orig. Area (sq. in.)	Machine Number	A\U\R
1-01-T-01	F42604	Room	107.4	89.5	23	71	29.0	---	10670	8891	0.3556	0.1911	1.40	1.72	0.09931467	M14	R
2-01-T-01	F42605	Room	108.9	91.7	22	70	30.7	---	10880	9160	0.3566	0.1954	1.40	1.71	0.09987403	M14	R
3-01-T-01	F42606	Room	100.2	83.3	24	76	29.0	---	9992	8311	0.3564	0.1746	1.40	1.73	0.09976203	M14	R
1-01-T-02	F50761	Room	106.4	89.1	22	71	31.7	---	21330	17860	0.5053	0.2725	2.00	2.44	0.20053421	M10	R
2-01-T-02	F50762	Room	108.5	91.9	22	71	32.2	---	21810	18460	0.5058	0.2739	2.00	2.43	0.20093127	M10	R
3-01-T-02	F50763	Room	103.1	87.0	23	74	32.3	D	20710	17480	0.5058	0.2567	2.00	2.45	0.20093127	M10	R

A\U\R: A=ACCEPTABLE, U=UNACCEPTABLE, R=REPORT

D - Ruptured outside middle half of gage length.

Matthew Wojton 5-22-07
Roy E. Starr\Matt Wojton
____ Technical Services Manager___ Tensile Supervisor May 22, 2007

KNOWINGLY OR WILLFULLY FALSIFYING OR CONCEALING A MATERIAL FACT ON THIS FORM OR MAKING FALSE, FICTITIOUS OR FRAUDULENT STATEMENTS OR REPRESENTATIONS HEREIN COULD CONSTITUTE A FELONY PUNISHABLE UNDER FEDERAL STATUTES. THIS CERTIFICATE OR REPORT SHALL NOT BE REPRODUCED EXCEPT IN FULL, WITHOUT THE WRITTEN APPROVAL OF WMTR, INC

WESTMORELAND MECHANICAL TESTING & RESEARCH, Inc

Stress vs. Strain

Phone: (724)537-3131

Customer: Stress Engineering Services Inc.
WMT&R Report: 7-29300

P.O. No.: 72883-YOK-20070417
WMT&R Quote No.: QN270777

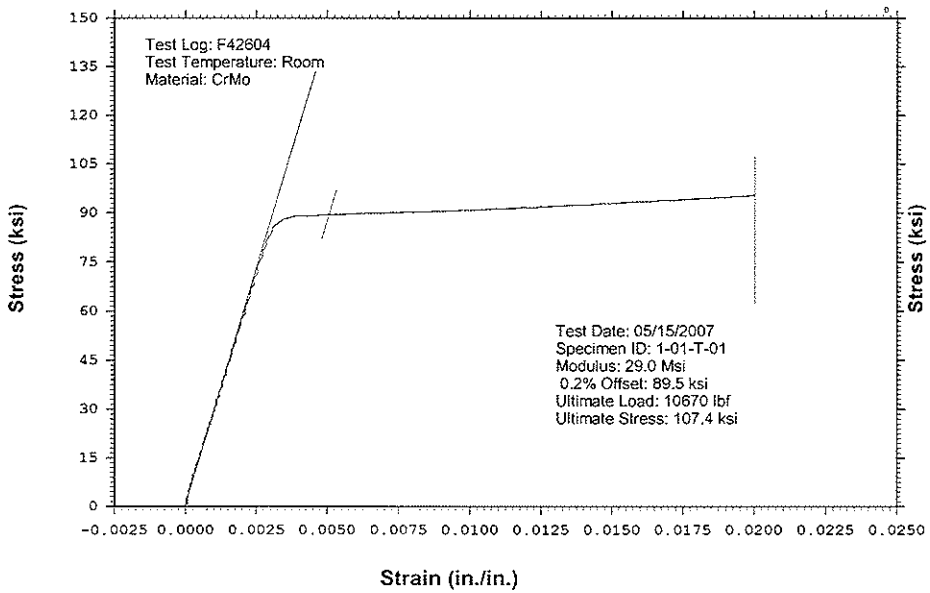

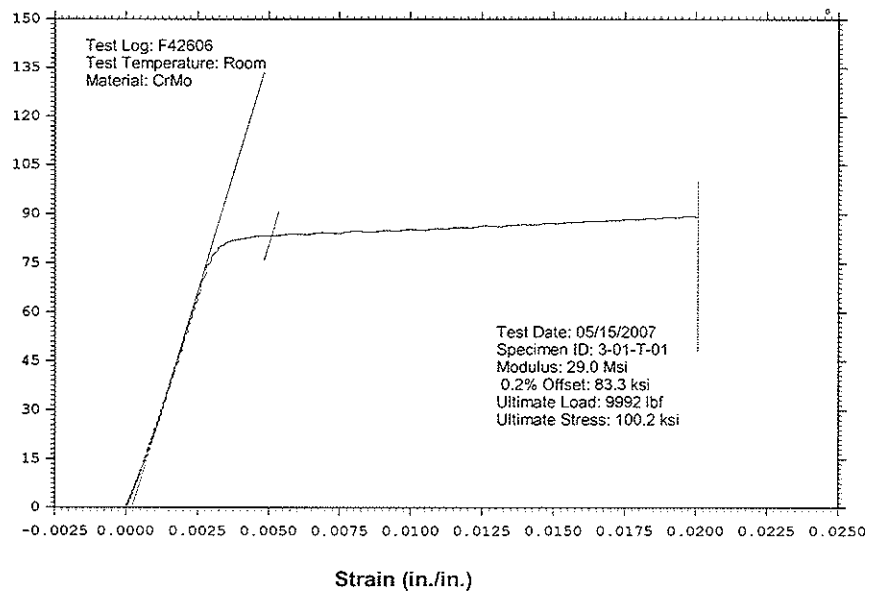

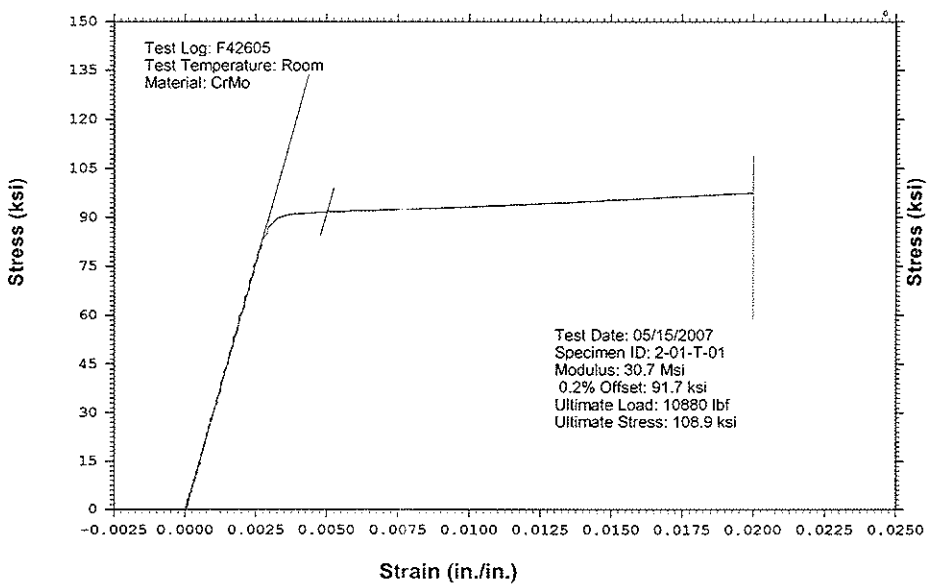

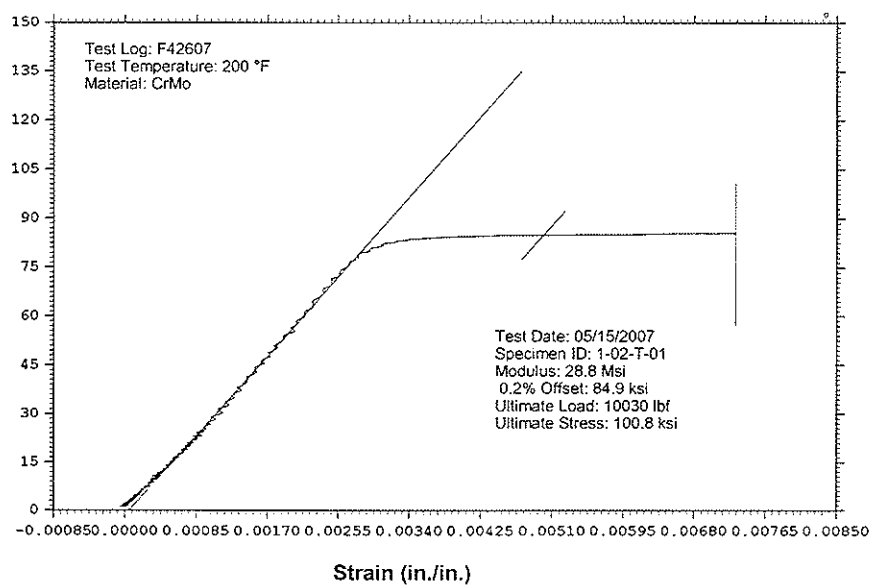

KNOWINGLY OR WILLFULLY FALSIFYING OR CONCEALING A MATERIAL FACT ON THIS FORM OR MAKING FALSE, FICTITIOUS OR FRAUDULENT STATEMENTS OR REPRESENTATIONS HEREIN COULD CONSTITUTE A FELONY PUNISHABLE UNDER FEDERAL STATUTES.

WESTMORELAND MECHANICAL TESTING & RESEARCH, Inc

Stress vs. Strain

Phone: (724)537-3131

Customer: Stress Engineering Services Inc.
WMT&R Report: 7-29300

P.O. No.: 72883-YOK-20070417
WMT&R Quote No.: QN270777

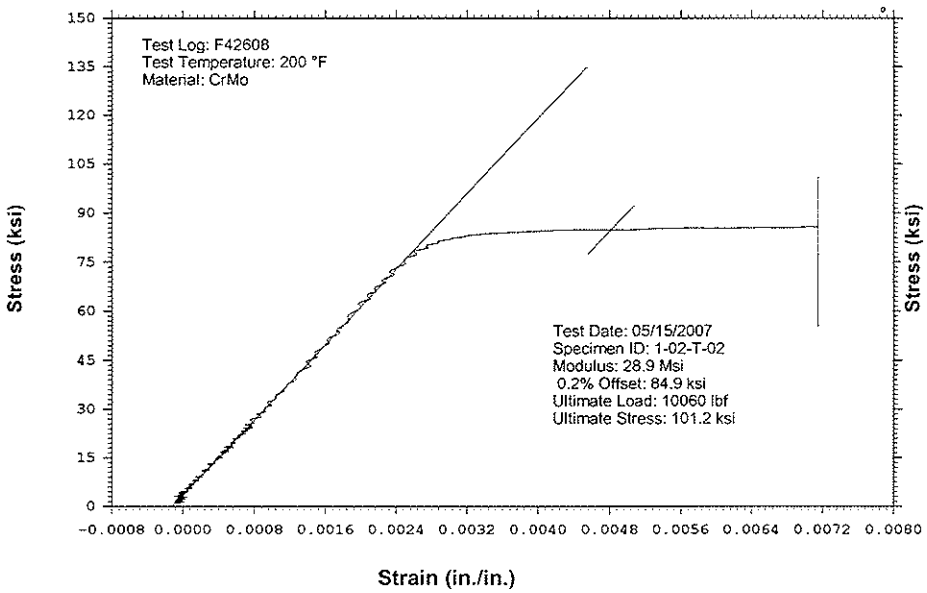

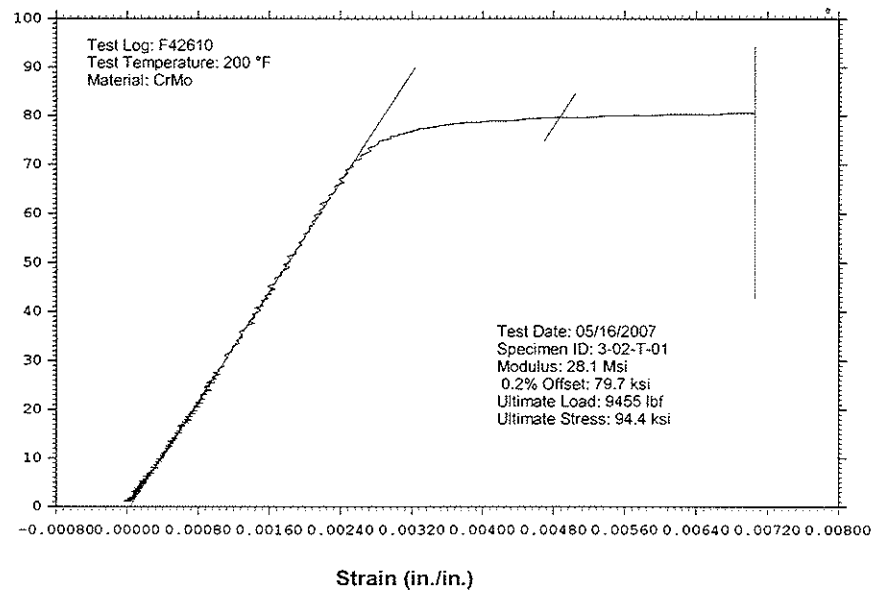

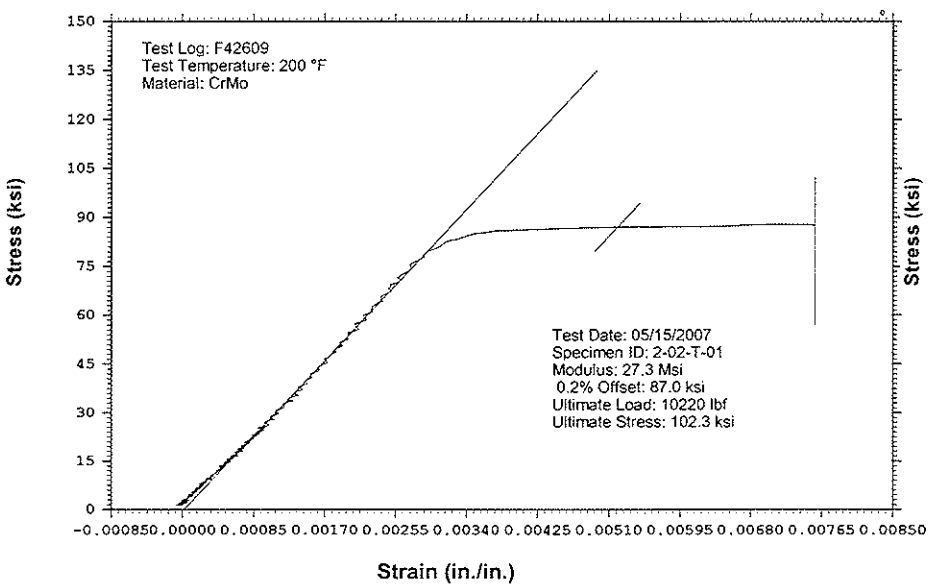

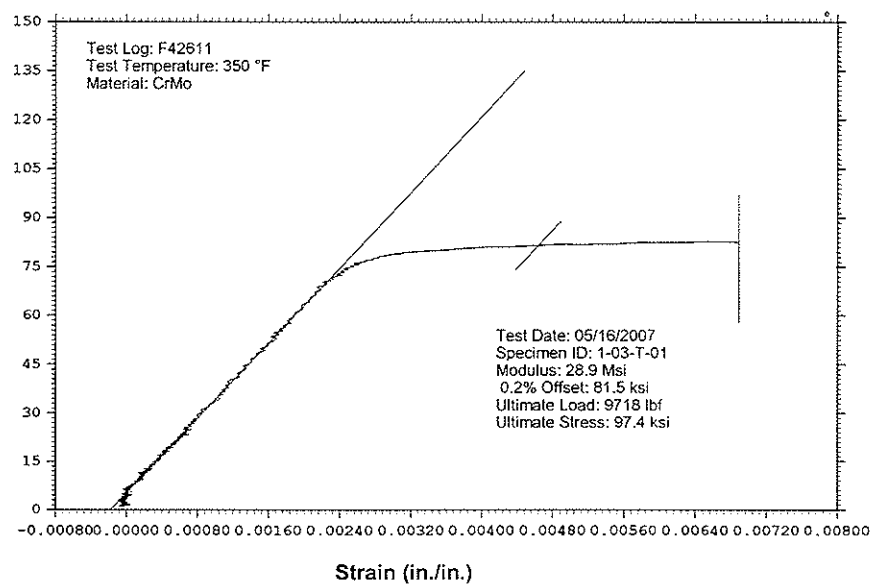

KNOWINGLY OR WILLFULLY FALSIFYING OR CONCEALING A MATERIAL FACT ON THIS FORM OR MAKING FALSE. FICTITIOUS OR FRAUDULENT STATEMENTS OR REPRESENTATIONS HEREIN COULD CONSTITUTE A FELONY PUNISHABLE UNDER FEDERAL STATUTES.

WESTMORELAND MECHANICAL TESTING & RESEARCH, Inc

Stress vs. Strain

Phone: (724)537-3131

Customer: Stress Engineering Services Inc.
WMT&R Report: 7-29300

P.O. No.: 72883-YOK-20070417
WMT&R Quote No.: QN270777

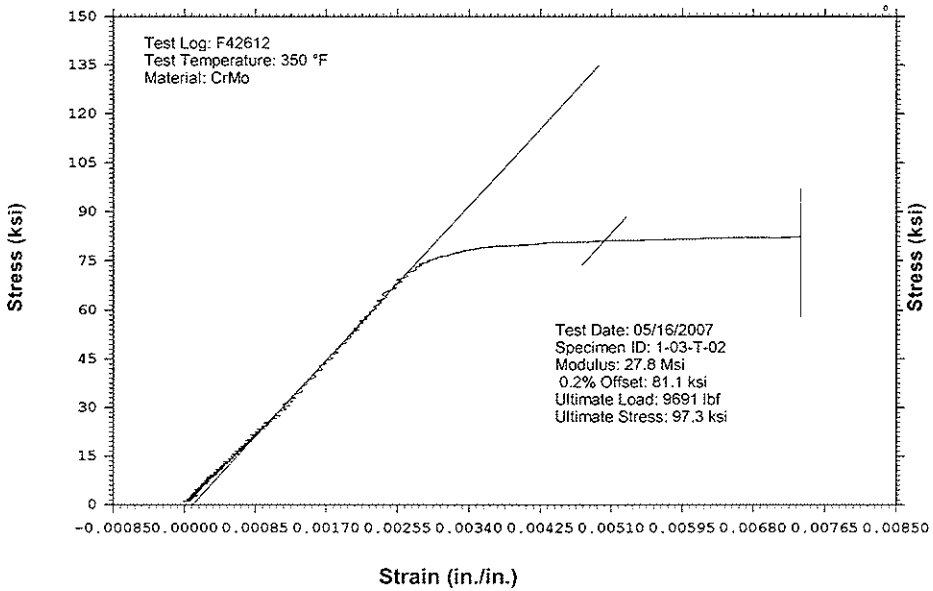

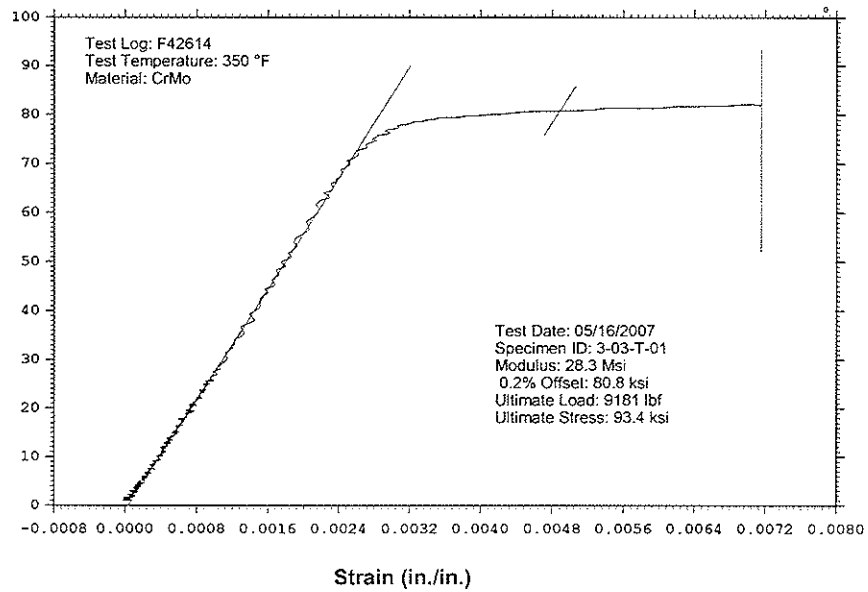

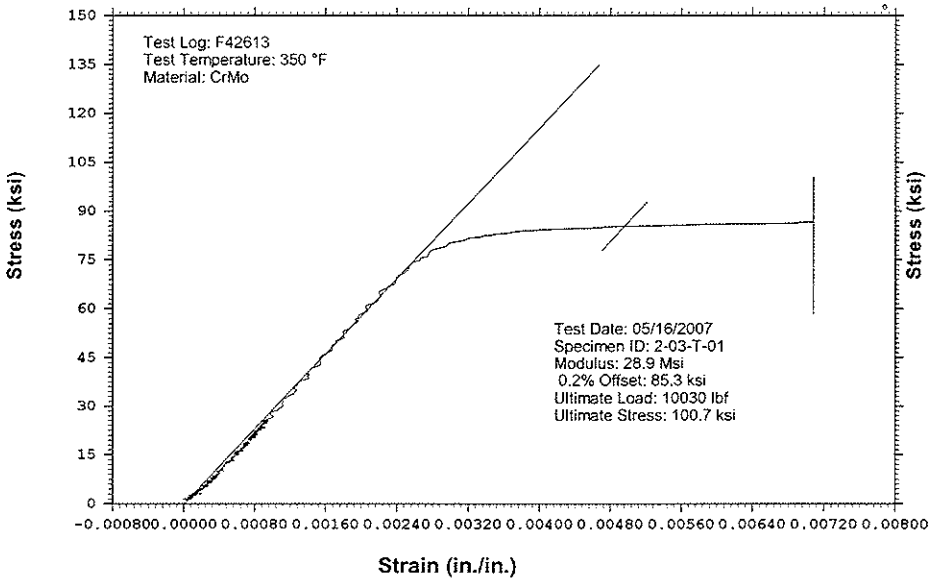

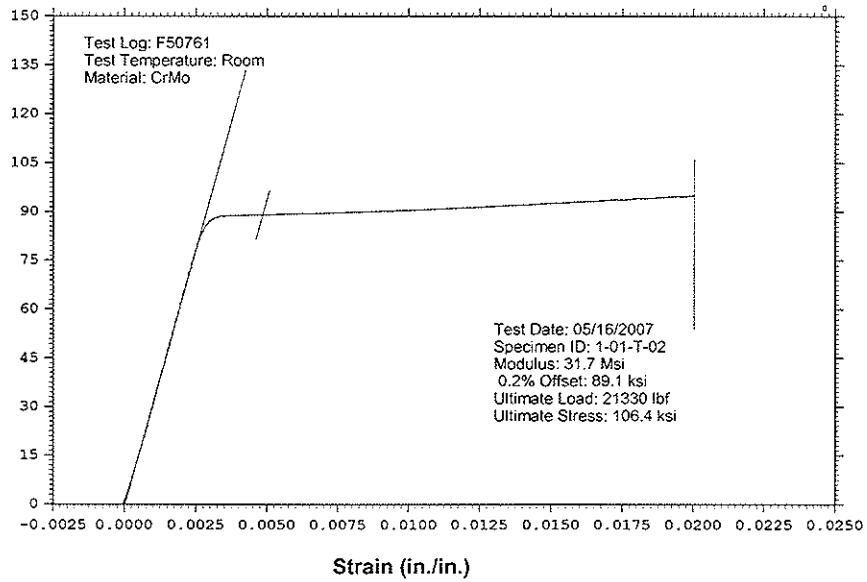

KNOWINGLY OR WILLFULLY FALSIFYING OR CONCEALING A MATERIAL FACT ON THIS FORM OR MAKING FALSE, FICTITIOUS OR FRAUDULENT STATEMENTS OR REPRESENTATIONS HEREIN COULD CONSTITUTE A FELONY PUNISHABLE UNDER FEDERAL STATUTES.

WESTMORELAND MECHANICAL TESTING & RESEARCH, Inc

Stress vs. Strain

Phone: (724)537-3131

Customer: Stress Engineering Services Inc.
WMT&R Report: 7-29300

P.O. No.: 72883-YOK-20070417
WMT&R Quote No.: QN270777

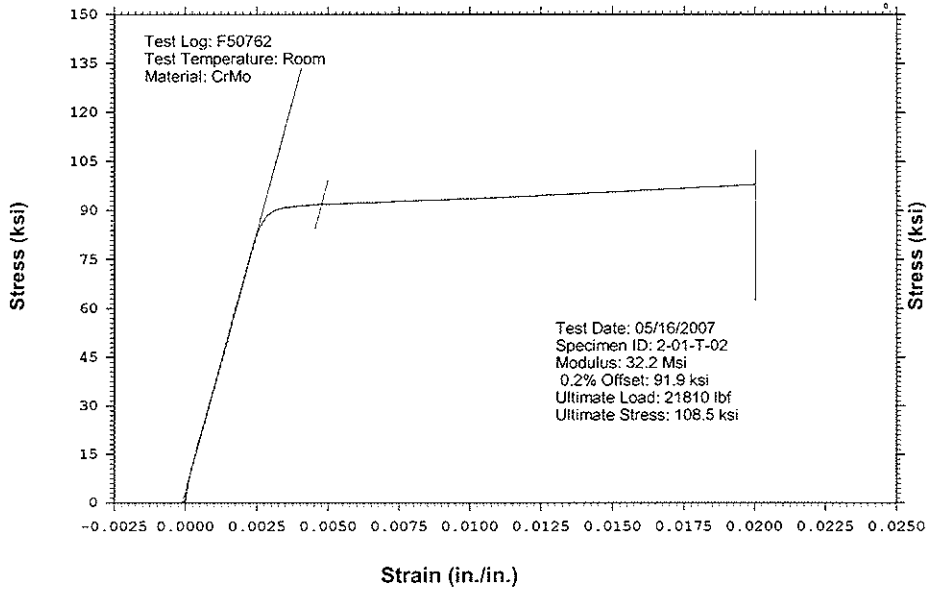

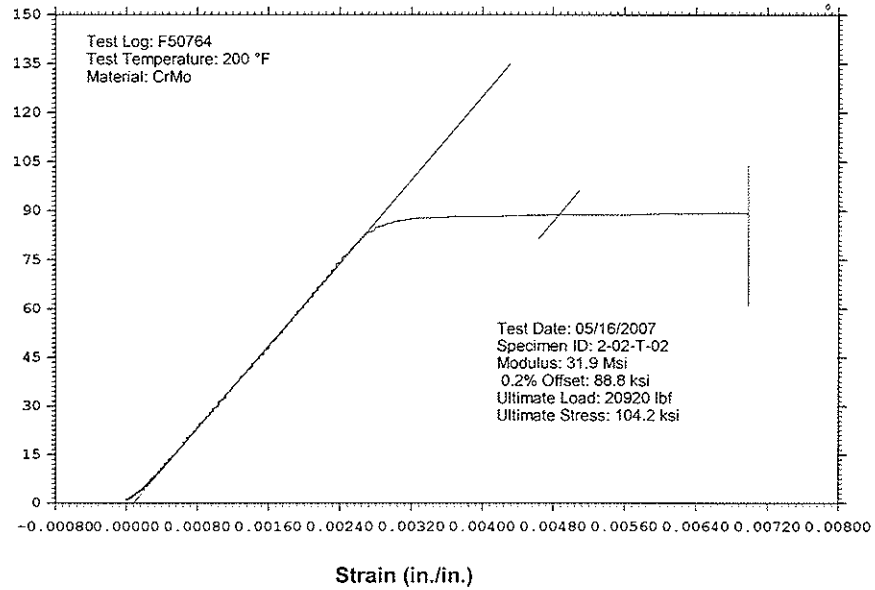

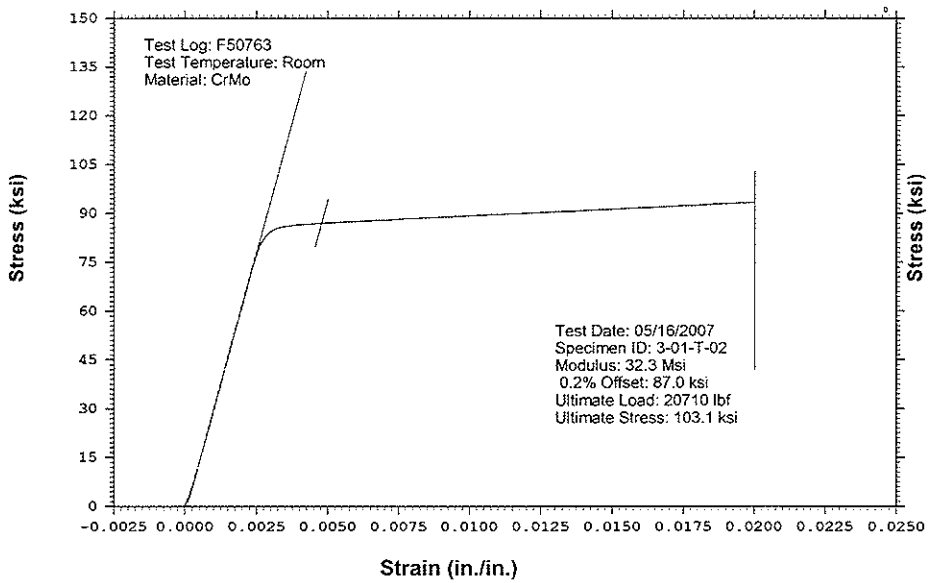

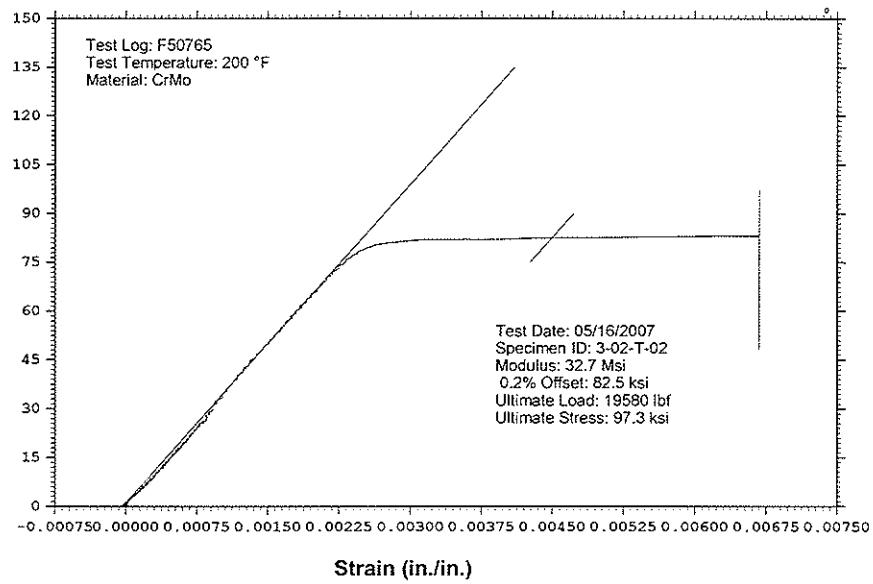

KNOWINGLY OR WILLFULLY FALSIFYING OR CONCEALING A MATERIAL FACT ON THIS FORM OR MAKING FALSE, FICTITIOUS OR FRAUDULENT STATEMENTS OR REPRESENTATIONS HEREIN COULD CONSTITUTE A FELONY PUNISHABLE UNDER FEDERAL STATUTES.

WESTMORELAND MECHANICAL TESTING & RESEARCH, Inc

Stress vs. Strain

Phone: (724)537-3131

Customer: Stress Engineering Services Inc.
WMT&R Report: 7-29300

P.O. No.: 72883-YOK-20070417
WMT&R Quote No.: QN270777

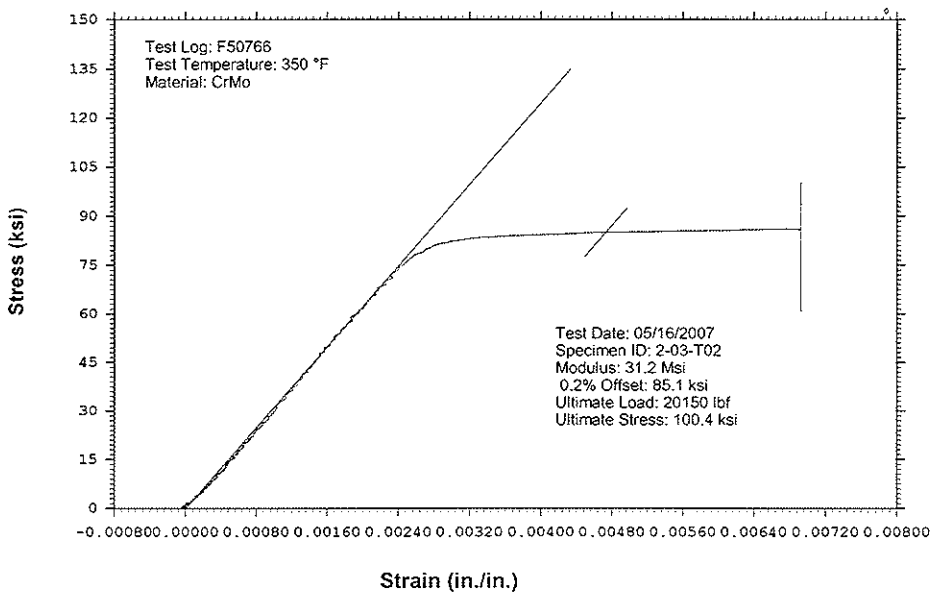

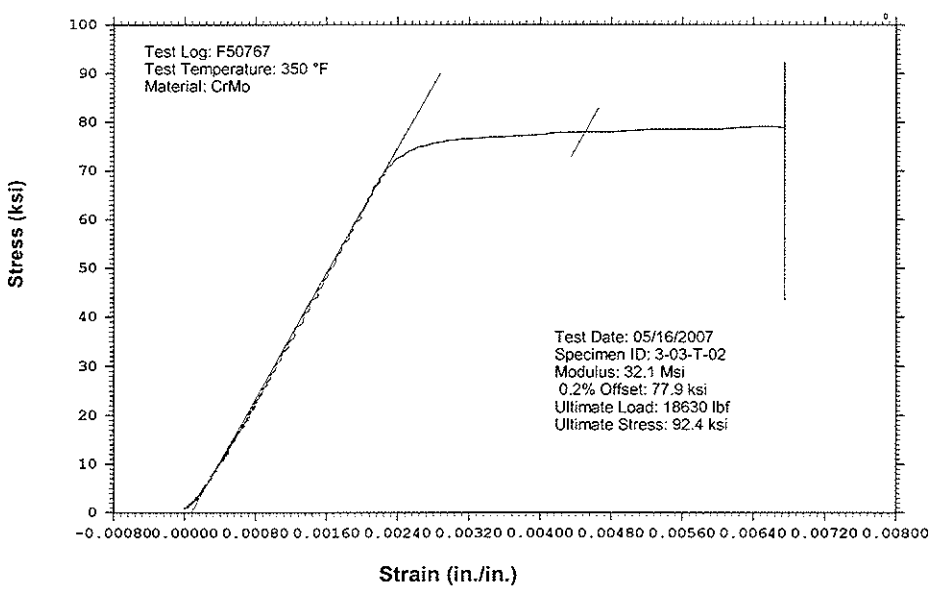

KNOWINGLY OR WILLFULLY FALSIFYING OR CONCEALING A MATERIAL FACT ON THIS FORM OR MAKING FALSE, FICTITIOUS OR FRAUDULENT STATEMENTS OR REPRESENTATIONS HEREIN COULD CONSTITUTE A FELONY PUNISHABLE UNDER FEDERAL STATUTES.

Annex D.2. Tension Test Data Analysis

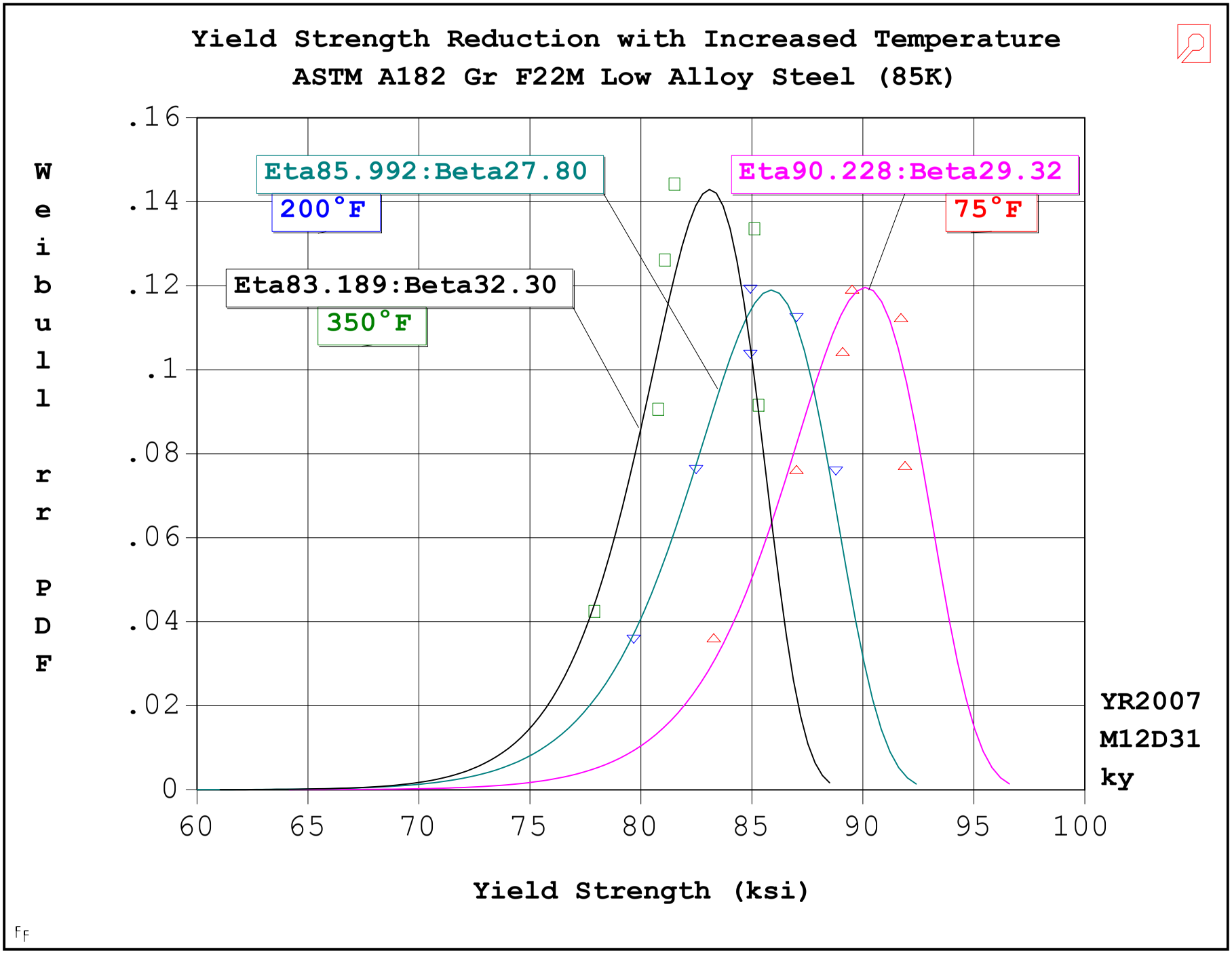
Yield Strength Reduction with Increased Temperature
ASTM A182 Gr F22M Low Alloy Steel (85K)
Eta85.992:Beta27.80
200°F
Eta83.189:Beta32.30
350°F
Eta90.228:Beta29.32
75°F
Weibull PDF
.16
.14
.12
.1
.08
.06
.04
.02
0
60
65
70
75
80
85
90
95
100
Yield Strength (ksi)
YR2007
M12D31
ky

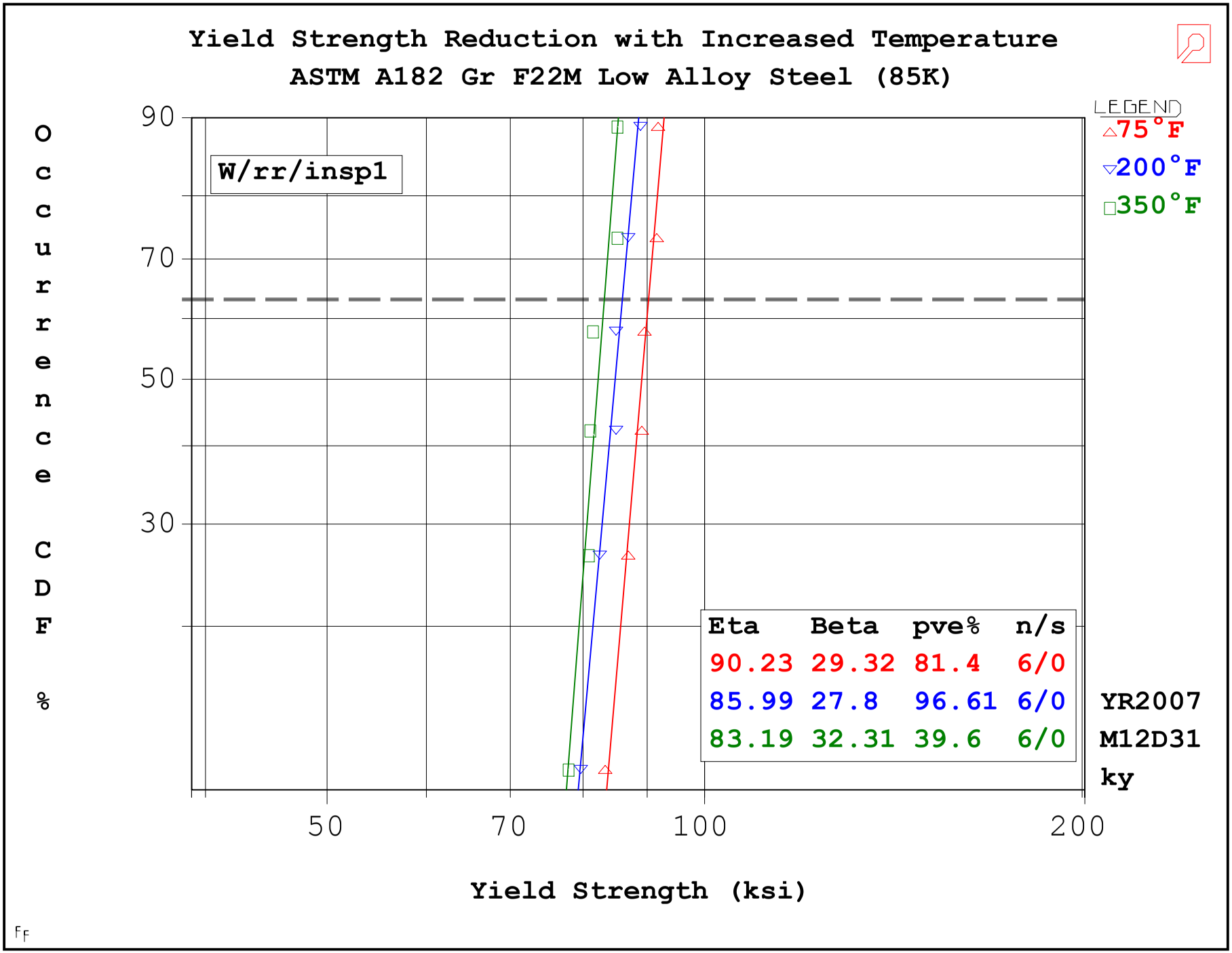
Yield Strength Reduction with Increased Temperature
ASTM A182 Gr F22M Low Alloy Steel (85K)
W/rr/insp1
LEGEND
75°F
200°F
350°F
Occurrence CDF %
90
70
50
30
50
70
100
200
Yield Strength (ksi)
Eta Beta pve% n/s
90.23 29.32 81.4 6/0
85.99 27.8 96.61 6/0
83.19 32.31 39.6 6/0
YR2007
M12D31
ky

Weibull Analysis Report

By ky - Set 1 - 75°F Date: YR2007-M12-D31
Yield Strength Reduction with Increased Temperature ASTM A182 Gr F22M Low Alloy
Correlation(r)=.98133 r^2=.963 ccc^2=.8203 pve%=81.4 (Okay)
Characteristic Value=90.23 Weibull Slope=29.32 Method=rr/insp1
Mean=88.55 Std. Deviation=3.781 Cv%=4.27
Point Quantity=6 (Susp=0)

B%	Yield Strength (k
1	77.12
2	78.98
5	81.53
10	83.56
20	85.73
50	89.11

Weibull Analysis Report

By ky - Set 2 - 200°F Date: YR2007-M12-D31
Yield Strength Reduction with Increased Temperature ASTM A182 Gr F22M Low Alloy
Correlation(r)=.99448 r^2=.989 ccc^2=.8076 pve%=96.61 (Okay)
Characteristic Value=85.99 Weibull Slope=27.8 Method=rr/insp1
Mean=84.31 Std. Deviation=3.792 Cv%=4.498
Point Quantity=6 (Susp=0)

B%	Yield Strength (k
1	72.88
2	74.73
5	77.28
10	79.3
20	81.47
50	84.87

Weibull Analysis Report

By ky - Set 3 - 350°F Date: YR2007-M12-D31
Yield Strength Reduction with Increased Temperature ASTM A182 Gr F22M Low Alloy
Correlation(r)=.95237 r^2=.907 ccc^2=.8203 pve%=39.6 (Okay)
Characteristic Value=83.19 Weibull Slope=32.3 Method=rr/insp1
Mean=81.78 Std. Deviation=3.176 Cv%=3.883
Point Quantity=6 (Susp=0)

B%	Yield Strength (k
1	72.15
2	73.72
5	75.88
10	77.59
20	79.41
50	82.25

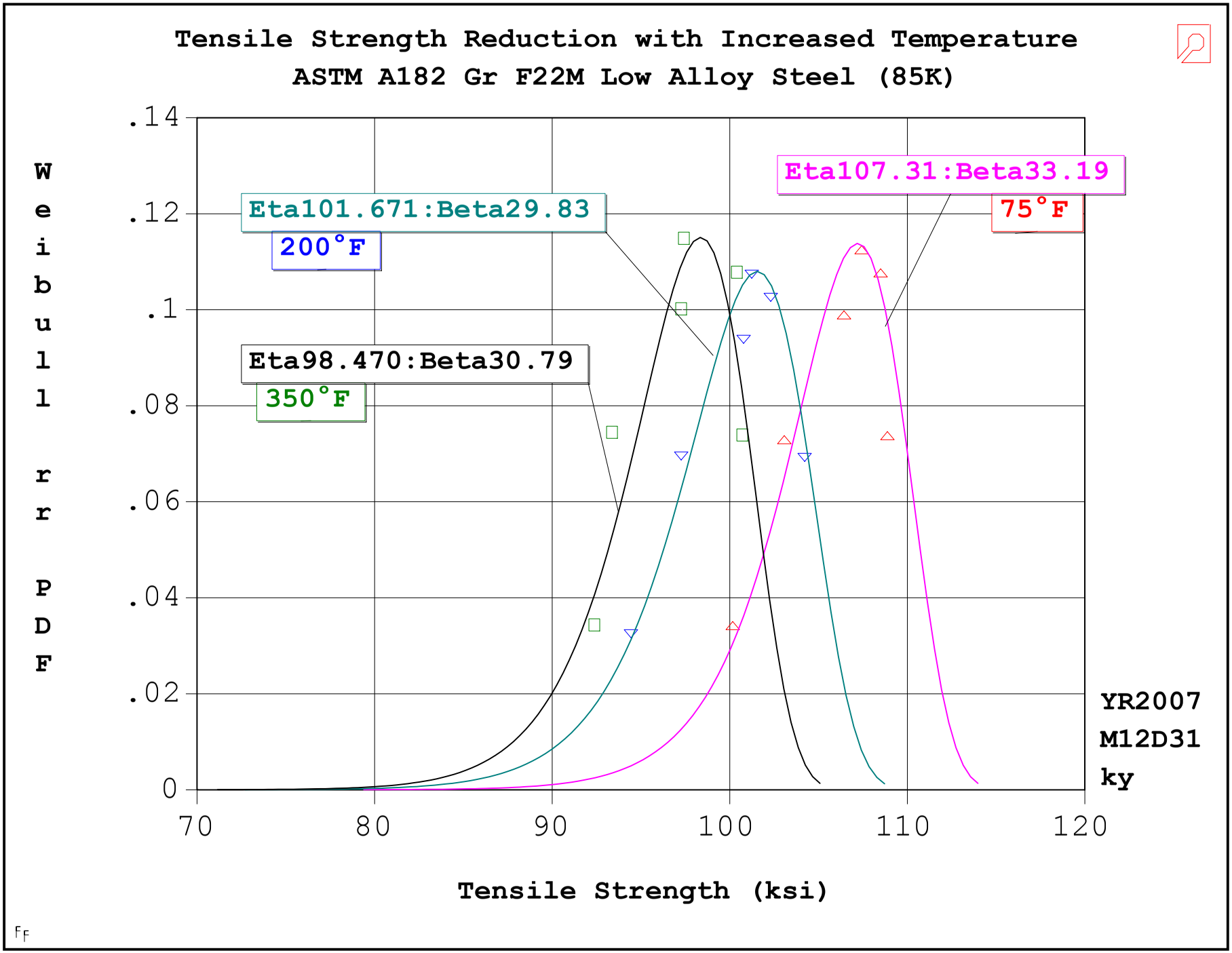
Tensile Strength Reduction with Increased Temperature
ASTM A182 Gr F22M Low Alloy Steel (85K)
Weibull PDF
.14
.12
.1
.08
.06
.04
.02
0
70
80
90
100
110
120
Tensile Strength (ksi)
Eta101.671:Beta29.83
200°F
Eta98.470:Beta30.79
350°F
Eta107.31:Beta33.19
75°F
YR2007
M12D31
ky

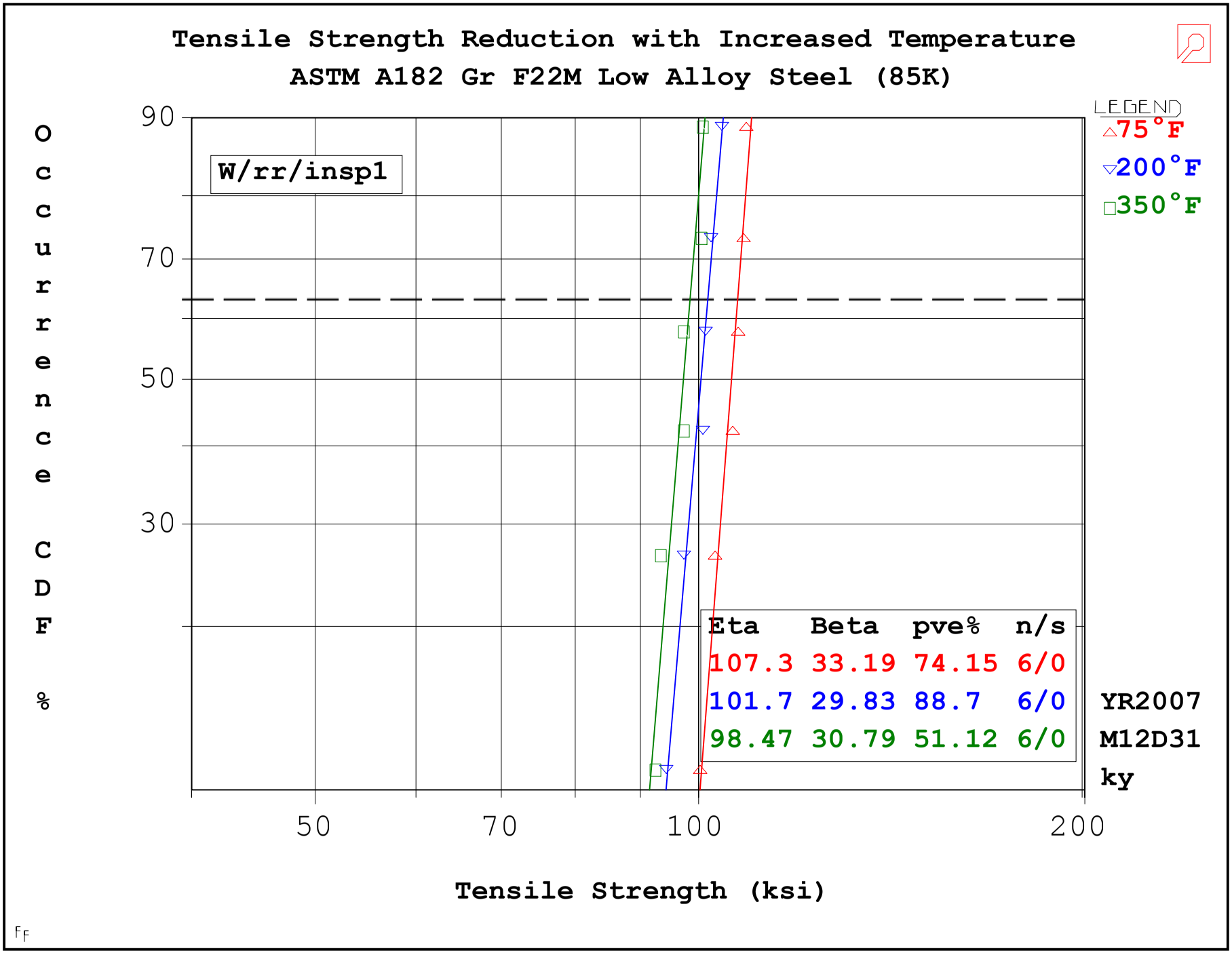
Tensile Strength Reduction with Increased Temperature
ASTM A182 Gr F22M Low Alloy Steel (85K)
W/rr/insp1
LEGEND
75°F
200°F
350°F
Occurrence CDF %
90
70
50
30
50
70
100
200
Tensile Strength (ksi)
Eta Beta pve% n/s
107.3 33.19 74.15 6/0
101.7 29.83 88.7 6/0
98.47 30.79 51.12 6/0
YR2007
M12D31
ky

Weibull Analysis Report

By ky - Set 1 - 75°F Date: YR2007-M12-D31
Tensile Strength Reduction with Increased Temperature ASTM A182 Gr F22M Low All
Correlation(r)=.97673 r^2=.954 ccc^2=.8203 pve%=74.15 (Okay)
Characteristic Value=107.3 Weibull Slope=33.19 Method=rr/insp1
Mean=105.5 Std. Deviation=3.991 Cv%=3.782
Point Quantity=6 (Susp=0)

B%	Tensile Strength
1	93.42
2	95.41
5	98.12
10	100.3
20	102.6
50	106.1

Weibull Analysis Report

By ky - Set 2 - 200°F Date: YR2007-M12-D31
Tensile Strength Reduction with Increased Temperature ASTM A182 Gr F22M Low All
Correlation(r)=.98641 r^2=.973 ccc^2=.8203 pve%=88.7 (Okay)
Characteristic Value=101.7 Weibull Slope=29.83 Method=rr/insp1
Mean=99.81 Std. Deviation=4.19 Cv%=4.198
Point Quantity=6 (Susp=0)

B%	Tensile Strength
1	87.14
2	89.21
5	92.04
10	94.28
20	96.69
50	100.4

Weibull Analysis Report

By ky - Set 3 - 350°F Date: YR2007-M12-D31
Tensile Strength Reduction with Increased Temperature ASTM A182 Gr F22M Low All
Correlation(r)=.96229 r^2=.926 ccc^2=.8203 pve%=51.12 (Okay)
Characteristic Value=98.47 Weibull Slope=30.79 Method=rr/insp1
Mean=96.72 Std. Deviation=3.937 Cv%=4.071
Point Quantity=6 (Susp=0)

B%	Tensile Strength
1	84.8
2	86.75
5	89.41
10	91.53
20	93.79
50	97.3

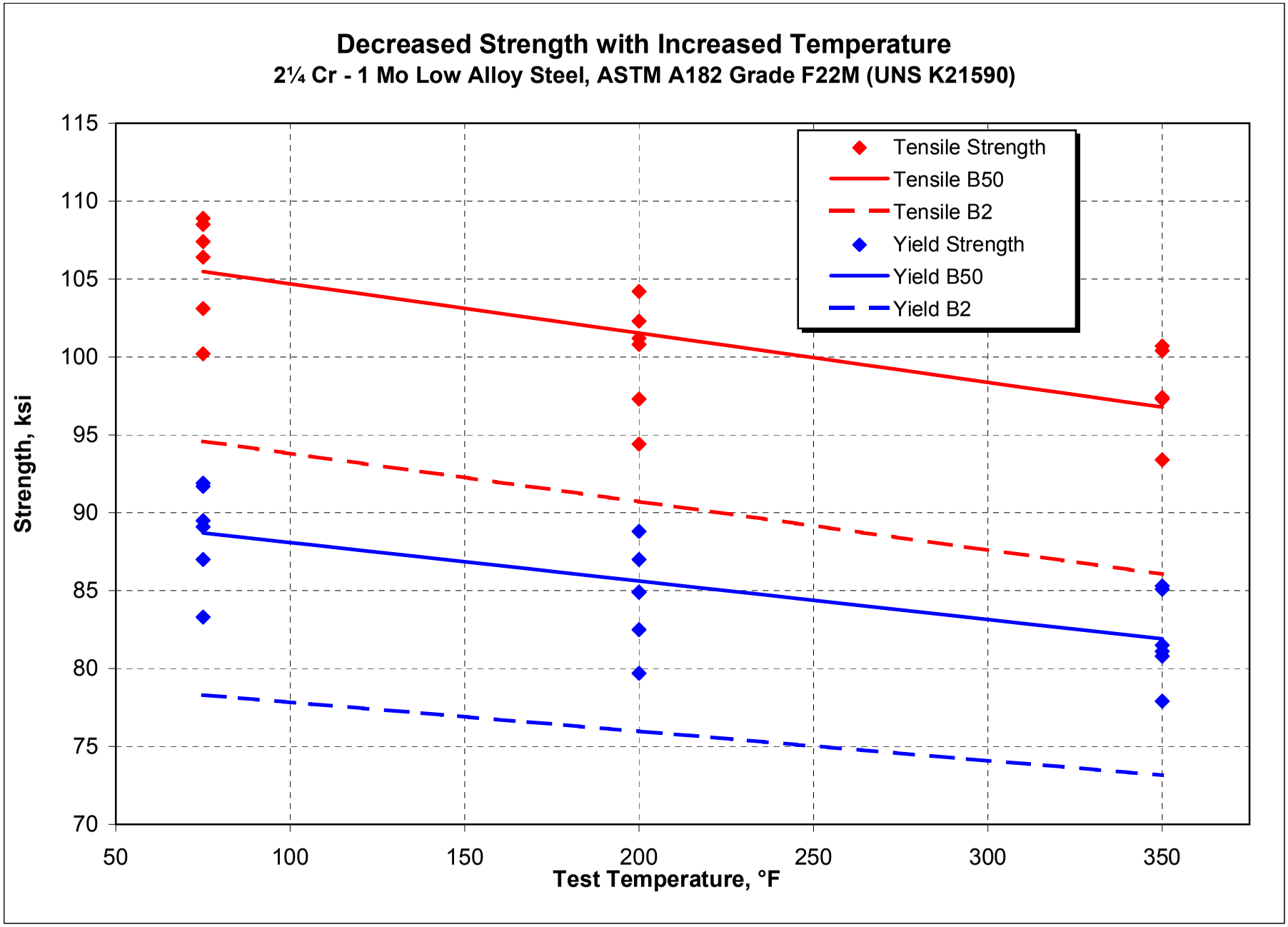

Figure 5 172883 Test Results.xls 2/19/2008

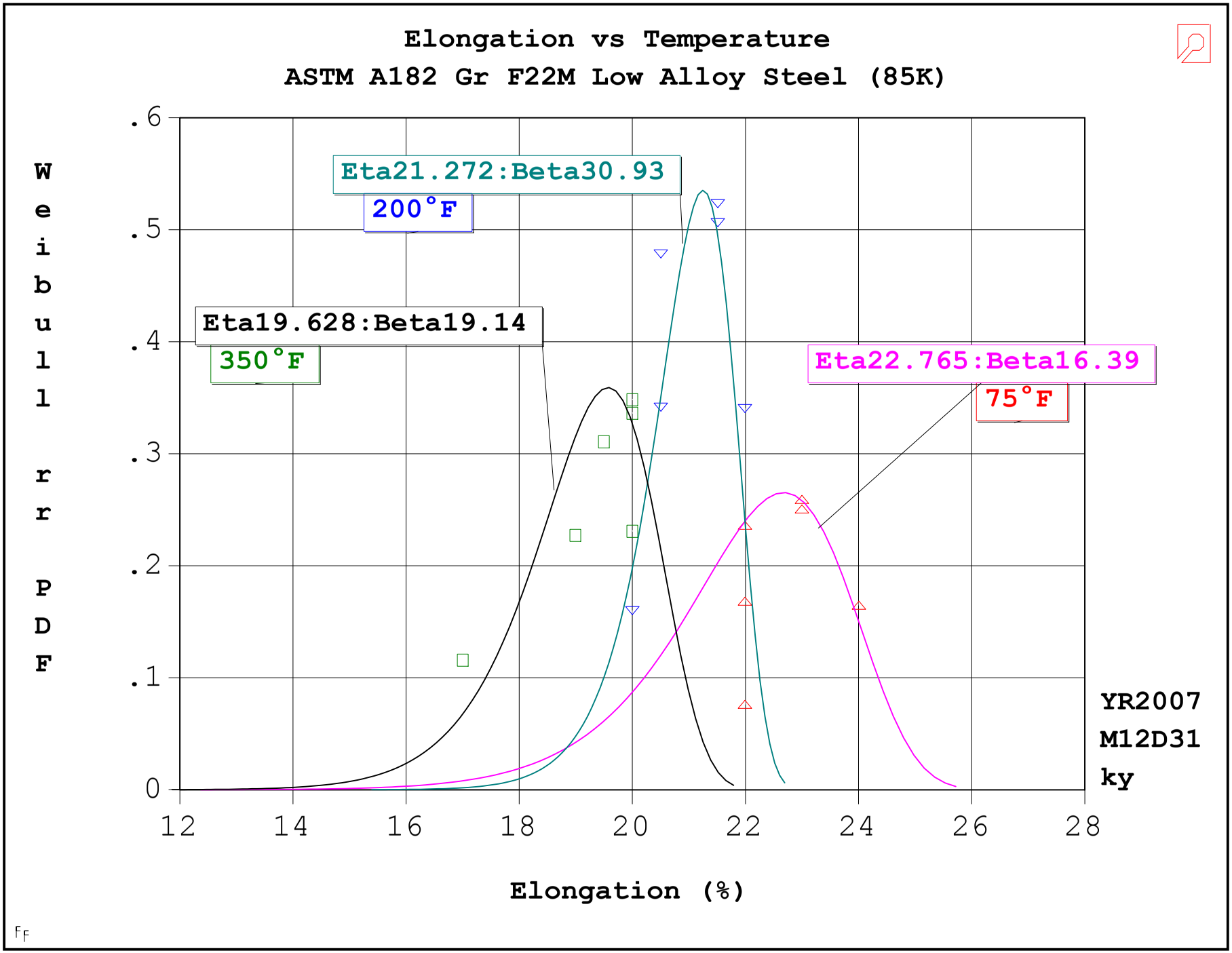
Elongation vs Temperature
ASTM A182 Gr F22M Low Alloy Steel (85K)
Weibull rr PDF
.6
.5
.4
.3
.2
.1
0
12
14
16
18
20
22
24
26
28
Elongation (%)
Eta21.272:Beta30.93
200°F
Eta19.628:Beta19.14
350°F
Eta22.765:Beta16.39
75°F
YR2007
M12D31
ky

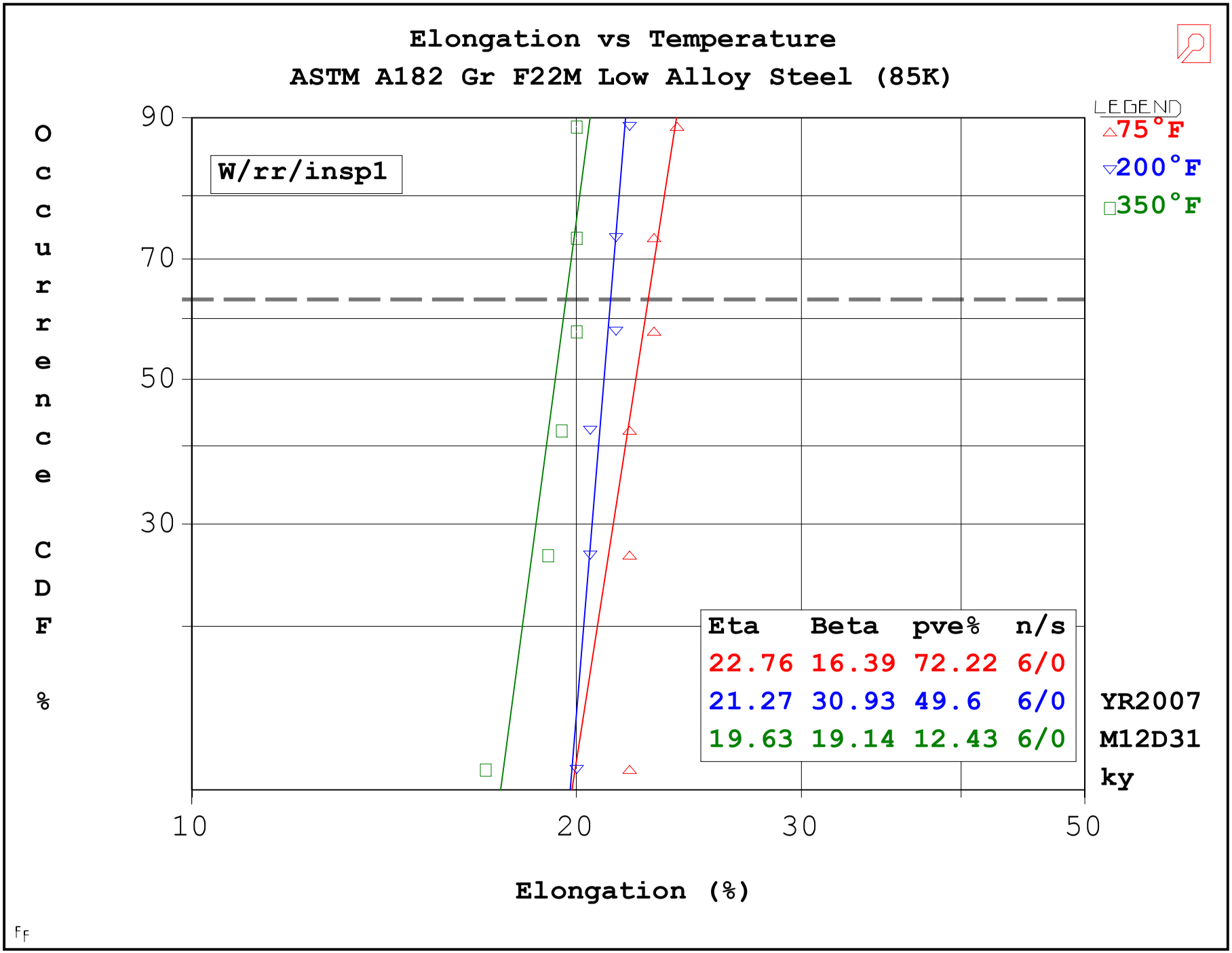
Elongation vs Temperature
ASTM A182 Gr F22M Low Alloy Steel (85K)
W/rr/insp1
LEGEND
75°F
200°F
350°F
Occurrence CDF %
90
70
50
30
10
20
30
50
Elongation (%)
Eta Beta pve% n/s
22.76 16.39 72.22 6/0
21.27 30.93 49.6 6/0
19.63 19.14 12.43 6/0
YR2007
M12D31
ky

Weibull Analysis Report

By ky - Set 1 - 75°F Date: YR2007-M12-D31
Elongation vs Temperature ASTM A182 Gr F22M Low Alloy Steel (85K)
Correlation(r)=.98995 r^2=.980 ccc^2=.792 pve%=72.22 (Okay)
Characteristic Value=22.76 Weibull Slope=16.39 Method=rr/insp1
Mean=22.04 Std. Deviation=1.655 Cv%=7.508
Point Quantity=6 (Susp=0)

B%	Elongation (%)
1	17.19
2	17.94
5	18.99
10	19.84
20	20.77
50	22.26

Weibull Analysis Report

By ky - Set 2 - 200°F Date: YR2007-M12-D31
Elongation vs Temperature ASTM A182 Gr F22M Low Alloy Steel (85K)
Correlation(r)=.96021 r^2=.922 ccc^2=.7991 pve%=49.6 (Okay)
Characteristic Value=21.27 Weibull Slope=30.93 Method=rr/insp1
Mean=20.9 Std. Deviation=.8467 Cv%=4.052
Point Quantity=6 (Susp=0)

B%	Elongation (%)
1	18.33
2	18.75
5	19.32
10	19.78
20	20.27
50	21.02

Weibull Analysis Report

By ky - Set 3 - 350°F Date: YR2007-M12-D31
Elongation vs Temperature ASTM A182 Gr F22M Low Alloy Steel (85K)
Correlation(r)=.89944 r^2=.809 ccc^2=.7991 pve%=12.43 (Okay)
Characteristic Value=19.63 Weibull Slope=19.14 Method=rr/insp1
Mean=19.09 Std. Deviation=1.234 Cv%=6.466
Point Quantity=6 (Susp=0)

B%	Elongation (%)
1	15.43
2	16.01
5	16.81
10	17.45
20	18.15
50	19.26

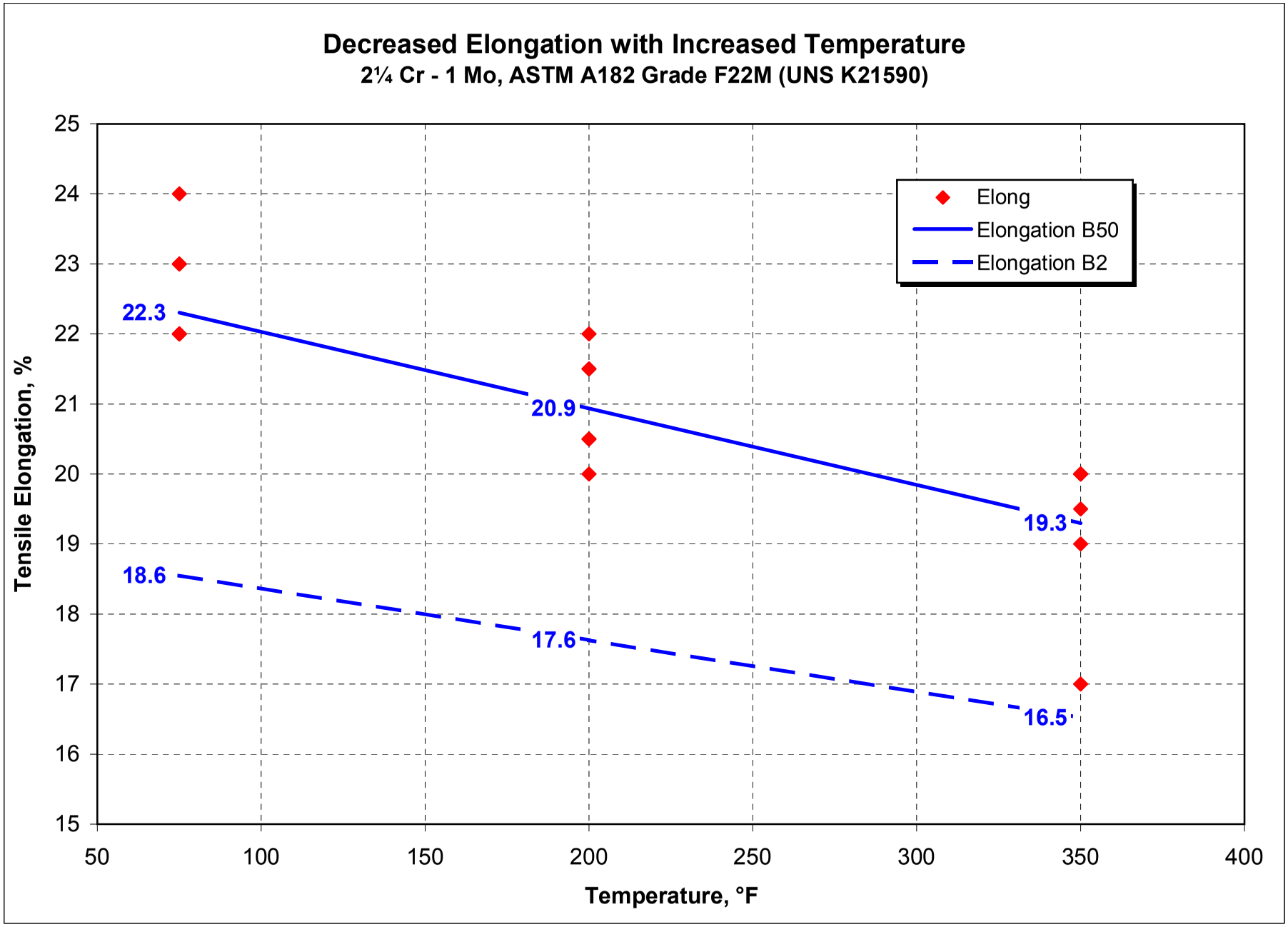

Figure 6 172883 Test Results.xls 2/19/2008

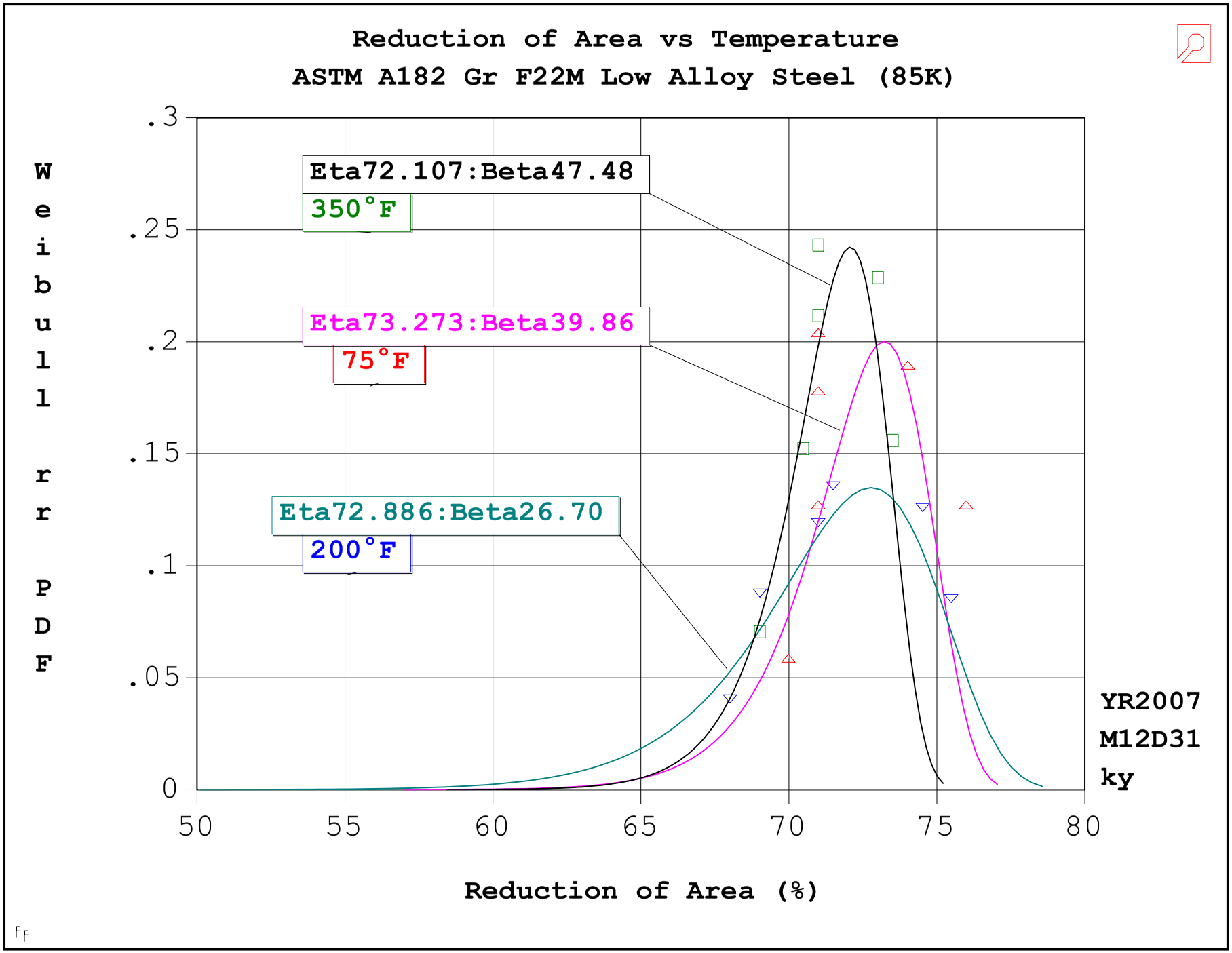
Reduction of Area vs Temperature
ASTM A182 Gr F22M Low Alloy Steel (85K)
Eta72.107:Beta47.48
350°F
Eta73.273:Beta39.86
75°F
Eta72.886:Beta26.70
200°F
Weibull rr PDF
.3
.25
.2
.15
.1
.05
0
50
55
60
65
70
75
80
Reduction of Area (%)
YR2007
M12D31
ky

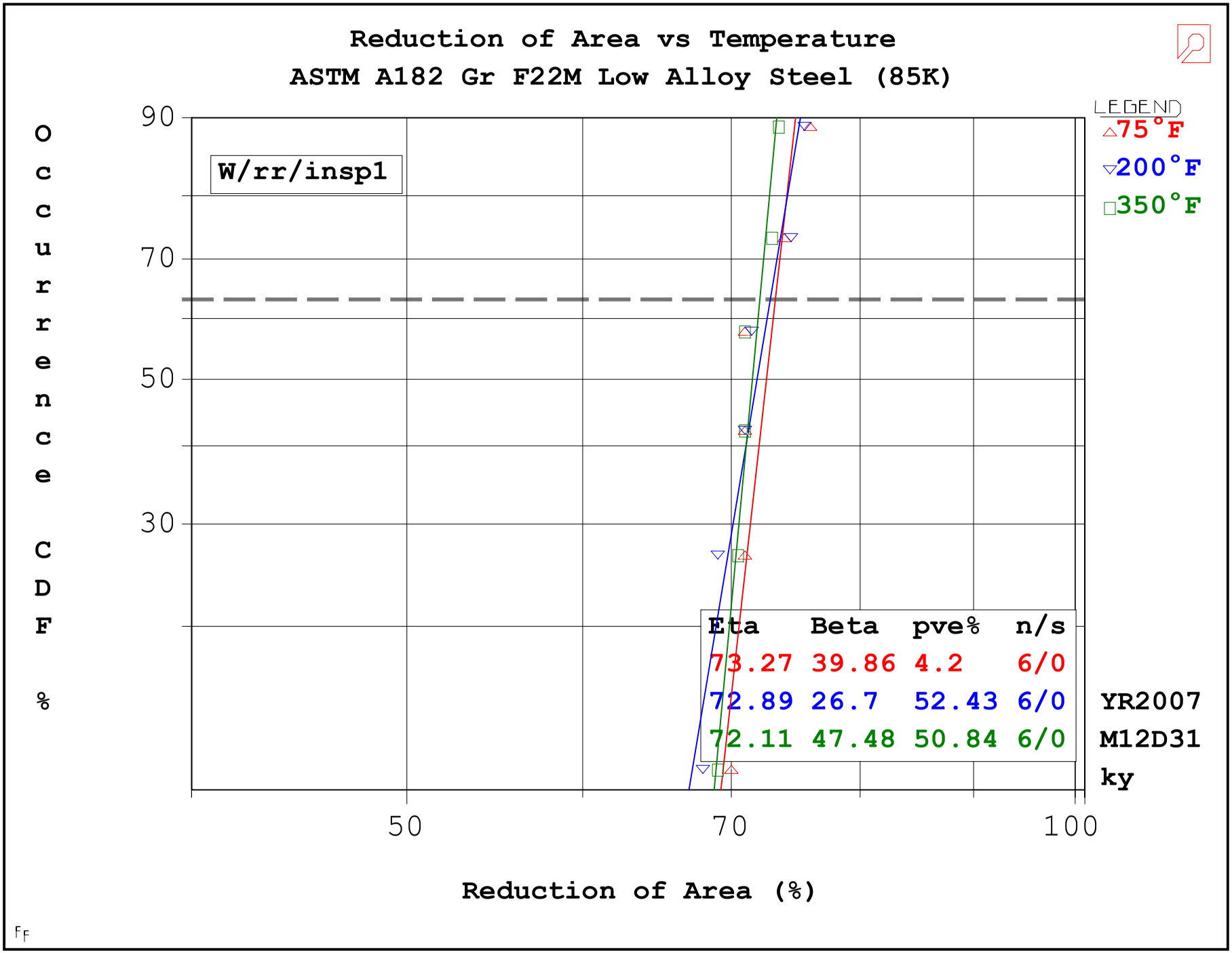
Reduction of Area vs Temperature
ASTM A182 Gr F22M Low Alloy Steel (85K)
W/rr/insp1
LEGEND
75°F
200°F
350°F
Occurrence CDF %
90
70
50
30
50
70
100
Reduction of Area (%)
Eta Beta pve% n/s
73.27 39.86 4.2 6/0
72.89 26.7 52.43 6/0
72.11 47.48 50.84 6/0
YR2007
M12D31
ky

Weibull Analysis Report

By ky - Set 1 - 75°F Date: YR2007-M12-D31
Reduction of Area vs Temperature ASTM A182 Gr F22M Low Alloy Steel (85K)
Correlation(r)=.8579 r^2=.736 ccc^2=.7991 pve%=4.2 (pve%<10!)
Characteristic Value=73.27 Weibull Slope=39.86 Method=rr/insp1
Mean=72.26 Std. Deviation=2.283 Cv%=3.16
Point Quantity=6 (Susp=0)

B%	Reduction of Area
1	65.29
2	66.44
5	68.01
10	69.25
20	70.57
50	72.6

Weibull Analysis Report

By ky - Set 2 - 200°F Date: YR2007-M12-D31
Reduction of Area vs Temperature ASTM A182 Gr F22M Low Alloy Steel (85K)
Correlation(r)=.96333 r^2=.928 ccc^2=.8203 pve%=52.44 (Okay)
Characteristic Value=72.89 Weibull Slope=26.7 Method=rr/insp1
Mean=71.41 Std. Deviation=3.341 Cv%=4.678
Point Quantity=6 (Susp=0)

B%	Reduction of Area
1	61.35
2	62.98
5	65.21
10	66.99
20	68.9
50	71.89

Weibull Analysis Report

By ky - Set 3 - 350°F Date: YR2007-M12-D31
Reduction of Area vs Temperature ASTM A182 Gr F22M Low Alloy Steel (85K)
Correlation(r)=.96073 r^2=.923 ccc^2=.8076 pve%=50.84 (Okay)
Characteristic Value=72.11 Weibull Slope=47.48 Method=rr/insp1
Mean=71.26 Std. Deviation=1.895 Cv%=2.66
Point Quantity=6 (Susp=0)

B%	Reduction of Area
1	65.45
2	66.42
5	67.73
10	68.77
20	69.86
50	71.55

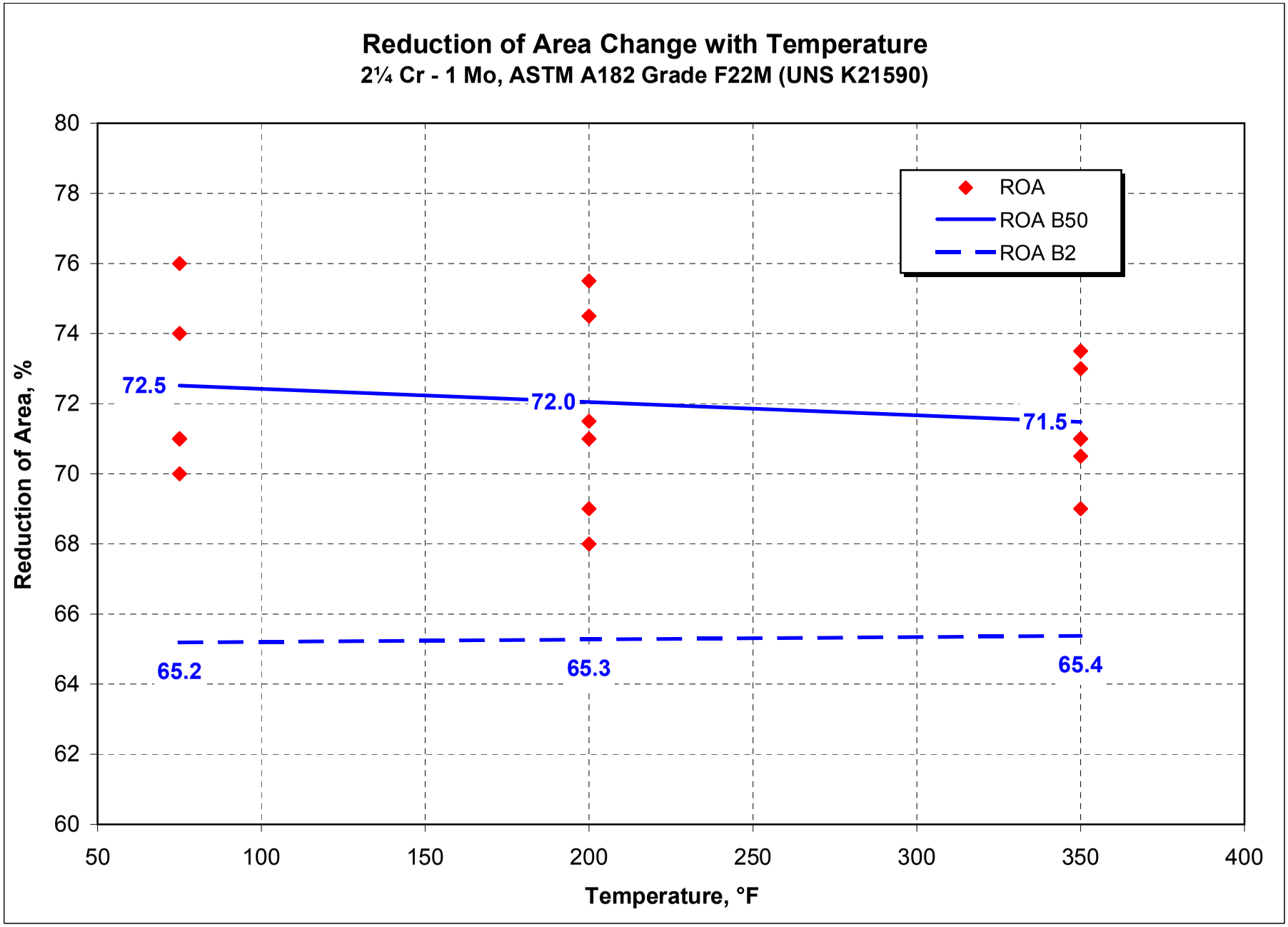

Figure 7 172883 Test Results.xls 2/19/2008

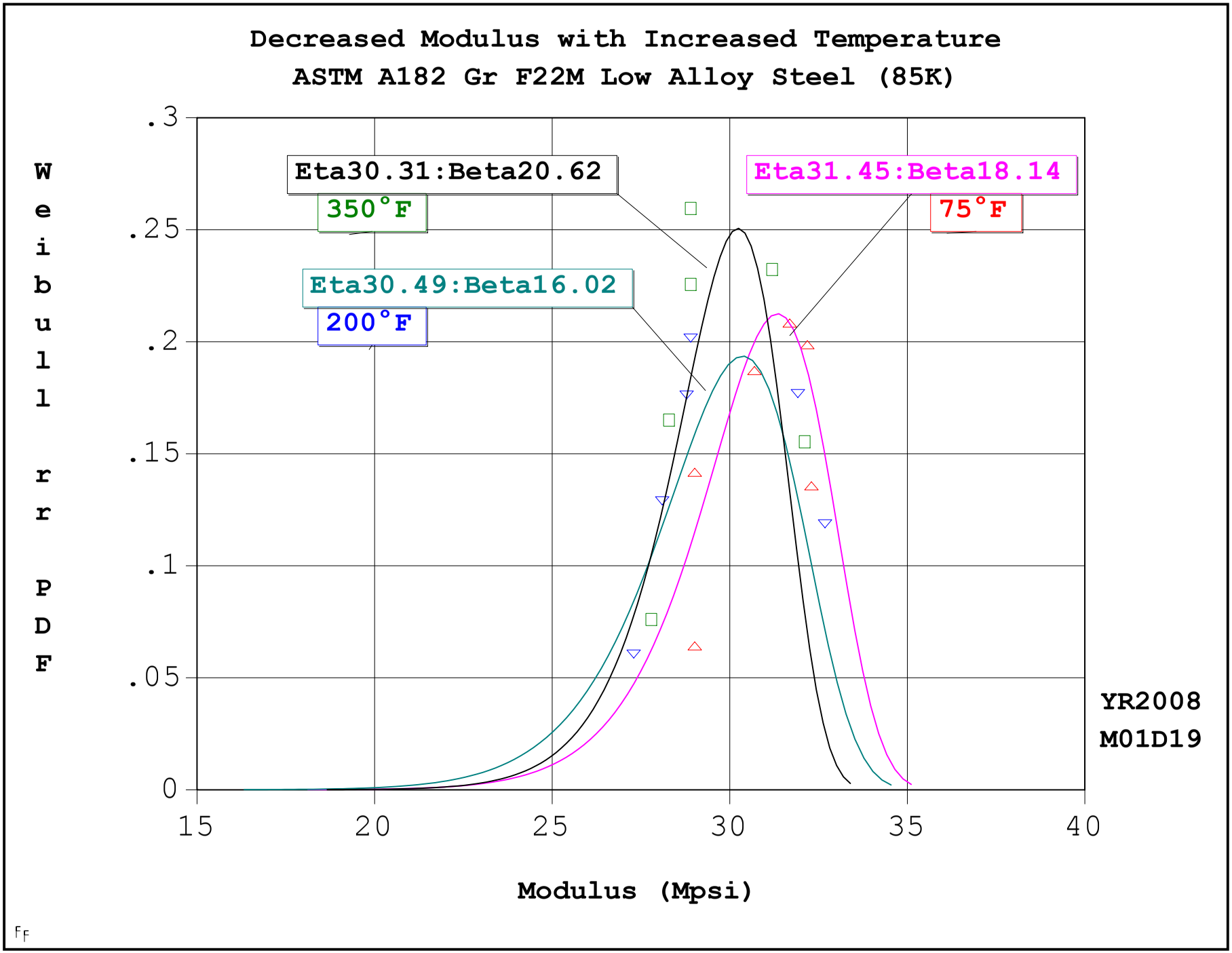
Decreased Modulus with Increased Temperature
ASTM A182 Gr F22M Low Alloy Steel (85K)
Eta30.31:Beta20.62
350°F
Eta30.49:Beta16.02
200°F
Eta31.45:Beta18.14
75°F
Weibull rr PDF
.3
.25
.2
.15
.1
.05
0
15
20
25
30
35
40
Modulus (Mpsi)
YR2008
M01D19

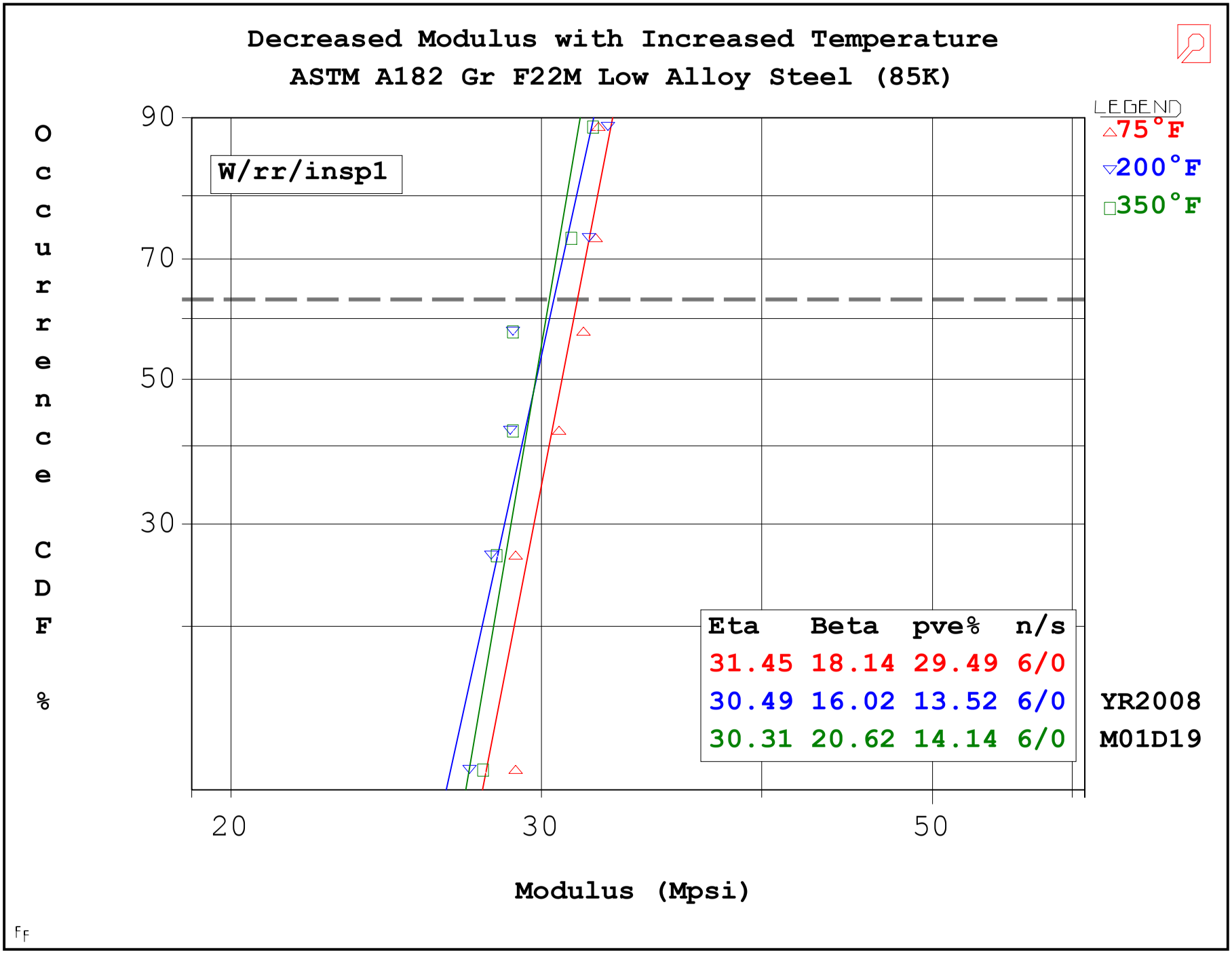
Decreased Modulus with Increased Temperature
ASTM A182 Gr F22M Low Alloy Steel (85K)
W/rr/insp1
LEGEND
75°F
200°F
350°F
Occurrence CDF %
90
70
50
30
20
30
50
Modulus (Mpsi)
Eta Beta pve% n/s
31.45 18.14 29.49 6/0
30.49 16.02 13.52 6/0
30.31 20.62 14.14 6/0
YR2008
M01D19

Weibull Analysis Report

Set 1 - 75°F Date: YR2008-M01-D19
Decreased Modulus with Increased Temperature ASTM A182 Gr F22M Low Alloy Steel
Correlation(r)=.93808 r^2=.880 ccc^2=.8076 pve%=29.49 (Okay)
Characteristic Value=31.45 Weibull Slope=18.14 Method=rr/insp1
Mean=30.54 Std. Deviation=2.079 Cv%=6.807
Point Quantity=6 (Susp=0)

B%	Modulus (Mpsi)
1	24.4
2	25.36
5	26.7
10	27.78
20	28.95
50	30.82

Weibull Analysis Report

Set 2 - 200°F Date: YR2008-M01-D19
Decreased Modulus with Increased Temperature ASTM A182 Gr F22M Low Alloy Steel
Correlation(r)=.91652 r^2=.840 ccc^2=.8203 pve%=13.52 (Okay)
Characteristic Value=30.49 Weibull Slope=16.02 Method=rr/insp1
Mean=29.5 Std. Deviation=2.265 Cv%=7.676
Point Quantity=6 (Susp=0)

B%	Modulus (Mpsi)
1	22.88
2	23.9
5	25.33
10	26.49
20	27.76
50	29.8

Weibull Analysis Report

Set 3 - 350°F Date: YR2008-M01-D19
Decreased Modulus with Increased Temperature ASTM A182 Gr F22M Low Alloy Steel
Correlation(r)=.91104 r^2=.830 ccc^2=.8076 pve%=14.14 (Okay)
Characteristic Value=30.31 Weibull Slope=20.62 Method=rr/insp1
Mean=29.53 Std. Deviation=1.776 Cv%=6.013
Point Quantity=6 (Susp=0)

B%	Modulus (Mpsi)
1	24.25
2	25.09
5	26.25
10	27.18
20	28.18
50	29.78

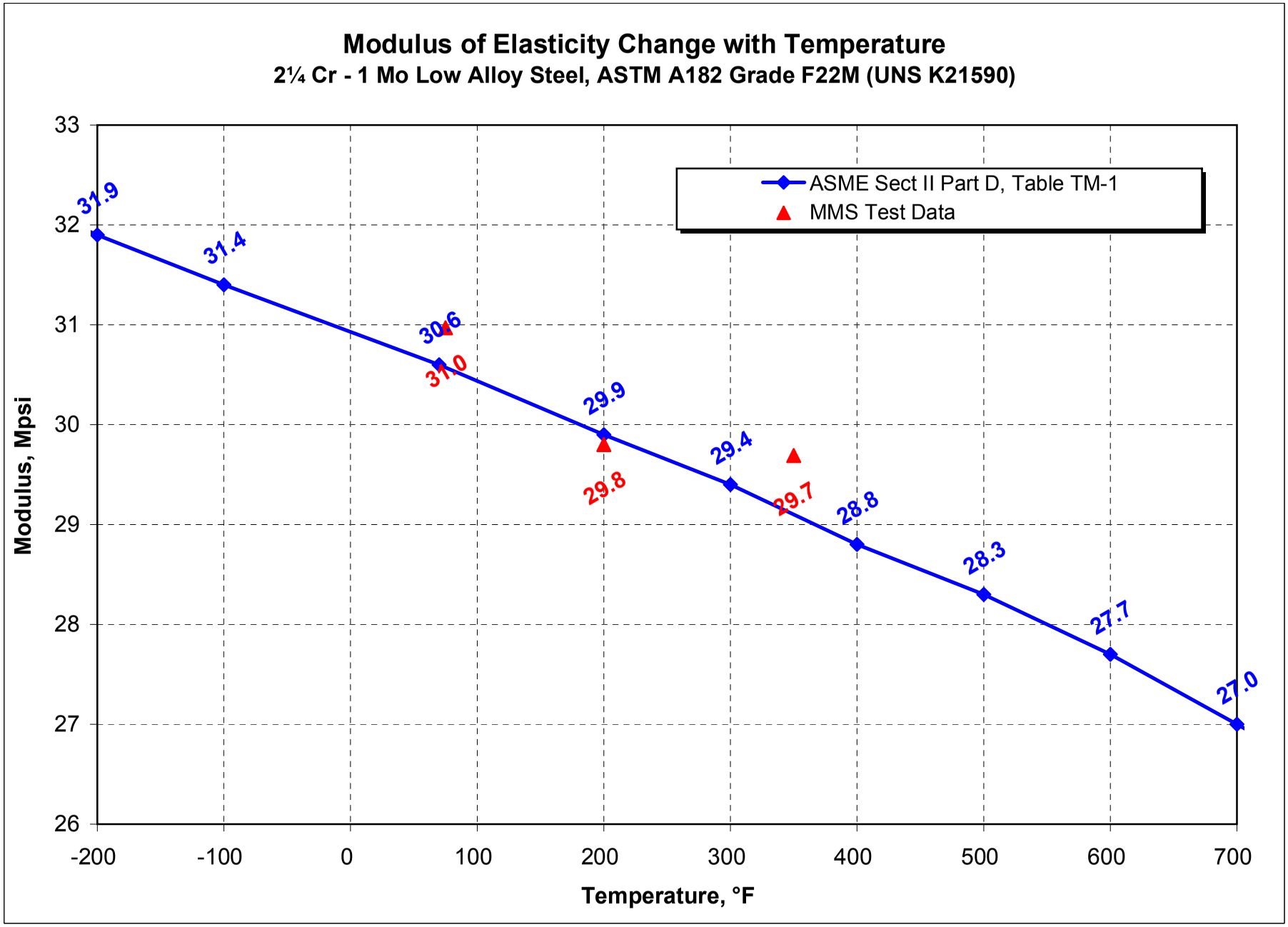

Figure 8 172883 Test Results.xls 2/19/2008

Annex E. Results from Charpy V-notch Tests

Annex E.1. Lab Charpy Test Data

BRYAN LABORATORY, INC.

METALLURGICAL CONSULTATION - INSPECTION - TESTING
ANALYTICAL SERVICES - FAILURE ANALYSIS
6919 ALMEDA ROAD (77021)
P. O. BOX 300366
HOUSTON, TX 77230-0366
TELEPHONE 713/747-7470 800/922-7470 FAX 713/747-7477

REPORT

Lab. No. B0L7-0434 **April 27, 2007**

ON: Steel

TO: Stress Engineering Services, Inc.
13800 Westfair East Drive
Houston, Texas 77041-1101

Attention: Mr. Kenneth Young

IDENTITY: Purchase Order No. 172883-YOK-20070420; Four blanks identified as from Block 1, four blanks identified as from Block 2 and four blanks identified as from Block 3

IMPACT TESTS

Specimen Type - Transverse, Full size, Charpy V-notch

Test Temperature - -20°F

Block No., Specimen		Absorbed Energy, Foot-Pounds	Percent Shear	Lateral Expansion, mils
1-1	-	85	66	58
1-2	-	98	80	66
1-3	-	100	85	66
1-4	-	98	80	62
2-1	-	123	100	76
2-2	-	121	100	74
2-3	-	102	75	66
2-4	-	124	100	83
3-1	-	145	100	86
3-2	-	140	100	84
3-3	-	144	100	89
3-4	-	108	80	71

Respectfully submitted,
BRYAN LABORATORY, INC.

Signature on Original Only

Walter T. Bryan

1/bb

NOTICE
The samples and/or specimens remaining from these tests or analyses will be discarded seven days after the date of this report, unless arrangements are made to the contrary.

BRYAN LABORATORY, INC.

METALLURGICAL CONSULTATION - INSPECTION - TESTING
ANALYTICAL SERVICES - FAILURE ANALYSIS
6919 ALMEDA ROAD (77021)
P. O. BOX 300366
HOUSTON, TX 77230-0366
TELEPHONE 713/747-7470 800/922-7470 FAX 713/747-7477

REPORT

Lab. No. B0L7-1202 **October 31, 2007**

ON: Steel

TO: Stress Engineering Services, Inc.
13800 Westfair East Drive
Houston, Texas 77041-1101

Attention: Mr. Kenneth Young

IDENTITY: Purchase Order No. 172883-YOK-20071026; Three blanks identified as from Block 1, Block 2 and Block 3

IMPACT TESTS

Specimens - Full Size, Charpy V notch

Sample Specimen		Test Temperature, °F	Absorbed Energy, Foot-Pounds	Percent Shear	Lateral Expansion, mils
1-1	-	-75	26	20	19
1-2	-	10	117	75	72
1-3	-	40	124	100	78
1-4	-	-50	27	25	22
1-7	-	75	120	100	73
2-1	-	-75	42	15	29
2-2	-	10	128	100	82
2-3	-	40	122	100	79
2-4	-	-50	63	30	44
2-7	-	75	130	100	75
3-1	-	-75	64	20	44
3-2	-	10	148	100	82
3-3	-	40	140	100	84
3-4	-	-50	90	50	60
3-7	-	75	130	100	76

Respectfully submitted,
BRYAN LABORATORY, INC.

Walter T. Bryan

1/bb

NOTICE
The samples and/or specimens remaining from these tests or analyses will be discarded seven days after the date of this report, unless arrangements are made to the contrary.

Annex E.2. Charpy Data Analysis

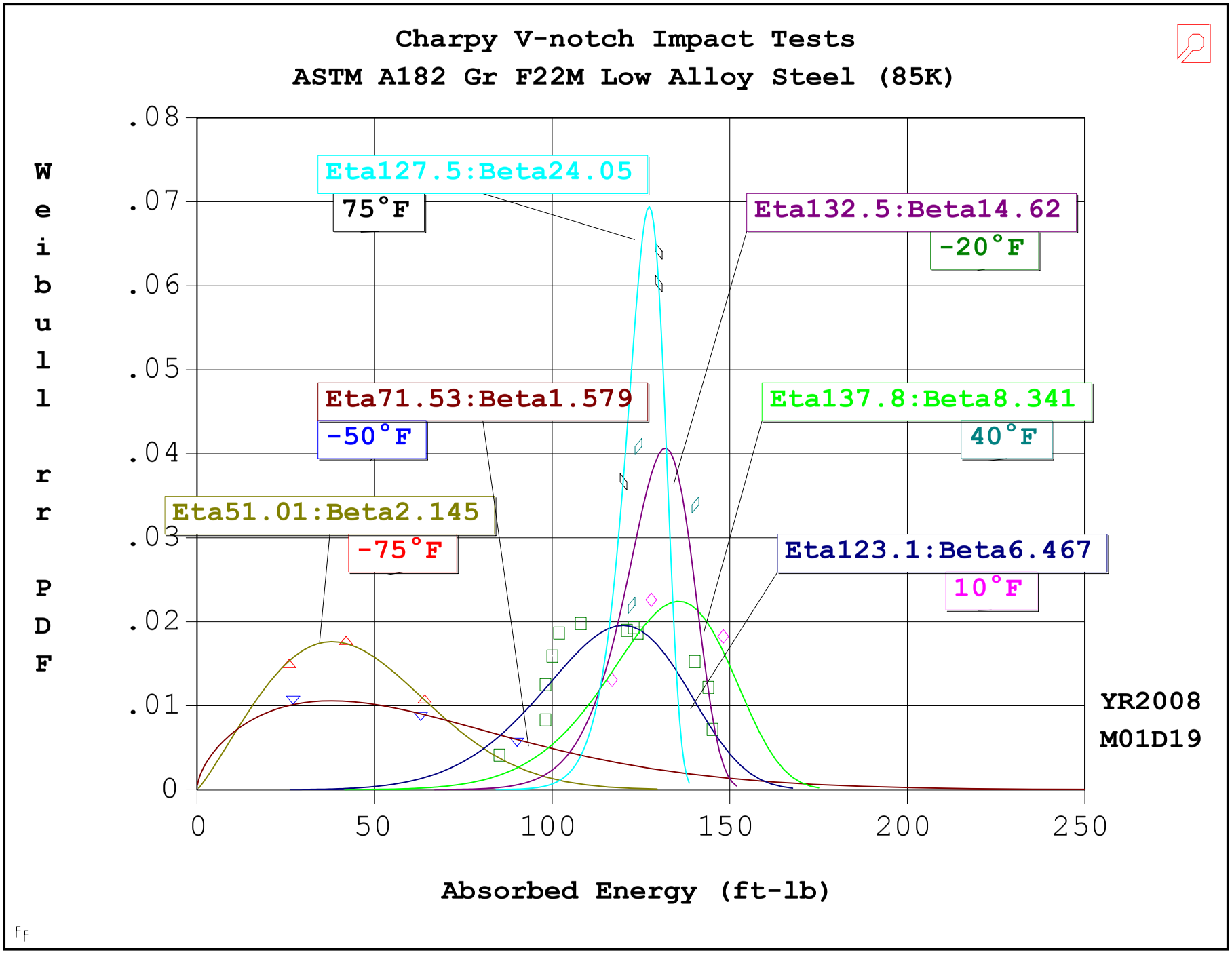
Charpy V-notch Impact Tests
ASTM A182 Gr F22M Low Alloy Steel (85K)
Weibull rr PDF
.08
.07
.06
.05
.04
.03
.02
.01
0
0
50
100
150
200
250
Absorbed Energy (ft-lb)
Eta127.5:Beta24.05
75°F
Eta132.5:Beta14.62
-20°F
Eta71.53:Beta1.579
-50°F
Eta137.8:Beta8.341
40°F
Eta51.01:Beta2.145
-75°F
Eta123.1:Beta6.467
10°F
YR2008
M01D19

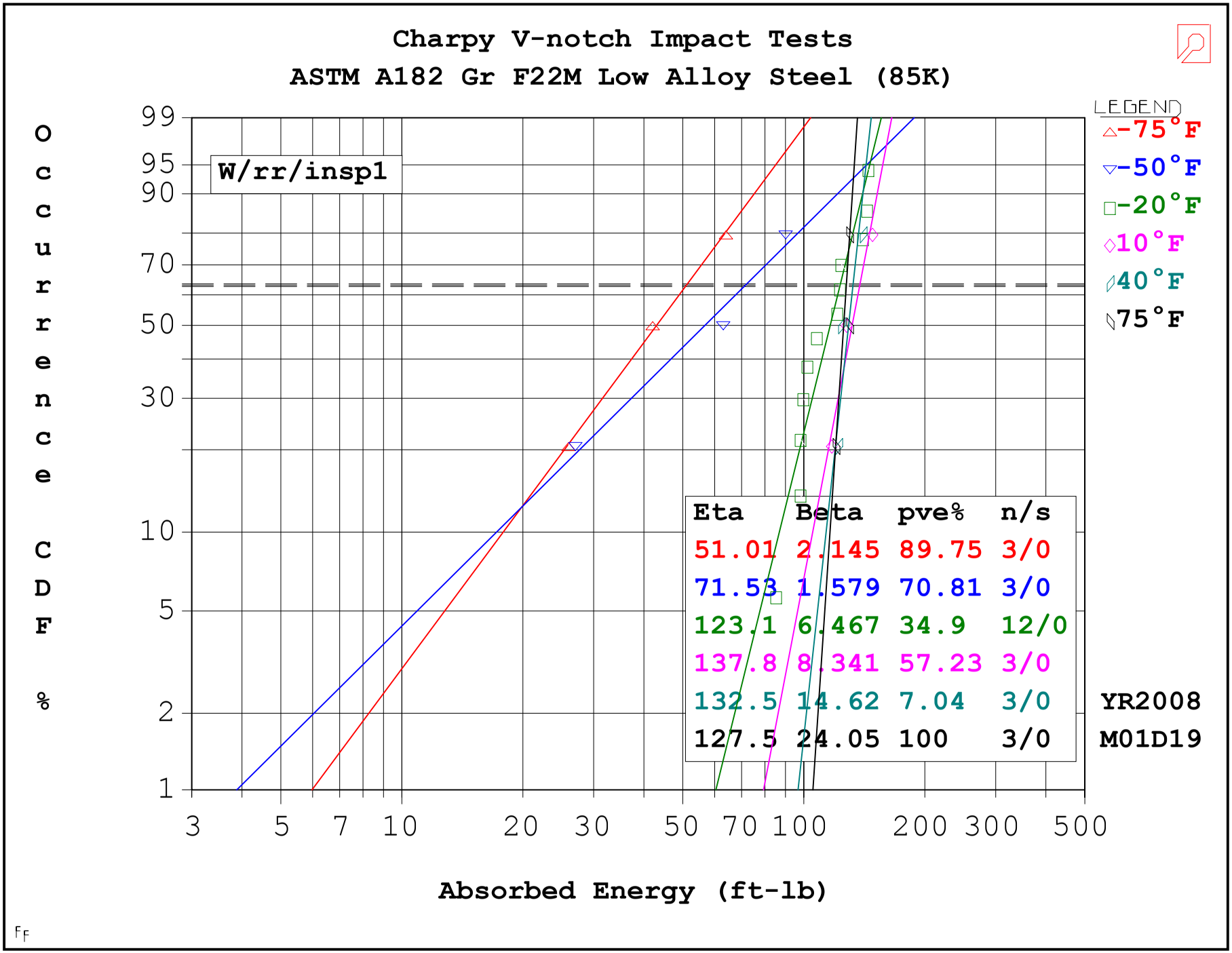
Charpy V-notch Impact Tests
ASTM A182 Gr F22M Low Alloy Steel (85K)
W/rr/insp1
Occurrence CDF %
99
95
90
70
50
30
10
5
2
1
3
5
7
10
20
30
50
70
100
200
300
500
Absorbed Energy (ft-lb)
LEGEND
-75°F
-50°F
-20°F
10°F
40°F
75°F
Eta Beta pve% n/s
51.01 2.145 89.75 3/0
71.53 1.579 70.81 3/0
123.1 6.467 34.9 12/0
137.8 8.341 57.23 3/0
132.5 14.62 7.04 3/0
127.5 24.05 100 3/0
YR2008
M01D19

Weibull Analysis Report

Set 1 - -75°F Date: YR2008-M01-D19
Charpy V-notch Impact Tests ASTM A182 Gr F22M Low Alloy Steel (85K)
Correlation(r)=.9985 r^2=.997 ccc^2=.792 pve%=89.75 (Okay)
Characteristic Value=51.01 Weibull Slope=2.145 Method=rr/insp1
Mean=45.18 Std. Deviation=22.17 Cv%=49.08
Point Quantity=3 (Susp=0)

B%	Absorbed Energy (
1	5.975
2	8.274
5	12.77
10	17.87
20	25.35
50	43

Weibull Analysis Report

Set 2 - -50°F Date: YR2008-M01-D19
Charpy V-notch Impact Tests ASTM A182 Gr F22M Low Alloy Steel (85K)
Correlation(r)=.98894 r^2=.978 ccc^2=.792 pve%=70.81 (Okay)
Characteristic Value=71.53 Weibull Slope=1.579 Method=rr/insp1
Mean=64.21 Std. Deviation=41.59 Cv%=64.76
Point Quantity=3 (Susp=0)

B%	Absorbed Energy (
1	3.885
2	6.045
5	10.9
10	17.2
20	27.67
50	56.71

Weibull Analysis Report

Set 3 - -20°F Date: YR2008-M01-D19
Charpy V-notch Impact Tests ASTM A182 Gr F22M Low Alloy Steel (85K)
Correlation(r)=.96125 r^2=.924 ccc^2=.8663 pve%=34.9 (Okay)
Characteristic Value=123.1 Weibull Slope=6.467 Method=rr/insp1
Mean=114.7 Std. Deviation=20.73 Cv%=18.08
Point Quantity=12 (Susp=0)

B%	Absorbed Energy (
1	60.44
2	67.33
5	77.77
10	86.92
20	97.62
50	116.3

Weibull Analysis Report

Set 4 - 10°F Date: YR2008-M01-D19
Charpy V-notch Impact Tests ASTM A182 Gr F22M Low Alloy Steel (85K)
Correlation(r)=.97622 r^2=.953 ccc^2=.792 pve%=57.23 (Okay)
Characteristic Value=137.8 Weibull Slope=8.341 Method=rr/insp1
Mean=130 Std. Deviation=18.54 Cv%=14.26
Point Quantity=3 (Susp=0)

B%	Absorbed Energy (
1	79.36
2	86.29
5	96.48
10	105.2
20	115.1
50	131.8

Weibull Analysis Report

Set 5 - 40°F Date: YR2008-M01-D19
Charpy V-notch Impact Tests ASTM A182 Gr F22M Low Alloy Steel (85K)
Correlation(r)=.87807 r^2=.771 ccc^2=.792 pve%=7.04 (pve%<10!)
Characteristic Value=132.5 Weibull Slope=14.62 Method=rr/insp1
Mean=127.9 Std. Deviation=10.71 Cv%=8.379
Point Quantity=3 (Susp=0)

B%	Absorbed Energy (
1	96.74
2	101.5
5	108.2
10	113.6
20	119.6
50	129.2

Weibull Analysis Report

Set 6 - 75°F Date: YR2008-M01-D19
Charpy V-notch Impact Tests ASTM A182 Gr F22M Low Alloy Steel (85K)
Correlation(r)=1 r^2=1 ccc^2=0 pve%=100 (Okay)
Characteristic Value=127.5 Weibull Slope=24.05 Method=rr/insp1
Mean=124.7 Std. Deviation=6.459 Cv%=5.179
Point Quantity=3 (Susp=0)

B%	Absorbed Energy (
1	105.3
2	108.4
5	112.7
10	116.2
20	119.8
50	125.6

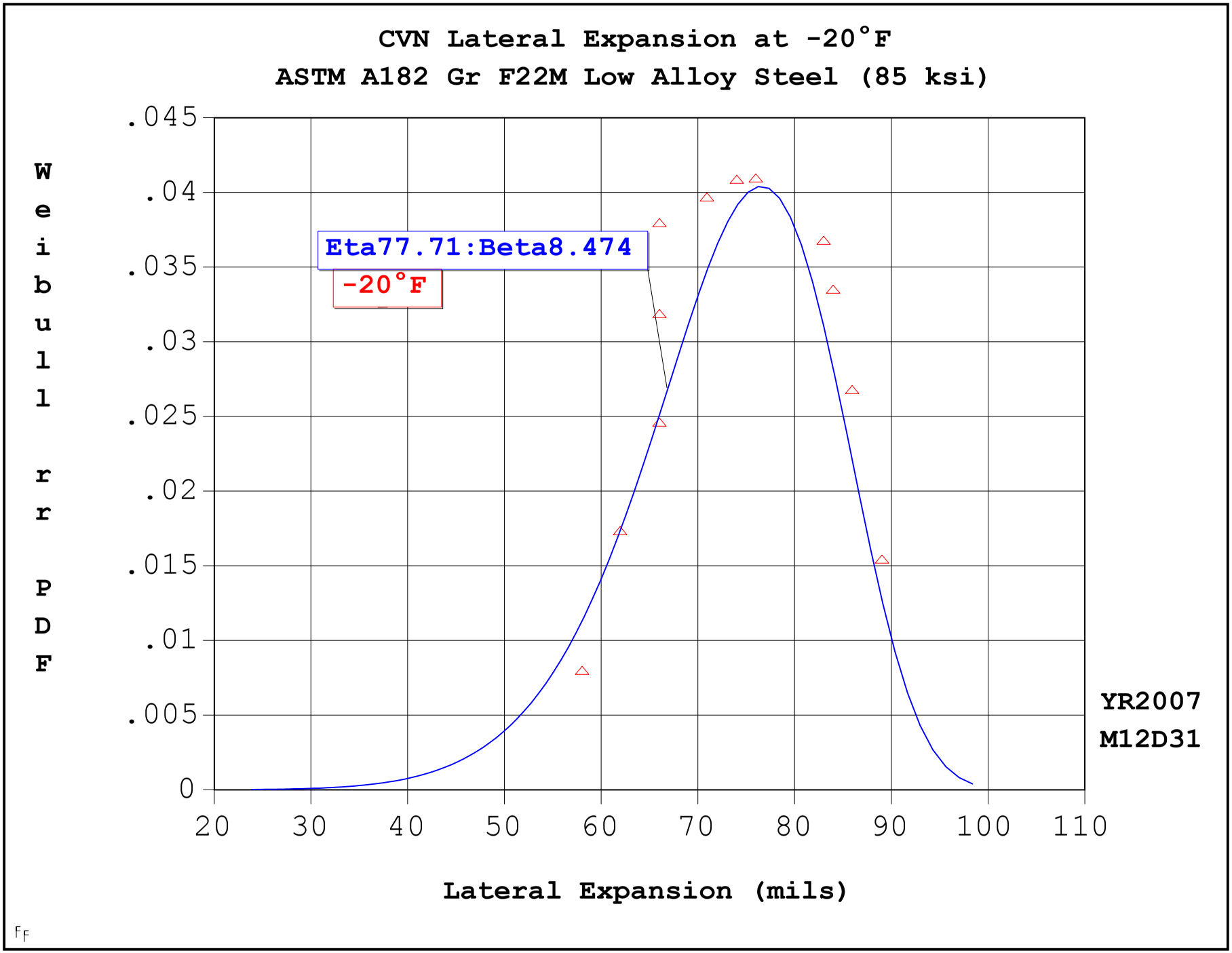
CVN Lateral Expansion at -20°F
ASTM A182 Gr F22M Low Alloy Steel (85 ksi)
Weibull rr PDF
.045
.04
.035
.03
.025
.02
.015
.01
.005
0
20
30
40
50
60
70
80
90
100
110
Lateral Expansion (mils)
Eta77.71:Beta8.474
-20°F
YR2007
M12D31

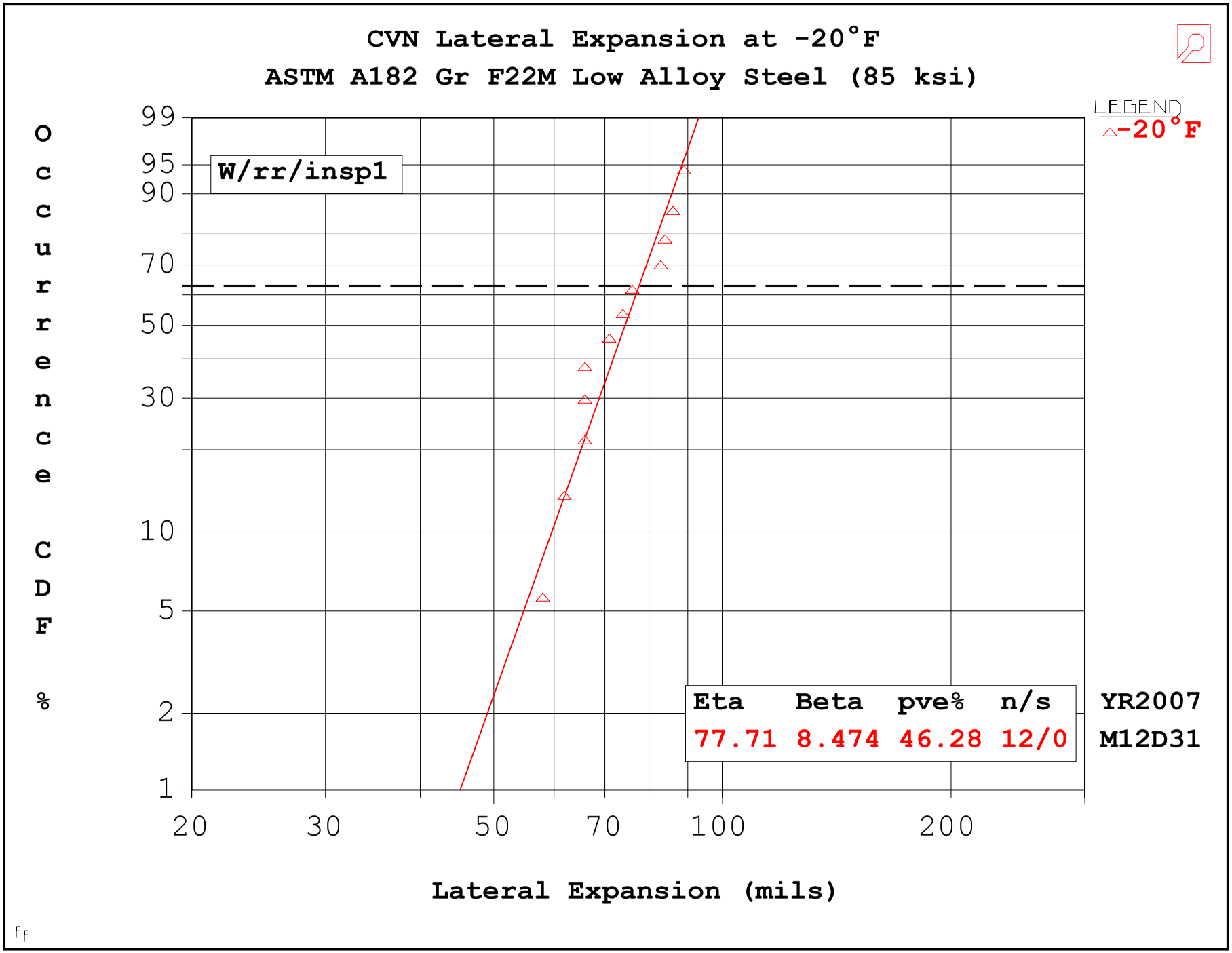
CVN Lateral Expansion at -20°F
ASTM A182 Gr F22M Low Alloy Steel (85 ksi)
LEGEND
-20°F
W/rr/insp1
Occurrence CDF %
99
95
90
70
50
30
10
5
2
1
20
30
50
70
100
200
Lateral Expansion (mils)
Eta Beta pve% n/s
77.71 8.474 46.28 12/0
YR2007
M12D31

Weibull Analysis Report

Set 1 - -20°F Date: YR2007-M12-D31
CVN Lateral Expansion at -20°F ASTM A182 Gr F22M Low Alloy Steel (85 ksi)
Correlation(r)=.96644 r^2=.934 ccc^2=.8594 pve%=46.28 (Okay)
Characteristic Value=77.71 Weibull Slope=8.474 Method=rr/insp1
Mean=73.38 Std. Deviation=10.31 Cv%=14.05
Point Quantity=12 (Susp=0)

B%	Lateral Expansion
1	45.15
2	49.03
5	54.73
10	59.58
20	65.1
50	74.42

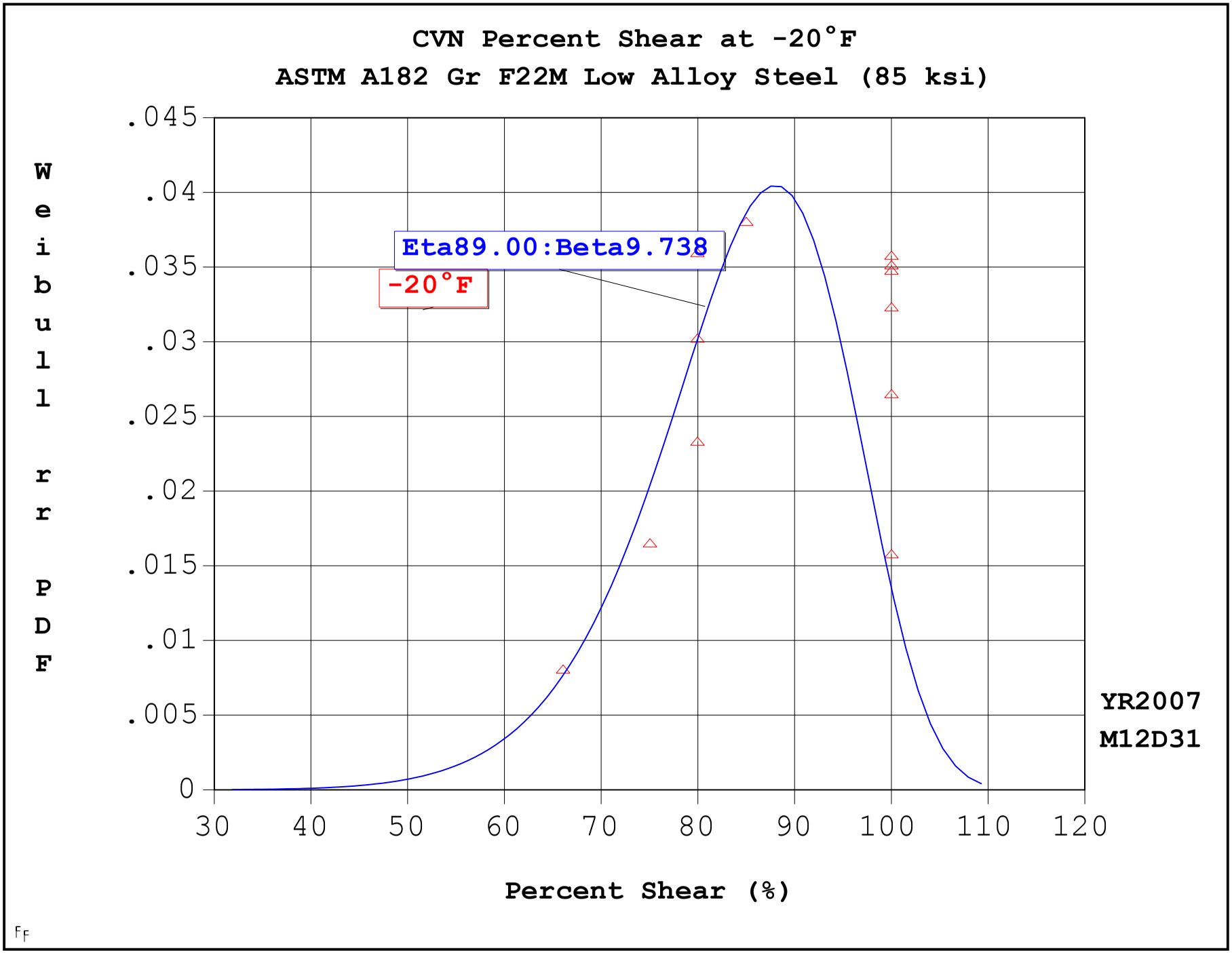
CVN Percent Shear at -20°F
ASTM A182 Gr F22M Low Alloy Steel (85 ksi)
Weibull rr PDF
.045
.04
.035
.03
.025
.02
.015
.01
.005
0
30
40
50
60
70
80
90
100
110
120
Percent Shear (%)
Eta89.00:Beta9.738
-20°F
YR2007
M12D31

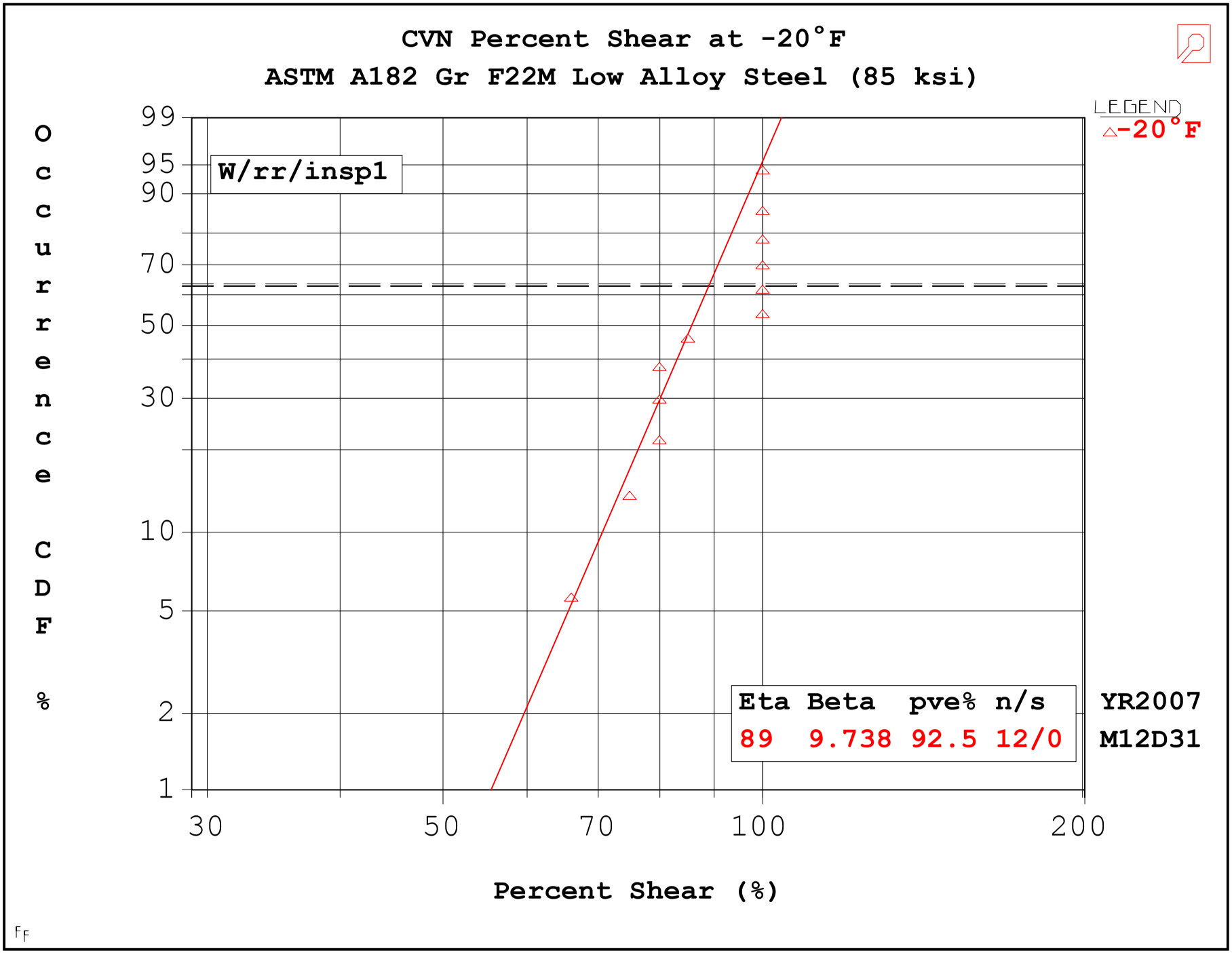
CVN Percent Shear at -20°F
ASTM A182 Gr F22M Low Alloy Steel (85 ksi)
LEGEND
-20°F
W/rr/insp1
Occurrence CDF %
99
95
90
70
50
30
10
5
2
1
30
50
70
100
200
Percent Shear (%)
Eta Beta pve% n/s
89 9.738 92.5 12/0
YR2007
M12D31

Weibull Analysis Report

Set 1 - -20°F Date: YR2007-M12-D31
CVN Percent Shear at -20°F ASTM A182 Gr F22M Low Alloy Steel (85 ksi)
Correlation(r)=.99045 r^2=.981 ccc^2=.8076 pve%=92.5 (Okay)
Characteristic Value=89 Weibull Slope=9.738 Method=rr/insp1
Mean=84.58 Std. Deviation=10.43 Cv%=12.33
Point Quantity=12 (Susp=0)

B%	Percent Shear (%)
1	55.49
2	59.62
5	65.6
10	70.64
20	76.3
50	85.71

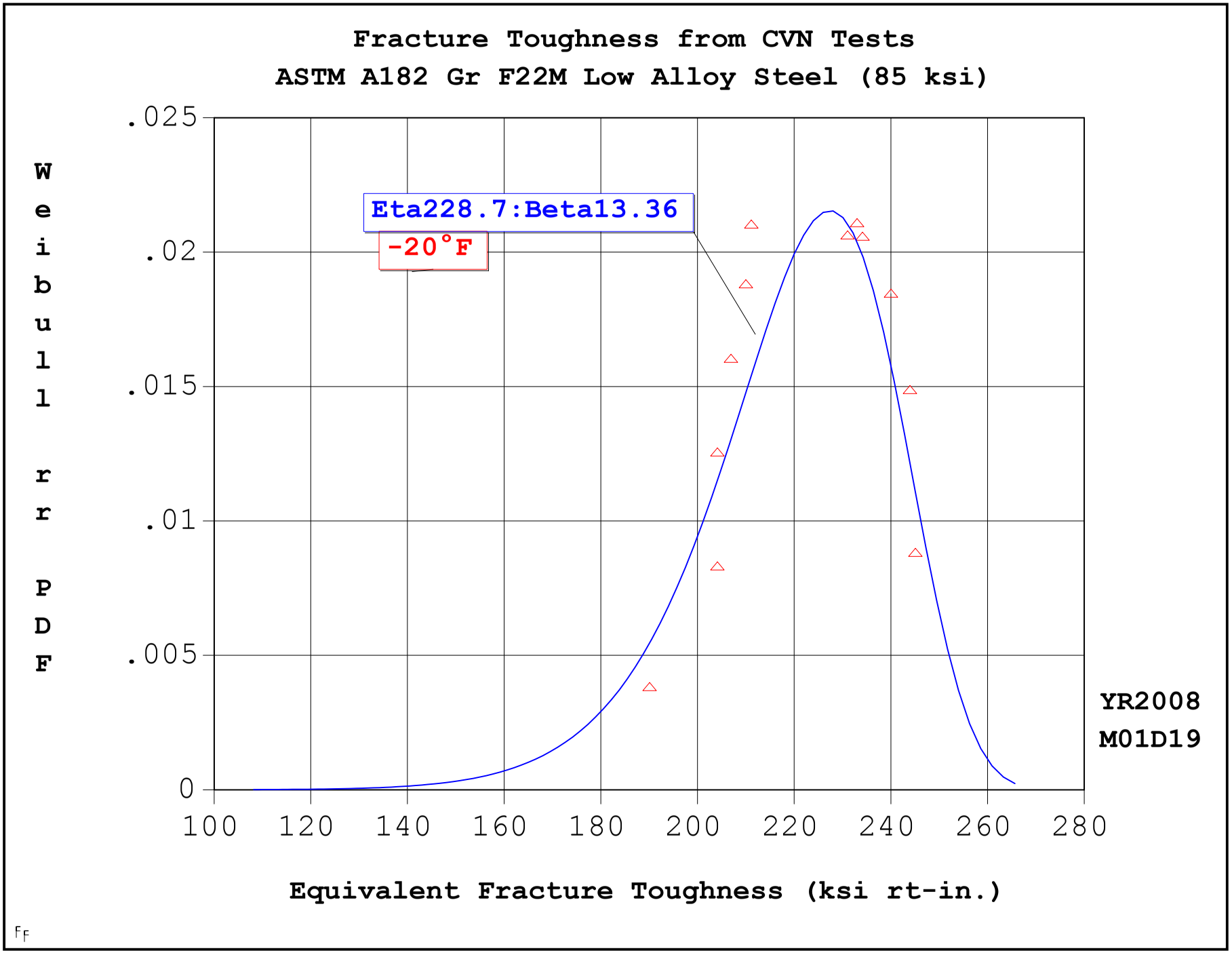
Fracture Toughness from CVN Tests
ASTM A182 Gr F22M Low Alloy Steel (85 ksi)
Eta228.7:Beta13.36
-20°F
Weibull PDF
.025
.02
.015
.01
.005
0
100
120
140
160
180
200
220
240
260
280
Equivalent Fracture Toughness (ksi rt-in.)
YR2008
M01D19

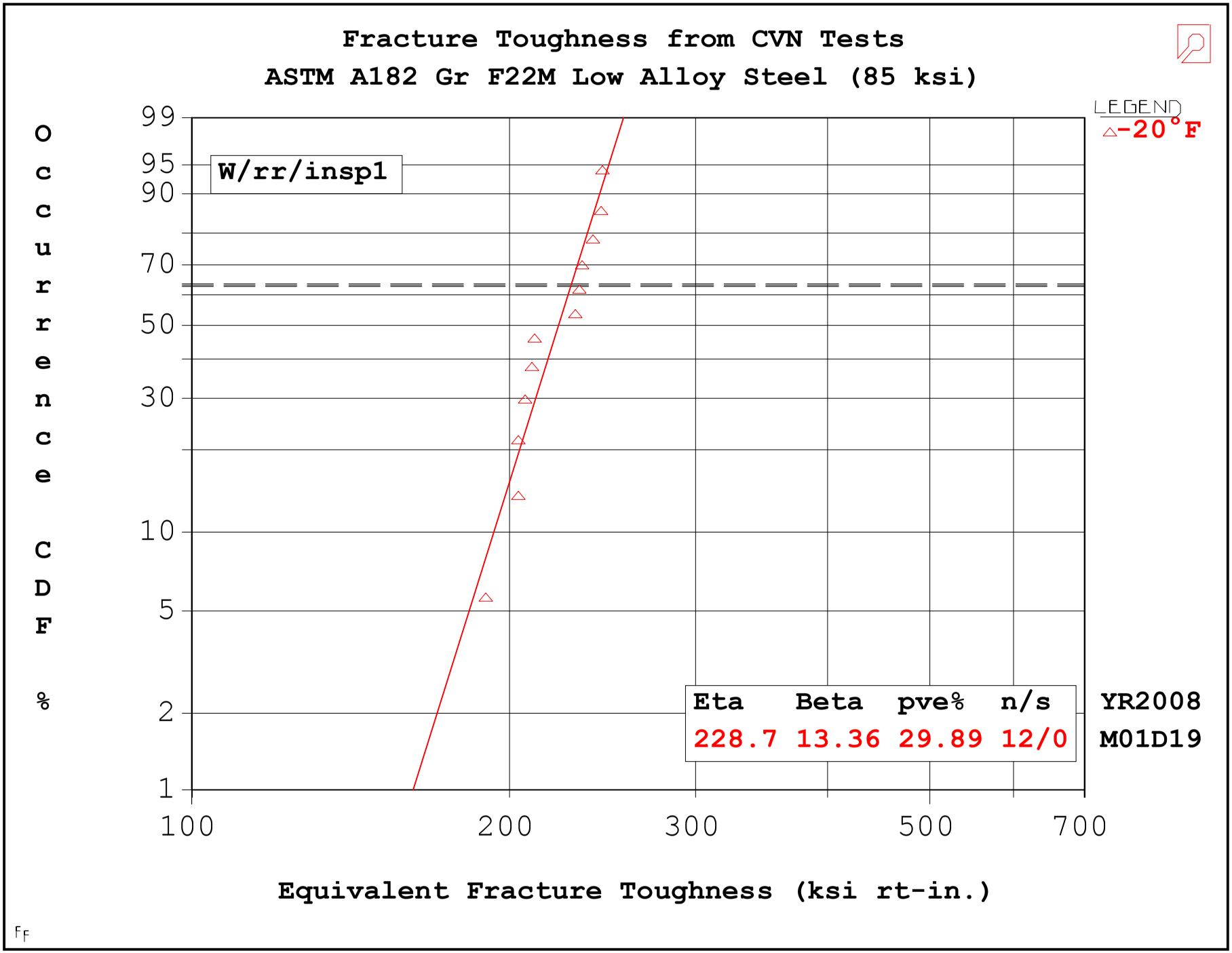
Fracture Toughness from CVN Tests
ASTM A182 Gr F22M Low Alloy Steel (85 ksi)
LEGEND
△-20°F
W/rr/insp1
Occurrence CDF %
99
95
90
70
50
30
10
5
2
1
100
200
300
500
700
Eta Beta pve% n/s
228.7 13.36 29.89 12/0
YR2008
M01D19
Equivalent Fracture Toughness (ksi rt-in.)

Weibull Analysis Report

Set 1 - -20°F Date: YR2008-M01-D19
Fracture Toughness from CVN Tests ASTM A182 Gr F22M Low Alloy Steel (85 ksi)
Correlation(r)=.9576 r^2=.917 ccc^2=.8663 pve%=29.89 (Okay)
Characteristic Value=228.7 Weibull Slope=13.36 Method=rr/insp1
Mean=220 Std. Deviation=20.1 Cv%=9.136
Point Quantity=12 (Susp=0)

B%	Equivalent Fractu
1	162.1
2	170.8
5	183.1
10	193.3
20	204.4
50	222.5

Annex F. Results from Fracture Toughness Tests

Annex F.1. Lab Toughness Test Data

Stress Engineering Services
13800 Westfair East Drive
Houston TX
77041

Report No. 703400
Date 01/25/08

Slow Strain Fracture Toughness Analysis of F22 Grade Steel using Mild Sour and Cathodic Protection Pre-Charging Test Methods.

Eighteen pre-cut test blocks were delivered to Bodycote Testing Group by Stress Engineering identified by an individual serial number and color coded for notch placement purposes.

The blocks were machined to a compact tension C(T) specimen geometry according to ASTM E1820 figure A2.1 with a nominal width of 2-inch and thickness of 1-inch and notched in the S-T orientation.

All samples were tested and analyzed within the general guidelines of ASTM E1820 with the exception of a slower applied strain rate as per project requirements.

Summary of Contents

Specimen Configuration ..... Page 3

Specimen Preparation and Test Parameters ..... Pages 4 through 7

Final Test Value Summary ..... Pages 8 through 9

Specimen Dimensions and Crack Length Summary ..... Pages 10 through 20

J-R and Load vs. COD (Clip Gauge Openning Displacement Plots) ... Pages 21 through 40

- Air as Recieved ..... Pages 22 through 27
- CP Charged ..... Pages 28 through 33
- H_2S Mild Sour ..... Pages 34 through 39
- Air as Received Control sample ..... Page 40

Fracture Face Photographs ..... Pages 41 through 51

- Air as Recieved Fracture Faces ..... Pages 42 through 44
- CP Charged Fracture Faces ..... Pages 45 through 47
- H_2S Mild Sour Fracture Faces ..... Pages 48 through 50
- Air as Received Control sample ..... Page 51

Tabulated Step Data ..... Pages 52 through 67

- Air as Received Step Data ..... Pages 52 through 57
- CP Charged Step Data ..... Pages 58 through 63
- H_2S Mild Sour Step Data ..... Pages 64 through 66
- Air as Received Control sample ..... Page 67

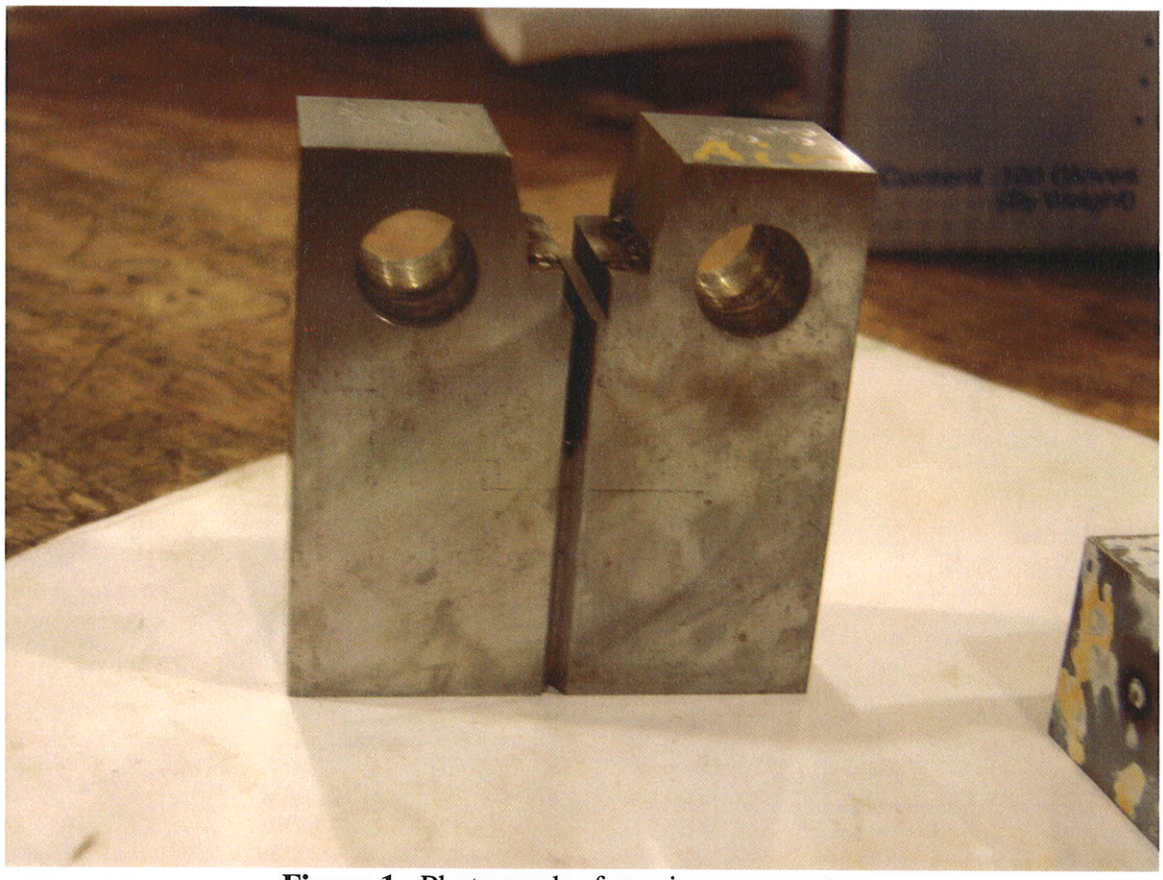

Figure 1. Photograph of specimen geometry

Due to material constraints the compact tension specimen design was selected for this particular test program.

The overall test method has also been proven effective on three-point bend (SEN(B)) samples. The three-point bend design also allows for CP charging during testing (see recommendations).

Eighteen samples were submitted for testing and separated into three main categories:

1. Slow strain tests in laboratory air conditions.
2. Slow strain tests that were pre-charged in a mild sour (H_2S) environment.
3. Slow strain tests that were CP pre-charged in seawater.

Test Method for Stress Engineering Hydrogen-charged Fracture Toughness Testing.

Specimen Preparation

- Specimens were machined into compact tension specimen geometry with a surface ground finish on all faces. Wire EDM was used to machine the notches.

- The holes were first initiated by drilling an initial hole, The EDM wire was then passed through to allow finishing the final required hole size .

- C(T) specimens were pre-cracked to achieve an a/W ratio of approximately 0.5. After pre-cracking side grooves of approximately 0.1B on each side were machined into the specimen prior to exposure to H_2S environment.

Hydrogen Charging

- Specimens were placed in individual test cells with a capacity of approximately 0.8 liters and exposed to a simulated sour environment for a minimum of five days prior to testing. During exposure the cracks were protected from the corrosive environment by using adhesive putty to avoid any corrosive crack tip blunting.

- A buffered solution chemistry was employed, comprising of 5 wt % sodium chloride and 0.4 wt % sodium acetate in deionized water (e.g. 50.0 g of NaCl and 4.0 g of sodium acetate dissolved in 946 g of deionized water). The test solution pH before H_2S saturation was adjusted to 4.0 using hydrochloric acid. A certified premixed test gas was used, comprising 7.0 mol % H_2S, balance nitrogen with a bubble rate of 10ml/min.

Test Method

- After the minimum exposure time had been reached, the first specimen was removed from the H_2S environment immediately prior to testing. The remaining specimens were exposed to environment until required.

- The test specimen was placed immediately in the test machine and tested in air using the unloading compliance method outlined in ASTM E1820 at a test

temperature of 20 Deg C. The nominal displacement rate during the test did not exceed 0.008 mm/min. The partial unloadings/reloadings were performed at loading rates of 0.15 kN/sec.

- J-R curve loading parameters: (Load versus Clip Gauge Displacement)

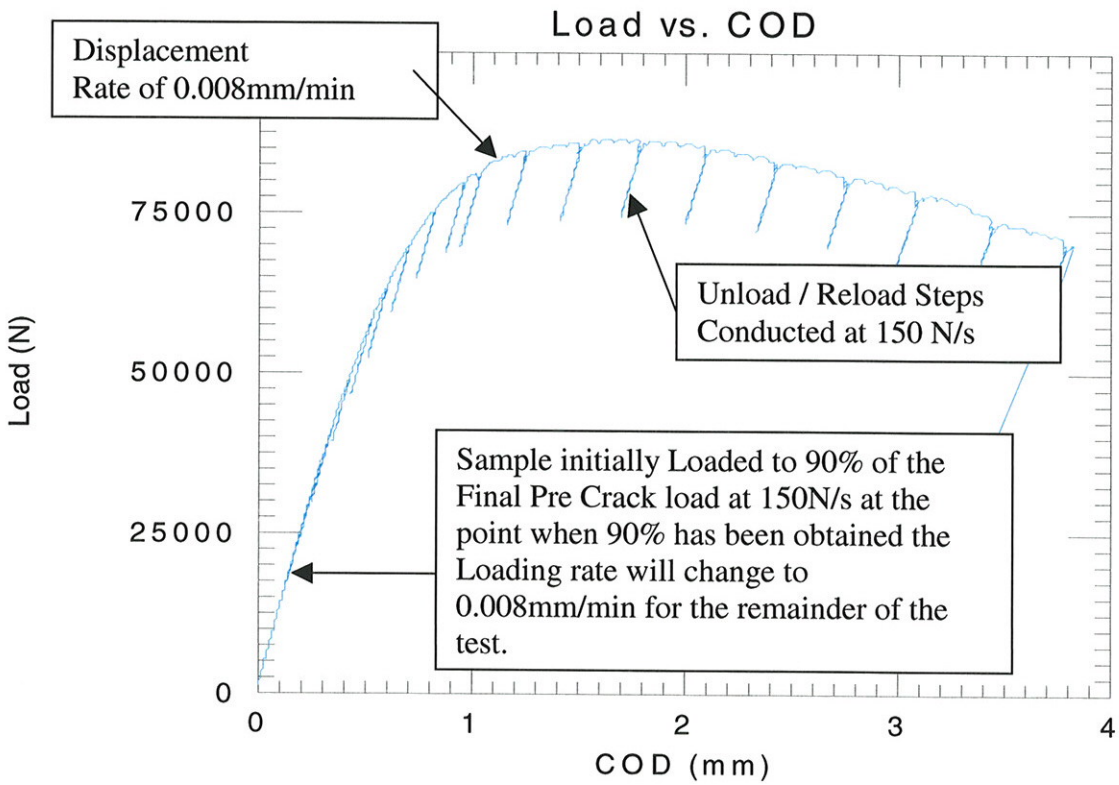

Figure 2. J-R curve loading parameters.

- At the completion of the test each specimen was heat tinted and analyzed in accordance with ASTM E1820.

<u>Test Method For Stress Engineering CP Charged Fracture Toughness Testing.</u>

Specimen Preparation

- Knife-edges were attached to the compact tension specimens of nominal dimensions of 1" x 2" and an electrical connection was made by spot welding a PVC-insulated solid-drawn 0.030" nickel-chromium wire to one end face.

- The specimens were then cleaned and degreased in an alkaline detergent solvent, followed by a two-step solvent rinse with ethanol then acetone, and air-dried. The effectiveness of degreasing was verified by means of the ASTM F21 atomizer test.

Polarization Requirements

- The polarized potential was –1100mV versus Ag/AgCl, KCl (sat'd) as per customer requirements.

- For the laboratory-testing program, double-junction Ag/AgCl, saturated KCl electrodes were used.

Test Solution Environment

- A synthetic seawater solution, prepared in accordance with ASTM D1141 (Stock Solution No. 1 & Stock Solution No.2, without heavy metal ions), was used for all cathodic pre-charging and during the polarized tests. The pH of the freshly prepared solution was measured and, if necessary, adjusted to a value of 8.2 ± 0.1.

- A solution volume of approximately 6 liters was used during the cathodic pre-charging (giving an approximate ratio of 1 liter of test solution per specimen). The test solution was periodically replaced, at least weekly.

Test Equipment

- Cathodic pre-charging was performed in a two-gallon open-topped HDPE vessel at ambient temperature (75°F). A minimum charging period of 5 days was observed prior to mechanical testing.

- Specimens were placed in a Teflon rack to maintain separation between specimens and ensure contact with the test solution on all sides. The Ag/AgCl, KCl (sat'd) reference electrode was located as close as possible to the test specimens. A manually controlled electrochemical potentiostat rated at 1000mA was used to simulate the effects of the cathodic protection in the seawater environment.

- The potentiostat was operated in a three-electrode configuration, with the test specimen(s) connected to the Working Electrode (WE) terminal. A piece of Titanium tubing, 3.5" diameter x 12" long, was connected to the Auxiliary Electrode (AE) terminal, and the Ag/AgCl, KCl (sat'd) reference electrode connected to the Reference Electrode (RE) terminal.

- After the minimum exposure time was reached, the first specimen was removed from the CP charging environment and immediately tested. The remaining specimens were exposed to environment until required.

- The test specimen was immediately placed in the test machine and tested in air using the unloading compliance method outlined in ASTM E1820 at ambient temperature. The nominal displacement rate during the test did not exceed 0.008 mm/min. The partial unloadings/reloadings were performed at loading rates of 0.15 kN/sec.

Recommendations

- The test specimens were observed to develop an adherent calcareous scale during exposure in the synthetic seawater solution. The formation of this scale resulted in a marked decrease in the CP charging current over the exposure period. While this does mimic the actual in-service behavior, it was considered that it would result in the corresponding rate of hydrogen uptake being strongly time-dependent.

  This effect could be eliminated through the use of non scale-forming test environments e.g. a solution of sodium chloride, which would result in a sustained high rate of hydrogen uptake, and hence a more conservative test.

- It would be recommended in future work involving CP Charging that SEN(B) specimens should be utilized due to the inability to expose the clip gages to a saltwater environment. SEN(B) specimens would allow for the tests to be performed in the CP charged seawater because the clip gage is positioned up on the specimen above the environment.

Post Test Value Summary

Table 1. Test Results

Sample No.	Test Rate (mm/min)	Test Condition	CTOD Max Load (mm)	J Max Load (MPa-mm)	K Max Load (MPa√m)
1-05-T1	0.008	Air	0.218	245	233
1-05-T2	0.008	Air	0.244	272	249
2-05-T1	0.008	Air	0.271	295	260
2-05-T2	0.008	Air	0.261	285	255
3-05-T1	0.008	Air	0.298	323	272
3-05-T2	0.008	Air	0.310	344	280
1-06-T-1	0.008	H_2S Saturated	0.066	74	130
1-06-T-2	0.008	H_2S Saturated	0.066	72	128
2-06-T-1	0.008	H_2S Saturated	0.063	72	128
2-06-T-2	0.008	H_2S Saturated	0.066	74	130
3-06-T-1	0.008	H_2S Saturated	0.081	88	142
3-06-T-2	0.008	H_2S Saturated	0.086	100	151
1-05-T-1	0.008	CP Charged	0.231	252	240
1-05-T-2	0.008	CP Charged	0.287	313	267
2-05-T-1	0.008	CP Charged	0.244	262	245
2-05-T-2	0.008	CP Charged	0.250	270	248
3-05-T-1	0.008	CP Charged	0.352	346	281
3-05-T-2	0.008	CP Charged	0.304	330	275

A control sample tested in air using a ramp rate of 0.011mm/s in conjunction with a load / unload rate of 300 N/s

2-07-T-1	0.66	Air	0.430	506	340

Post Test Value Summary

Table 2. Test Results at 0.2-mm offset line

Sample No.	J (MPa-mm)	CTOD (mm)	K (MPa√m)
1-05-T1	244.7	0.218	236.5
1-05-T2	270.8	0.227	248.8
2-05-T1	259.8	0.223	243.7
2-05-T2	256.0	0.238	241.9
3-05-T1	253.2	0.228	240.6
3-05-T2	285.2	0.237	255.3
1-06-T-1	16.9	0.013	62.2
1-06-T-2	9.6	0.007	46.8
2-06-T-1	17.1	0.013	62.5
2-06-T-2	6.4	0.005	38.2
3-06-T-1	13.6	0.016	55.8
3-06-T-2	11.5	0.003	51.3
1-05-T-1	219.9	0.187	224.2
1-05-T-2	230.3	0.193	229.4
2-05-T-1	166.4	0.133	195.0
2-05-T-2	229.7	0.199	229.1
3-05-T-1	184.0	0.168	205.1
3-05-T-2	219.3	0.181	223.9
2-07-T-1	506	0.430	340.1

Interpretation of H_2S charged J-R test data should be viewed with caution as stable crack growth Δa begins almost immediately during the test, giving rise to a non-linear JQ / Jmax relationship.

Sample Dimension & Crack Length Data

Table 3. 1-05-T-1 & 2 (Air)

Compact Tension Configuration	1-05-T-1	1-05-T-2
B (mm)	25.48	25.48
W (mm)	50.76	50.78
Net Thickness (mm)	21.02	20.93
Modulus (MPa)	208000	208000
Poisson's Ratio	0.3	0.3
Yield Stress (MPa)	610	610
UTS (MPa)	727	727
Final Pre-crack Load (kN)	18.00	18.00
Pre-crack Stress Ratio	0.1	0.1
Pre-crack Temp (°C)	20	20
Cycles Recorded	46055	47712
Test Temp (°C)	RT	RT
Initial Crack Length (mm)	25.90	26.06
Final Crack Length (mm)	34.38	28.58
CTOD @ Max Load (mm)	0.22	0.24
J @ Max Load (MPa-mm)	239	272

Table 4. 2-05-T-1 & 2 (Air)

Compact Tension Configuration	2-05-T-1	2-05-T-2
B (mm)	25.50	25.52
W (mm)	50.67	50.75
Net Thickness (mm)	20.93	20.98
Modulus (MPa)	208000	208000
Poisson's Ratio	0.3	0.3
Yield Stress (MPa)	610	610
UTS (MPa)	727	727
Final Pre-crack Load (kN)	18.00	18.00
Pre-crack Stress Ratio	0.1	0.1
Pre-crack Temp (°C)	20	20
Cycles Recorded	47225	44803
Test Temp (°C)	RT	RT
Initial Crack Length (mm)	26.12	26.18
Final Crack Length (mm)	29.05	33.48
CTOD @ Max Load (mm)	0.27	0.26
J @ Max Load (MPa-mm)	295	285

Table 5. 3-05-T-1 & 2 (Air)

Compact Tension Configuration	3-05-T-1	3-05-T-2
B (mm)	25.51	25.47
W (mm)	50.77	50.72
Net Thickness (mm)	21.03	20.85
Modulus (MPa)	208000	208000
Poisson's Ratio	0.3	0.3
Yield Stress (MPa)	610	610
UTS (MPa)	727	727
Final Pre-crack Load (kN)	18.00	18.00
Pre-crack Stress Ratio	0.1	0.1
Pre-crack Temp (°C)	20	20
Cycles Recorded	46299	46932
Test Temp (°C)	RT	RT
Initial Crack Length (mm)	25.82	26.03
Final Crack Length (mm)	28.43	29.97
CTOD @ Max Load (mm)	0.30	0.31
J @ Max Load (MPa-mm)	323	344

Table 6. 1-06-T-1 & 2 (H_2S)

Compact Tension Configuration	1-06-T-1	1-06-T-2
B (mm)	25.49	25.47
W (mm)	50.71	50.76
Net Thickness (mm)	20.70	20.50
Modulus (MPa)	208000	208000
Poisson's Ratio	0.3	0.3
Yield Stress (MPa)	610	610
UTS (MPa)	727	727
Final Pre-crack Load (kN)	18.00	18.00
Pre-crack Stress Ratio	0.1	0.1
Pre-crack Temp (°C)	20	20
Cycles Recorded	44855	45162
Test Temp (°C)	RT	RT
Initial Crack Length (mm)	26.13	25.74
Final Crack Length (mm)	28.44	39.43
CTOD @ Max Load (mm)	0.06	0.06
J @ Max Load (MPa-mm)	74	72

Table 7. 2-06-T-1 & 2 (H_2S)

Compact Tension Configuration	2-06-T-1	2-06-T-2
B (mm)	25.48	25.49
W (mm)	50.76	50.77
Net Thickness (mm)	20.49	20.62
Modulus (MPa)	208000	208000
Poisson's Ratio	0.3	0.3
Yield Stress (MPa)	610	610
UTS (MPa)	727	727
Final Pre-crack Load (kN)	18.00	18.00
Pre-crack Stress Ratio	0.1	0.1
Pre-crack Temp (°C)	20	20
Cycles Recorded	47225	46662
Test Temp (°C)	RT	RT
Initial Crack Length (mm)	25.88	26.52
Final Crack Length (mm)	43.48	40.37
CTOD @ Max Load (mm)	0.06	0.06
J @ Max Load (MPa-mm)	72	74

Table 8. 3-06-T-1 & 2 (H_2S)

Compact Tension Configuration	3-06-T-1	3-06-T-2
B (mm)	25.48	25.48
W (mm)	50.78	50.78
Net Thickness (mm)	20.62	20.50
Modulus (MPa)	208000	208000
Poisson's Ratio	0.3	0.3
Yield Stress (MPa)	610	610
UTS (MPa)	727	727
Final Pre-crack Load (kN)	18.00	18.00
Pre-crack Stress Ratio	0.1	0.1
Pre-crack Temp (°C)	20	20
Cycles Recorded	45545	47649
Test Temp (°C)	RT	RT
Initial Crack Length (mm)	26.00	26.26
Final Crack Length (mm)	38.92	36.79
CTOD @ Max Load (mm)	0.08	0.09
J @ Max Load (MPa-mm)	88	100

Table 9. 1-05-T-1 & 2 (CP)

Compact Tension Configuration	1-05-T-1	1-05-T-2
B (mm)	25.47	25.47
W (mm)	50.67	50.80
Net Thickness (mm)	20.62	20.50
Modulus (MPa)	208000	208000
Poisson's Ratio	0.3	0.3
Yield Stress (MPa)	610	610
UTS (MPa)	727	727
Final Pre-crack Load (kN)	18.00	18.00
Pre-crack Stress Ratio	0.1	0.1
Pre-crack Temp (°C)	20	20
Cycles Recorded	46003	45112
Test Temp (°C)	RT	RT
Initial Crack Length (mm)	25.95	26.09
Final Crack Length (mm)	27.75	28.02
CTOD @ Max Load (mm)	0.23	0.29
J @ Max Load (MPa-mm)	252	313

Table 10. 2-05-T-1 & 2 (CP)

Compact Tension Configuration	2-05-T-1	2-05-T-2
B (mm)	25.53	25.47
W (mm)	50.77	50.76
Net Thickness (mm)	20.62	20.50
Modulus (MPa)	208000	208000
Poisson's Ratio	0.3	0.3
Yield Stress (MPa)	610	610
UTS (MPa)	727	727
Final Pre-crack Load (kN)	18.00	18.00
Pre-crack Stress Ratio	0.1	0.1
Pre-crack Temp (°C)	20	20
Cycles Recorded	46366	49371
Test Temp (°C)	RT	RT
Initial Crack Length (mm)	25.9	26.42
Final Crack Length (mm)	32.57	27.94
CTOD @ Max Load (mm)	0.24	0.25
J @ Max Load (MPa-mm)	262	370

Table 11. 3-05-T-1 & 2 (CP)

Compact Tension Configuration	3-05-T-1	3-05-T-2
B (mm)	25.47	25.47
W (mm)	50.78	50.79
Net Thickness (mm)	20.62	20.50
Modulus (MPa)	208000	208000
Poisson's Ratio	0.3	0.3
Yield Stress (MPa)	610	610
UTS (MPa)	727	727
Final Pre-crack Load (kN)	18.00	18.00
Pre-crack Stress Ratio	0.1	0.1
Pre-crack Temp (°C)	20	20
Cycles Recorded	44726	46632
Test Temp (°C)	RT	RT
Initial Crack Length (mm)	26.28	26.17
Final Crack Length (mm)	29.98	30.34
CTOD @ Max Load (mm)	0.35	0.30
J @ Max Load (MPa-mm)	346	330

Table 12. 2-07-T-1 (Air) Control Sample

Compact Tension Configuration	2-07-T-1
B (mm)	25.47
W (mm)	50.77
Net Thickness (mm)	21.05
Modulus (MPa)	208000
Poisson's Ratio	0.3
Yield Stress (MPa)	610
UTS (MPa)	727
Final Pre-crack Load (kN)	18.00
Pre-crack Stress Ratio	0.1
Pre-crack Temp (°C)	20
Cycles Recorded	49943
Test Temp (°C)	RT
Initial Crack Length (mm)	26.24
Final Crack Length (mm)	28.95
CTOD @ Max Load (mm)	0.43
J @ Max Load (MPa-mm)	506

J-R Curve and Load versus Clip Gage Data.

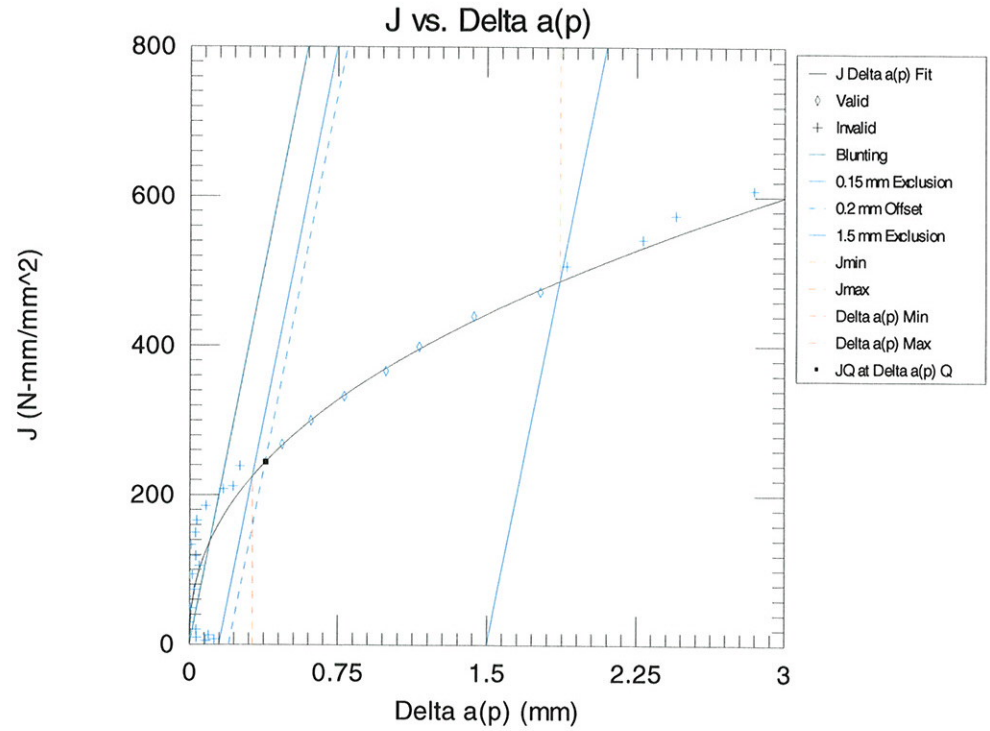

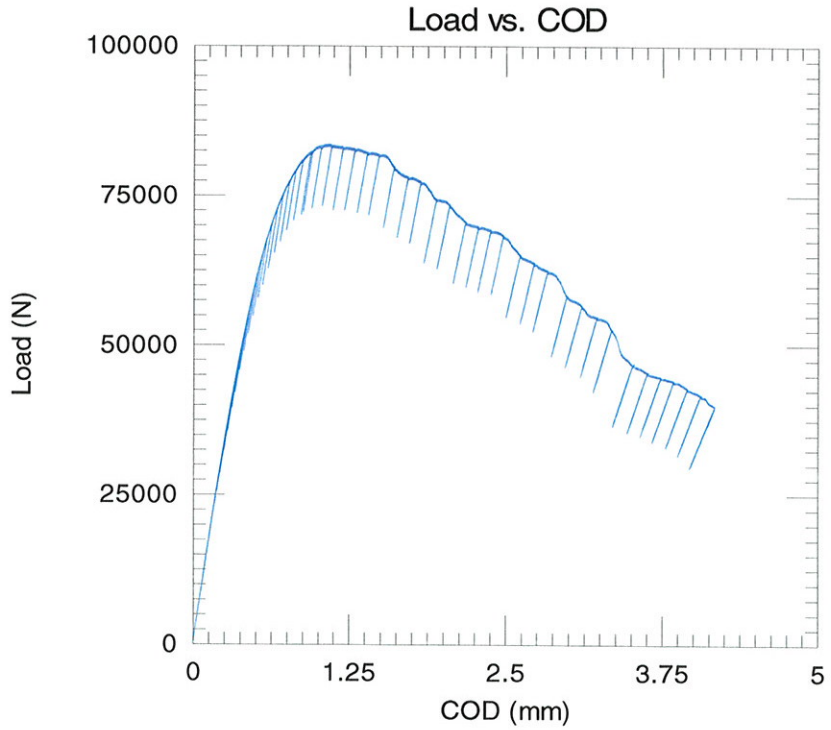

Figure 3. Specimen 1-05-T-1 (Lab Air)

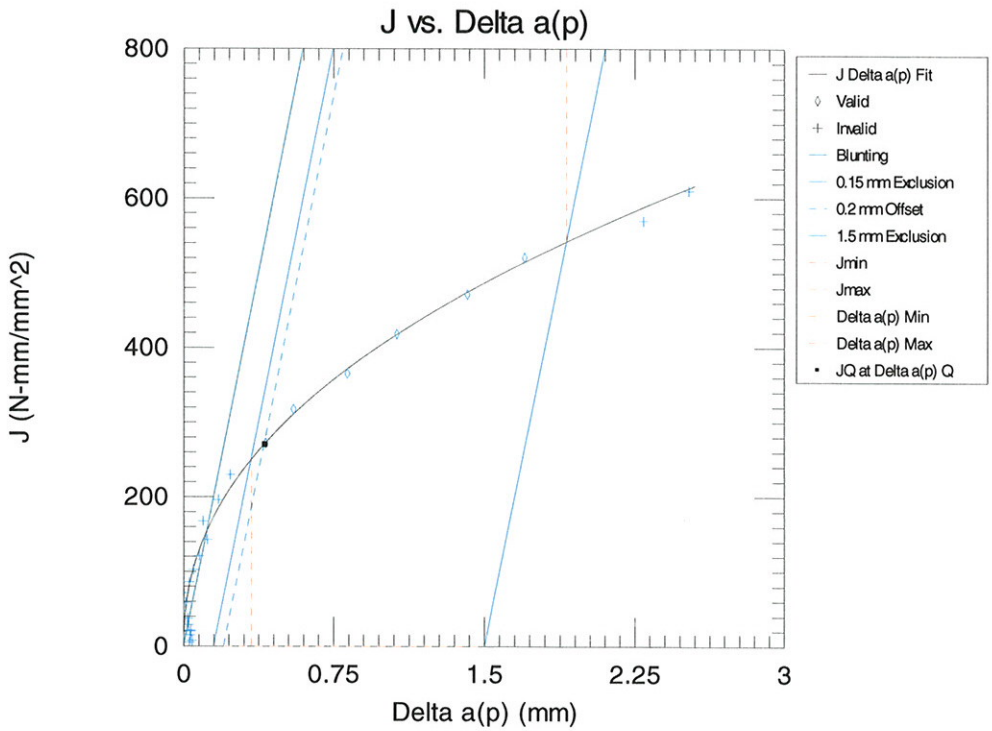

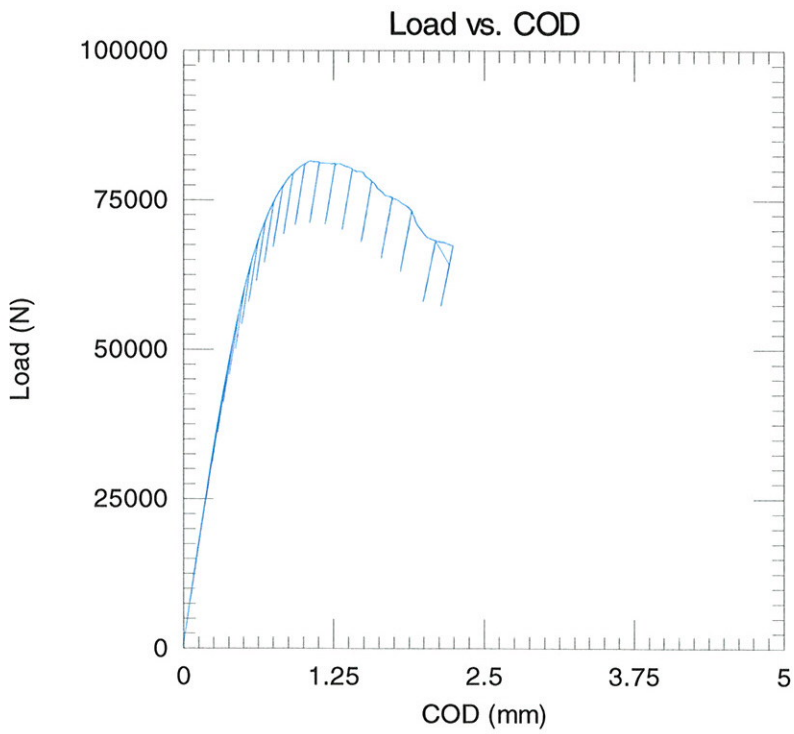

Figure 4. Specimen 1-05-T-2 (Lab Air)

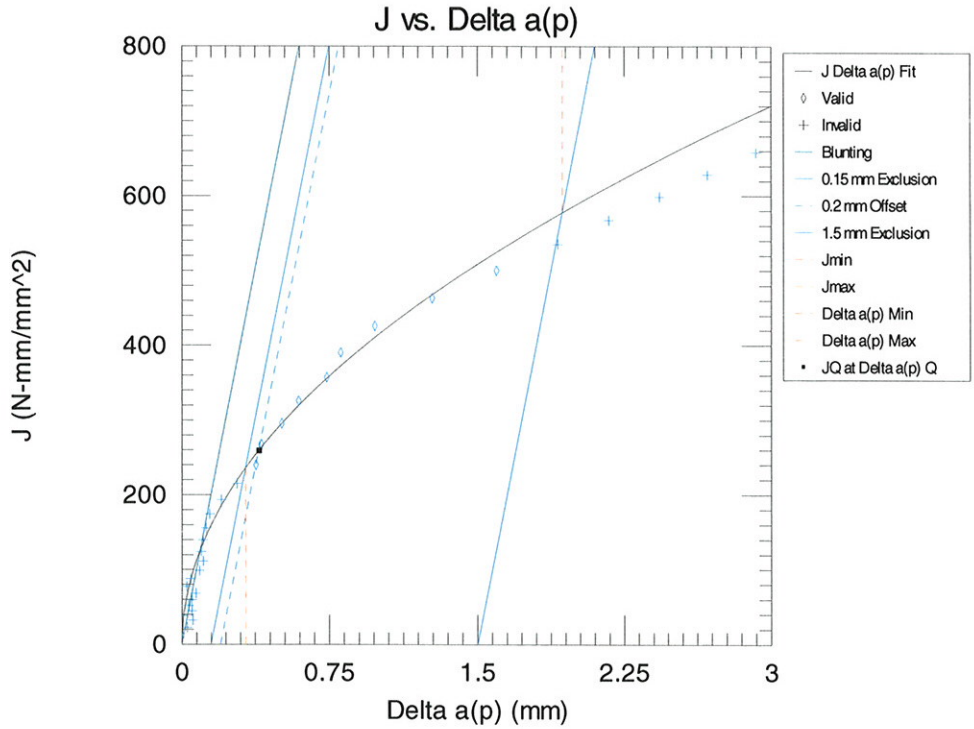

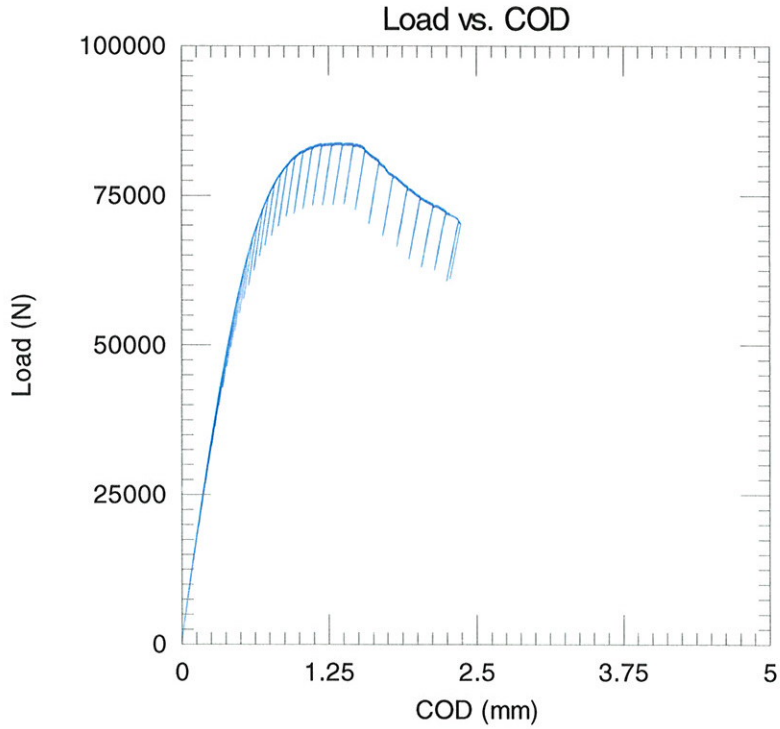

Figure 5. Specimen 2-05-T-1 (Lab Air)

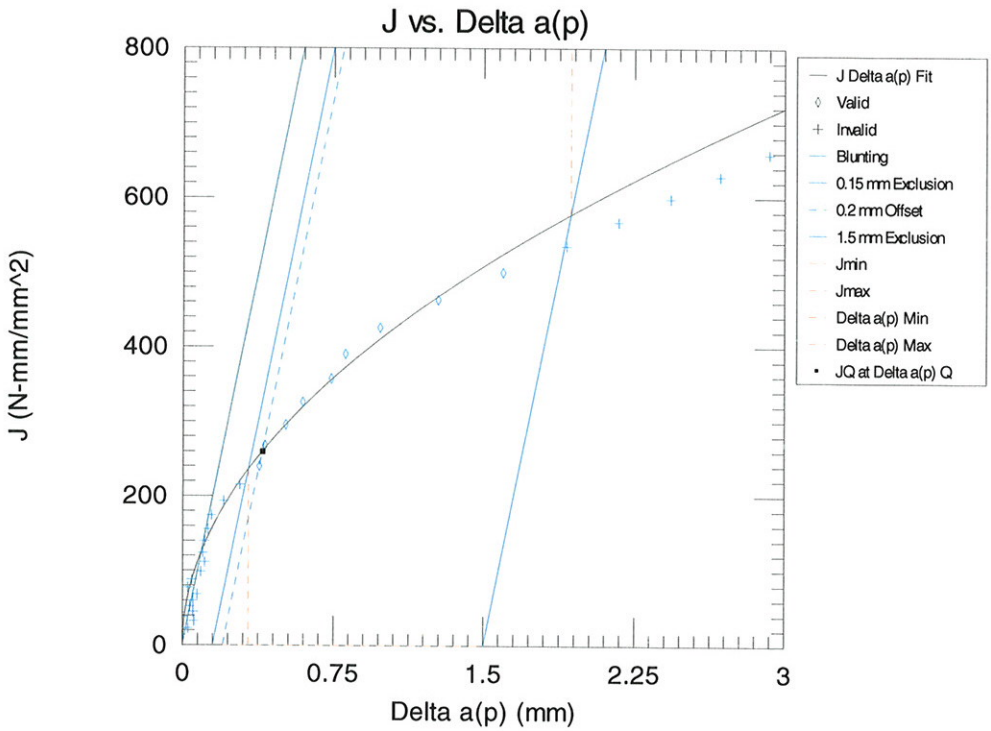

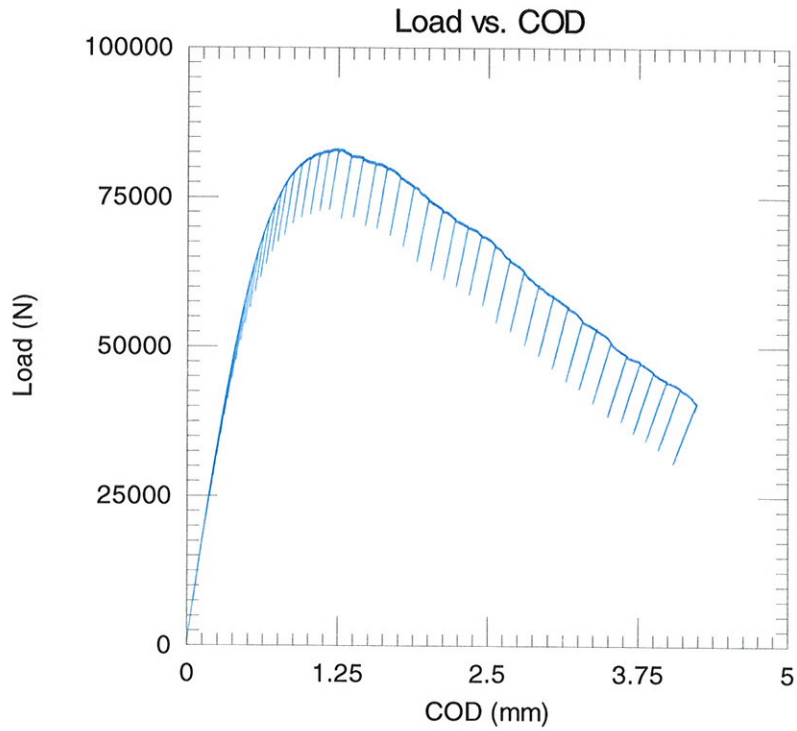

Figure 6. Specimen 2-05-T-2 (Lab Air)

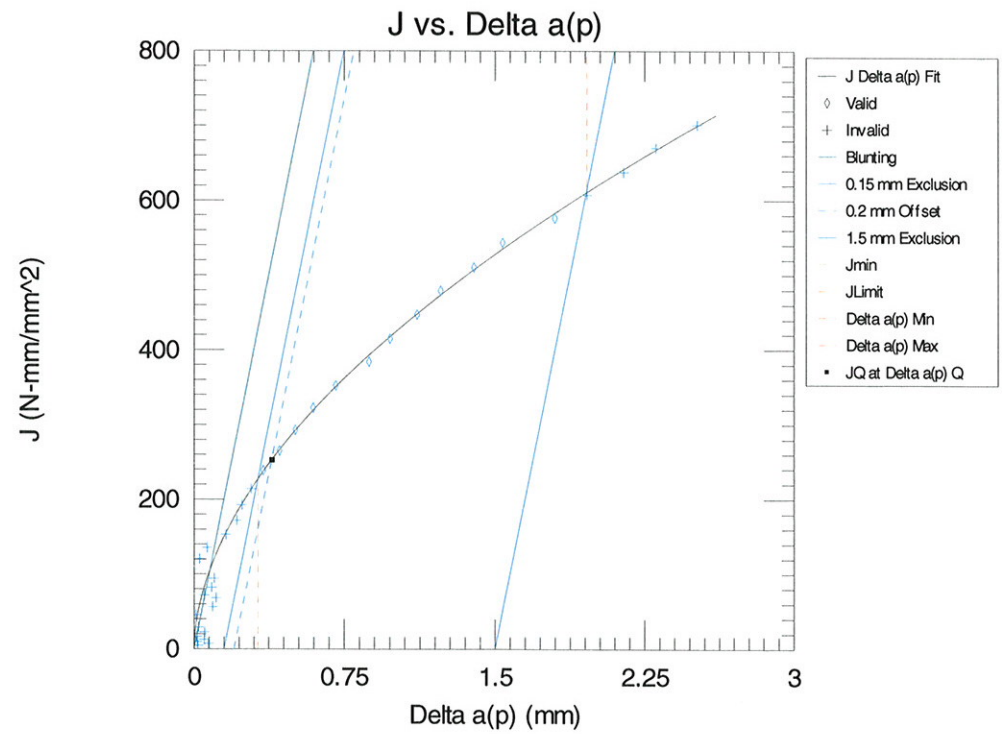

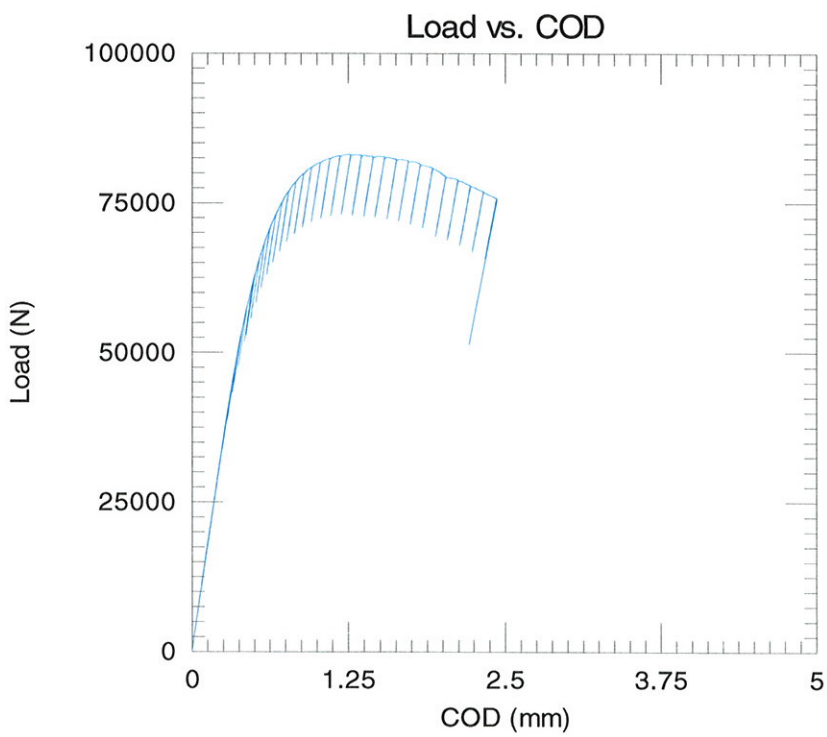

Figure 7. Specimen 3-05-T-1 (Lab Air)

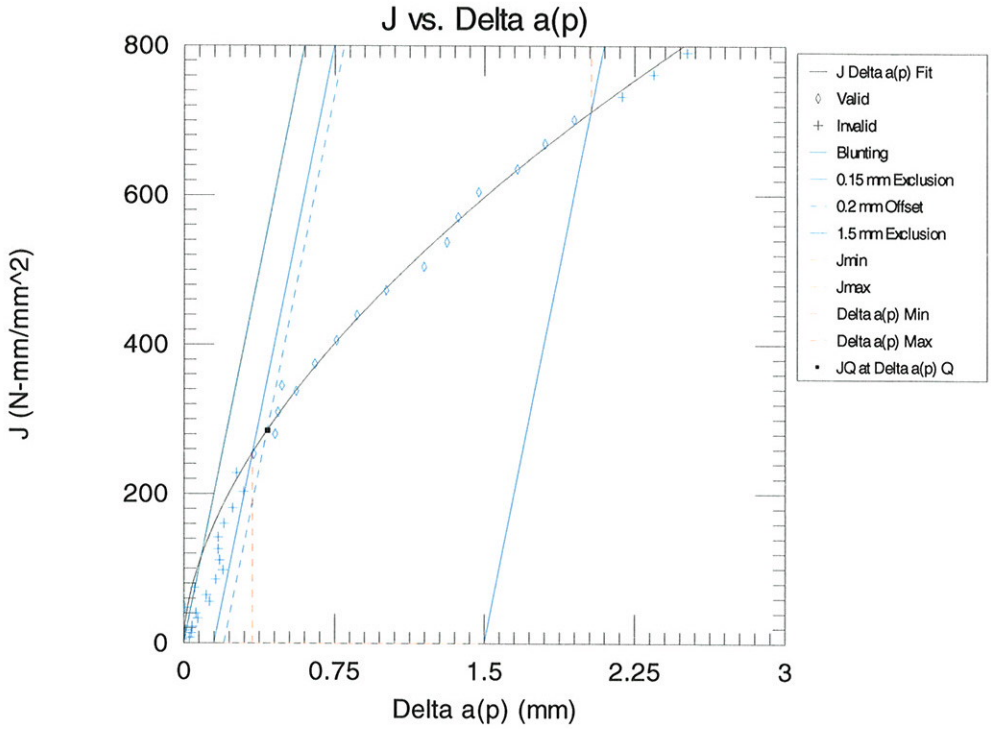

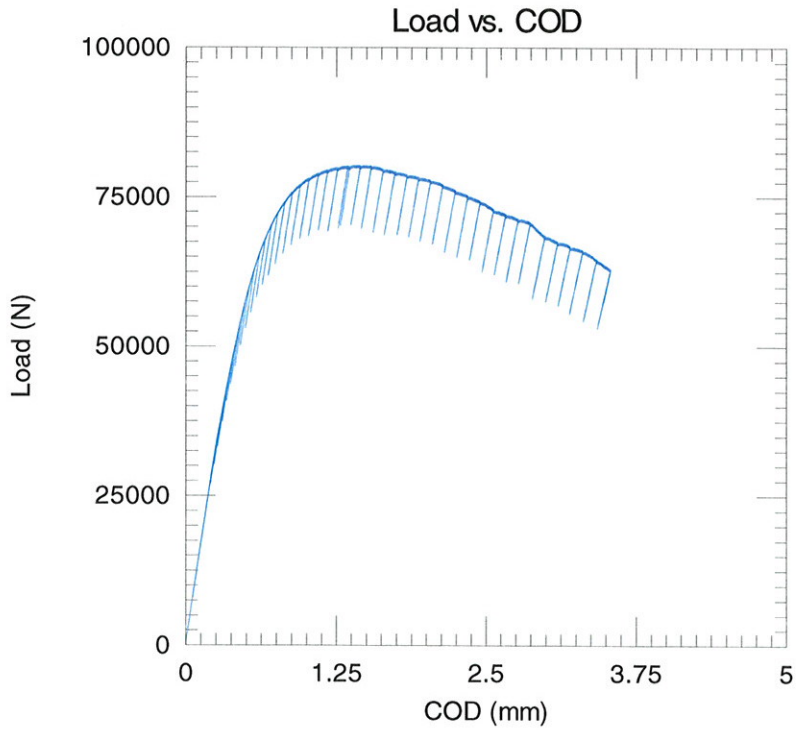

Figure 8. Specimen 3-05-T-2 (Lab Air)

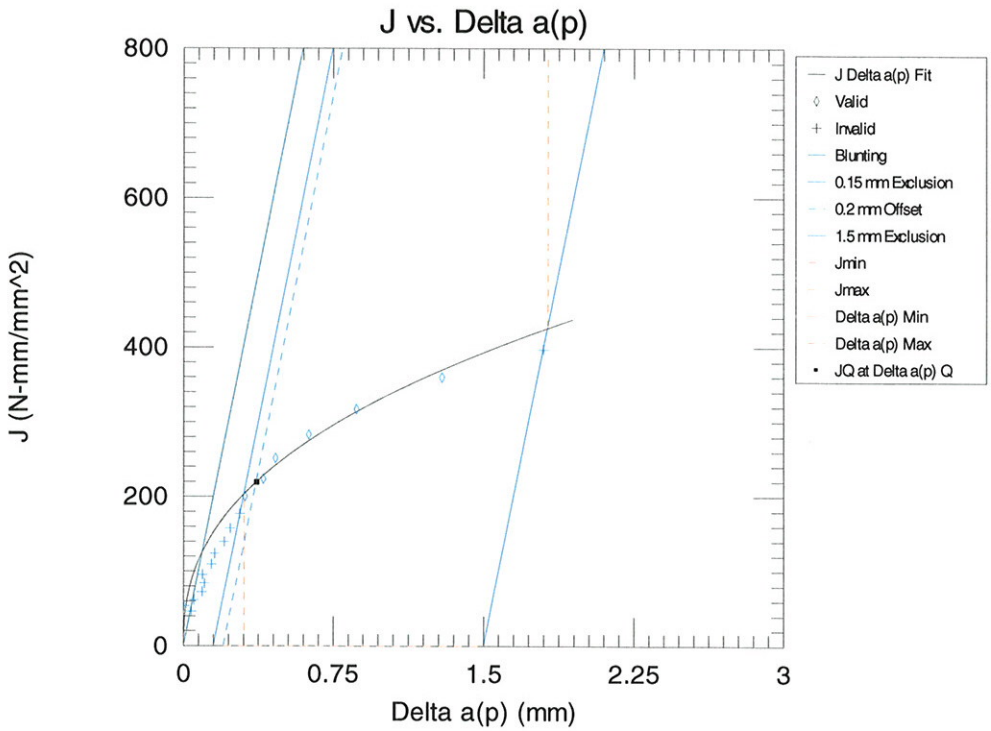

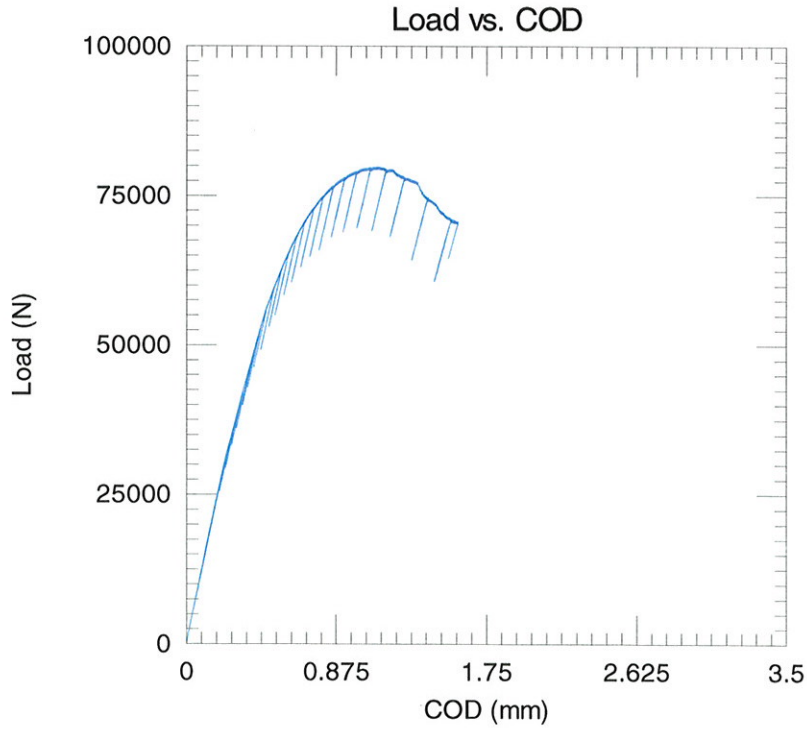

Figure 9. Specimen 1-05-T-1 (CP)

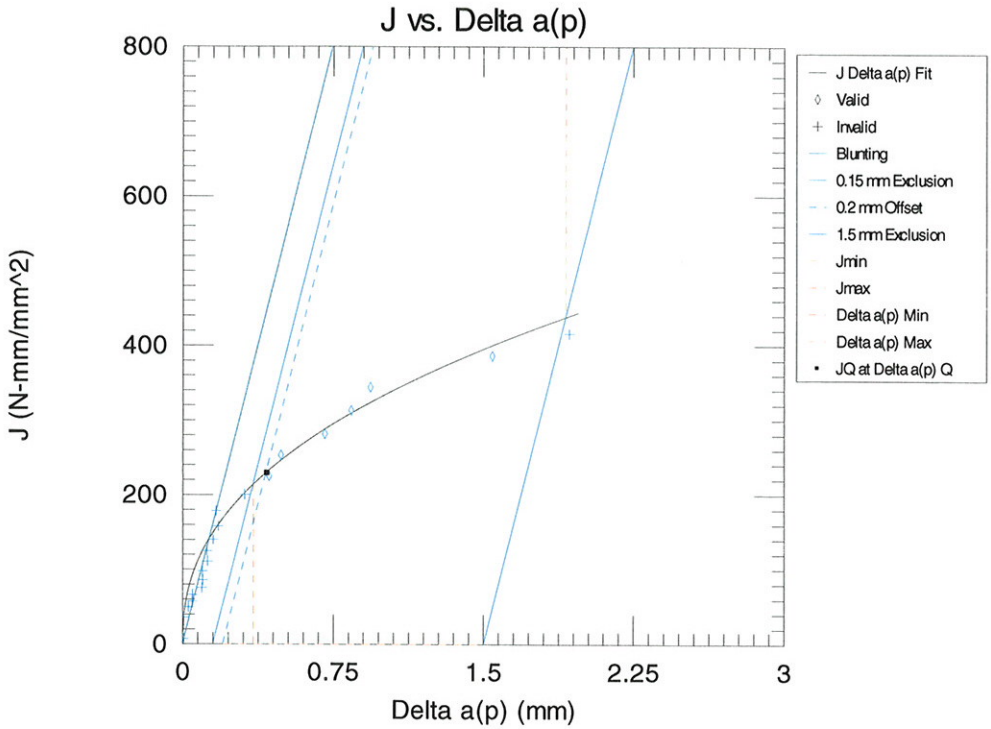

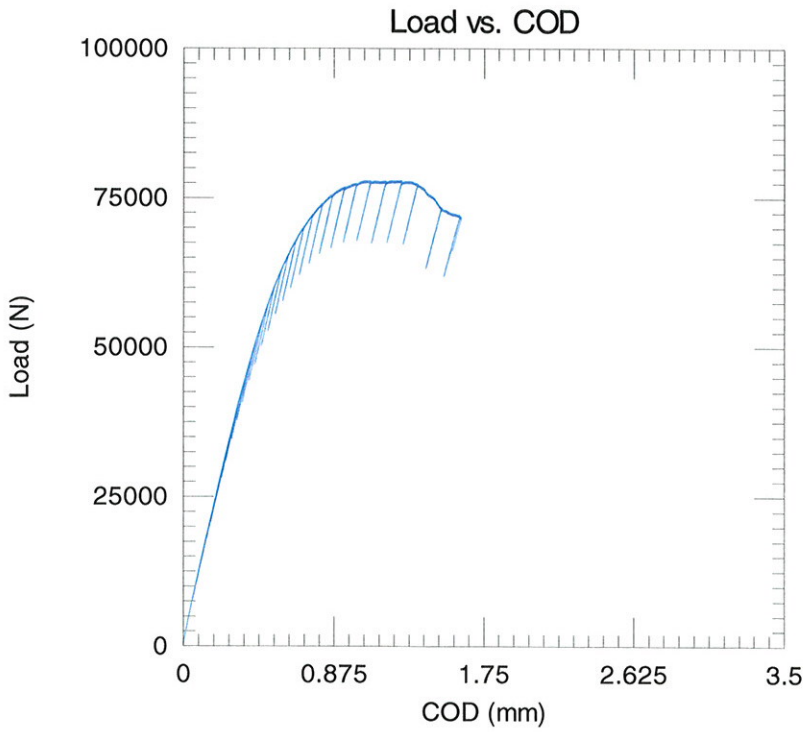

Figure 10. Specimen 1-05-T-2 (CP)

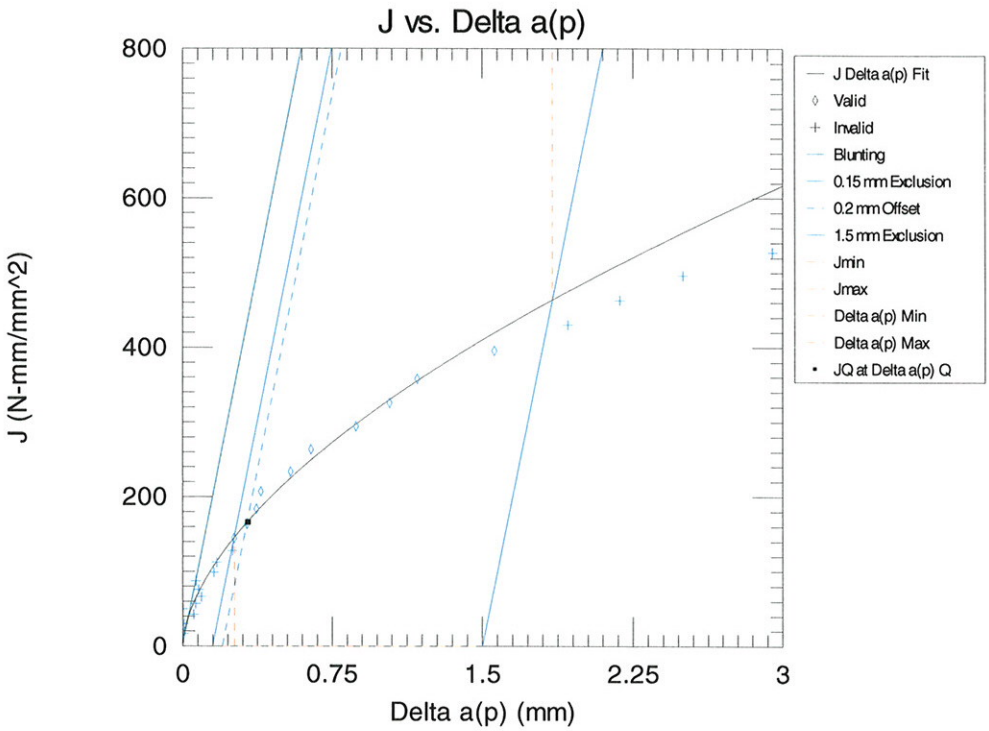

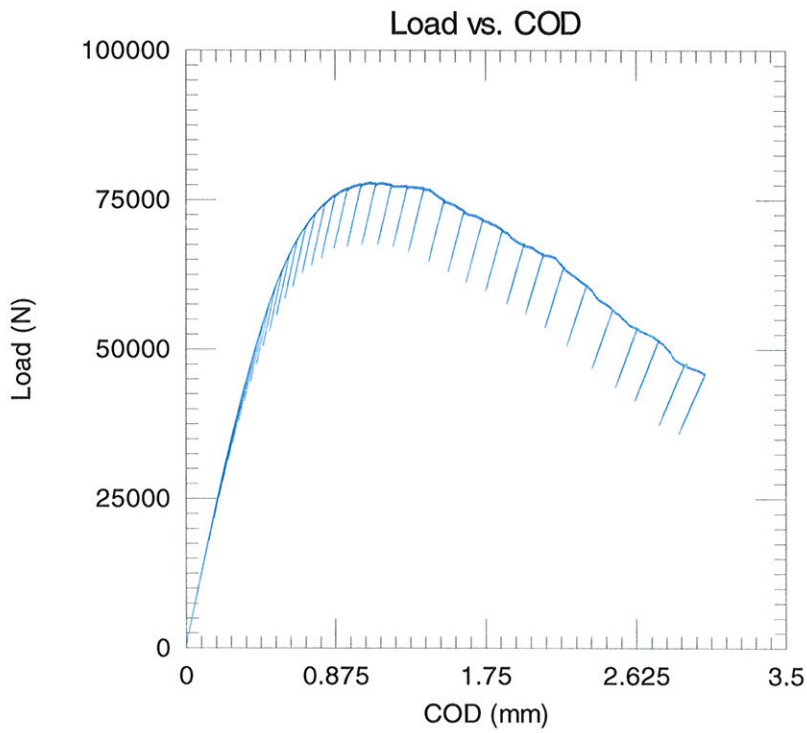

Figure 11. Specimen 2-05-T-1 (CP)

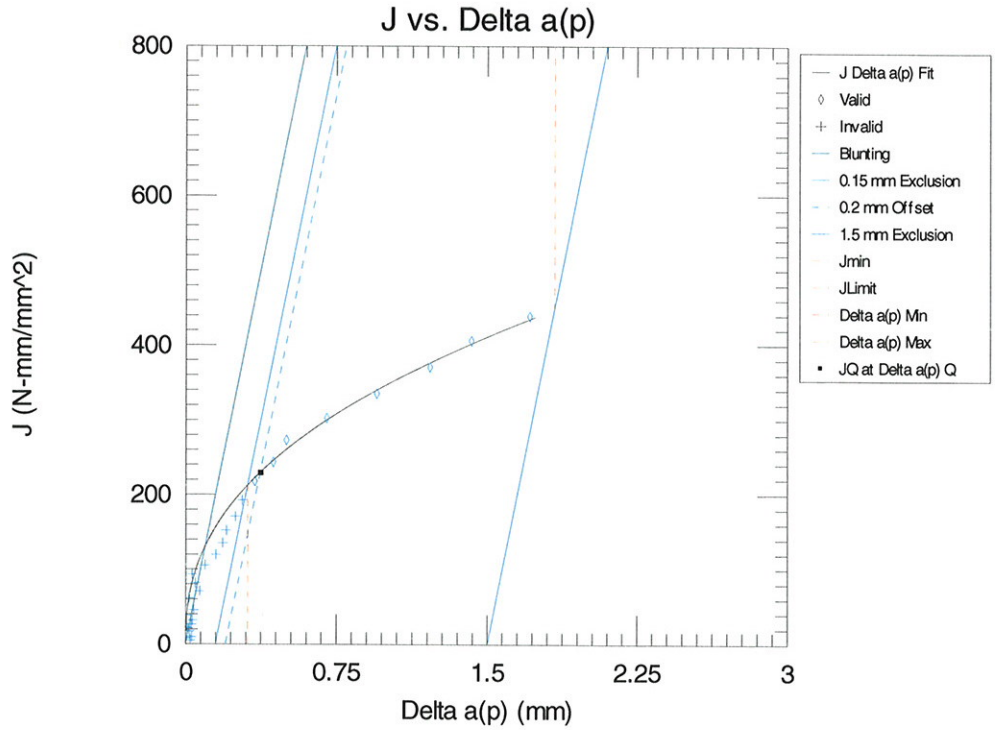

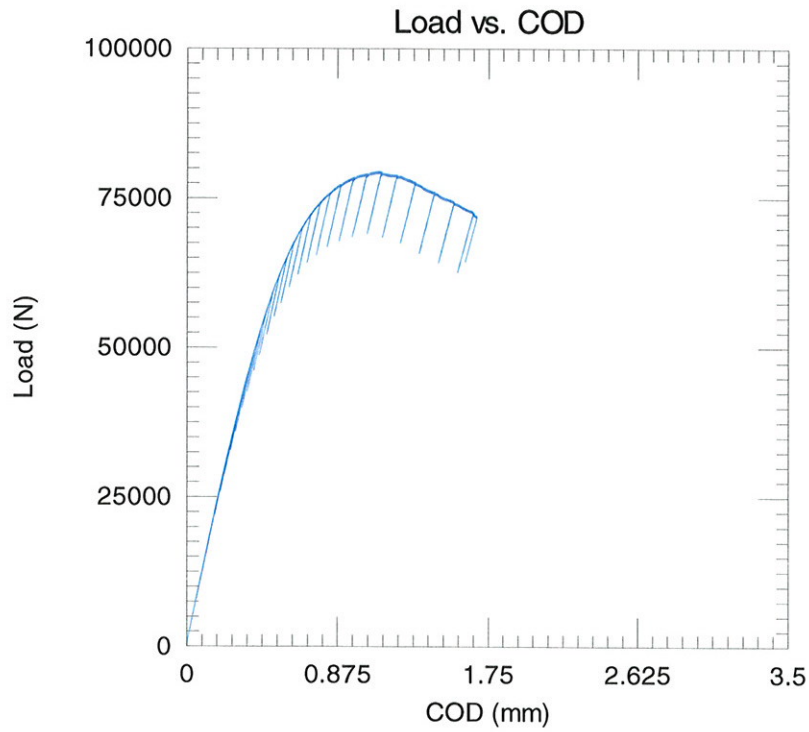

Figure 12. Specimen 2-05-T-2 (CP)

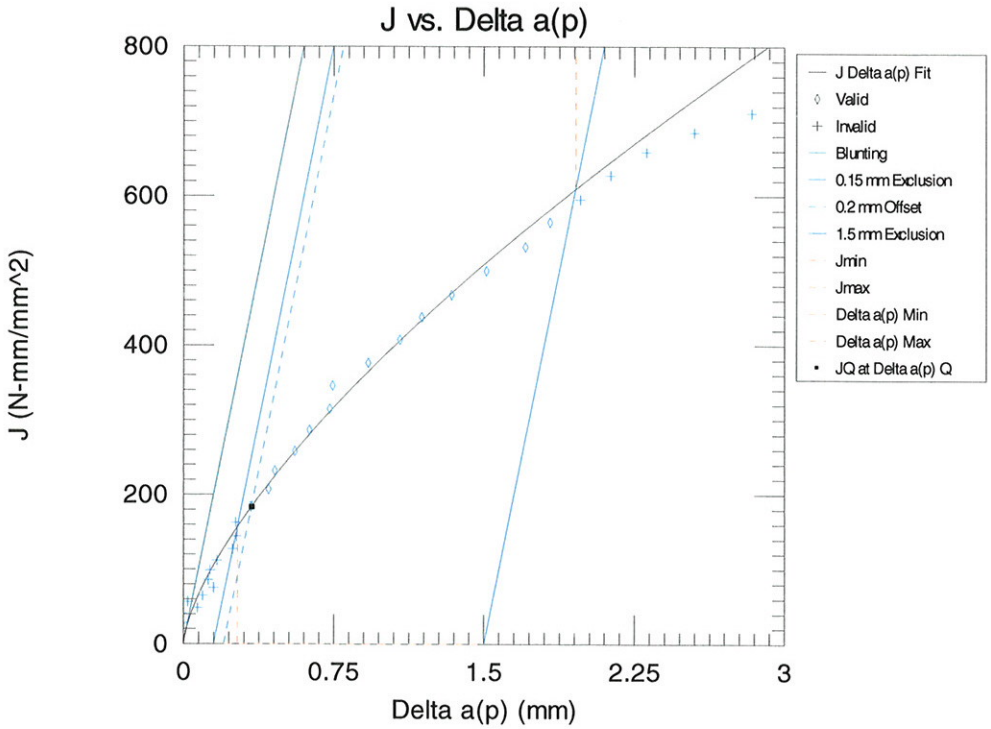

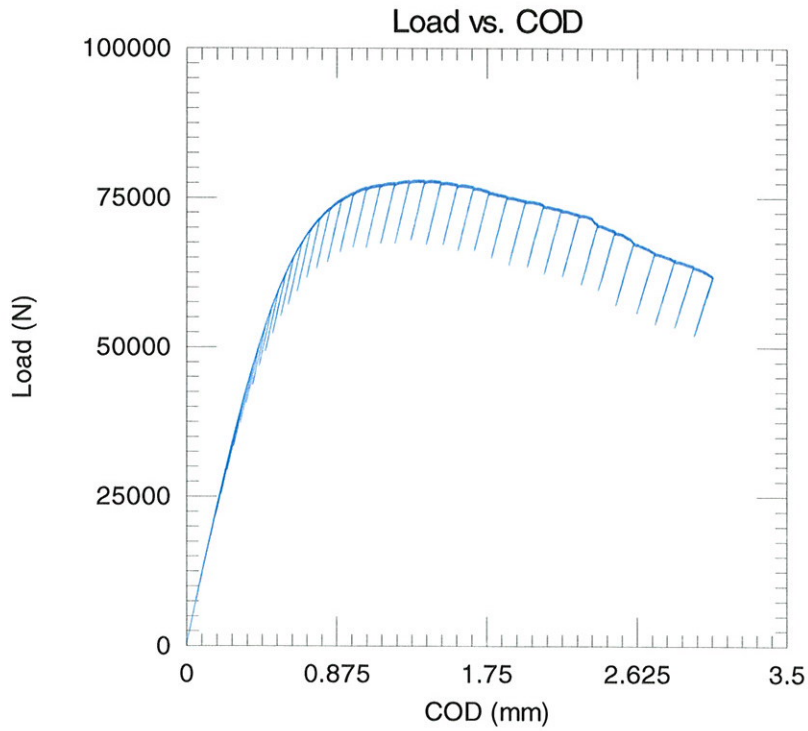

Figure 13. Specimen 3-05-T-1 (CP)

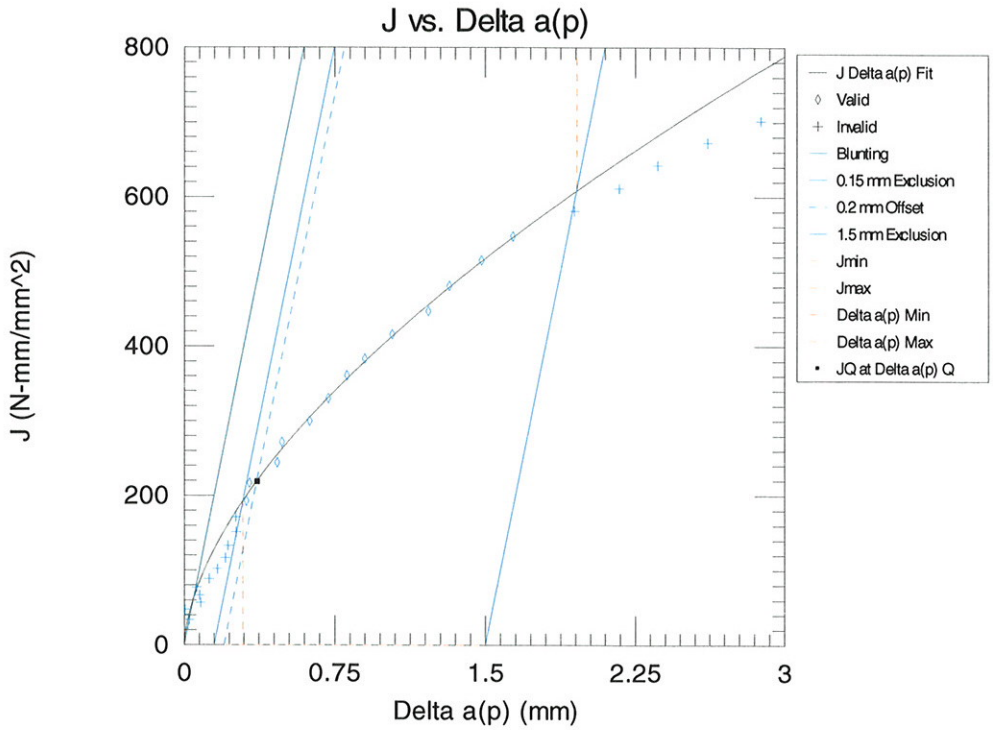

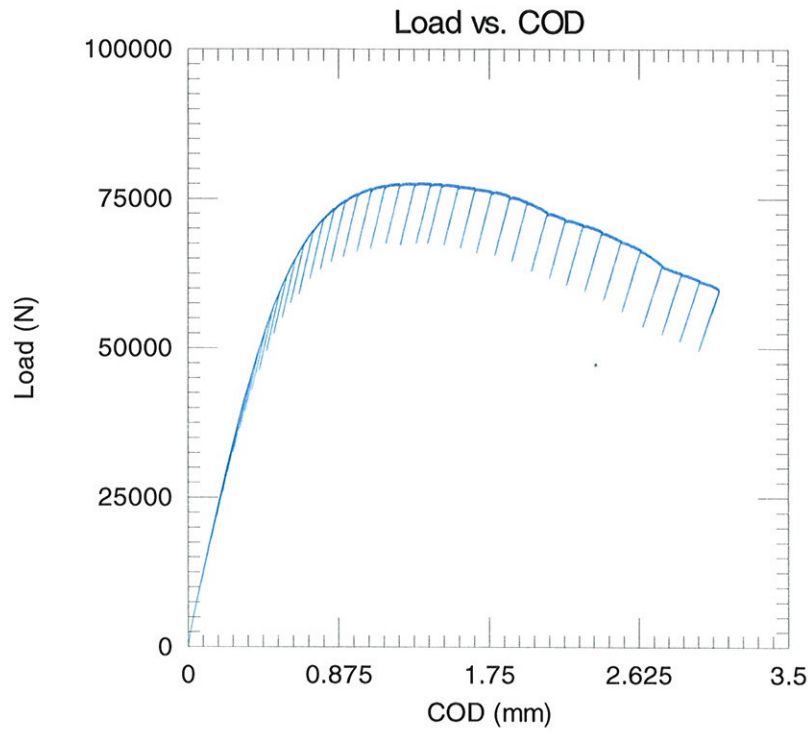

Figure 14. Specimen 3-05-T-2 (CP)

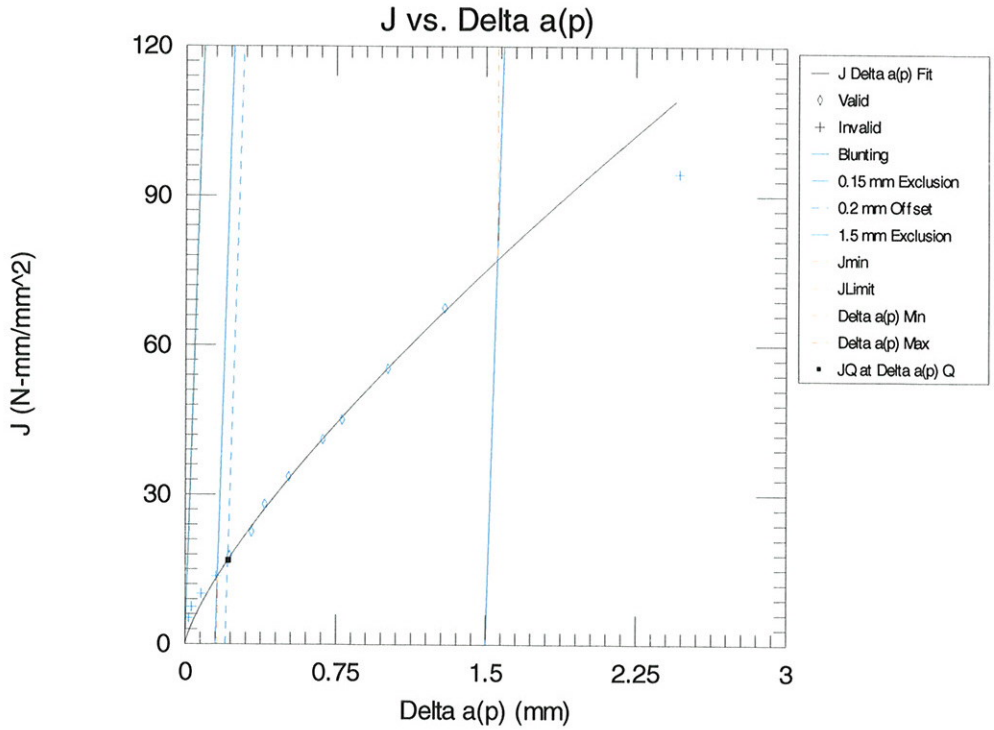

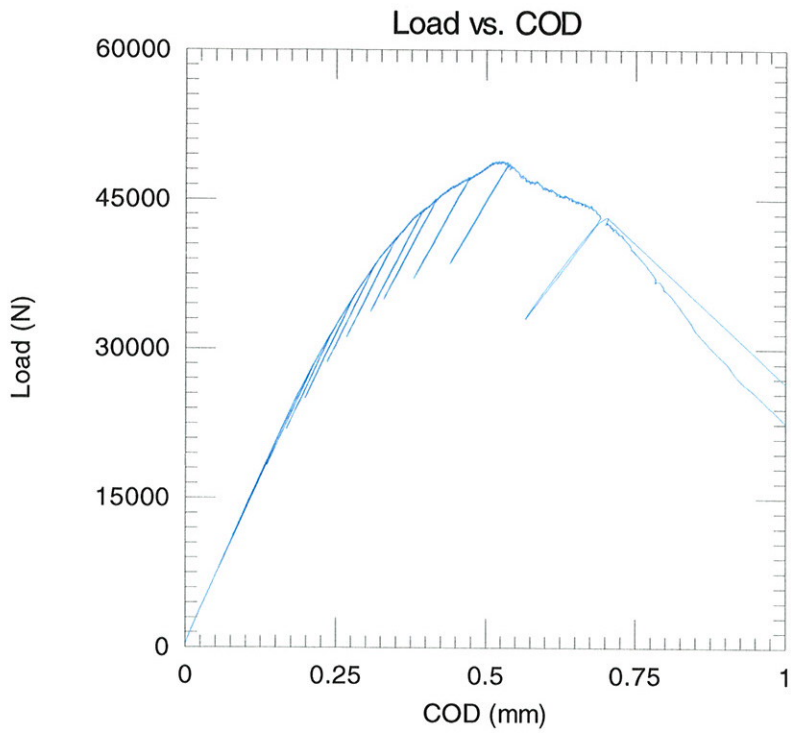

Figure 15. Specimen 1-06-T-1 (H_2S)

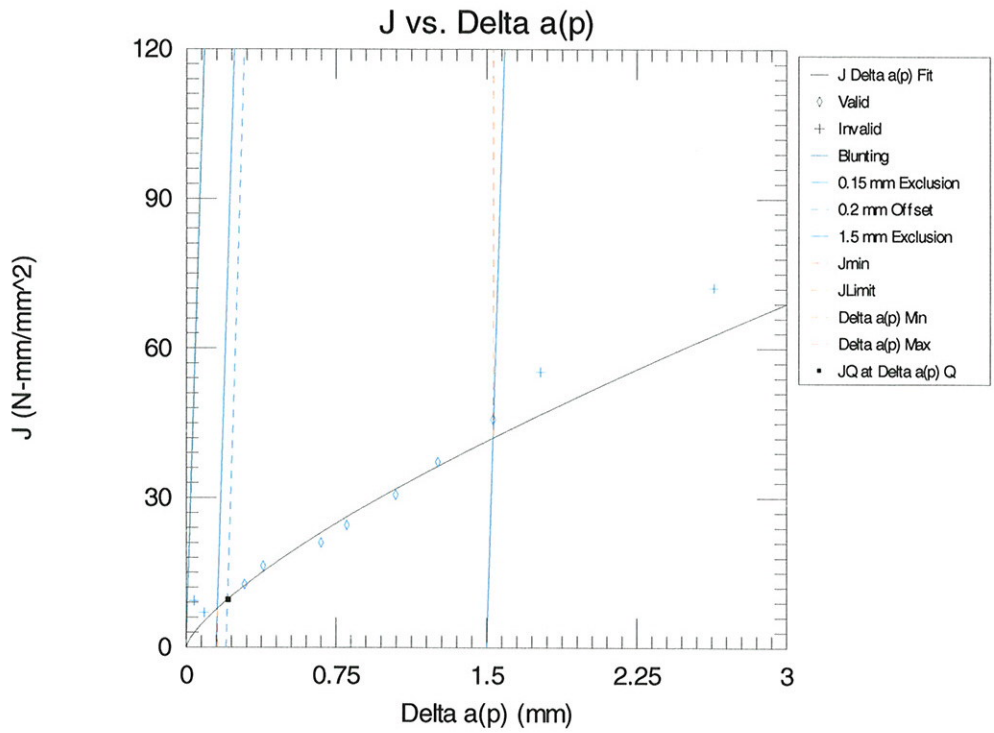

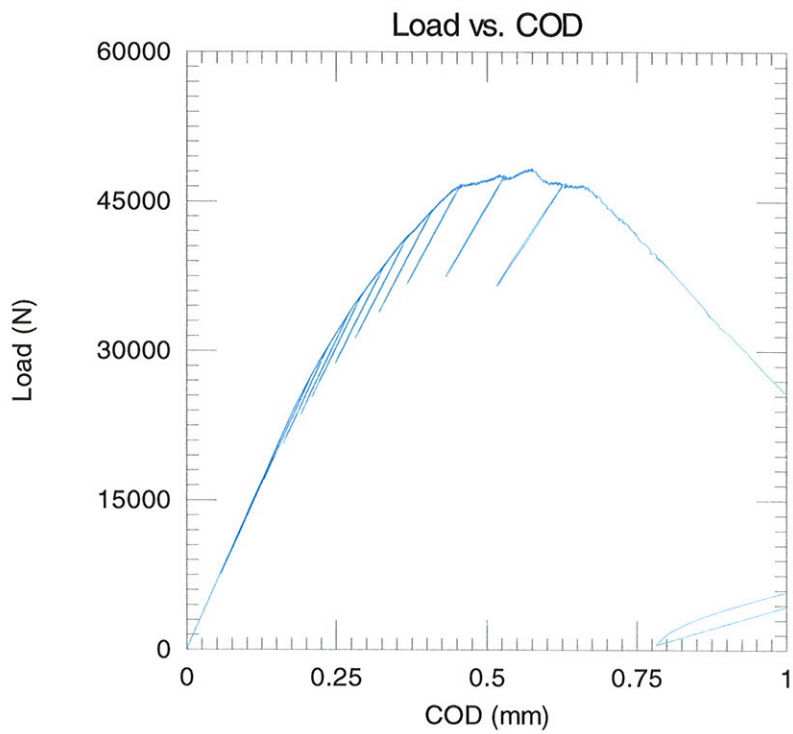

Figure 16. Specimen 1-06-T-2 (H_2S

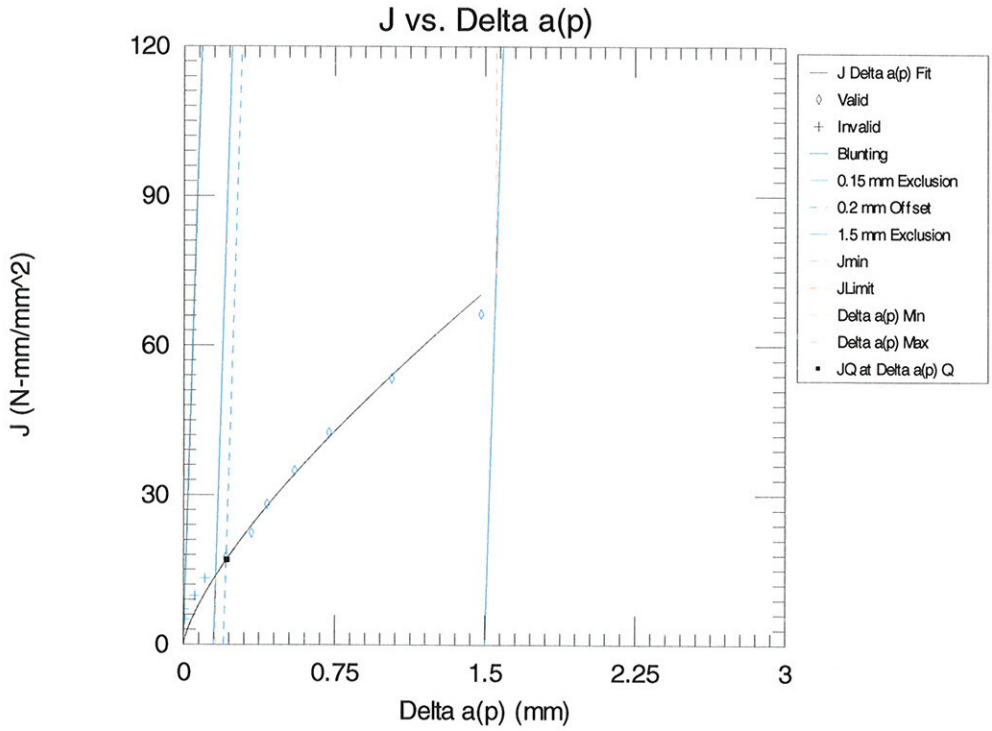

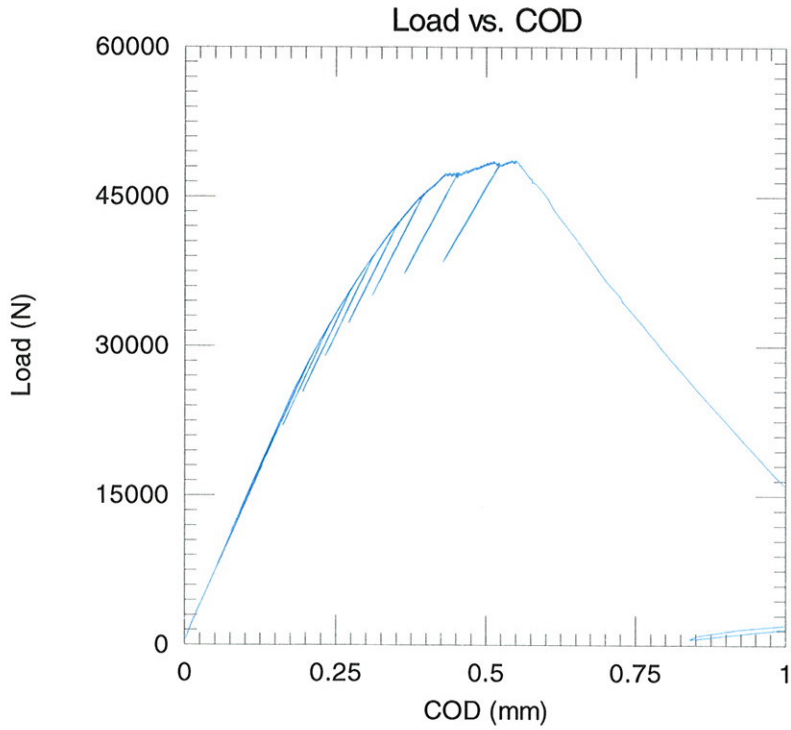

Figure 17. Specimen 2-06-T-1 (H_2S)

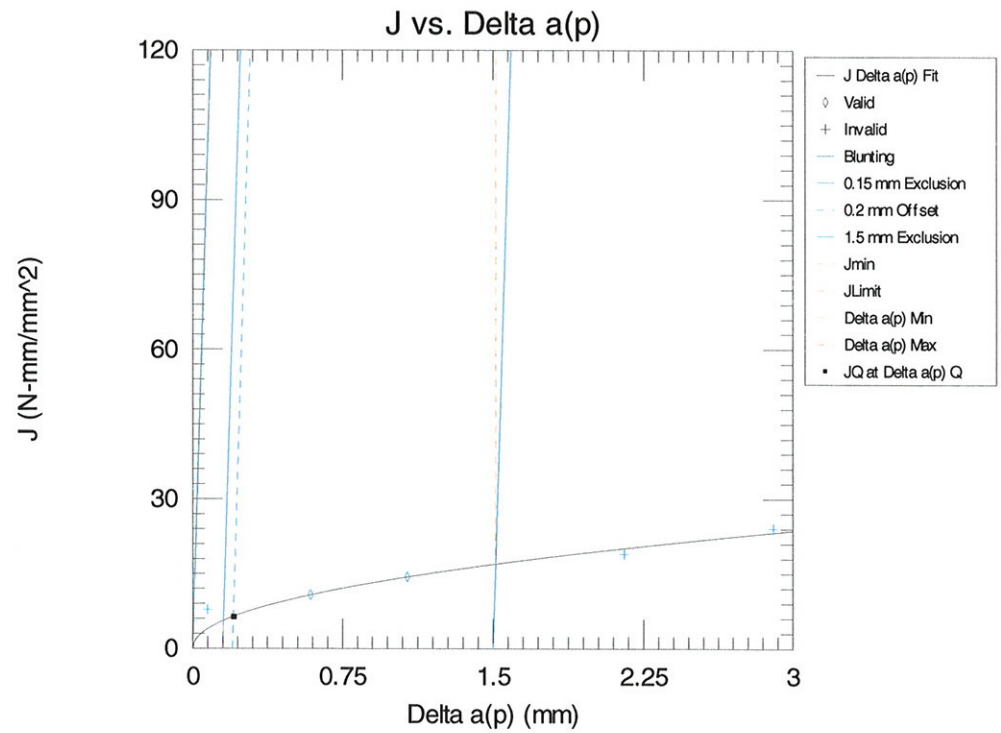

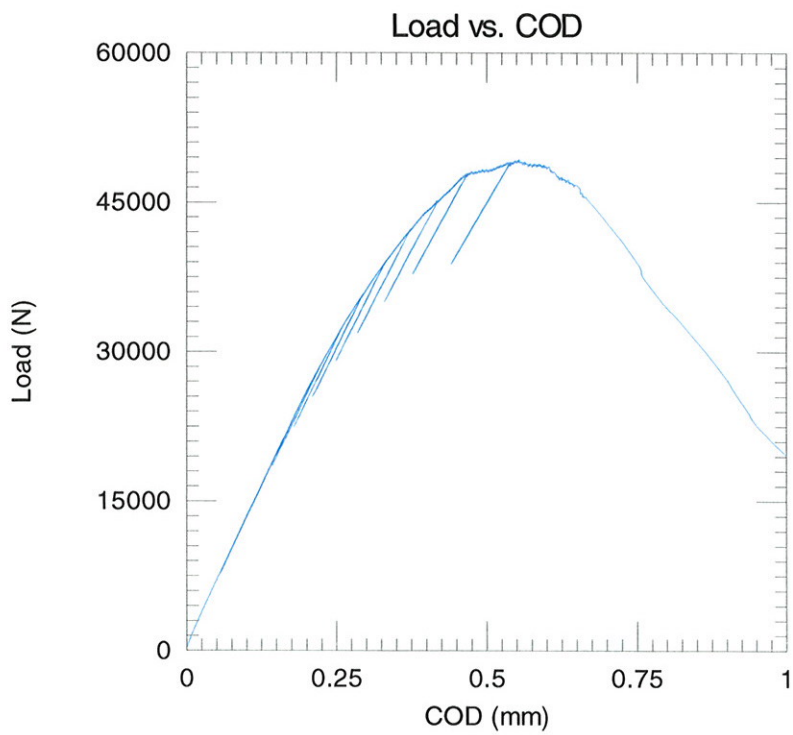

Figure 18. Specimen 2-06-T-2 (H_2S)

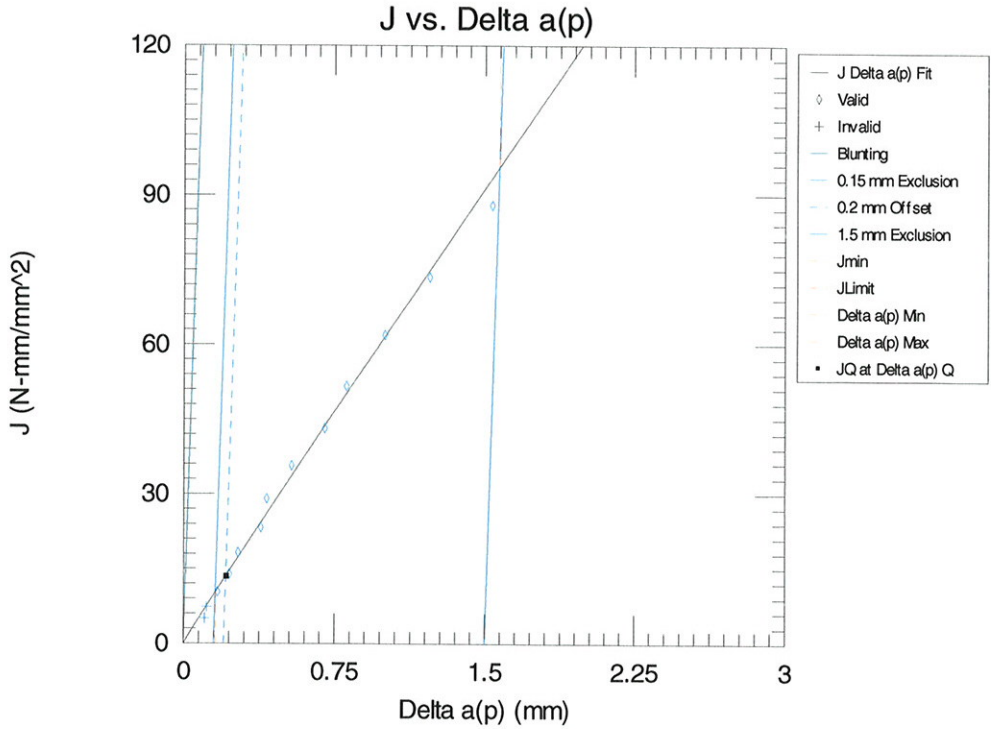

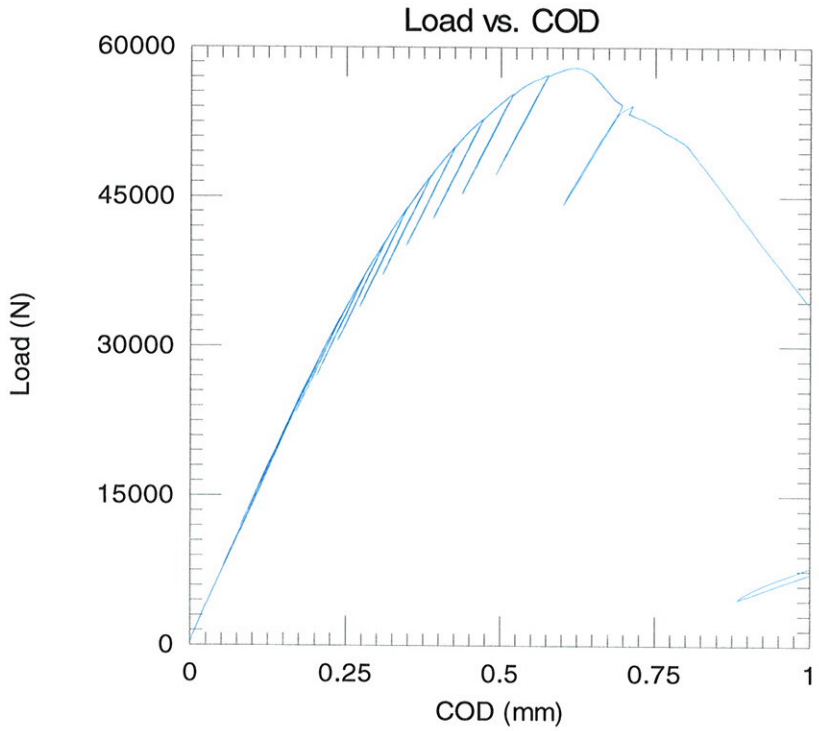

Figure 19. Specimen 3-06-T-1 (H_2S)

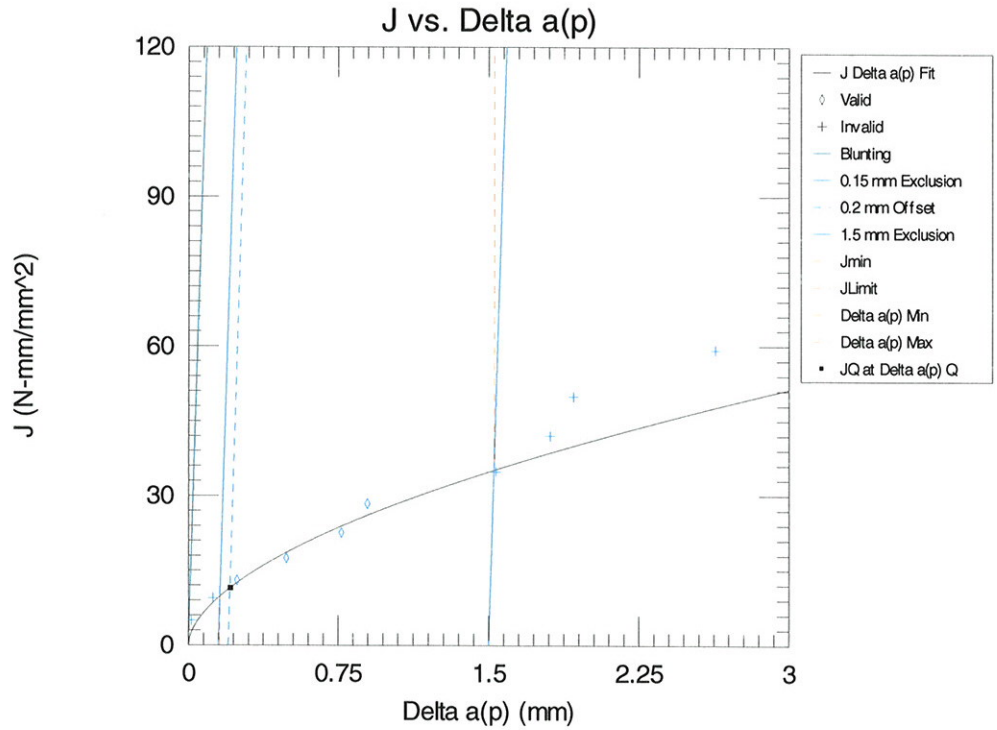

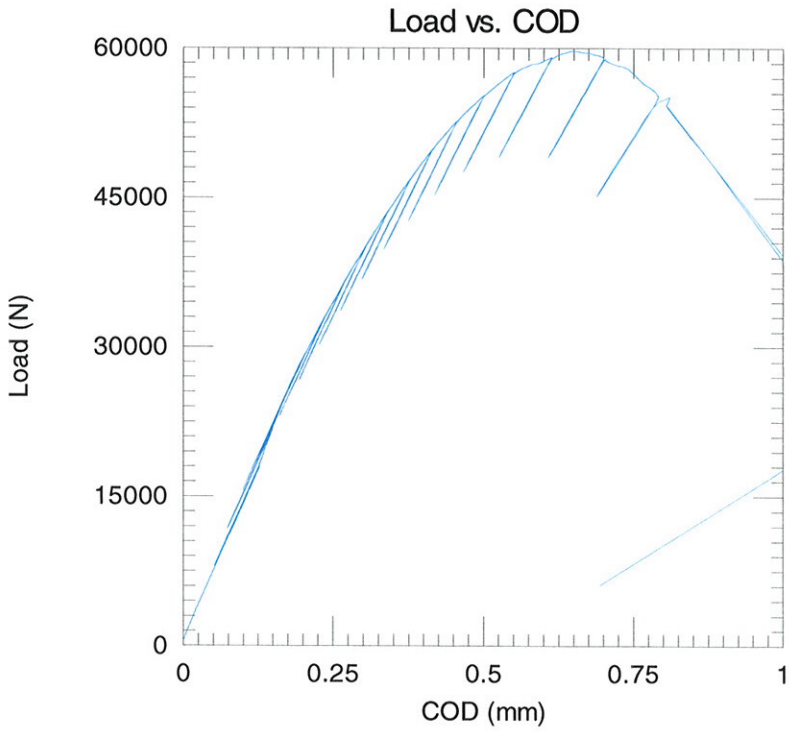

Figure 20. Specimen 3-06-T-2 (H_2S)

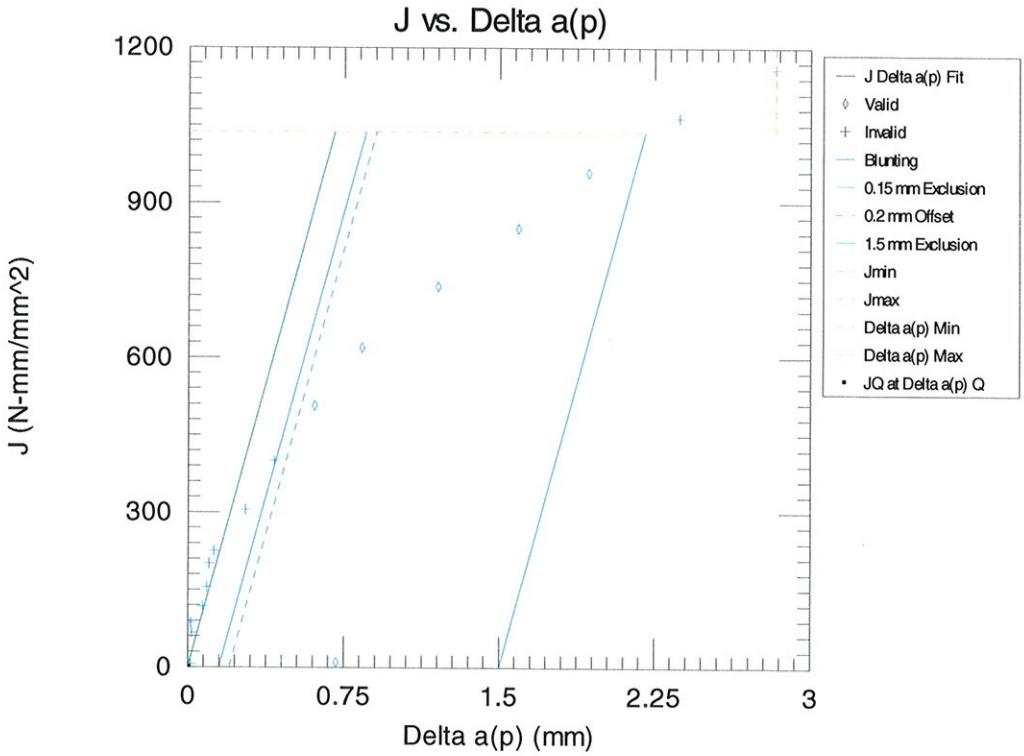

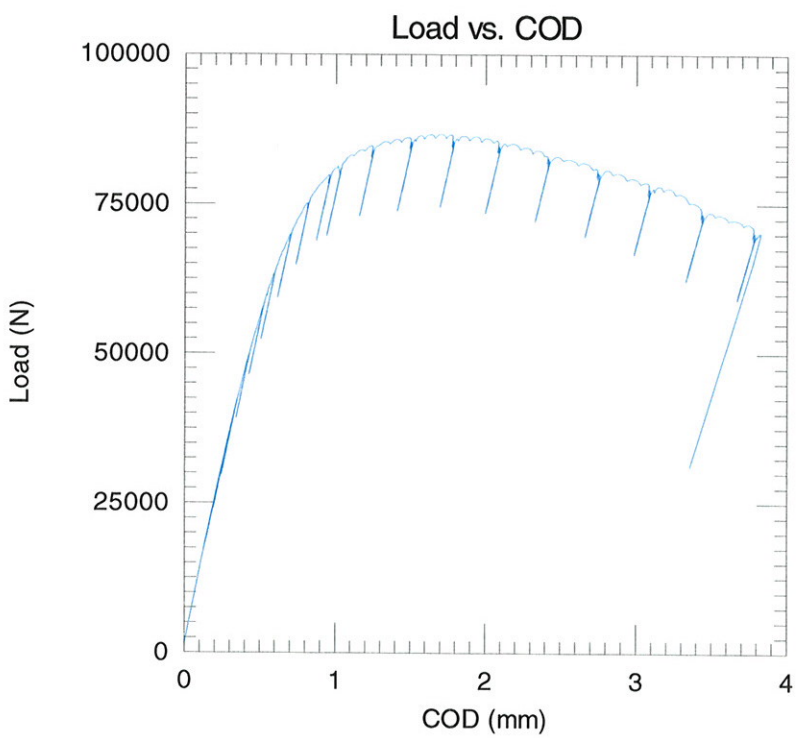

Figure 21. Specimen 2-07-T-1 (Lab Air) Control Sample

Fracture Face Photographs

Figure 22. 1-05-T-1 (Air)

Figure 23. 1-05-T-2 (Air)

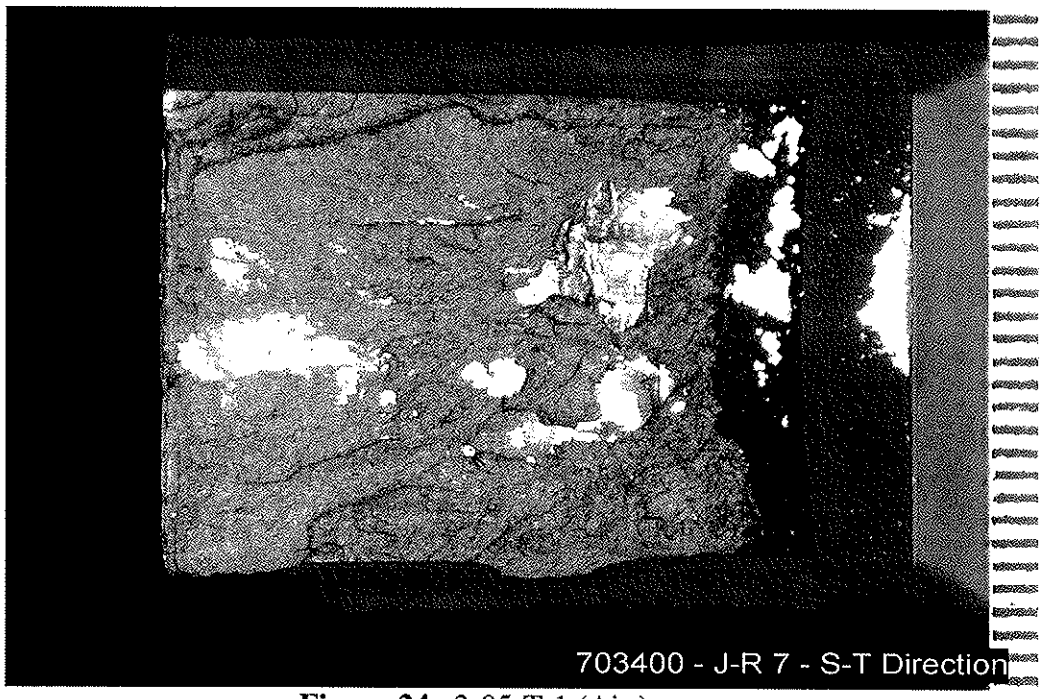

Figure 24. 2-05-T-1 (Air)

Figure 25. 2-05-T-2 (Air)

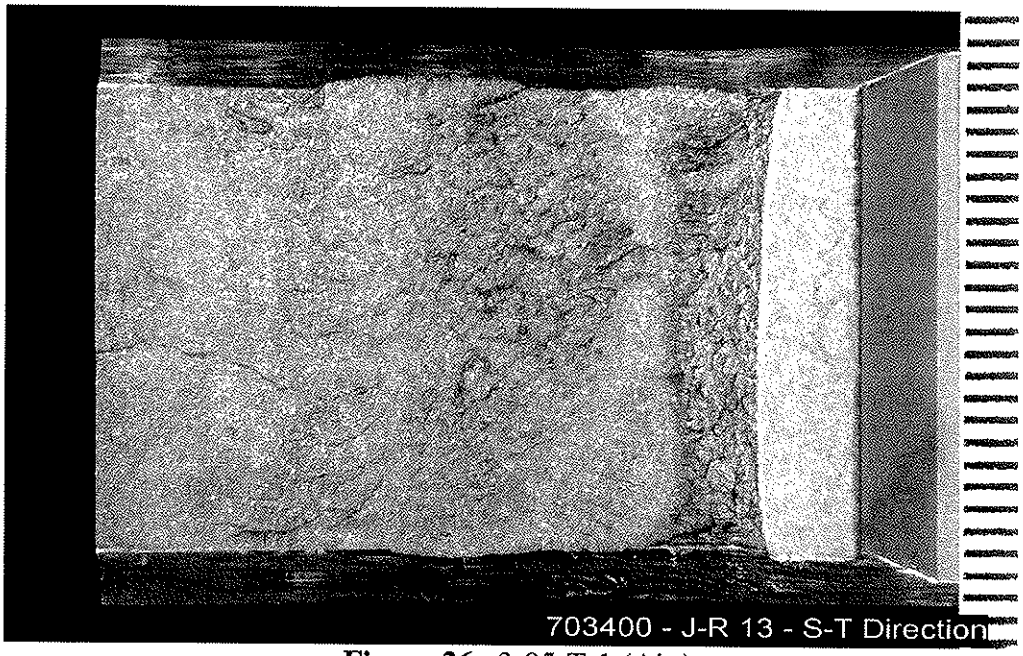

Figure 26. 3-05-T-1 (Air)

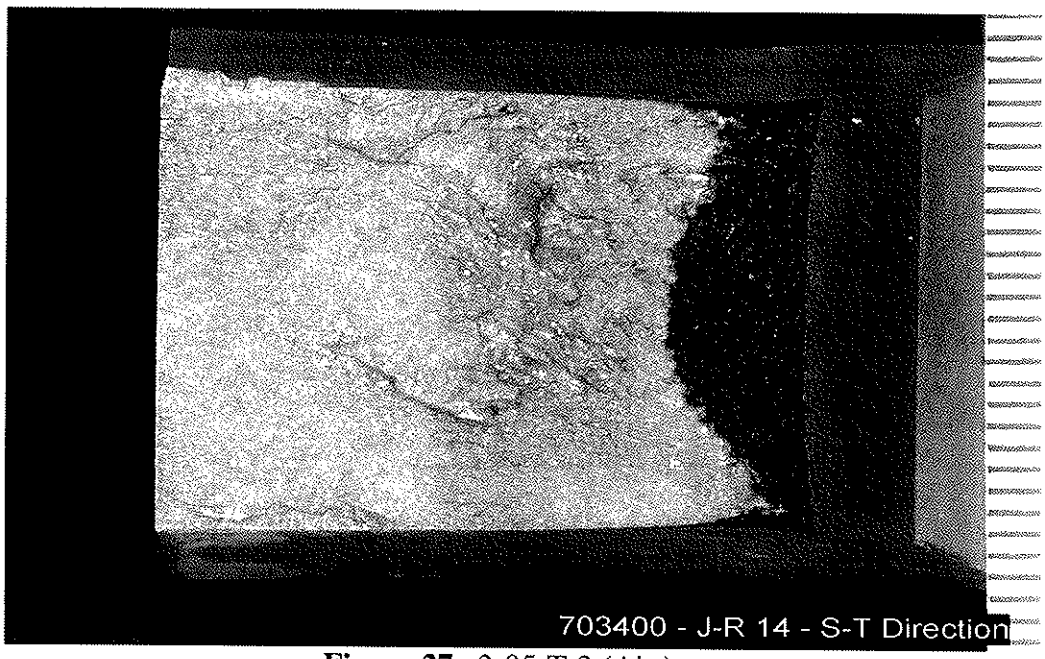

Figure 27. 3-05-T-2 (Air)

Figure 28. 1-05-T-1 (CP)

Figure 29. 1-05-T-2 (CP)

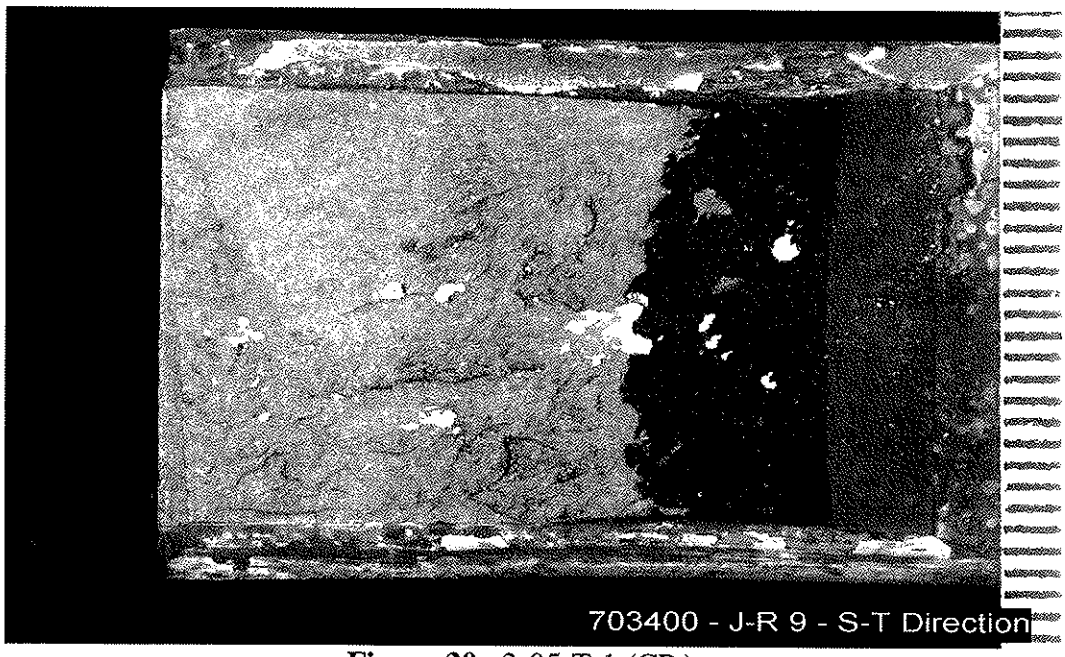

Figure 30. 2-05-T-1 (CP)

Figure 31. 2-05-T-2 (CP)

Figure 32. 3-05-T-1 (CP)

Figure 33. 3-05-T-2 (CP)

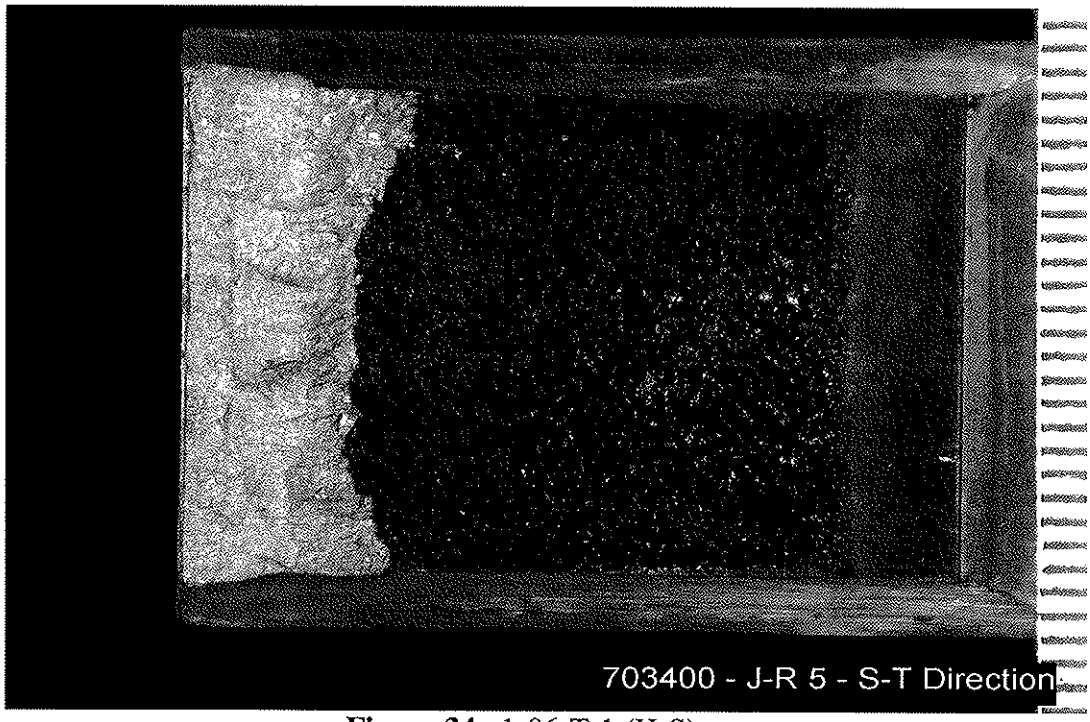

Figure 34. 1-06-T-1 (H_2S)

Figure 35. 1-06-T-2 (H_2S)

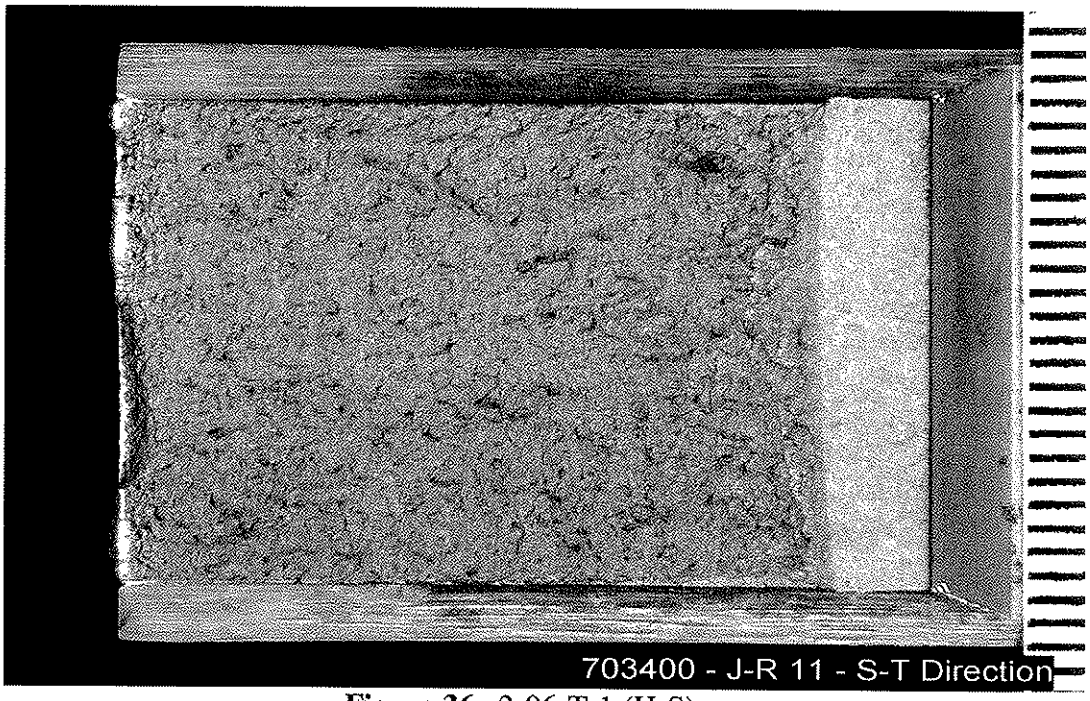

Figure 36. 2-06-T-1 (H_2S)

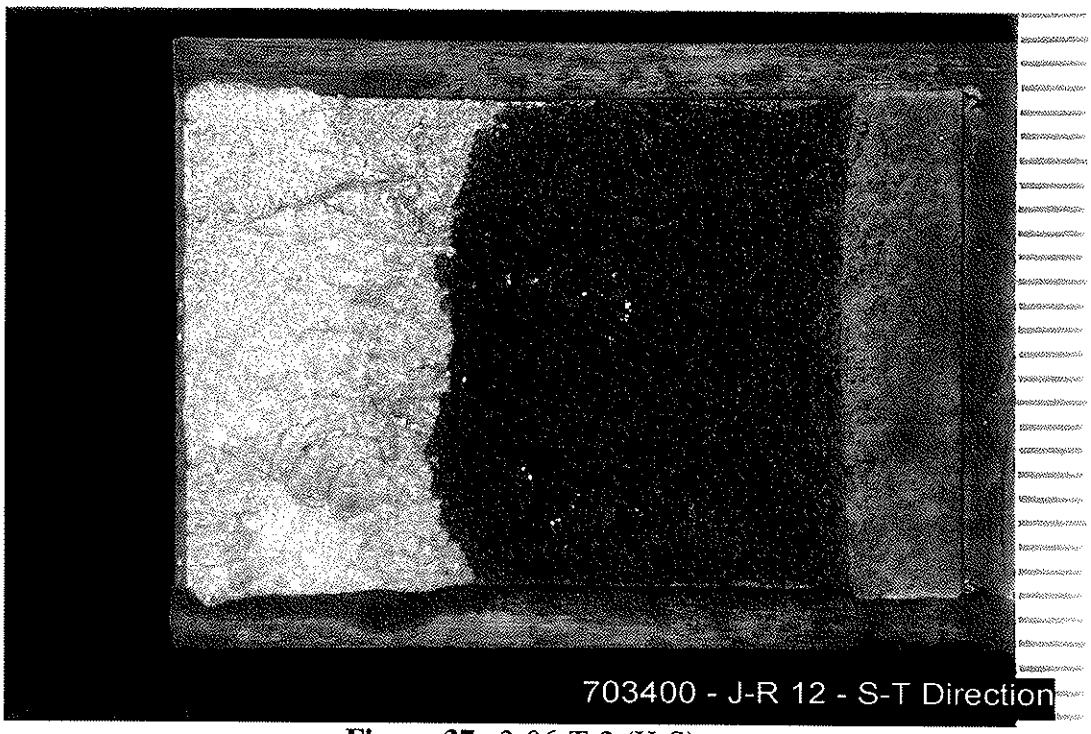

Figure 37. 2-06-T-2 (H_2S)

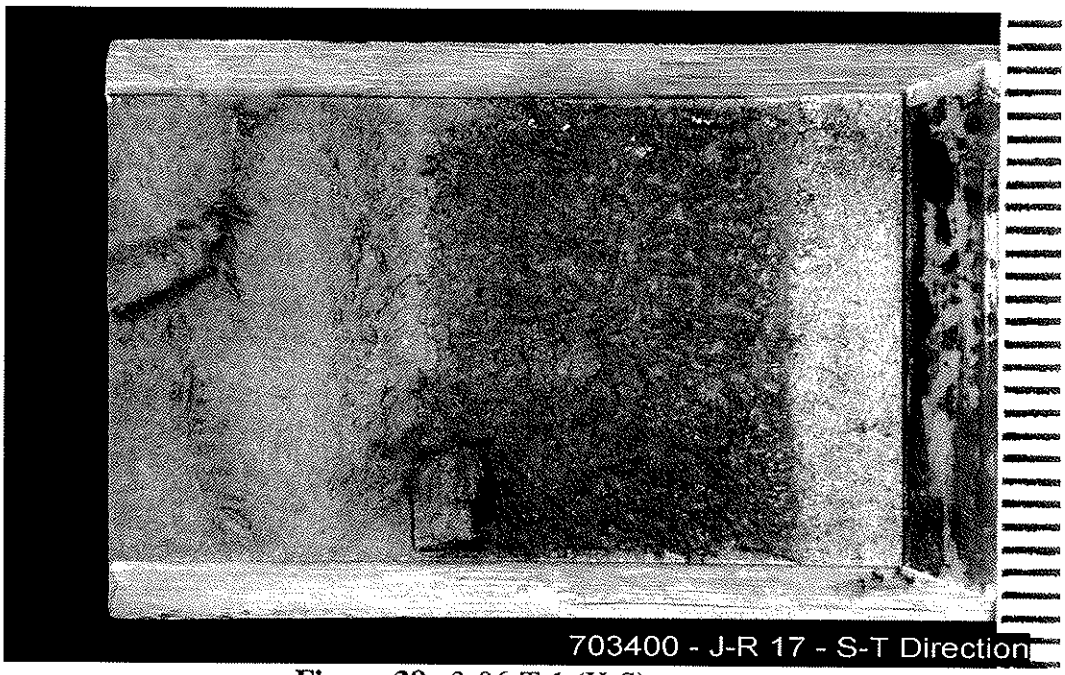

Figure 38. 3-06-T-1 (H_2S)

Figure 39. 3-06-T-2 (H_2S)

Figure 40. 2-07-T-1 (Lab Air) Control Sample

Value Step Data

Table 13. 1-05-T-1 (Air)

J (N-mm/mm^2)	CTOD (mm)	Delta a(p) (mm)	Load kN	Clip Gauge COD
5.2476	0.00325	0.114037	18023.8	0.129866
7.34852	0.004636	0.155008	21171.3	0.152209
9.82934	0.006999	0.070202	24916	0.179665
12.8492	0.009125	0.126522	28303.5	0.204894
16.3997	0.012987	0.017149	31857.8	0.232286
20.7339	0.016588	0.066803	35464.4	0.260944
25.3067	0.021261	0.017611	38907	0.289911
30.6359	0.026211	0.032486	42429.5	0.320031
36.7415	0.032131	0.027243	45747.5	0.349657
43.315	0.038712	-0.02004	49179.8	0.381133
50.2556	0.044832	0.043129	52623.3	0.413751
57.5593	0.052337	-0.0168	55318.1	0.442102
66.3189	0.060231	0.021235	58758.4	0.478078
75.7467	0.068782	0.058821	61960.5	0.514567
85.8211	0.07912	-0.02942	64983.5	0.552064
96.8855	0.0888	0.04862	67556.7	0.588131
108.751	0.099474	0.082731	70253.5	0.629093
122.492	0.112152	0.066143	73000.5	0.674008
137.617	0.12606	0.045555	75049.6	0.718086
154.098	0.140603	0.064653	77369.2	0.769739
170.864	0.155419	0.071392	79149.2	0.819019
190.932	0.172638	0.115137	80626.8	0.874171
213.873	0.191838	0.197643	82396.7	0.942812
217.572	0.195475	0.244617	81842.4	0.950563
245.117	0.218264	0.277807	83398.8	1.02966
274.462	0.243154	0.478651	83356.9	1.11162
306.722	0.270965	0.617226	82983.3	1.20339
339.535	0.299834	0.777349	82396.6	1.29461
373.846	0.330431	0.974981	81490	1.3908
406.989	0.360038	1.13345	81534.6	1.48799
448.356	0.397189	1.39239	79959.9	1.61373
481.138	0.432919	1.70697	77684.8	1.71725
516.238	0.466204	1.83072	77359.4	1.82365
551.824	0.506832	2.19382	74494.9	1.94836
584.708	0.541267	2.35127	73470.2	2.05249
618.603	0.584818	2.72343	70432.3	2.17731
647.469	0.619206	2.90714	69487.2	2.27875
677.819	0.652741	3.0276	69255.4	2.38175

Table 14. 1-05-T-2 (Air)

J (N-mm/mm^2)	CTOD (mm)	Delta a(p) (mm)	Load kN	Clip Gauge COD
5.2179	0.003388	-0.01771	17827.8	0.132077
7.83583	0.005069	-0.00407	22050.5	0.162272
11.2027	0.008238	-0.08569	26320.1	0.19467
15.3801	0.011448	-0.01527	30663.8	0.228465
20.5082	0.016098	-0.00998	35053.3	0.264486
21.8536	0.017324	-0.01107	36143.9	0.273318
29.225	0.024275	-0.02295	41251.9	0.317341
37.7438	0.03247	-0.02846	46173.3	0.36243
47.8808	0.042422	-0.06733	51076.2	0.410633
59.3966	0.053288	-0.03826	55752.1	0.460419
72.2156	0.065633	-0.0482	60090.7	0.511508
86.8207	0.07926	-0.01985	64217	0.565698
103.714	0.094908	0.004204	68012.2	0.624471
122.56	0.112053	0.0354	71458.5	0.686582
144.358	0.131442	0.080107	74563.9	0.75506
169.324	0.153813	0.057106	77183.2	0.830334
198.226	0.178774	0.141632	79322.6	0.915526
232.125	0.207823	0.209236	80864.7	1.01269
274.495	0.243957	0.4056	81171.9	1.13432
320.342	0.283708	0.561226	80958.5	1.26539
368.183	0.326552	0.860224	80067.5	1.40722
421.604	0.37614	1.13272	78035.5	1.56663
474.601	0.429865	1.52283	75301.7	1.73739
524.222	0.481679	1.83638	73051	1.89951
573.08	0.547757	2.49416	68037.1	2.09651
613.449	0.596201	2.74601	64239.7	2.21078

Table 15. 2-05-T-1 (Air)

J (N-mm/mm^2)	CTOD (mm)	Delta a(p) (mm)	Load kN	Clip Gauge COD
5.33675	0.003444	-0.01427	17401.1	0.124653
7.14918	0.005051	-0.06402	20491.5	0.146967
9.61308	0.00679	0.020307	23804	0.172071
12.5215	0.0097	-0.00356	27035.8	0.197474
15.5622	0.012305	0.020219	30093	0.22163
19.7551	0.016332	0.004157	33533.3	0.249619
24.5653	0.02049	0.059682	37221.6	0.28024
29.3204	0.025742	-0.01693	39953.6	0.304162
35.0801	0.030371	0.087251	43674.8	0.33696
41.3619	0.036799	0.033645	47084.4	0.368118
48.4009	0.042951	0.084088	50327.2	0.399083
56.0893	0.050578	0.067037	53390.9	0.431413
64.3618	0.058346	0.083259	56342.1	0.463542
73.3418	0.066559	0.103761	59207.1	0.495987
83.0057	0.076006	0.057847	62217.4	0.532521
94.1561	0.086311	0.076501	65275.9	0.572283
105.569	0.096458	0.121362	67566.1	0.607761
118.99	0.108301	0.139935	70612.7	0.654195
132.246	0.120632	0.129887	72518.7	0.694123
148.467	0.135009	0.139146	74751.6	0.742344
164.983	0.149543	0.155269	76772.3	0.79236
184.819	0.166532	0.172953	78351.6	0.846456
204.469	0.183142	0.23132	80115.7	0.905222
227.246	0.202268	0.308493	80863.6	0.964504
252.726	0.223399	0.402224	82012	1.03604
281.167	0.246808	0.429065	83109	1.11575
310.248	0.271088	0.528457	83515.9	1.19556
341.418	0.29716	0.611968	83427.6	1.27951
373.85	0.324528	0.75027	83340.3	1.36715
407.946	0.352952	0.819209	83303.4	1.46036
444.442	0.383951	0.986564	82571.4	1.56111
482.634	0.420122	1.26833	80505	1.67792
520.824	0.458314	1.58348	78409.6	1.79967
557.297	0.496237	1.88918	75998.4	1.91398
590.722	0.532316	2.14089	74642.7	2.02716
623.213	0.568262	2.39397	73233.8	2.13476
654.173	0.604152	2.63292	71915.6	2.23864
684.997	0.640385	2.87197	70661.5	2.35049

Table 16. 2-05-T-2 (Air)

J (N-mm/mm^2)	CTOD (mm)	Delta a(p) (mm)	Load kN	Clip Gauge COD
5.33595	0.002512	0.069838	17929.2	0.128132
7.42816	0.004454	-0.01451	21141.8	0.151128
10.1621	0.006564	0.002386	24705.7	0.177404
13.3805	0.009676	-0.04387	27856.8	0.202244
17.1686	0.012937	0.002301	31436.5	0.230796
21.3885	0.017032	-0.01141	34908.1	0.259535
26.1281	0.021344	0.011042	38262.1	0.287642
31.44	0.026705	-0.03019	41565.8	0.316952
37.4728	0.03249	-0.02354	44956.7	0.347702
44.1369	0.038537	0.016503	48357	0.379526
50.8251	0.045236	-0.02265	51465.7	0.410823
59.1924	0.052643	0.042225	55013.7	0.446437
67.4484	0.060876	0.011513	57843.4	0.478888
77.3447	0.069926	0.035006	60767.6	0.5143
87.5357	0.079119	0.080849	63635.2	0.550732
98.4451	0.089392	0.066927	66217.6	0.587936
110.856	0.101153	0.031229	68789.8	0.628995
124.788	0.113689	0.058905	71204.7	0.673152
139.843	0.126893	0.11241	73405	0.719557
155.819	0.140974	0.151949	75241	0.766015
172.33	0.155241	0.15905	76992.8	0.814525
193.489	0.173186	0.19944	79338.7	0.880577
216.588	0.193039	0.231356	80162.4	0.941672
242.054	0.21451	0.282706	81295.9	1.01366
269.974	0.237263	0.411274	82471.6	1.09465
297.566	0.260853	0.429678	82503.4	1.16833
326.569	0.285362	0.5705	82469.9	1.24733
363.871	0.317289	0.806649	81986.1	1.35802
397.837	0.347443	0.946211	81058.4	1.45036
434.142	0.379545	1.10624	80445.9	1.5577
468.386	0.41043	1.25101	80055.3	1.6566
503.538	0.445035	1.52538	78260.5	1.76412
539.879	0.481114	1.76556	76921.6	1.88028
575.936	0.520672	2.11997	74797.4	2.00514
609.429	0.558839	2.4017	72993	2.11926
640.651	0.594985	2.64359	71444.9	2.22802
670.872	0.63103	2.85287	69801.4	2.33085
702.241	0.668518	3.05544	68324.1	2.44122

Table 17. 3-05-T-1 (Air)

J (N-mm/mm^2)	CTOD (mm)	Delta a(p) (mm)	Load kN	Clip Gauge COD
5.12925	0.003311	-0.00754	17971.5	0.125239
7.55353	0.004791	0.069399	21817.9	0.152375
10.4943	0.007537	-0.00989	25713.3	0.180177
13.8991	0.009947	0.047171	29595.2	0.207578
17.984	0.013625	-0.00795	33611	0.236669
18.0453	0.01393	-0.05056	33710.5	0.237189
24.1051	0.018386	0.025086	38881.7	0.274269
31.335	0.024927	0.016827	43901.4	0.313537
39.6798	0.033051	-0.05252	48831.9	0.354254
49.2032	0.041661	-0.00924	53322	0.396084
60.4031	0.051888	0.058377	57703.3	0.441368
72.9928	0.064023	0.057787	61747.5	0.489083
77.0771	0.068334	0.013358	62883.9	0.504081
87.8979	0.078292	0.057293	65676	0.54219
100.414	0.09002	0.073271	68379.4	0.584566
113.002	0.102198	0.036272	70750.7	0.625888
127.805	0.115952	0.036831	73035.5	0.672913
143.469	0.130446	0.027325	75035.3	0.721281
161.506	0.146683	0.058814	76899.4	0.775807
181.029	0.164141	0.085682	78491.2	0.833506
202.147	0.182644	0.161004	79869.8	0.895219
224.21	0.201938	0.227131	80913.8	0.958706
249.077	0.223646	0.283165	81757.6	1.02943
276.758	0.247673	0.269812	82416.1	1.10633
304.627	0.272053	0.413256	82834.2	1.18623
335.128	0.298421	0.449786	83044	1.27087
365.12	0.325125	0.573233	82950.9	1.35658
397.327	0.354192	0.732714	82705	1.44981
429.9	0.382415	0.738224	82671.7	1.53889
462.532	0.412342	0.873911	82288	1.63375
494.083	0.442025	1.02302	81972	1.72686
526.333	0.47208	1.15183	81462.9	1.82144
560.429	0.504005	1.25095	80831.8	1.92054
594.676	0.538848	1.44386	79389.5	2.02737
625.867	0.570285	1.58565	78836.8	2.12381
657.112	0.603198	1.74979	77875.5	2.22331
689.786	0.637719	1.89491	76873.7	2.3268
719.927	0.672661	2.11433	75746.9	2.43141

Table 18. 3-05-T-2 (Air)

J (N-mm/mm^2)	CTOD (mm)	Delta a(p) (mm)	Load kN	Clip Gauge COD
5.36369	0.003785	-0.06017	18192.3	0.134457
7.82098	0.005472	-0.0268	22087.5	0.163195
10.7184	0.008075	-0.06333	25709.1	0.189616
14.0582	0.010281	-0.01883	29359.5	0.216283
17.6366	0.013615	-0.04367	33061.8	0.24541
22.8241	0.018478	-0.0157	36524.2	0.276872
28.2813	0.024497	-0.07362	40480.8	0.3128
34.0795	0.029576	0.010393	43695.7	0.343509
41.2278	0.03665	0.001463	47514.2	0.380139
48.7364	0.044347	-0.04569	50210.9	0.410271
56.9532	0.051532	0.061369	53760.7	0.448106
65.747	0.060375	0.04739	56694	0.484174
75.7219	0.070494	-0.00349	59909.2	0.525199
86.9279	0.080502	0.088533	62849.4	0.567433
99.5281	0.09239	0.120621	65673.3	0.612983
113.172	0.105582	0.105478	67717.2	0.656703
128.155	0.119624	0.100044	70309.6	0.709006
144.311	0.13491	0.099581	71695.3	0.757002
162.851	0.151691	0.125719	74038.6	0.818262
183.646	0.17044	0.164211	75106.7	0.877382
205.745	0.190106	0.212671	77036.2	0.949266
231.145	0.212727	0.180967	77794.1	1.02054
256.394	0.23521	0.256687	78576.5	1.09559
283.08	0.258696	0.350836	79203.3	1.17496
312.685	0.28464	0.364246	79696.4	1.26042
341.082	0.310012	0.44462	79259.3	1.339
348.415	0.315882	0.381649	79988.3	1.36147
377.736	0.342542	0.527805	79766.8	1.44682
409.285	0.37065	0.624147	79950.6	1.54134
443.426	0.401625	0.716246	79432.8	1.64159
476.752	0.432119	0.845909	79343	1.74245
508.426	0.463543	1.01418	78368.8	1.83725
541.358	0.494678	1.11506	77872.6	1.93474
575.016	0.525678	1.16629	77503.6	2.03443
608.763	0.55825	1.25777	76671.9	2.13479
639.703	0.591373	1.43033	75330.5	2.23571
673.975	0.626288	1.5536	74890.7	2.34532
705.988	0.66029	1.68213	73918.7	2.44876
737.854	0.697773	1.89439	72892.7	2.56555
767.56	0.731447	2.03422	72180.8	2.66836
796.887	0.766243	2.18125	71235.7	2.77006
827.598	0.799244	2.25756	70102.7	2.86703

Table 19. 1-05-T-1 (CP)

J (N-mm/mm^2)	CTOD (mm)	Delta a(p) (mm)	Load kN	Clip Gauge COD
5.1999	0.003662	-0.06345	17836.9	0.130921
7.40077	0.005528	-0.11737	21114.3	0.154082
9.93847	0.006889	-0.04665	25019.2	0.181438
13.173	0.009892	-0.11	28531.8	0.20815
16.8665	0.012777	-0.04017	31984.4	0.235332
22.295	0.018663	-0.06879	35566.1	0.269195
27.8719	0.023801	-0.00192	39385.5	0.303887
34.4174	0.030083	0.013577	43177.7	0.338903
41.1025	0.036705	0.014651	46345.8	0.370327
48.0941	0.042586	0.097393	49844.5	0.402835
55.253	0.049767	0.055737	52516.6	0.430532
63.797	0.057163	0.113169	56527.5	0.472027
74.9579	0.067704	0.160029	59492.6	0.512503
87.0612	0.079027	0.174351	62888.9	0.557555
98.7143	0.090307	0.162861	65476.1	0.598547
113.378	0.103424	0.213377	68437	0.647369
128.073	0.116862	0.233927	70718.2	0.693646
144.277	0.131398	0.288256	72863.7	0.744488
162.691	0.147833	0.323264	74627.9	0.797958
182.85	0.16548	0.378464	76284.8	0.858054
206.292	0.185621	0.408755	78077.4	0.928029
230.429	0.20637	0.51615	78908.2	0.996466
259.206	0.231229	0.586834	79096.3	1.0736
291.492	0.258653	0.779887	79386.9	1.16978
326.692	0.290778	1.05774	77756.4	1.2715
370.56	0.332736	1.54949	74711.5	1.4131
409.155	0.375493	2.13444	71067.9	1.54779

Table 20. 1-05-T-2 (CP)

J (N-mm/mm^2)	CTOD (mm)	Delta a(p) (mm)	Load kN	Clip Gauge COD
5.17459	0.002961	-0.00832	17642.7	0.129509
7.62857	0.005209	0.020504	20970.3	0.15608
10.3866	0.007879	-0.01154	24456.6	0.183574
13.4321	0.01063	-0.00611	27659.8	0.208906
17.1677	0.014199	-0.02449	31438.6	0.239856
21.3001	0.017959	-0.01352	34590.6	0.26647
26.0683	0.022545	0.001323	37850.5	0.294583
31.3842	0.027592	-0.02809	41604.5	0.327121
37.4216	0.033205	0.018831	44826.3	0.35804
44.1001	0.040012	-0.03268	48161.8	0.390856
51.3514	0.046427	0.042301	51232.8	0.422576
59.47	0.05416	0.061302	54116.6	0.455199
68.5519	0.062809	0.062513	57466.3	0.494156
78.1276	0.071555	0.108991	60071.1	0.528288
88.6987	0.08175	0.112245	62886.1	0.568553
100.869	0.093214	0.111252	65269.1	0.608571
114.254	0.105533	0.135879	67801.3	0.654472
128.676	0.118801	0.132557	70268.9	0.70331
144.36	0.133067	0.163343	71998.8	0.75089
162.581	0.149591	0.187637	73580.3	0.80435
183.112	0.167843	0.176595	75403.7	0.867424
205.606	0.187472	0.317009	76030.5	0.931416
230.55	0.209004	0.436714	77153.2	1.00648
259.042	0.233712	0.495062	77549.1	1.088
287.899	0.259631	0.710817	77186.8	1.17305
320.067	0.287188	0.839641	77608.6	1.26842
351.581	0.316175	0.933117	76630.6	1.35646
394.61	0.359886	1.53215	73320.2	1.50483
425.126	0.393605	1.91031	71721.2	1.60816

Table 21. 2-05-T-1 (CP)

J (N-mm/mm^2)	CTOD (mm)	Delta a(p) (mm)	Load kN	Clip Gauge COD
5.41696	0.003541	0.003941	17632.8	0.127454
7.70023	0.005563	0.018614	21274.2	0.154796
10.4622	0.007884	0.012699	24539.7	0.179651
13.7579	0.011008	-0.00582	28653.6	0.211627
17.6601	0.01439	0.040947	32145.7	0.24049
22.1056	0.018818	0.030067	35534.6	0.268637
25.795	0.022653	0.001614	37822.9	0.289083
31.1778	0.027643	0.043932	41375.2	0.32078
37.4046	0.033961	0.012034	44998.3	0.354698
44.3145	0.040006	0.089483	48339.2	0.387092
51.4746	0.047456	0.040054	51362.3	0.418342
59.2689	0.054604	0.099663	54015.6	0.448663
68.7619	0.063457	0.125582	57750.2	0.490001
78.4946	0.072985	0.113745	59824.6	0.521416
90.2443	0.084253	0.100712	63429.8	0.568481
102.204	0.094931	0.184818	65895.5	0.609084
116.169	0.108029	0.198158	68180.7	0.653821
132.026	0.122103	0.273329	70812.1	0.706648
148.779	0.13757	0.281801	72367.1	0.756039
168.232	0.154673	0.341513	74526.1	0.817342
188.702	0.172735	0.386288	75920.8	0.878368
212.601	0.194082	0.407539	76439.5	0.944118
239.623	0.217306	0.548363	77382.6	1.02552
269.638	0.244047	0.644548	77587.2	1.11171
300.882	0.272173	0.85507	76952.4	1.20077
332.654	0.30062	1.01338	77011.3	1.29452
365.547	0.33051	1.14296	76946.8	1.39401
403.434	0.367183	1.50233	75058.6	1.51304
438.651	0.404039	1.84564	73257.3	1.62833
471.645	0.43924	2.08735	71759.3	1.7365
505.267	0.476961	2.38181	69842.9	1.84796
537.046	0.518292	2.80364	66983.7	1.9672
567.008	0.556442	3.15674	65891.7	2.08744

Table 22. 2-05-T-2 (CP)

J (N-mm/mm^2)	CTOD (mm)	Delta a(p) (mm)	Load kN	Clip Gauge COD
5.67673	0.003783	0.089422	17977.3	0.130491
8.0252	0.005715	0.059614	20878.1	0.151273
10.676	0.007494	0.098942	24667	0.178666
14.3785	0.011137	0.027138	28561.7	0.208875
18.7588	0.014755	0.086252	32092.8	0.236998
23.598	0.019415	0.074886	35350.7	0.264551
28.7911	0.024064	0.096373	39294.9	0.297411
34.7095	0.029675	0.104652	42401.1	0.325413
41.4504	0.036331	0.061359	46163.1	0.360147
49.3024	0.043306	0.112263	49512.1	0.392729
57.25	0.051433	0.028643	52941.3	0.42771
66.5996	0.059795	0.084169	56252.6	0.463857
76.1911	0.068282	0.148321	59311.6	0.499856
87.6956	0.079056	0.12121	62302.4	0.539152
99.8543	0.090534	0.101225	64719	0.577692
112.895	0.101671	0.180237	67677.8	0.623022
128.014	0.114969	0.245302	70067.5	0.668999
144.518	0.129494	0.2854	71993.8	0.717134
162.387	0.14514	0.308535	73552.4	0.767851
182.069	0.161761	0.36297	75745.8	0.82936
204.889	0.180889	0.40523	76916.9	0.892296
230.969	0.202356	0.479668	78557.7	0.968129
258.126	0.224905	0.591007	79144.5	1.04412
288.767	0.2502	0.67008	79446.6	1.12864
320.056	0.277333	0.9128	78849.9	1.21875
354.922	0.308835	1.20979	77139.3	1.31747
392.284	0.34325	1.52788	75723.3	1.4325
429.642	0.378526	1.77805	74050.7	1.54526
464.559	0.41429	2.13146	71950.8	1.65537

Table 23. 3-05-T-1 (CP)

J (N-mm/mm^2)	CTOD (mm)	Delta a(p) (mm)	Load kN	Clip Gauge COD
5.27316	0.003935	-0.07515	17586.3	0.130012
7.6857	0.005726	-0.01139	21183.4	0.157322
10.7082	0.008639	-0.06376	24779.9	0.185531
13.9282	0.011559	-0.03118	28288.4	0.213343
18.3878	0.015689	-0.02968	32407	0.247652
22.9689	0.02004	0.002624	35613	0.275834
28.4879	0.025553	0.004591	39160.4	0.307944
30.2549	0.027117	0.019743	40383.1	0.318745
36.494	0.033431	-0.01711	44036.1	0.353416
43.5003	0.040097	0.014255	46863.7	0.38329
51.2516	0.047127	0.088984	50546.9	0.421432
59.9076	0.056063	0.043392	53401.6	0.455559
68.6657	0.063861	0.113209	56644.5	0.494102
79.5542	0.074043	0.165226	59600.1	0.534414
90.553	0.084951	0.138544	62390.1	0.576395
104.151	0.097649	0.148456	65004.9	0.62185
117.838	0.110475	0.179974	67001.9	0.666284
133.58	0.124732	0.254068	69175.5	0.717582
151.196	0.140587	0.272753	71609.4	0.776931
170.469	0.158147	0.269384	73318.4	0.836741
191.851	0.177309	0.34083	73871.7	0.895965
215.685	0.198134	0.424536	75944.1	0.973743
241.408	0.220574	0.454586	76682.6	1.04885
268.062	0.24433	0.550499	76556.5	1.12401
297.229	0.270104	0.619644	77448.1	1.21307
326.116	0.295758	0.718241	77610.9	1.29627
357.654	0.322727	0.732084	77725.8	1.38795
389.323	0.352141	0.900742	77441.8	1.48196
421.043	0.381536	1.05238	77168.4	1.57921
451.777	0.410254	1.15537	76150.7	1.66668
482.09	0.438573	1.29841	76151.8	1.76512
514.918	0.471086	1.46295	74767.4	1.86423
547.778	0.504983	1.64836	73698.8	1.96661
581.465	0.537819	1.76475	73559.3	2.07682
612.854	0.570794	1.90839	72224.5	2.17364
645.776	0.605296	2.05275	71725.2	2.28229
677.817	0.64054	2.22308	70378.7	2.39455
705.036	0.674379	2.45116	69480.6	2.4983
731.582	0.711542	2.72409	67037.7	2.60157
763.71	0.753345	2.95498	65786	2.72883

Table 24. 3-05-T-2 (CP)

J (N-mm/mm^2)	CTOD (mm)	Delta a(p) (mm)	Load kN	Clip Gauge COD
5.324	0.0023	-0.03604	17048.1	0.123498
7.81481	0.004506	-0.04154	21373.5	0.157115
10.8575	0.007171	-0.04445	24555.5	0.182304
14.1629	0.010245	-0.02837	27873.9	0.210012
18.2919	0.014201	-0.03611	31491	0.240486
23.4829	0.018979	-0.00177	35540.9	0.275822
28.6744	0.024585	-0.09257	38885.5	0.305445
35.5354	0.030389	0.02446	42960.6	0.344381
42.4081	0.037479	-0.0029	46095	0.376363
49.4675	0.044269	0.006056	49228.1	0.409774
59.2545	0.053138	0.080763	52743.5	0.449423
69.5966	0.063192	0.074705	56432.1	0.493627
80.4706	0.073946	0.061261	58808	0.530198
92.1796	0.084738	0.120388	61903.8	0.574898
106.094	0.097595	0.159333	64708.4	0.624084
121.052	0.111393	0.197369	66994.1	0.672063
137.848	0.126724	0.211277	69805.1	0.731248
156.859	0.143957	0.250214	71052.4	0.78359
177.247	0.162188	0.248434	73422.2	0.851699
198.829	0.181327	0.298897	74639.7	0.914573
223.443	0.203014	0.313383	75700.6	0.986785
251.326	0.227016	0.44394	76823.6	1.06871
279.431	0.251469	0.467081	77282.2	1.14809
307.988	0.276973	0.596808	77342.7	1.23101
339.009	0.30404	0.683735	77564.8	1.32038
370.338	0.331979	0.771181	77056.7	1.40649
393.141	0.352527	0.855126	76744.9	1.47089
426.256	0.382003	0.985144	76545	1.56741
458.137	0.412316	1.15618	76501.7	1.66763
492.569	0.443445	1.25497	76177	1.76813
527.205	0.476693	1.40647	75153.9	1.871
560.302	0.509119	1.55502	74453.3	1.97499
594.916	0.547279	1.84678	72748.9	2.09286
625.861	0.58158	2.05945	71573.2	2.19853
657.392	0.616645	2.24237	70427.2	2.30004
688.612	0.653199	2.48123	69619.2	2.41453
718.664	0.69108	2.73322	67671.9	2.52153
750.466	0.729644	2.90548	65927.9	2.63151

Table 25. 1-06-T-1 (H_2S)

J (N-mm/mm^2)	CTOD (mm)	Delta a(p) (mm)	Load kN	Clip Gauge COD
5.42192	0.003343	0.064241	17977.3	0.130824
7.73578	0.004894	0.091408	21472	0.156239
10.5212	0.006766	0.182995	24711	0.181116
14.2817	0.009809	0.320396	28552.9	0.214343
18.7115	0.013817	0.448021	31884.1	0.24593
24.0263	0.018102	0.651604	34990.4	0.277844
30.1555	0.023891	0.775591	38377	0.314849
36.5367	0.029539	0.99921	40798	0.347598
45.3523	0.037102	1.31936	43287	0.389501
50.0627	0.041261	1.49986	45012.7	0.417848
62.5105	0.052118	1.92933	47311.4	0.474653
77.6363	0.065879	2.45896	48550.3	0.538792
112.788	0.10026	4.6531	43209	0.701788

Table 26. 1-06-T-2 (H_2S)

J (N-mm/mm^2)	CTOD (mm)	Delta a(p) (mm)	Load kN	Clip Gauge COD
5.42574	0.00479	0.092926	17960	0.134404
7.41203	0.00567	0.189461	20909	0.154868
9.96596	0.008022	0.144489	23808	0.176996
13.4204	0.010439	0.37237	27641.9	0.210189
17.303	0.014388	0.457993	30346.9	0.236825
22.2306	0.01815	0.723818	33782.2	0.271695
25.9182	0.021497	0.842735	35689.3	0.293754
32.2543	0.027228	1.06245	38401.5	0.32824
39.1193	0.033613	1.25276	41085.7	0.364716
47.9602	0.041571	1.50251	44194.1	0.4103
57.8004	0.051092	1.71807	46114.3	0.451139
74.8958	0.066116	2.50557	47580.4	0.531501
96.6889	0.088804	3.47914	46346.1	0.623045

Table 27. 2-06-T-1 (H_2S)

J (N-mm/mm^2)	CTOD (mm)	Delta a(p) (mm)	Load kN	Clip Gauge COD
5.15077	0.003093	0.025831	17931.5	0.127532
7.18267	0.004209	0.013491	21515.4	0.152008
10.0496	0.005995	0.104177	24924.3	0.176665
13.7444	0.009241	0.187113	28424.3	0.206023
18.1944	0.013104	0.358494	32199.4	0.240284
23.5752	0.017446	0.567308	35863.5	0.277156
29.8108	0.023481	0.695257	38972.4	0.312187
37.2684	0.030032	0.920343	41992	0.350471
45.9837	0.03755	1.20078	45151.8	0.394702
58.7318	0.048431	1.71275	47440.9	0.455489
74.5469	0.062784	2.44687	48100.9	0.522355

Table 28. 2-06-T-2 (H_2S)

J (N-mm/mm^2)	CTOD (mm)	Delta a(p) (mm)	Load kN	Clip Gauge COD
5.75044	0.003534	0.001936	18056.9	0.136906
8.21683	0.005491	0.013744	21611.4	0.16493
11.2784	0.00782	0.084456	25134.1	0.192778
15.0676	0.011126	0.151312	28597.1	0.223309
19.9585	0.015191	0.300541	31903.4	0.255093
25.3008	0.020228	0.403889	35369.9	0.291168
31.9845	0.026277	0.567619	38795.6	0.330501
39.8529	0.033051	0.794708	41953	0.371205
49.196	0.041148	1.05383	45037.8	0.418156
60.2221	0.051096	1.29434	47709	0.466348
77.0384	0.066152	1.93511	48935.3	0.539393

Table 29. 3-06-T-1 (H_2S)

J (N-mm/mm^2)	CTOD (mm)	Delta a(p) (mm)	Load kN	Clip Gauge COD
5.25302	0.002778	0.041895	17968.1	0.127909
7.66881	0.004087	0.050932	21962.1	0.155089
10.7572	0.006132	0.099943	25909.5	0.183954
14.4981	0.009342	0.152649	29677.5	0.214146
18.9975	0.013525	0.192356	33385.9	0.246012
24.2102	0.018048	0.294762	37023.2	0.278916
30.2311	0.02401	0.321384	40541.8	0.313557
37.1197	0.030328	0.434019	43909.2	0.349705
44.9102	0.037262	0.584593	47138.3	0.387418
53.6455	0.045713	0.6824	50043.8	0.427025
64.2399	0.055748	0.855377	52785.7	0.472198
76.2355	0.066862	1.05681	55283.9	0.520736
91.1257	0.08076	1.34164	57208	0.57829
125.894	0.111372	2.48899	54163.9	0.714274

Table 30. 3-06-T-2 (H_2S)

J (N-mm/mm^2)	CTOD (mm)	Delta a(p) (mm)	Load kN	Clip Gauge COD
5.06618	0.002214	0.018068	17981.8	0.126281
7.00834	0.002214	-0.00341	21775.9	0.14888
9.64067	0.003359	0.048472	25567.9	0.1744
13.2464	0.006177	0.082542	29296.6	0.20436
17.7116	0.010396	0.151793	33041.6	0.237003
22.8869	0.015068	0.229565	36697.1	0.270741
28.8228	0.020995	0.266129	40227.3	0.305739
35.3705	0.026336	0.445335	43599.5	0.34081
42.6828	0.033299	0.521229	46783.9	0.377204
50.658	0.041389	0.553905	49750.2	0.414384
60.2861	0.049712	0.752819	52631.6	0.45626
71.1436	0.059814	0.910181	55225.3	0.500934
84.0101	0.071455	1.13427	57534.7	0.551326
100.72	0.086863	1.44548	59052	0.614205
124.982	0.108905	2.05709	59003.2	0.703879
152.094	0.132203	3.05705	55123.4	0.810432

Table 31. 2-07-T-1 (Air) Control Sample

J (N-mm/mm^2)	CTOD (mm)	Delta a(p) (mm)	Load kN	Clip Gauge COD
5.72038	0.000571	0.013919	17503.5	0.131642
9.59667	-0.00057	0.71506	23003.6	0.177211
14.7257	0.008733	-0.04312	28471.9	0.224299
20.8987	0.014486	-0.03128	33603.4	0.271091
29.155	0.022456	-0.03589	39343.7	0.325418
30.3947	0.023648	-0.04526	39921.3	0.331195
46.4871	0.039376	-0.06009	48537.1	0.420205
66.6273	0.058073	0.018527	56068.7	0.50864
86.1056	0.076528	0.013994	62112.8	0.588567
117.77	0.104959	0.072896	68838.1	0.696398
155.192	0.138217	0.091428	74493.9	0.818059
200.934	0.177854	0.102664	78660.6	0.955923
225.627	0.199515	0.125348	79567	1.02417
305.68	0.265327	0.277463	82752	1.2426
400.648	0.34291	0.4171	83731.7	1.49889
506.462	0.429566	0.609647	84093.5	1.78054
618.769	0.523718	0.837785	83295.8	2.0886
737.497	0.628835	1.20406	81842.4	2.42514
849.566	0.733385	1.59132	79377.8	2.75933
957.817	0.844532	1.93153	76142.6	3.08352
1064.24	0.962733	2.36834	72504.8	3.44549
1158.67	1.08163	2.83184	69107	3.78654

Tested by,

Gary Keith
Fracture Mechanics Specialist

Reviewed by,

Dustin McKnight
Fracture Mechanics Specialist

Unless otherwise directed by the customer, items or samples are retained for 30 days after completion of the project and then discarded.

Annex F.2. Toughness Data Analysis

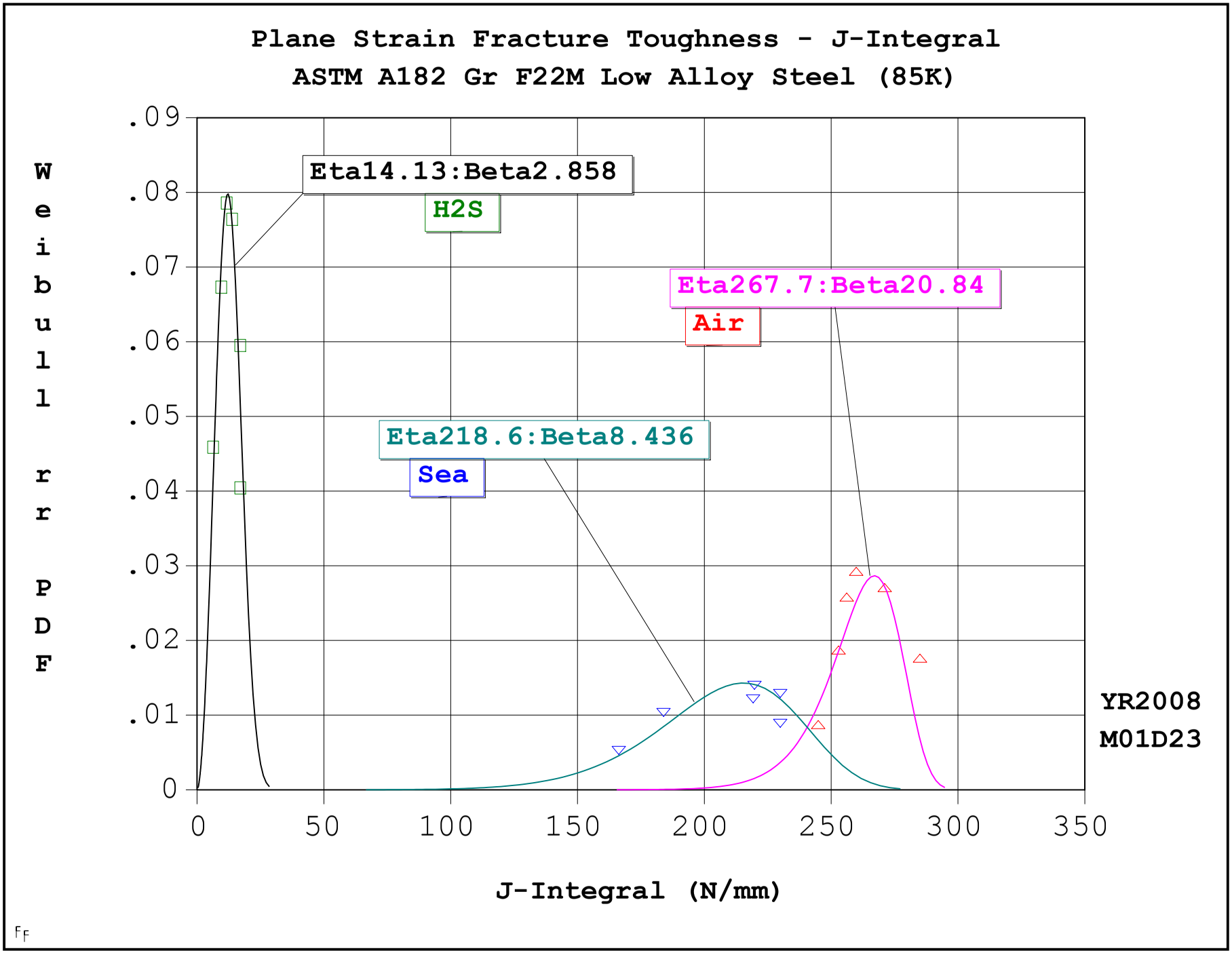
Plane Strain Fracture Toughness - J-Integral
ASTM A182 Gr F22M Low Alloy Steel (85K)
Weibull rr PDF
.09
.08
.07
.06
.05
.04
.03
.02
.01
0
Eta14.13:Beta2.858
H2S
Eta267.7:Beta20.84
Air
Eta218.6:Beta8.436
Sea
0
50
100
150
200
250
300
350
J-Integral (N/mm)
YR2008
M01D23

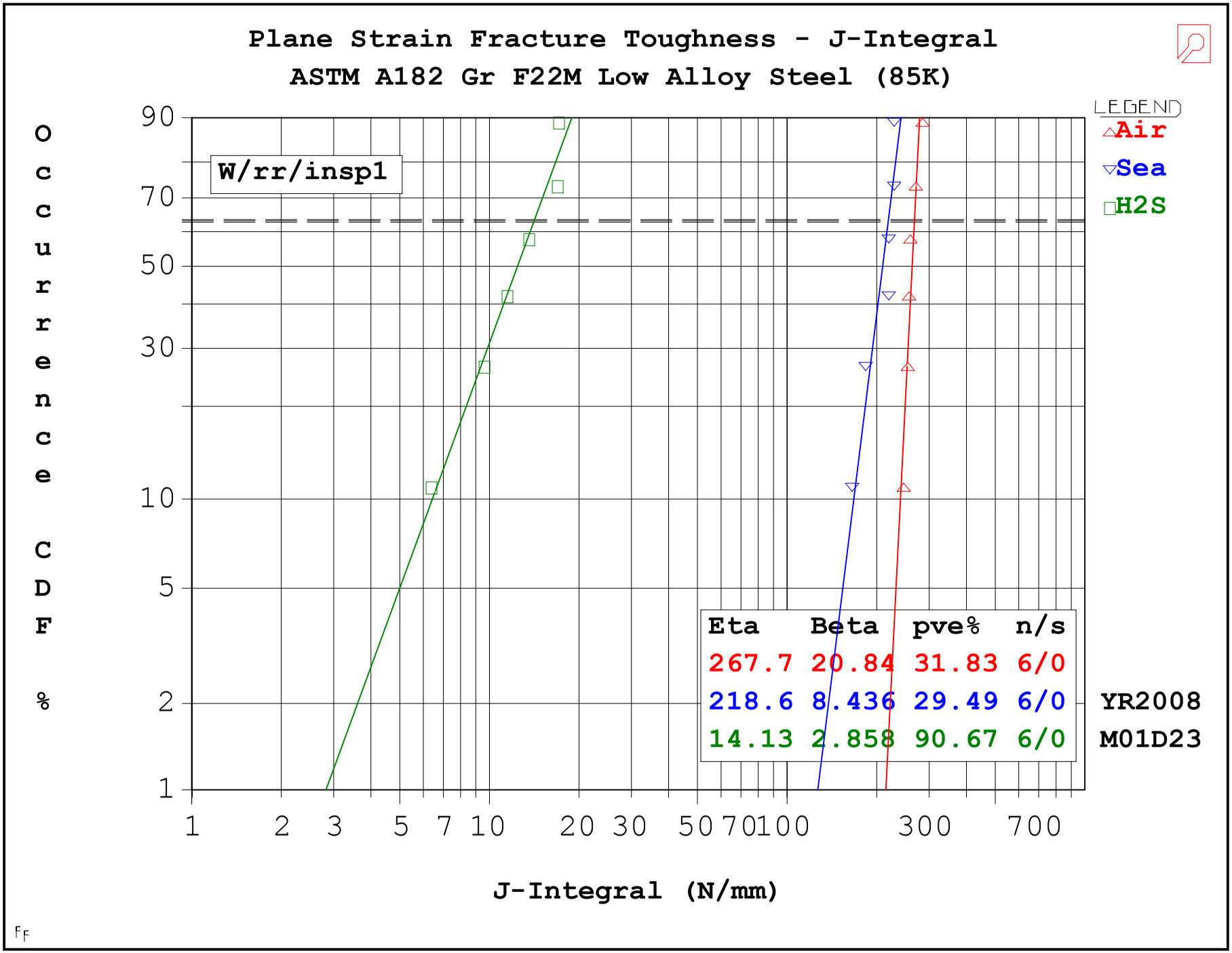
Plane Strain Fracture Toughness - J-Integral
ASTM A182 Gr F22M Low Alloy Steel (85K)
Occurrence CDF %
90
70
50
30
10
5
2
1
W/rr/insp1
LEGEND
Air
Sea
H2S
Eta Beta pve% n/s
267.7 20.84 31.83 6/0
218.6 8.436 29.49 6/0
14.13 2.858 90.67 6/0
YR2008
M01D23
1 2 3 5 7 10 20 30 50 70 100 300 700
J-Integral (N/mm)

Weibull Analysis Report

Set 1 - Air Date: YR2008-M01-D23
Plane Strain Fracture Toughness - J-Integral ASTM A182 Gr F22M Low Alloy Steel
Correlation(r)=.94446 r^2=.892 ccc^2=.8203 pve%=31.83 (Okay)
Characteristic Value=267.7 Weibull Slope=20.84 Method=rr/insp1
Mean=260.9 Std. Deviation=15.53 Cv%=5.954
Point Quantity=6 (Susp=0)

B%	J-Integral (N/mm)
1	214.7
2	222
5	232.1
10	240.3
20	249.1
50	263

Weibull Analysis Report

Set 2 - Sea Date: YR2008-M01-D23
Plane Strain Fracture Toughness - J-Integral ASTM A182 Gr F22M Low Alloy Steel
Correlation(r)=.93808 r^2=.880 ccc^2=.8076 pve%=29.49 (Okay)
Characteristic Value=218.6 Weibull Slope=8.436 Method=rr/insp1
Mean=206.4 Std. Deviation=29.13 Cv%=14.11
Point Quantity=6 (Susp=0)

B%	J-Integral (N/mm)
1	126.7
2	137.7
5	153.8
10	167.4
20	183
50	209.3

Weibull Analysis Report

Set 3 - H2S Date: YR2008-M01-D23
Plane Strain Fracture Toughness - J-Integral ASTM A182 Gr F22M Low Alloy Steel
Correlation(r)=.98793 r^2=.976 ccc^2=.8203 pve%=90.67 (Okay)
Characteristic Value=14.13 Weibull Slope=2.858 Method=rr/insp1
Mean=12.59 Std. Deviation=4.778 Cv%=37.96
Point Quantity=6 (Susp=0)

B%	J-Integral (N/mm)
1	2.824
2	3.606
5	4.996
10	6.427
20	8.357
50	12.43

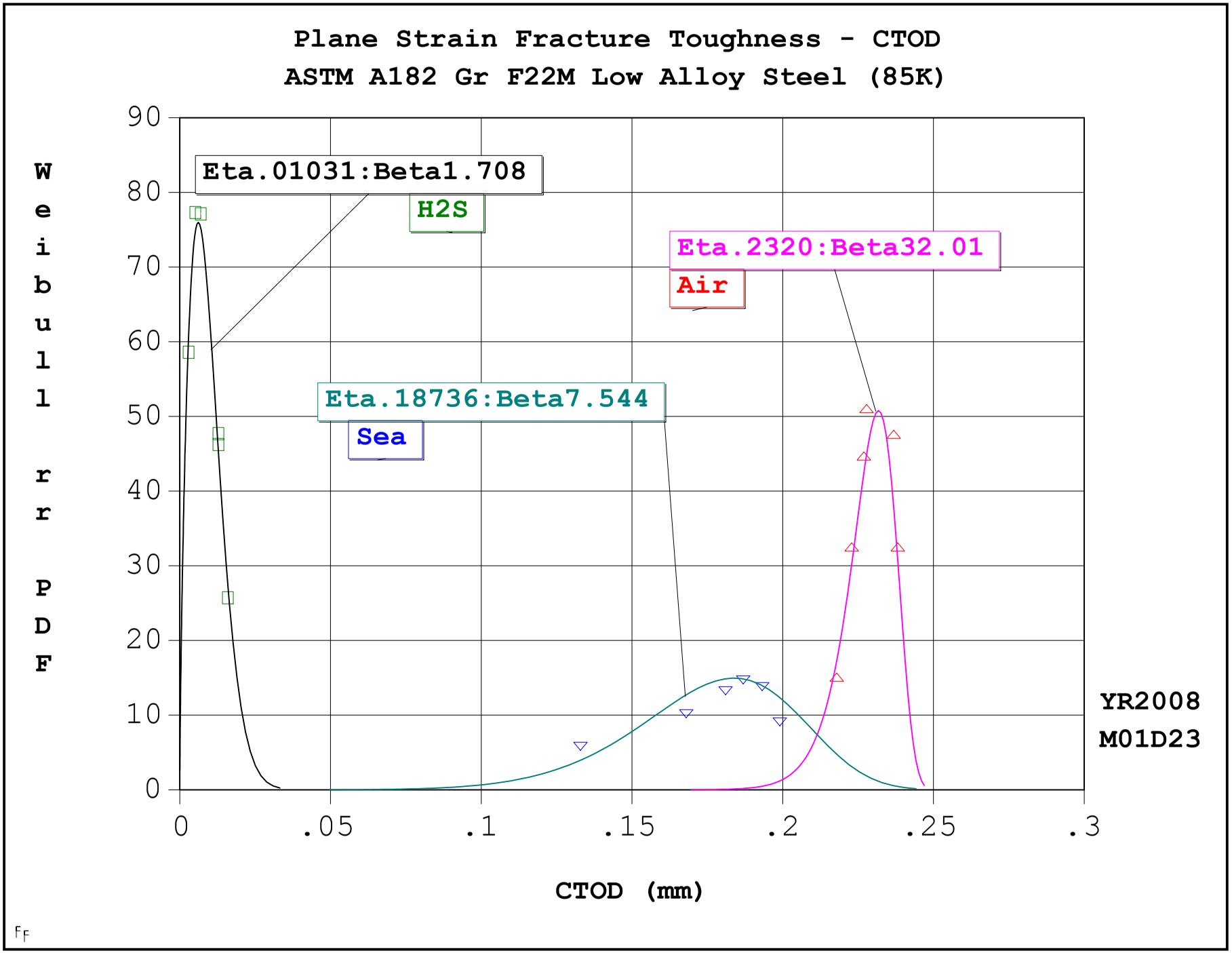
Plane Strain Fracture Toughness - CTOD
ASTM A182 Gr F22M Low Alloy Steel (85K)
Weibull rr PDF
Eta.01031:Beta1.708
H2S
Eta.2320:Beta32.01
Air
Eta.18736:Beta7.544
Sea
YR2008
M01D23
CTOD (mm)
0
10
20
30
40
50
60
70
80
90
0
.05
.1
.15
.2
.25
.3

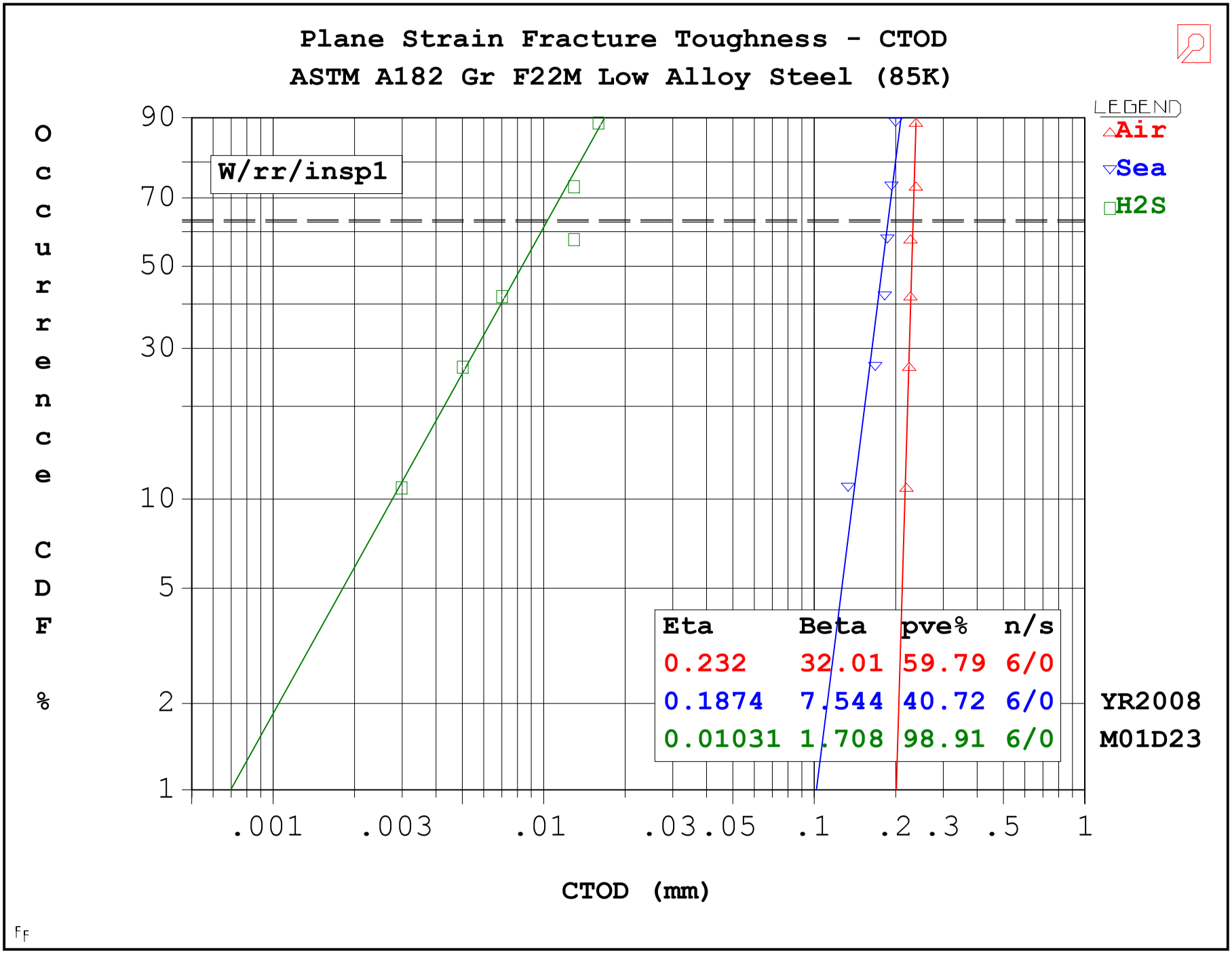
Plane Strain Fracture Toughness - CTOD
ASTM A182 Gr F22M Low Alloy Steel (85K)
Occurrence CDF %
90
70
50
30
10
5
2
1
W/rr/insp1
LEGEND
Air
Sea
H2S
Eta Beta pve% n/s
0.232 32.01 59.79 6/0
0.1874 7.544 40.72 6/0
0.01031 1.708 98.91 6/0
YR2008
M01D23
.001 .003 .01 .03 .05 .1 .2 .3 .5 1
CTOD (mm)

Weibull Analysis Report

Set 1 - Air Date: YR2008-M01-D23
Plane Strain Fracture Toughness - CTOD ASTM A182 Gr F22M Low Alloy Steel (85K)
Correlation(r)=.96799 r^2=.937 ccc^2=.8203 pve%=59.79 (Okay)
Characteristic Value=.232 Weibull Slope=32.01 Method=rr/insp1
Mean=.228 Std. Deviation=.0089339 Cv%=3.918
Point Quantity=6 (Susp=0)

B%	CTOD (mm)
1	.2009
2	.2054
5	.2114
10	.2162
20	.2214
50	.2293

Weibull Analysis Report

Set 2 - Sea Date: YR2008-M01-D23
Plane Strain Fracture Toughness - CTOD ASTM A182 Gr F22M Low Alloy Steel (85K)
Correlation(r)=.95341 r^2=.909 ccc^2=.8203 pve%=40.72 (Okay)
Characteristic Value=.1874 Weibull Slope=7.544 Method=rr/insp1
Mean=.1759 Std. Deviation=.02757 Cv%=15.67
Point Quantity=6 (Susp=0)

B%	CTOD (mm)
1	.1018
2	.1117
5	.1264
10	.139
20	.1536
50	.1785

Weibull Analysis Report

Set 3 - H2S Date: YR2008-M01-D23
Plane Strain Fracture Toughness - CTOD ASTM A182 Gr F22M Low Alloy Steel (85K)
Correlation(r)=.9975 r^2=.995 ccc^2=.8076 pve%=98.91 (Okay)
Characteristic Value=.01031 Weibull Slope=1.708 Method=rr/insp1
Mean=.0091938 Std. Deviation=.0055444 Cv%=60.31
Point Quantity=6 (Susp=0)

B%	CTOD (mm)
1	.0006968
2	.0010488
5	.0018101
10	.0027592
20	.004282
50	.0083161

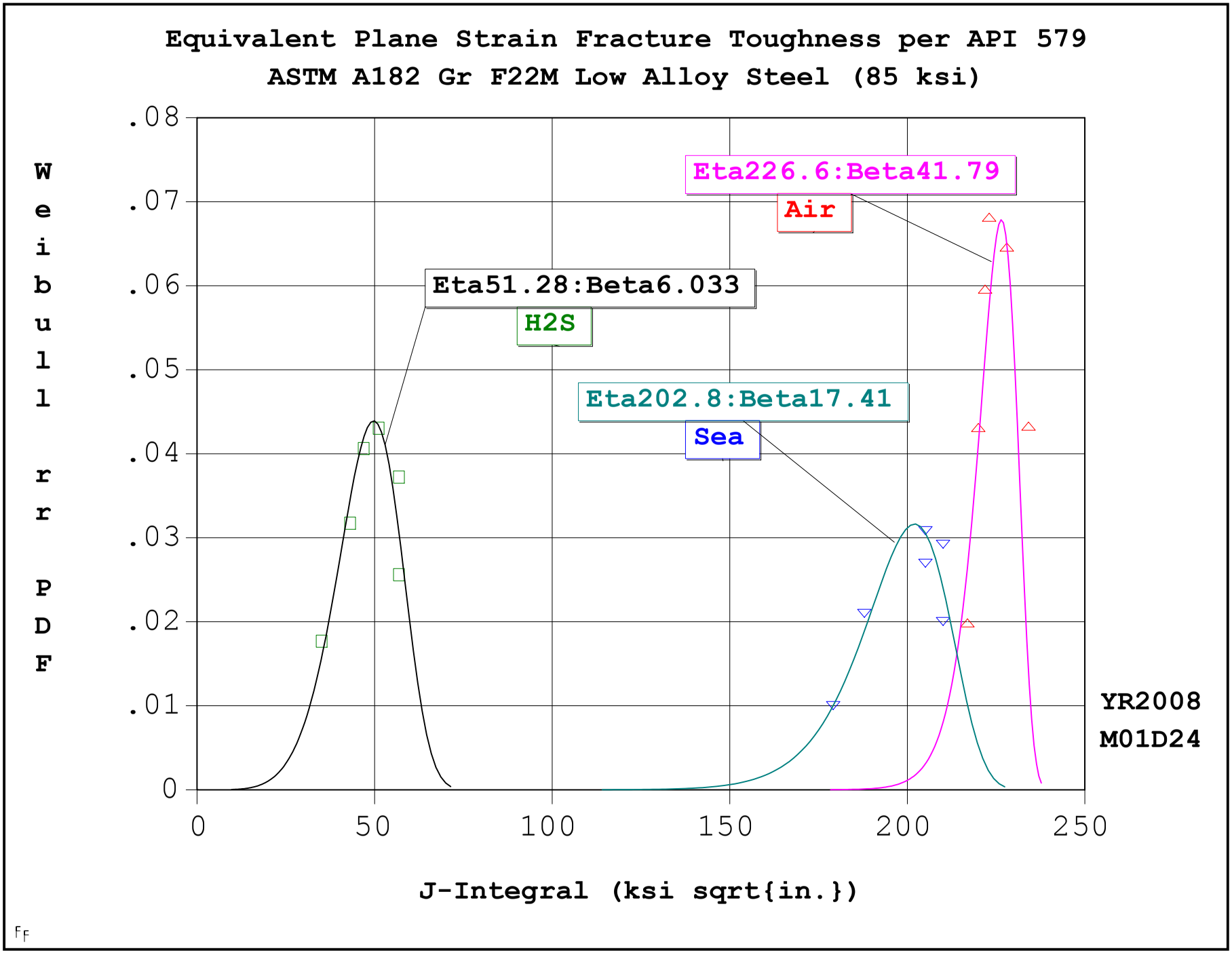
Equivalent Plane Strain Fracture Toughness per API 579
ASTM A182 Gr F22M Low Alloy Steel (85 ksi)
Weibull PDF
.08
.07
.06
.05
.04
.03
.02
.01
0
0
50
100
150
200
250
J-Integral (ksi sqrt{in.})
Eta226.6:Beta41.79
Air
Eta51.28:Beta6.033
H2S
Eta202.8:Beta17.41
Sea
YR2008
M01D24

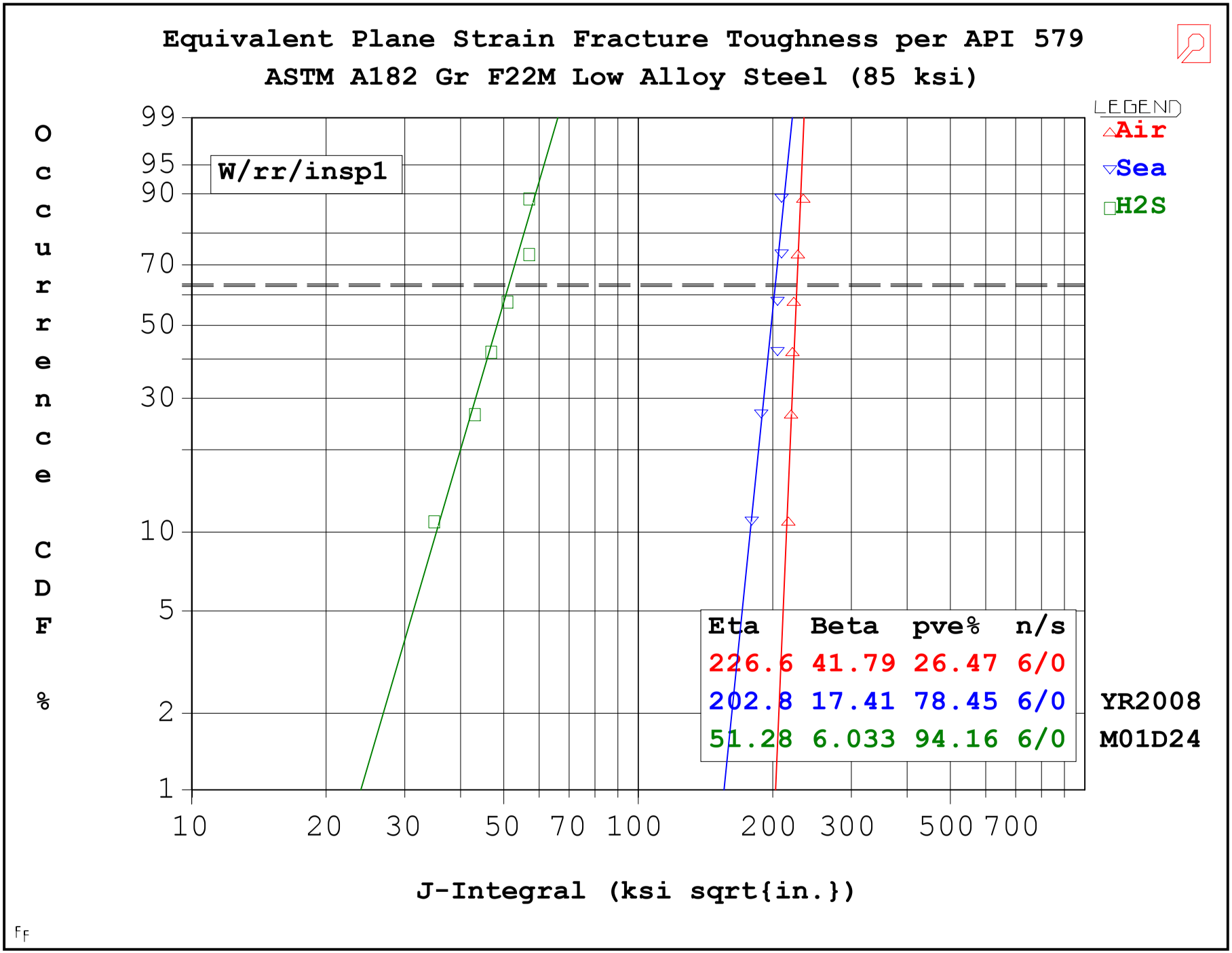
Equivalent Plane Strain Fracture Toughness per API 579
ASTM A182 Gr F22M Low Alloy Steel (85 ksi)
W/rr/insp1
LEGEND
Air
Sea
H2S
Occurrence CDF %
99
95
90
70
50
30
10
5
2
1
10
20
30
50
70
100
200
300
500
700
J-Integral (ksi sqrt{in.})
Eta Beta pve% n/s
226.6 41.79 26.47 6/0
202.8 17.41 78.45 6/0
51.28 6.033 94.16 6/0
YR2008
M01D24

Weibull Analysis Report

Set 1 - Air Date: YR2008-M01-D24
Equivalent Plane Strain Fracture Toughness per API 579 ASTM A182 Gr F22M Low Al
Correlation(r)=.93808 r^2=.880 ccc^2=.8203 pve%=26.47 (Okay)
Characteristic Value=226.6 Weibull Slope=41.79 Method=rr/insp1
Mean=223.6 Std. Deviation=6.744 Cv%=3.016
Point Quantity=6 (Susp=0)

B%	J-Integral (ksi s
1	203
2	206.4
5	211.1
10	214.7
20	218.6
50	224.7

Weibull Analysis Report

Set 2 - Sea Date: YR2008-M01-D24
Equivalent Plane Strain Fracture Toughness per API 579 ASTM A182 Gr F22M Low Al
Correlation(r)=.98285 r^2=.966 ccc^2=.7991 pve%=78.45 (Okay)
Characteristic Value=202.8 Weibull Slope=17.41 Method=rr/insp1
Mean=196.7 Std. Deviation=13.93 Cv%=7.084
Point Quantity=6 (Susp=0)

B%	J-Integral (ksi s
1	155.7
2	162
5	171
10	178.2
20	186
50	198.5

Weibull Analysis Report

Set 3 - H2S Date: YR2008-M01-D24
Equivalent Plane Strain Fracture Toughness per API 579 ASTM A182 Gr F22M Low Al
Correlation(r)=.99197 r^2=.984 ccc^2=.8076 pve%=94.16 (Okay)
Characteristic Value=51.28 Weibull Slope=6.033 Method=rr/insp1
Mean=47.59 Std. Deviation=9.172 Cv%=19.27
Point Quantity=6 (Susp=0)

B%	J-Integral (ksi s
1	23.92
2	26.86
5	31.34
10	35.31
20	39.99
50	48.25

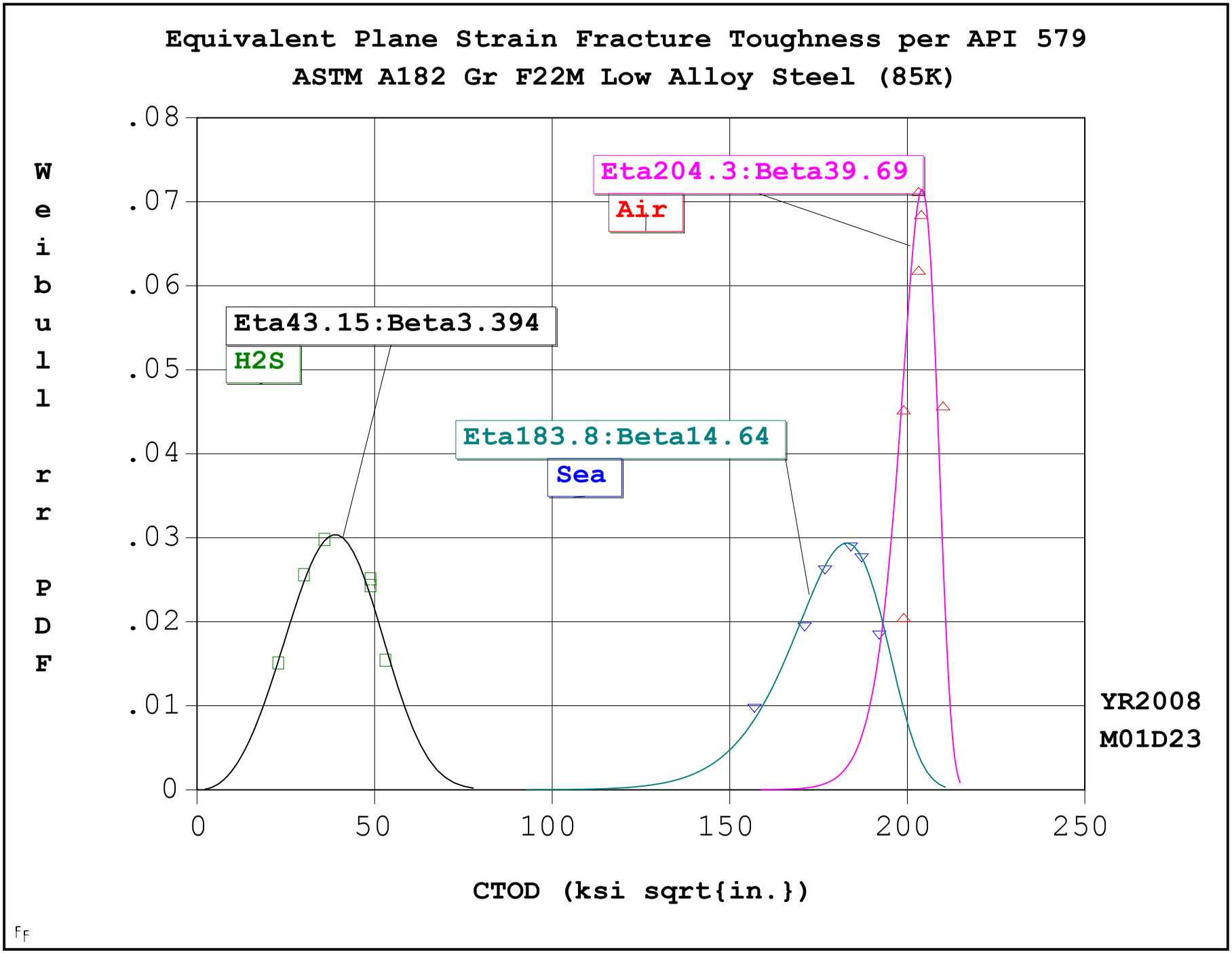
Equivalent Plane Strain Fracture Toughness per API 579
ASTM A182 Gr F22M Low Alloy Steel (85K)
Weibull PDF
.08
.07
.06
.05
.04
.03
.02
.01
0
0
50
100
150
200
250
CTOD (ksi sqrt{in.})
Eta204.3:Beta39.69
Air
Eta43.15:Beta3.394
H2S
Eta183.8:Beta14.64
Sea
YR2008
M01D23

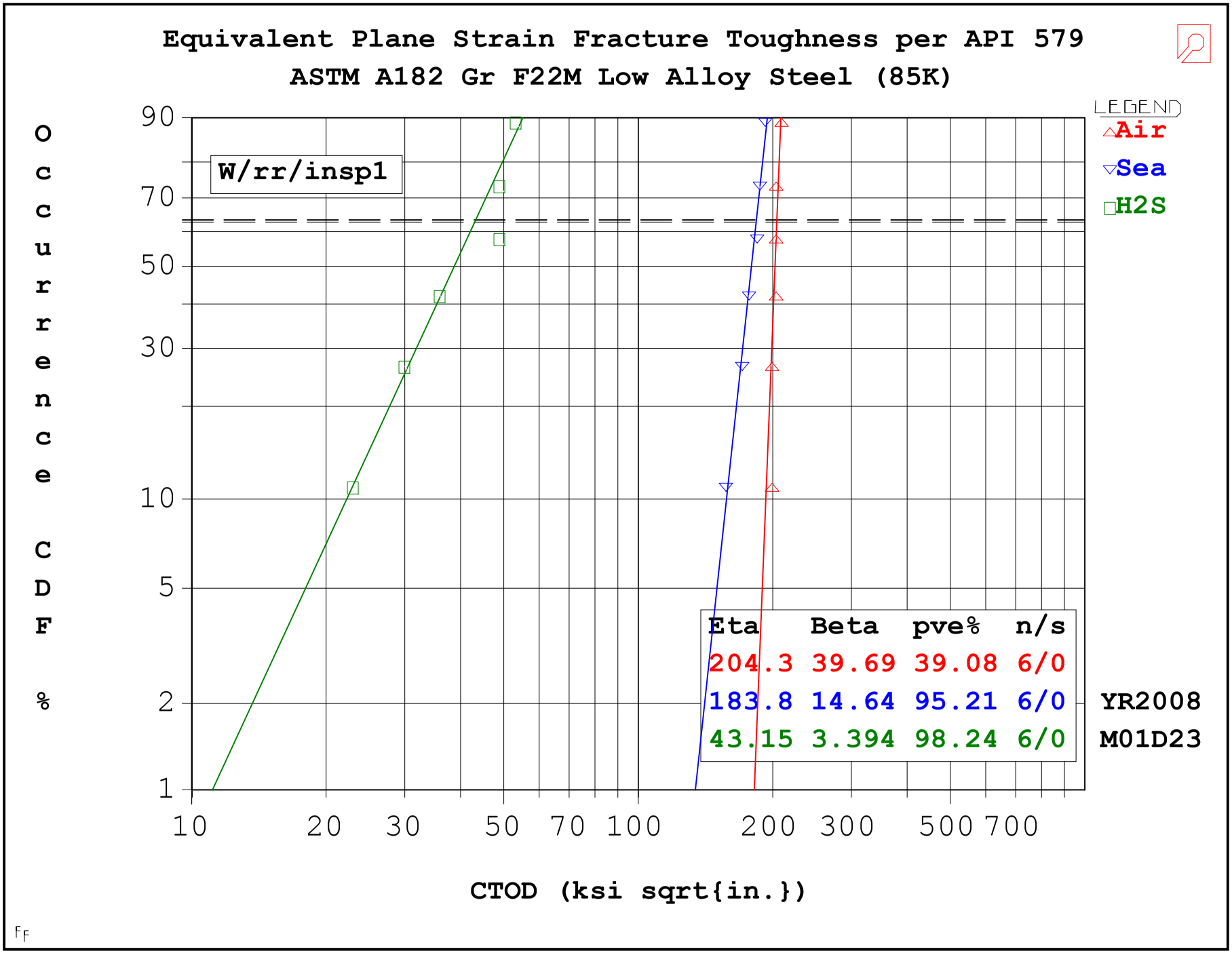
Equivalent Plane Strain Fracture Toughness per API 579
ASTM A182 Gr F22M Low Alloy Steel (85K)
W/rr/insp1
LEGEND
Air
Sea
H2S
Eta Beta pve% n/s
204.3 39.69 39.08 6/0
183.8 14.64 95.21 6/0
43.15 3.394 98.24 6/0
YR2008
M01D23
Occurrence CDF %
90
70
50
30
10
5
2
1
10
20
30
50
70
100
200
300
500
700
CTOD (ksi sqrt{in.})

Weibull Analysis Report

Set 1 - Air Date: YR2008-M01-D23
Equivalent Plane Strain Fracture Toughness per API 579 ASTM A182 Gr F22M Low Al
Correlation(r)=.94868 r^2=.900 ccc^2=.7991 pve%=39.08 (Okay)
Characteristic Value=204.3 Weibull Slope=39.69 Method=rr/insp1
Mean=201.4 Std. Deviation=6.392 Cv%=3.173
Point Quantity=6 (Susp=0)

B%	CTOD (ksi sqrt{in
1	181.9
2	185.2
5	189.5
10	193
20	196.7
50	202.4

Weibull Analysis Report

Set 2 - Sea Date: YR2008-M01-D23
Equivalent Plane Strain Fracture Toughness per API 579 ASTM A182 Gr F22M Low Al
Correlation(r)=.99197 r^2=.984 ccc^2=.8203 pve%=95.21 (Okay)
Characteristic Value=183.8 Weibull Slope=14.64 Method=rr/insp1
Mean=177.3 Std. Deviation=14.84 Cv%=8.367
Point Quantity=6 (Susp=0)

B%	CTOD (ksi sqrt{in
1	134.2
2	140.8
5	150
10	157.6
20	165.9
50	179.2

Weibull Analysis Report

Set 3 - H2S Date: YR2008-M01-D23
Equivalent Plane Strain Fracture Toughness per API 579 ASTM A182 Gr F22M Low Al
Correlation(r)=.99649 r^2=.993 ccc^2=.8076 pve%=98.24 (Okay)
Characteristic Value=43.15 Weibull Slope=3.394 Method=rr/insp1
Mean=38.77 Std. Deviation=12.61 Cv%=32.53
Point Quantity=6 (Susp=0)

B%	CTOD (ksi sqrt{in
1	11.13
2	13.67
5	17.99
10	22.24
20	27.74
50	38.74

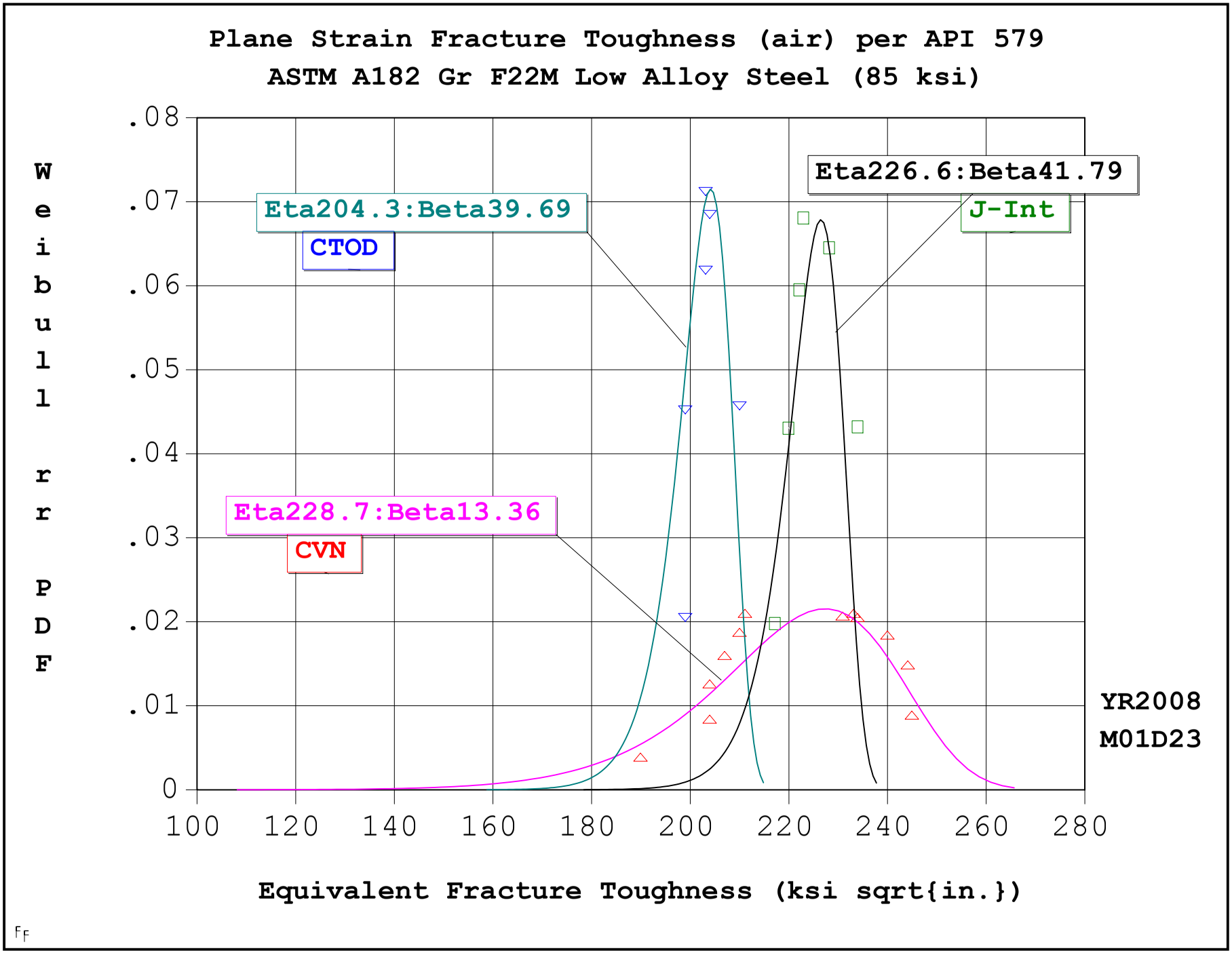
Plane Strain Fracture Toughness (air) per API 579
ASTM A182 Gr F22M Low Alloy Steel (85 ksi)
Weibull rr PDF
.08
.07
.06
.05
.04
.03
.02
.01
0
100
120
140
160
180
200
220
240
260
280
Eta204.3:Beta39.69
CTOD
Eta226.6:Beta41.79
J-Int
Eta228.7:Beta13.36
CVN
YR2008
M01D23
Equivalent Fracture Toughness (ksi sqrt{in.})

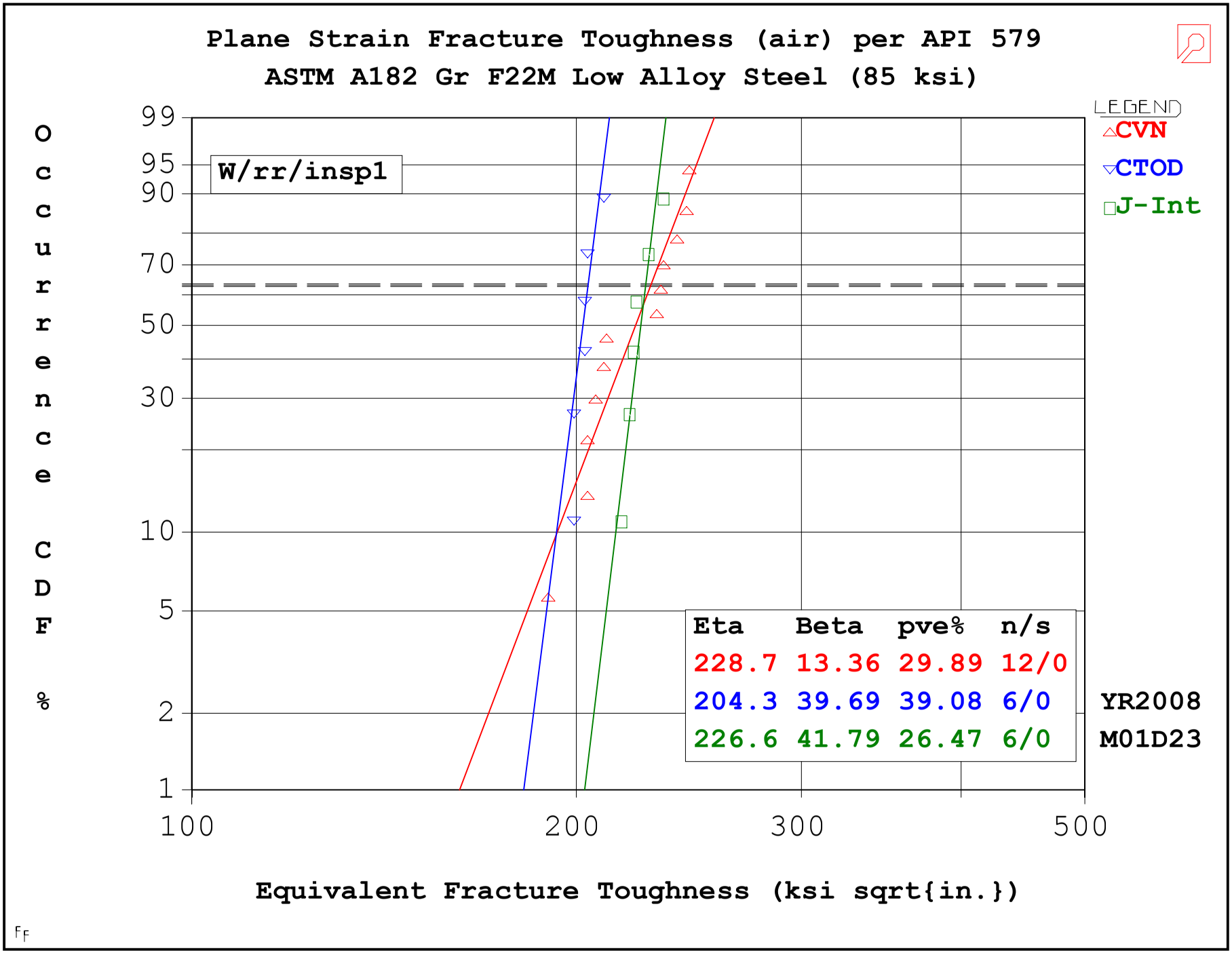
Plane Strain Fracture Toughness (air) per API 579
ASTM A182 Gr F22M Low Alloy Steel (85 ksi)
W/rr/insp1
LEGEND
CVN
CTOD
J-Int
Occurrence CDF %
99
95
90
70
50
30
10
5
2
1
100
200
300
500
Eta Beta pve% n/s
228.7 13.36 29.89 12/0
204.3 39.69 39.08 6/0
226.6 41.79 26.47 6/0
YR2008
M01D23
Equivalent Fracture Toughness (ksi sqrt{in.})

Weibull Analysis Report

Set 1 - CVN Date: YR2008-M01-D23
Plane Strain Fracture Toughness (air) per API 579 ASTM A182 Gr F22M Low Alloy S
Correlation(r)=.9576 r^2=.917 ccc^2=.8663 pve%=29.89 (Okay)
Characteristic Value=228.7 Weibull Slope=13.36 Method=rr/insp1
Mean=220 Std. Deviation=20.1 Cv%=9.136
Point Quantity=12 (Susp=0)

B%	Equivalent Fractu
1	162.1
2	170.8
5	183.1
10	193.3
20	204.4
50	222.5

Weibull Analysis Report

Set 2 - CTOD Date: YR2008-M01-D23
Plane Strain Fracture Toughness (air) per API 579 ASTM A182 Gr F22M Low Alloy S
Correlation(r)=.94868 r^2=.900 ccc^2=.7991 pve%=39.08 (Okay)
Characteristic Value=204.3 Weibull Slope=39.69 Method=rr/insp1
Mean=201.4 Std. Deviation=6.392 Cv%=3.173
Point Quantity=6 (Susp=0)

B%	Equivalent Fractu
1	181.9
2	185.2
5	189.5
10	193
20	196.7
50	202.4

Weibull Analysis Report

Set 3 - J-Int Date: YR2008-M01-D23
Plane Strain Fracture Toughness (air) per API 579 ASTM A182 Gr F22M Low Alloy S
Correlation(r)=.93808 r^2=.880 ccc^2=.8203 pve%=26.47 (Okay)
Characteristic Value=226.6 Weibull Slope=41.79 Method=rr/insp1
Mean=223.6 Std. Deviation=6.744 Cv%=3.016
Point Quantity=6 (Susp=0)

B%	Equivalent Fractu
1	203
2	206.4
5	211.1
10	214.7
20	218.6
50	224.7

Material 85K, 2¼ Cr - 1 Mo Low Alloy Steel

Test Lab Bodycote

Test Date Aug - Nov 2007

Plane Strain Fracture Toughness Test Data, ASTM E 1820 (0.2 mm offset, J_Q)

Data	S/N	Environment	CTOD Test Data		CTOD Equivalent K_{IC}			J-Integral Test Data		J-Integral Equivalent K_{IC}	Comments
					ASME	API 579	Barson Rolfe				
			mm	in.	ksi·√in.	ksi·√in.	ksi·√in.	N / mm	lb / in	ksi·√in.	
8/31/2007	2-07-T-1	Air	0.430	0.01695	218	283	297	506	2890	312	Std strain rate 0.66 mm/min
9/17/2007	1-05-T-1	Air	0.218	0.00860	153	199	209	245	1395	217	Slow strain rate 0.008 mm/min
8/31/2007	1-05-T-2	Air	0.227	0.00895	156	203	214	271	1545	228	Slow strain rate 0.008 mm/min
9/17/2007	2-05-T-1	Air	0.223	0.00880	157	204	214	260	1485	223	Slow strain rate 0.008 mm/min
9/18/2007	2-05-T-2	Air	0.238	0.00935	162	210	221	256	1460	222	Slow strain rate 0.008 mm/min
9/11/2007	3-05-T-1	Air	0.228	0.00900	153	199	209	253	1445	220	Slow strain rate 0.008 mm/min
10/3/2007	3-05-T-2	Air	0.237	0.00935	156	203	213	285	1630	234	Slow strain rate 0.008 mm/min
		Weibull eta	**0.232**		**157.2**	**204.3**	**215.1**	**267.7**		**226.6**	
		Weibull beta	**32.01**		**37.39**	**39.69**	**41.00**	**20.84**		**41.79**	
		Weibull B50	**0.229**		**156**	**202**	**213**	**263**		**225**	
		Weibull B2	**0.205**		**142**	**185**	**196**	**222**		**206**	
		Weibull B1	**0.201**		**139**	**182**	**192**	**215**		**203**	
		COV	**3.9%**		**3.4%**	**3.2%**	**3.1%**	**6.0%**		**3.0%**	
9/19/2007	1-05-T-1	Seawater w/ CP	0.187	0.00735	142	184	194	220	1255	205	Slow strain rate 0.008 mm/min
9/19/2007	1-05-T-2	Seawater w/ CP	0.193	0.00760	144	187	197	230	1315	210	Slow strain rate 0.008 mm/min
9/19/2007	2-05-T-1	Seawater w/ CP	0.133	0.00525	121	157	165	166	950	179	Slow strain rate 0.008 mm/min
9/19/2007	2-05-T-2	Seawater w/ CP	0.199	0.00785	148	192	202	230	1310	210	Slow strain rate 0.008 mm/min
9/19/2007	3-05-T-1	Seawater w/ CP	0.168	0.00660	131	171	179	184	1050	188	Slow strain rate 0.008 mm/min
9/19/2007	3-05-T-2	Seawater w/ CP	0.181	0.00715	136	177	186	219	1250	205	Slow strain rate 0.008 mm/min
		Weibull eta	**0.187**		**141.5**	**183.8**	**193.4**	**218.6**		**202.8**	
		Weibull beta	**7.54**		**14.47**	**14.64**	**14.37**	**8.44**		**17.41**	
		Weibull B50	**0.179**		**138**	**179**	**189**	**209**		**199**	
		Weibull B2	**0.112**		**108**	**141**	**147**	**138**		**162**	
		Weibull B1	**0.102**		**103**	**134**	**140**	**127**		**156**	
		COV	**15.7%**		**8.5%**	**8.4%**	**8.5%**	**14.1%**		**7.1%**	
9/12/2007	1-06-T-1	7% H2S, 4 ph	0.013	0.00050	37	49	51	16.9	95	57	Slow strain rate 0.008 mm/min
9/14/2007	1-06-T-2	7% H2S, 4 ph	0.007	0.00030	27	36	38	9.6	55	43	Slow strain rate 0.008 mm/min
9/12/2007	2-06-F-1	7% H2S, 4 ph	0.013	0.00050	38	49	52	17.1	100	57	Slow strain rate 0.008 mm/min
9/13/2007	2-06-T-2	7% H2S, 4 ph	0.005	0.00020	24	30	32	6.4	35	35	Slow strain rate 0.008 mm/min
9/11/2007	3-06-T-1	7% H2S, 4 ph	0.016	0.00065	41	53	55	13.6	80	51	Slow strain rate 0.008 mm/min
9/11/2007	3-06-T-2	7% H2S, 4 ph	0.003	0.00010	18	23	24	11.5	65	47	Slow strain rate 0.008 mm/min
		Weibull eta	**0.010**		**34.35**	**43.15**	**46.86**	**14.13**		**51.28**	
		Weibull beta	**1.71**		**3.364**	**3.394**	**3.296**	**2.858**		**6.033**	
		Weibull B50	**0.008**		**31**	**39**	**42**	**12**		**48**	
		Weibull B2	**0.001**		**11**	**14**	**14**	**3.6**		**27**	
		Weibull B1	**0.001**		**8.8**	**11**	**12**	**2.8**		**24**	
		COV	**60.3%**		**32.8%**	**32.5%**	**33.4%**	**38.0%**		**19.3%**	

	HT 1	HT 2	HT 3		
Yield strength	89.32	91.81	85.31	ksi	Weibull B50 value from Westmoreland data at 75°F
Ultimate strength	106.9	108.7	101.8	ksi	Weibull B50 value from Westmoreland data at 75°F
Modulus	30,600			ksi	ASME Sect II Part D data at 75°F
Poission's ratio	0.30				

Equivalent Plane Strain Fracture Toughness - J_Q Summary

Weibull distribution value	Environment	CVN	CTOD ASME	CTOD API 579	CTOD Barson Rolfe	J-Integral ASME	J-Integral API 579	J-Integral Barson Rolfe
		ksi·√in.	ksi·√in.	ksi·√in.	ksi·√in.	ksi·√in.	ksi·√in.	ksi·√in.
B50 value	Air, -20°F	223						
	Air, 75°F		156	202	213	225	225	225
	Seawater w/ CP		138	179	189	199	199	199
	7% H2S, 4 ph		31	39	42	48	48	48
B2 value	Air, -20°F	171						
	Air, 75°F		142	185	196	206	206	206
	Seawater w/ CP		108	141	147	162	162	162
	7% H2S, 4 ph		11	14	14	27	27	27
B1 value	Air, -20°F	162						
	Air, 75°F		139	182	192	203	203	203
	Seawater w/ CP		103	134	140	156	156	156
	7% H2S, 4 ph		9	11	12	24	24	24

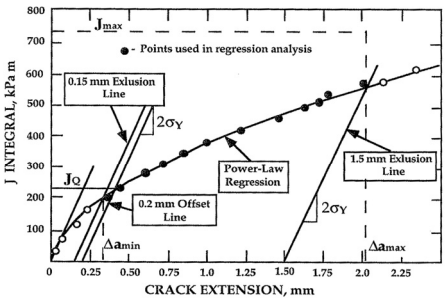

FIGURE 7.21 Determination of J_Q from a J-R curve [5].

Plane Strain Fracture Toughness Test Data, ASTM E 1820 (max Load, J_{max})											
Data	S/N	Environment	CTOD					J-Integral			Comments
			Test Data		Equivalent K_{IC}			Test Data		Equivalent K_{IC}	
					ASME	API 579	Barson Rolfe				
			mm	in.	ksi·√in.	ksi·√in.	ksi·√in.	N / mm	lb / in	ksi·√in.	
8/31/2007	2-07-T-1	Air	0.430	0.01695	218	283	297	506	2890	312	Std strain rate 0.66 mm/min
9/17/2007	1-05-T-1	Air	0.218	0.00860	153	199	209	245	1400	217	Slow strain rate 0.008 mm/min
8/31/2007	1-05-T-2	Air	0.244	0.00960	162	211	221	272	1555	229	Slow strain rate 0.008 mm/min
9/17/2007	2-05-T-1	Air	0.271	0.01065	173	222	236	295	1685	238	Slow strain rate 0.008 mm/min
9/18/2007	2-05-T-2	Air	0.261	0.01030	170	218	231	285	1625	234	Slow strain rate 0.008 mm/min
9/11/2007	3-05-T-1	Air	0.298	0.01175	175	233	239	323	1845	249	Slow strain rate 0.008 mm/min
10/3/2007	3-05-T-2	Air	0.310	0.01220	178	237	244	344	1965	257	Slow strain rate 0.008 mm/min
		Weibull eta	**0.282**		**173**	**224**	**236**	**309**		**244**	
		Weibull beta	**8.22**		**19.03**	**19.12**	**18.69**	**8.84**		**17.81**	
		Weibull B50	**0.270**		**170**	**220**	**231**	**297**		**239**	
		Weibull B2	**0.175**		**141**	**183**	**192**	**199**		**196**	
		Weibull B1	**0.161**		**136**	**176**	**185**	**184**		**188**	
		COV	**14.5%**		**6.5%**	**6.5%**	**6.6%**	**13.5%**		**6.9%**	
9/19/2007	1-05-T-1	Seawater w/ CP	0.231	0.00910	158	205	215	252	1440	220	Slow strain rate 0.008 mm/min
9/19/2007	1-05-T-2	Seawater w/ CP	0.287	0.01130	176	228	240	313	1785	245	Slow strain rate 0.008 mm/min
9/19/2007	2-05-T-1	Seawater w/ CP	0.244	0.00960	164	213	224	262	1495	224	Slow strain rate 0.008 mm/min
9/19/2007	2-05-T-2	Seawater w/ CP	0.250	0.00985	166	216	227	270	1540	228	Slow strain rate 0.008 mm/min
9/19/2007	3-05-T-1	Seawater w/ CP	0.352	0.01385	190	247	260	346	1975	258	Slow strain rate 0.008 mm/min
9/19/2007	3-05-T-2	Seawater w/ CP	0.304	0.01195	177	230	241	330	1885	252	Slow strain rate 0.008 mm/min
		Weibull eta	**0.295**		**177**	**230**	**241**	**311**		**245**	
		Weibull beta	**7.09**		**16.74**	**16.63**	**16.47**	**8.45**		**16.78**	
		Weibull B50	**0.280**		**173**	**225**	**236**	**298**		**239**	
		Weibull B2	**0.170**		**140**	**182**	**190**	**196**		**194**	
		Weibull B1	**0.154**		**134**	**174**	**183**	**181**		**186**	
		COV	**16.6%**		**7.4%**	**7.4%**	**7.5%**	**14.1%**		**7.3%**	
9/12/2007	1-06-T-1	7% H2S, 4 ph	0.066	0.00260	84	110	115	74	425	119	Slow strain rate 0.008 mm/min
9/14/2007	1-06-T-2	7% H2S, 4 ph	0.066	0.00260	84	110	115	72	410	118	Slow strain rate 0.008 mm/min
9/12/2007	2-06-F-1	7% H2S, 4 ph	0.063	0.00250	83	108	114	72	410	118	Slow strain rate 0.008 mm/min
9/13/2007	2-06-T-2	7% H2S, 4 ph	0.066	0.00260	85	111	116	74	425	119	Slow strain rate 0.008 mm/min
9/11/2007	3-06-T-1	7% H2S, 4 ph	0.081	0.00320	91	119	125	88	500	130	Slow strain rate 0.008 mm/min
9/11/2007	3-06-T-2	7% H2S, 4 ph	0.086	0.00340	94	122	128	100	570	139	Slow strain rate 0.008 mm/min
		Weibull eta	**0.075**		**89**	**116**	**121**	**84**		**127**	
		Weibull beta	**9.69**		**24.19**	**24.52**	**25.37**	**6.03**		**19.37**	
		Weibull B50	**0.072**		**87**	**114**	**119**	**79**		**124**	
		Weibull B2	**0.050**		**75**	**99**	**104**	**44**		**104**	
		Weibull B1	**0.046**		**73**	**96**	**101**			**100**	
		COV	**12.4%**		**5.2%**	**5.1%**	**4.9%**	**19.3%**		**6.4%**	

Equivalent Plane Strain Fracture Toughness - J_{max} Summary								
Weibull distribution value	Environment	CVN	CTOD			J-Integral		
			ASME	API 579	Barson Rolfe	ASME	API 579	Barson Rolfe
		ksi·√in.	ksi·√in.	ksi·√in.	ksi·√in.	ksi·√in.	ksi·√in.	ksi·√in.
B50 value	Air, -20°F	223						
	Air, 75°F		170	220	231	239	239	239
	Seawater w/ CP		173	225	298	239	239	239
	7% H2S, 4 ph		87	114	79	124	124	124
B2 value	Air, -20°F	171						
	Air, 75°F		141	183	192	196	196	196
	Seawater w/ CP		140	182	190	194	194	194
	7% H2S, 4 ph		75	99	104	104	104	104

Annex G. Results from Fatigue Crack Growth Rate Tests

Annex G.1. Lab Crack Growth Rate Test Data

THE FATIGUE CRACK GROWTH RATE BEHAVIOR OF FORGED A182 STEEL IN LAB AIR, CATHODICALLY PROTECTED SEAWATER BRINE AND SOUR BRINE

SwRI® Project No. 18.13349.01.001
REVISED FINAL REPORT

Prepared by

Peter C. McKeighan
James H. Feiger
Dustin H. McKnight

Southwest Research Institute (SwRI)
San Antonio, TX

Prepared for

Mohr Engineering Division
Stress Engineering Services, Inc.
13602 Westland East Blvd.
Houston, TX 77041-1205

March 2008

SOUTHWEST RESEARCH INSTITUTE®
SAN ANTONIO HOUSTON WASHINGTON, DC

THE FATIGUE CRACK GROWTH RATE BEHAVIOR OF FORGED A182 STEEL IN LAB AIR, CATHODICALLY PROTECTED SEAWATER BRINE AND SOUR BRINE

SwRI® Project No. 18.13349.01.001
REVISED FINAL REPORT

Prepared by

Peter C. McKeighan
James H. Feiger
Dustin H. McKnight

Southwest Research Institute (SwRI)
San Antonio, TX

Prepared for

Mohr Engineering Division
Stress Engineering Services, Inc.
13602 Westland East Blvd.
Houston, TX 77041-1205

March 2008

APPROVED:

Ben H. Thacker, Ph.D., Director
Materials Engineering Department

TABLE OF CONTENTS

Section **Page**

List of Tables iv

List of Figures iv

Abstract vi

1.0 Introduction 1

2.0 Material and Methods 3
- 2.1 Material and Specimen Extraction 3
- 2.2 Specimen Geometry 3
- 2.3 Overall Test Matrix 4
- 2.4 Procedural Details 5
- 2.5 Compression Precracking Test Methodology 6

3.0 Results and Discussion 15
- 3.1 Preliminary, Methods Development Testing 15
- 3.2 Baseline Lab Air Data 16
- 3.3 Environmental Fatigue Crack Growth Rates – Cathodically Protected Brine 18
- 3.4 Environmental Fatigue Crack Growth Rates – Sour Gas in Brine 19
- 3.5 Fractography 20

4.0 Summary 33

5.0 References 35

LIST OF TABLES

Table **Page**

2-1 Blanks provided for fatigue crack growth testing 9

2-2 Specimen test matrix 9

LIST OF FIGURES

Figure **Page**

2-1 Specimen blank used to fabricate C(T) specimens (3-09-T-2 shown) 10

2-2 Specimen extraction orientation (supplied by Stress Engineering Services, Inc.) 10

2-3 Fatigue crack growth coupon utilized during lab air, seawater, and H_2S testing 11

2-4 Typical 2-in. C(T) coupon with a dual probe DCPD configuration 11

2-5 Representative setup showing clevis grips, specimen, and DCPD hardware 12

2-6 Initial crack (from EDM notch) created by compression precracking 13

2-7 Typical precracking performance under compression-compression loading 14

3-1 FCG results from the preliminary (methods development) phase of testing 21

3-2 Influence of low and high load ratio R on fatigue crack growth rate behavior 22

3-3 Influence of cathodically protected saltwater on fatigue crack growth rate behavior 23

3-4 Influence of sour saltwater brine on fatigue crack growth rate behavior 24

3-5 Average FCG rate response for the low and high load ratio data 25

3-6 Average growth rate increase associated with load ratio 26

3-7 Different crack growth rate responses as a function of environmental and R 27

LIST OF FIGURES (Continued)

Figure **Page**

3-8 Comparison between literature and physically measured cathodically protected seawater FCG data....28

3-9 Comparison between experimentally measured sour and CP FCG rate data....29

3-10 Fracture surface for specimen 1-09-T-1 (seawater w/CP)....30

3-11 Fracture surface for specimen 1-09-T-2 (seawater w/CP)....30

3-12 Fracture surface for specimen 3-09-T-1 (seawater w/CP)....31

3-13 Fracture surface for specimen 2-10-T-1 (sour brine)....32

3-14 Fracture surface for specimen 3-10-T-1 (sour brine)....32

3-15 Fracture surface for specimen 3-10-T-3 (sour brine)....32

ABSTRACT

Fatigue crack growth (FCG) rate testing was performed on an A182 Grade F22M (85K) steel forging. Testing was performed in lab air, cathodically protected (CP) seawater brine and sour brine environments. Little difference was observed between FCG test data at R = 0.1 and 0.5 in lab air. Environmental FCG testing, under low load ratio conditions, showed higher growth rates in CP brine when compared with lab air. The A182 data generated under CP brine compared favorably to data from the literature although the literature data tended to be slightly more conservative than the measured data. The sour brine FCG data exhibited higher growth rates than the CP brine data although only by a factor of 2-5x greater. The sour brine crack growth rates were on the order of 5-10x greater than the lab air data. Finally, compression-compression precracking proved effective in preconditioning the crack tip to start FCG tests at lower ΔK and generate sour data at lower growth rates.

1.0 INTRODUCTION

When designing damage tolerant structure, the fatigue properties of the given material must be understood in the relevant environments. The focus of the testing performed herein is quantifying the fatigue crack growth characteristics of an ASTM A182 Grade F22M (85K) steel forging material.

Fatigue crack growth properties, namely da/dN versus ΔK, have been generated in lab air at both low (R = 0.1) as well as high (R = 0.5) load ratio conditions. Testing has also been performed in seawater under cathodic protection at -1100 mV and in sour brine under freely corroding conditions. The environmental testing was performed under low load ratio (R = 0.1) cycling conditions.

To date few fatigue crack growth rate data have been generated under cathodic protection. The vast majority of previous testing in seawater brine has been under free corrosion conditions. An element of this program also concerned further development of the fatigue crack growth test methodology. Previous crack growth testing with sour brine has been under constant-K_{max}, increasing-K_{min} test conditions where the load ratio varies during the test from low R at high ΔK to high R at low ΔK at the completion of testing. This method was utilized because in past testing crack arrest occurred when the environment was introduced. This forced the initial starting ΔK to be in the range of 10-20 ksi$\sqrt{\text{in.}}$ under fixed load ratio constant amplitude loading conditions.

An alternate approach was applied herein where compression-compression loading was used to grow the precrack (prior to the crack growth rate test starting). This results in a short precrack that has virtually no load history effects on it. By omitting the decreasing ΔK region associated with a conventional precrack procedure, the starting ΔK level was considerably lower than during previous conventional testing procedures. This eliminated the time-consuming crack arrest situation that was observed during previous testing.

This page intentionally left blank.

2.0 MATERIAL AND METHODS

The material that was supplied by the customer will be described in this section as well as unusual features of the testing. Recall that all tests were performed in accordance with the relevant ASTM E647 standard [1] for fatigue crack growth testing.

2.1 Material and Specimen Extraction

Material for specimen extraction was provided to SwRI from Stress Engineering. The steel was noted to be ASTM A182 Grade F22M. The strength level was reported to be 85 ksi and the material meets NACE MR0175 / ISO 15156 and API Spec 6A (PSL 3). The material is forged material typically used for drill-through equipment. Forgings were obtained from three different heats of material with the original forging size being 8" by 8" by 9". The received material was in saw cut blanks having nominal dimensions of 2.6" by 2.75" by 1.13" and stamped with the numbering scheme shown in Table 2-1. A schematic of the specimen extraction is shown in Figure 2-1. Blanks were excised from the 1/4T location and had a specimen orientation of S-T (see Figure 2-2).

2.2 Specimen Geometry

A 2-inch compact tension, C(T), fatigue crack growth coupon was utilized during this effort and is presented in Figure 2-3. Given the compressive precracking approach used in the effort, key features need to be noted when describing the specimens. First considering the notch geometry, both height and tip conditions are intended to facilitate compressive precracking. Second, recessed divots are located on the top and bottom faces of the specimen inline with the load-line. One of these divots can be observed on the top face in Figure 2-3. These divots were machined to accommodate round-ended pins that contact the top and bottom face and apply the compressive load precrack boundary conditions. Lastly, the specimen was thick enough (B = 0.25 inch) to prevent out-of-plane buckling during the compressive loading. Although the E647 standard allows a possible range of thicknesses (for a 2-inch specimen, the thickness range is 0.1

to 0.5 inch), the 0.25 inch utilized is the optimum in terms of generating growth rate data absent from crack curvature effects which can be significant for forged product.

Prior to testing, each specimen was polished to aid in visual crack length measurements. Dual probe, DC potential drop instrumentation was also configured on each specimen to provide a continuous measure of crack length during the test. Overall, current input-output leads, active voltage probes, and reference voltage probes are spot welded to the specimen at predetermined locations. A representative image of a specimen with direct current, potential drop (DCPD) instrumentation (leads and probes) is presented in Figure 2-4.

2.3 Overall Test Matrix

In total, sixteen different fatigue crack growth rate tests were performed. These tests are further identified by condition and specimen ID number in Table 2-2. Testing was divided up into four different phases:

- In the first preliminary phase, several different test methods for generating da/dN data on the forged material were investigated. The original SOW supplied by Stress Engineering advocated using a K-decreasing procedure to generate the data. The effect of this approach was compared to a compression-compression precracking procedure followed by a K-increasing approach. All subsequent testing used compression-compression precracking followed by a K-increasing approach.

- During the second phase of the program, FCG data at low load ratio (ratio of minimum to maximum load, denoted R) and high load ratio, specifically R = 0.1 and 0.5, was generated. This testing was performed in lab air.

- The third and four phases of the program focused on low load ratio (R = 0.1) testing in both seawater brine (with cathodic protection) and de-aerated brine with the addition of H_2S/CO_2 gas.

As can be ascertained from this testing, the overall objective of testing is to characterize the fatigue crack growth rate behavior of A182 Grade F22M, forged steel at two stress ratios, R = 0.1 and 0.5 (lab air only), in lab air, cathodically protected seawater and sour brine conditions.

2.4 Procedural Details

Four 20-kip servohydraulic test frames were utilized to characterize the fatigue crack growth properties. Integrated into the test frames was an MTS 458 analog controller and FTA software package used to control and monitor the testing. Standard fatigue crack growth clevis grips were used for both setups. However, additional design features included in the grips allowed for compressive precracking (described in a later section). A cyclic frequency of 25 Hz was used for all lab air tests. During environmental testing, frequency was decreased to ensure that the environmental attack was allowed to fully occur. Frequencies of 1 Hz and 0.33 Hz were used during seawater and sour brine testing, respectively. The nominal lab conditions were 72°F and 30-50% RH during this testing.

System crack length measurements were made using DCPD measurements while visual crack length measurements were made with the use of traveling microscopes. DCPD allows a continuous measurement of crack length as the test progresses. For the testing performed herein, a dual probe (active and reference sets of probes) setup was utilized. The benefit of a dual probe setup is the thermal stability gained by normalizing out the thermal couple effects at the spot weld locations. Both front and back crack lengths were visually measured periodically during testing for post-test correction of the data. Any nonvisual crack length measurement method requires post-test correction of the crack length data to ensure that the physical crack lengths (visual measurements) are properly accounted for during the test. Approximately five to six visual crack length measurements were made during a lab air test for post-test processing of the data. With regard to the environmental testing, an initial and final crack length were visually measured for post-test processing. After completion of the test, the final crack length was visually measured and the data processed to establish the fatigue crack growth properties.

The technique used to characterize the fatigue crack growth behavior included a K-control technique in which the crack length is actively monitored to allow the system to adjust the load levels. Unlike a constant amplitude fatigue crack growth test where load is fixed for the duration of testing, a K-control approach adjusts the load levels according to the crack length. For the testing performed herein, the typical fixed K-gradient parameter (C = dK/Kda) was +6 $in.^{-1}$ although other magnitudes were used for some of the testing as detailed in Table 2-2.

The third and fourth phases of this effort included testing in seawater (with cathodic protection) and H_2S/CO_2 gas, respectively. The seawater solution provided for testing was defined as the following: 5.00% by weight sodium chloride and 0.40% by weight of sodium acetate in deionized water. Containment of the seawater solution was accomplished using a Teflon "bag" that sealed at the clevis pins/holes. The cathodic protection hardware was integrated through the top of the bag to provide the required corrosion protection. It is important to note that the seawater solution was not purged with nitrogen or carbon dioxide, leaving the cathodic protection setup to mitigate corrosion of the specimen.

The H_2S conditions utilized during this effort were provided by Stress Engineering and included the same seawater solution provided above in addition to the 7.0% (by moles) H_2S and N_2 as the balance. Prior to adding the hydrogen sulfide and nitrogen, the test solution pH was adjusted to 4.0 using hydrochloric acid. It should be also noted that the seawater solution was purged of oxygen with nitrogen prior to being transferred to the test chamber. The sour environment was contained during testing using an SwRI-designed setup that included the primary containment vessel, a secondary envelope that was purged with nitrogen, and finally a shroud that had a slight negative pressure (vacuum) with the exhaust located on the roof of the test lab.

Finally, at the start of each type of environmental test, the complete system was allowed to "soak" for 24 hours prior to initiating the fatigue crack growth rate test. This soak occurred at minimum load conditions.

2.5 Compression Precracking Test Methodology

Prior to establishing the final testing protocol, a developmental effort was conducted to investigate possible testing strategies as it relates to methodologies including compressive precracking and K-decreasing testing from initially high ΔK values. In the strictest sense, the ASTM test standard does not allow K-decreasing tests in the manner recommended in the statement-of-work. However if testing can show that the crack growth testing method does not impact the properties obtained, the ASTM test standard is open to alternative control strategies.

The test control issue is most important for testing in sour environments. Some of the first testing SwRI performed in sour gas environments was conventional fixed load ratio (R = 0.1) tests on moderate strength pipeline steel. It is worth reviewing some of the findings from this period of testing since they apply to the work performed herein. This fixed load ratio technique proved difficult to apply though with the crack typically arresting as soon as the gas was introduced at ΔK levels in the range of 10-20 ksi$\sqrt{\text{in}}$. At the time, the crack arrest was attributed to two effects: inevitable load history effects from precracking combined with corrosion fatigue issues associated with corrosion product build-up and crack closure. However lab air testing indicated that the materials being tested had virtually no load ratio effects (in other words FCG test data at low and high R were coincident at the same ΔK). Consequently, a technique utilizing variable load ratio testing was utilized. This test, termed a constant-K_{max}-increasing-K_{min} test (constant-K_{max} for short), traverses the crack growth rate curve backward starting at low R (0.1) and completing the test at high R (0.9) conditions. In addition, the shed rate can be aggressive at -10 to -15 in.$^{-1}$. This strategy allowed tests to be performed in slow frequency in approximately one month as opposed to 3-5 months for the fixed load ratio technique. However since the loading that most offshore structure is subjected to differs from these artificial conditions, it is arguable whether this approach yields data suitable for offshore structure.

The technique that was used herein to precrack test specimen is called the compression-precracking-constant-amplitude (CPCA) test method [2] and has been used successfully for generating near-threshold growth rate data where there is high sensitivity to load history effects. Although the first reference of the technique in the literature was 1969 [3], the method has

gained in popularity of late and is currently in draft form as an annex to ASTM E647. It is being reviewed for inclusion into the standard and there are a sufficient number of individuals currently interested in the methods so that it is likely that the method will eventually become part of E647. SwRI has been using the compression precracking technique for years to compressively precrack beryllium samples for fracture toughness measurement.

Fully compressive loading (maximum and minimum load is compressive) is applied to the C(T) specimen on the top face of the specimen. Special dual loading clevis grips are employed to perform this loading as shown in Figure 2-5. Although as photographed the horizontal pins are loading the specimen, if they were removed the vertical pins would load the top and bottom face of the specimen in compression. The target was to precrack the specimen 40 mils (0.040 inch) at R = 10, or more specifically with K_{min} = -60 ksi√in. and K_{max} = -6 ksi√in.

The compressive loading causes some reverse tensile loading to occur in the near-crack region. Examples of the resulting precrack are shown in Figure 2-6 where some surface rippling is clearly evident at short crack lengths. Precracking durations were usually fairly short as indicated in Figure 2-7. In no cases did they exceed 10K cycles, with 5-7K more typical for all of the specimens precracked.

After compressive precracking, a constant ΔK of 3-ksi√in. segment was performed in order to grow away from the compressive precracking regime. Typically, this growth was over 25-50 mils of crack length. However, the final decision on when to conclude this segment was when the growth rate became constant and reached steady state.

The ΔK range of interest for the lab air testing was from 3-ksi√in. and up the fatigue crack growth curve into the stage 3 regime. Given the compressive precracking procedure performed, there was no K-decreasing strategy required because the K-increasing testing could initiate at the desired ΔK of 3-ksi√in. For environmental testing, the tests typically started at higher ΔK (5 ksi√in. or so).

Table 2-1. Blanks provided for fatigue crack growth testing.

Specimen ID	Group Numbers
1-08-T	1,2
1-09-T	1,2
1-10-T	2,3
2-08-T	1,2
2-09-T	2,3
2-10-T	1,2
3-08-T	1,2
3-09-T	1,2
3-10-T	1,3

Table 2-2. Specimen test matrix.

Program Phase	Test Env.	Specimen ID No.	Precracking Procedure	Load Ratio, R	Test Strategy
Preliminary	lab air	3-09-T-2a	conventional load shedding	0.1	high ΔK C=-4 in.$^{-1}$
		2-09-T-3b	conventional load shedding	0.1	high ΔK C=-6 in.$^{-1}$
		3-09-T-2b	compression-compression	0.1	C = +2 in.$^{-1}$
		3-09-T-2c	compression-compression	0.1	C = +6 in.$^{-1}$
Baseline	lab air	1-08-T-1	compression-compression	0.1	C = +6 in.$^{-1}$
		2-08-T-1	compression-compression	0.1	C = +6 in.$^{-1}$
		3-08-T-1	compression-compression	0.1	C = +6 in.$^{-1}$
		1-08-T-2	compression-compression	0.5	C = +6 in.$^{-1}$
		2-08-T-2	compression-compression	0.5	C = +6 in.$^{-1}$
		3-08-T-2	compression-compression	0.5	C = +6 in.$^{-1}$
Seawater (with CP)	SW brine	1-09-T-1	compression-compression	0.1	C = +6 in.$^{-1}$
		1-09-T-2	compression-compression	0.1	C = +6 in.$^{-1}$
		3-09-T-1	compression-compression	0.1	C = +6 in.$^{-1}$
Sour	sour brine	2-10-T-1	compression-compression	0.1	C = +6 in.$^{-1}$
		3-10-T-3	compression-compression	0.1	C = +6 in.$^{-1}$
		3-10-T-1	compression-compression	0.1	C = +6 in.$^{-1}$

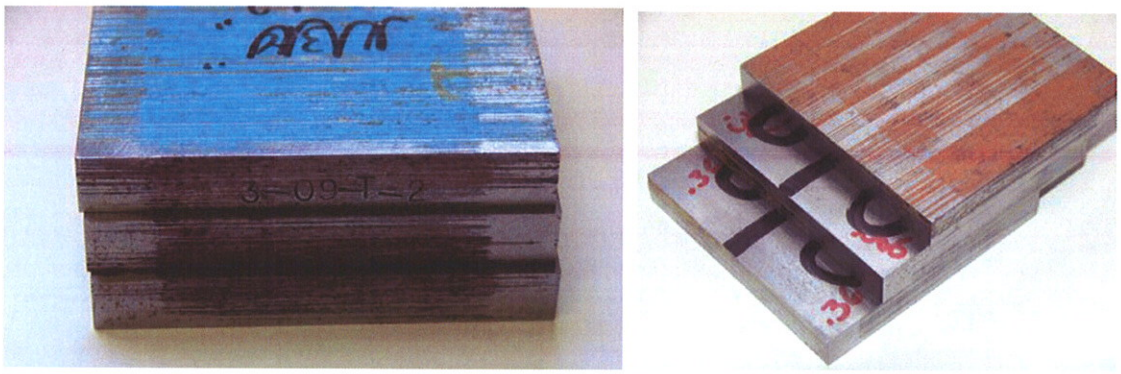

Figure 2-1. Specimen blank used to fabricate C(T) specimens (3-09-T-2 shown).

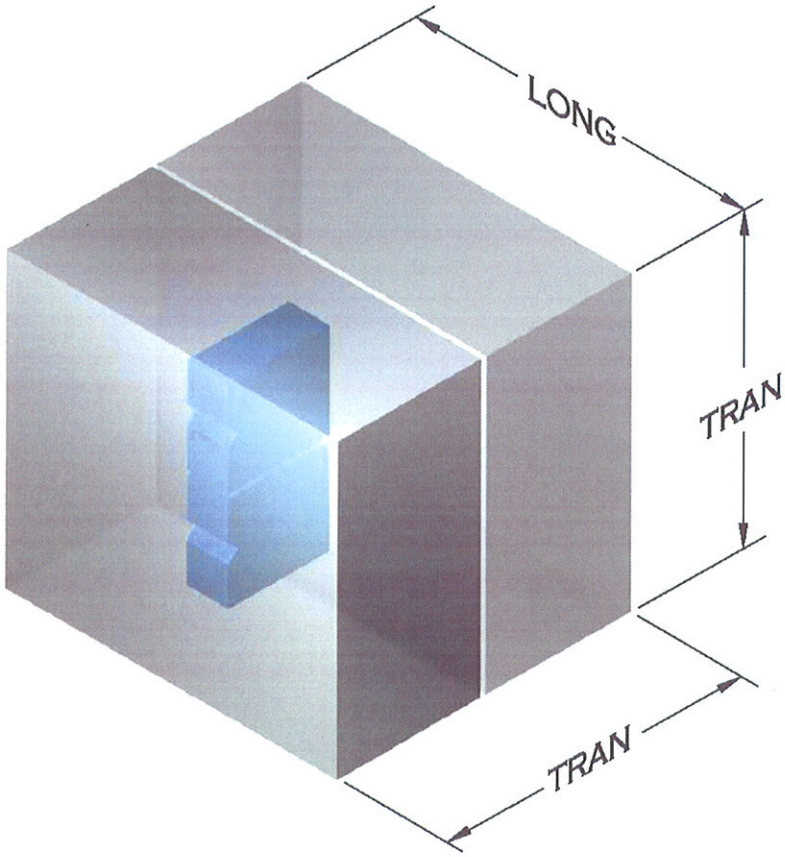

Figure 2-2. Specimen extraction orientation (supplied by Stress Engineering Services, Inc.).

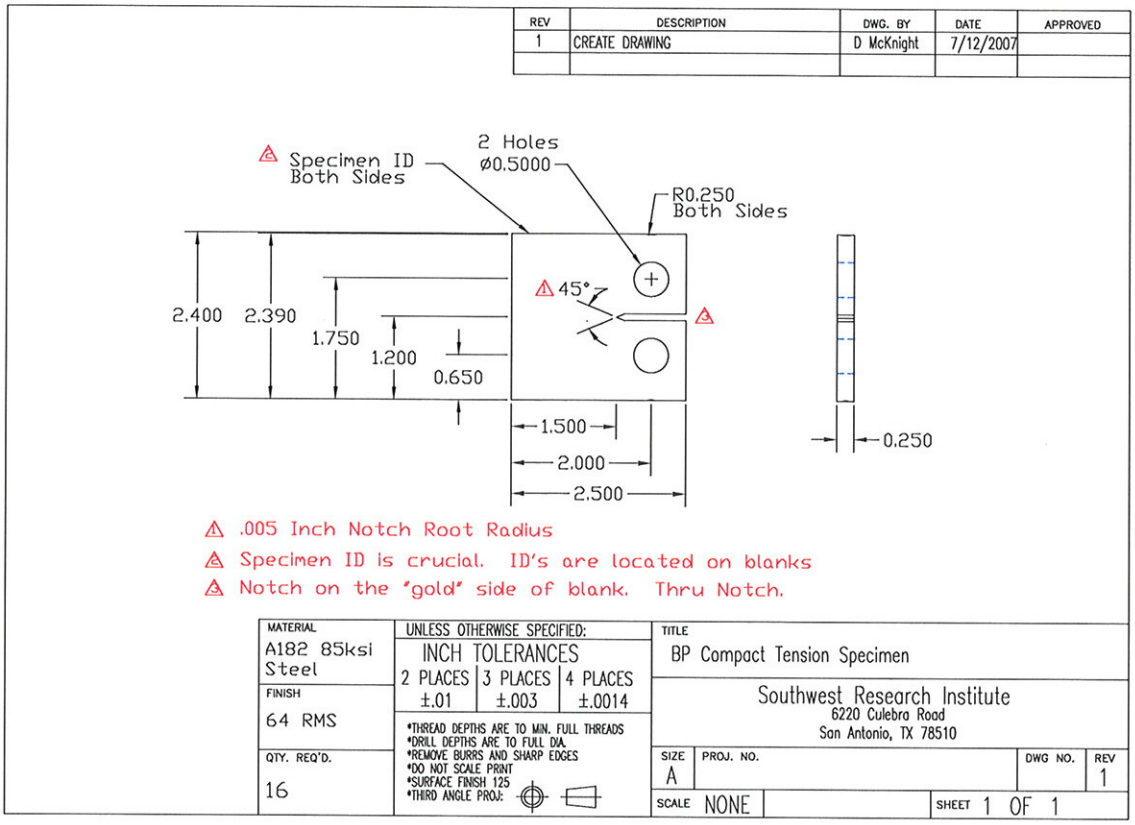

Figure 2-3. Fatigue crack growth coupon utilized during lab air, seawater, and H_2S testing.

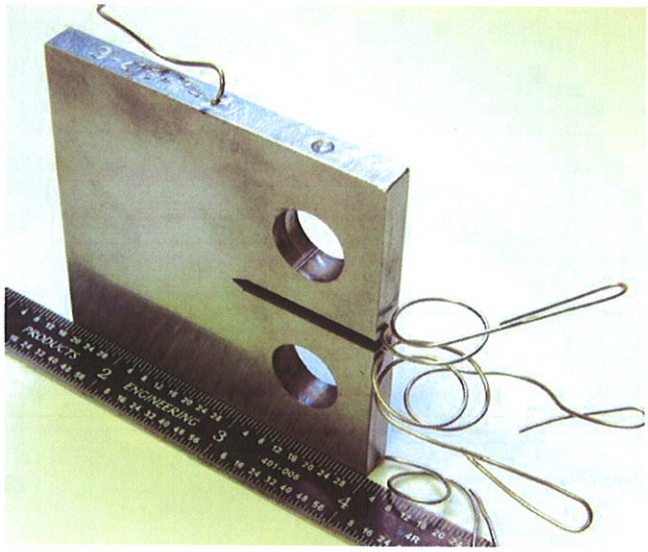

Figure 2-4. Typical 2-in. C(T) coupon with a dual probe DCPD configuration.

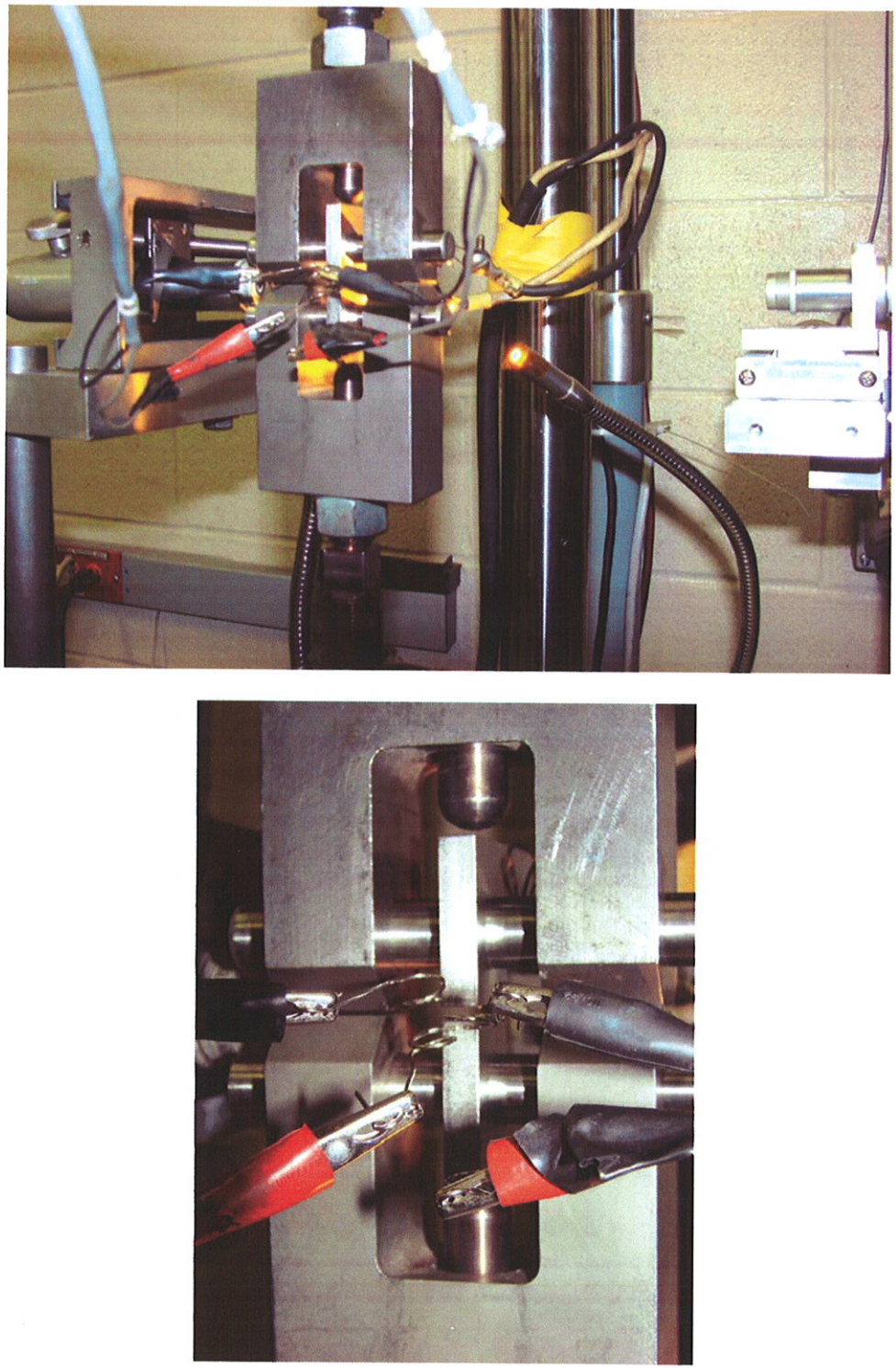

Figure 2-5. Representative setup showing clevis grips, specimen, and DCPD hardware.

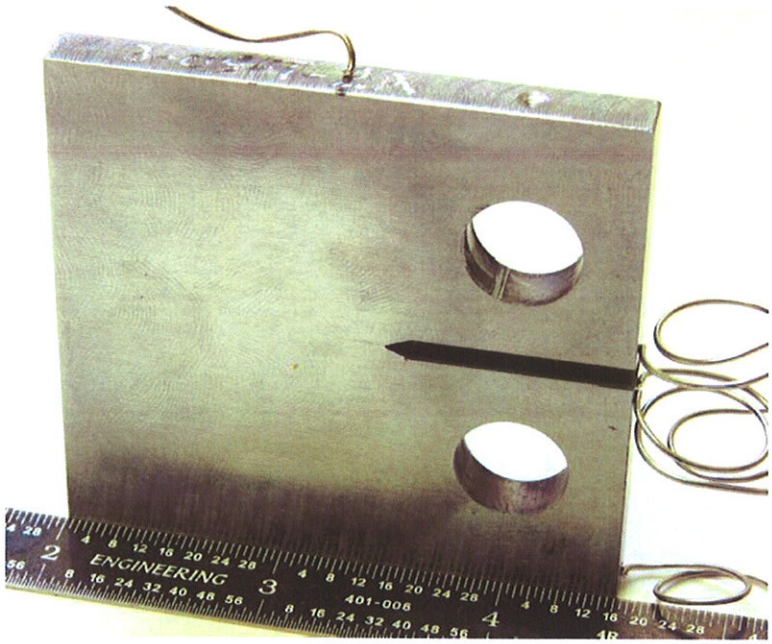

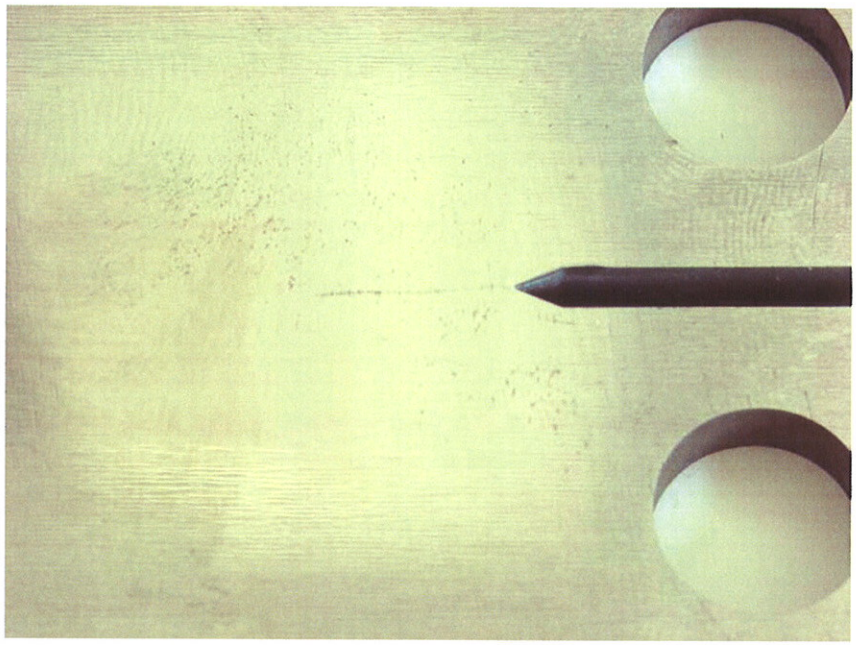

Figure 2-6. Initial crack (from EDM notch) created by compression precracking.

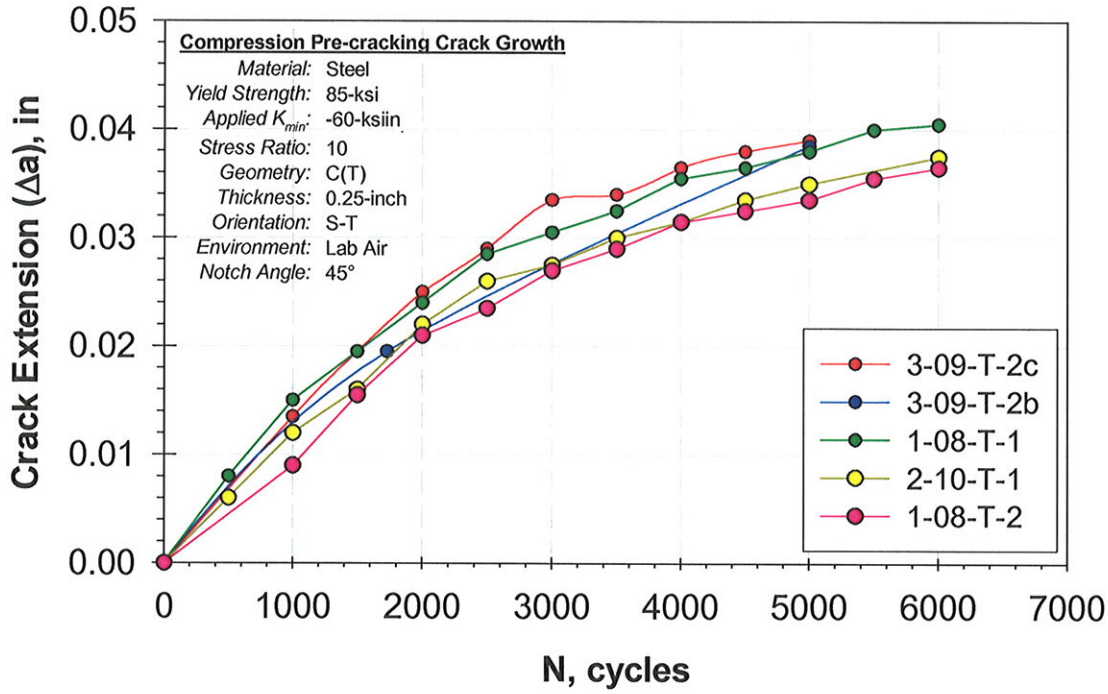

Figure 2-7. Typical precracking performance under compression-compression loading.

3.0 RESULTS AND DISCUSSION

The purpose of this section of the report is to present the results and interpret the inter-relationship between different variables perturbed in the testing. The resulting fatigue crack growth rate data for the four test series performed herein are shown in Figures 3-1 through 3-4. These data will be described below discussing different aspects of the trends observed.

3.1 Preliminary, Methods Development Testing

The fatigue crack growth rate results from the four specimens involved in the preliminary methods development phase of the program are shown in Figure 3-1. For comparative purposes, the low R HBC curve is also shown. This curve, detailed in Reference [4] based on research performed for the Ship Structure Committee [5], represents typical FCG behavior for a wide range of medium strength, structural steels. Although there are a number of other "standard" FCG relationships available [6,7] for HSLA and ferritic steels, they tend to be slightly more conservative[1] when compared to the HBC curves [4]. The low R HBC curve is defined by $da/dN = C\,\Delta K^{3.12}$ where C = 2.12e-10 with units of in./cycle and ksi$\sqrt{\text{in}}$.

The data shown in Figure 3-1 that were precracked under compression-compression conditions exhibit extremely linear growth rate with applied ΔK. This is contrasted to the behavior evident with the K-decreasing data that diverge from the more linear data. In fact, at higher ΔK levels, the K-decreasing data exhibits a 2x decrease in growth rate when compared to the compression precracked data. Given these differences, which response represents the typical growth rate behavior independent of test method?

The answer to this question is that the compression-compression precrack data in Figure 3-1 represents material behavior independent of test method. First, the FCG response is very linear, as expected for steel material. Second, the data obtained is in close agreement with the HBC curve. Third, the K-decreasing data tends to tail off to a threshold value on the order of

[1] In other words, the HBC curves tend to show slightly higher growth rates than the other relationships.

7 ksi√in. or so. This is much too high for lab air conditions and is believed to be an artifact of the high plasticity and resulting plastic wake from the initial, high ΔK loading. This artificially high threshold value (that also appears quite repeatable) is one of the reasons that the ASTM warns that one should not perform a K-decreasing test with an initially high growth rate (above 4e-7 in./cycle).

Finally, the compression precracking data in Figure 3-1 includes testing at two different C values, +2 and +6 in.$^{-1}$. The advantage with the higher C test is that it takes significantly fewer cycles (time) to run and it also allows covering a greater range of ΔK values. However, the ASTM test standard limits tests to C = +2 in.$^{-1}$ unless data can show that faster (*i.e.* higher) rates do not impact growth rate. The data in Figure 3-1 shows that the A182 material does not exhibit K-gradient effects and testing can be performed at C = +6 in.$^{-1}$. All subsequent testing was therefore performed at this level.

3.2 Baseline Lab Air Data

The fatigue crack growth rate data in lab air and at R = 0.1 and R = 0.5 is shown in Figure 3-2 with three tests for each of the different load ratios. The low R HBC curve is also indicated as well as the high R HBC curve. The high R HBC curve has the same ΔK exponent with a leading coefficient C = 5.81e-10 (units same as low R HBC curve). Note that the two HBC relationships suggest, by virtue of the ratio of the C coefficients, a factor of 2.74x between low and high R conditions.

What is interesting about the data in Figure 3-2 is that both load ratios lie at or below the low R HBC curve. In fact, there is little discernable difference between low and high R growth rates evident in the FCG data. This trend is similar to that observed in previous crack growth testing for the oil and gas industry when testing pipeline steels with strengths less than 100 ksi.

In an effort to further discern the difference between the data, each dataset was fed through an analysis program that interpolated the crack growth rate response at specific ΔK levels. This allowed a full comparison of both the variability of the data for a given condition as well as the

difference between low and high load ratio. Note that this analysis tool is explained more fully in a recent report [8] examining variability in fatigue crack growth rate data. The resulting data are shown in Figure 3-5 for low and high load ratio conditions. Note that the low R datasets have been augmented by the two compression precrack tests involved in the preliminary phase of testing (resulting in five datasets for low R versus three for high R).

The fatigue crack growth rate responses for a given load ratio in Figure 3-2 exhibit a low level of scatter. The variability, given by ratioing the growth rates at ±2 standard deviations of the mean at a given ΔK level, can be quantified:

- *Low R conditions:* variability (5 datasets) ranges from 1.12x to 2.72x, with a mean of 1.43x, and
- *High R conditions:* variability (3 datasets) ranges from 1.14x to 2.35x with a mean of 1.47x.

To put these numbers in context, in the recent round robin report [8] where variability was examined for a steel and two structural aluminum alloys, the intralaboratory variability was 1.55x and 1.48x under low and high load ratio conditions, respectively. Based on this comparison, the variability measured herein was consistent with the average level calculated from results from 18 different laboratories. What is surprising about this is that the low observed variability is unusual for a forged material. Forgings typically have grain flow and residual stress issues that greatly increase the observed variability in fatigue crack growth rate behavior.

The mean growth rate data in Figure 3-5 are ratioed to obtain the difference between low and high load ratio in Figure 3-6. The FCG rate ratio in Figure 3-6 indicates that the high load ratio growth rate is approximately 1.2x to 1.6x faster growth than the low load ratio growth rate. Also shown on Figure 3-6 is significantly higher 2.74x factor expected from the HBC relationship. Clearly, the observed load ratio effect for the A182 Grade F22M forging is fairly minor and not unlike that observed in the past for pipeline steels with strengths less than 100 ksi.

3.3 Environmental Fatigue Crack Growth Rates – Cathodically Protected Brine

The fatigue crack growth rate results for cathodically protected seawater brine are shown in Figure 3-3. As the annotation suggests, at a ΔK of 7.5 ksi$\sqrt{\text{in.}}$, the seawater brine portion of the test was initiated at a frequency of 1 Hz. Prior to this ΔK level, testing was in lab air at 20 Hz. Data from three tests is shown and in general a fair amount of scatter and test-to-test variability (approximately ½ of a decade in growth rate) was evident in the data.

These SW-CP (seawater – cathodic protection) tests proved to be the most difficult tests to perform in this sequence. One of the tests exhibited a rapid increase in growth rate when the environment was perturbed (1-09-T-1). However two of the three tests exhibited a transient growth rate slowdown immediately after introduction of the environment (note that there was a 24-hour hold upon introduction of the seawater and CP conditions before the test started). In one case, test 1-09-T-2, the crack slowed and then quickly restarted. In another case (3-09-T-1) the slowdown resulted in crack arrest and the load had to be gradually increased to restart the test (this resulted in a delay of nearly one month as the load was incremented and the crack cycled). This degree of inefficiency was the type of situation that occurred during previous fixed load ratio testing.

What is interesting to note is that all three tests basically reacted differently upon introduction of the environment. This suggests that there are conditions beyond the control of the test parameters that impact the environmental response (for instance, slightly differing crack closure levels in the propagating crack when the environment is introduced). It is interesting to note that the FCG behavior of 3-09-T-1 in Figure 3-3 was unusual even before the environment was introduced. Whereas the other two tests exhibited consistent behavior, the growth rate of this single test was faster than observed with the other tests. Why this one test exhibited odd behavior is unknown. It might have simply been an anomaly or possibly a consequence of the different forging block used (a "3" specimen as opposed to a "1" specimen).

FCG data in seawater with cathodic protection is not plentiful. Nevertheless, some data is available for structural steels from a 1984 reference by Burnside *et al.* [5]. The so-called HBC curves [4] were also originally derived in Reference [5]. In developing these curves, a literature survey was performed and data extracted from the scientific literature examining a wide range of conditions. A summary of the resulting crack growth curves, representing a wide variety of data, is presented in Figure 3-7 (be careful of these curves since they are in metric units). In a relative sense, the CP curve exhibits the highest threshold and highest observed growth rate, plateauing at a level where the actual growth rate observed is a function of frequency. At this point, the mechanical damage accumulates as a function of cycles and if the frequency is too fast the full environmental impact is not realized. However, in summary, at the CP curve's highest point, it exhibits a growth rate increase of approximately 5-8x that observed in freely corroding seawater.

A comparison between the CP curve in Figure 3-7 and the measured CP data herein is provided in Figure 3-8. The SW-CP curve at low R is more conservative (higher growth rate) than the data obtained herein, although the results are on balance fairly similar. Note that the threshold-like data at $\Delta K = 10$ ksi$\sqrt{\text{in.}}$ for the measured data involved in this program is artificial since this is the point that the seawater was actually introduced and a growth rate perturbation occurred.

3.4 Environmental Fatigue Crack Growth Rates – Sour Gas in Brine

The sour brine fatigue crack growth rate data is shown in Figure 3-4. However, the response is now split into three segments: lab air at 20 Hz before 7.5 ksi$\sqrt{\text{in.}}$, free corrosion in seawater at 1 Hz between 7.5-10.0 ksi$\sqrt{\text{in.}}$ and 0.33 Hz sour brine results for >10 ksi$\sqrt{\text{in.}}$ Curious results are evident upon introduction of seawater: for test 3-10-T1, a marked increase in growth rate is observed whereas for the other two tests a decrease followed by an increase is noted. By the time sour gas is introduced, all three sets of crack growth rate data are consistent until a growth rate of approximately 10^{-4} in./cycle when plateau behavior is evident and growth rate ceases to increase with applied ΔK.

It is interesting to note that the three sour brine tests tend to mirror each other with little observed variability. Overall it is somewhat unusual that the data with the largest observed variability is the cathodically protected seawater case. Nevertheless, the compression-compression precrack methodology has clearly shown that it can be used to push the starting point of sour crack growth tests to lower levels. None of these tests had any issue with crack arrest. What makes this even more significant is the fact that the ΔK where loading started was similar or even lower to where it was applied in previous testing when arrest was more of a problem.

Finally, it is instructive to compare the sour brine FCG results with the cathodically protected seawater and lab air results. The sour brine data are compared with the general zone where the CP-SW data fell in Figure 3-9. What is interesting to note is that the sour brine data falls just above the cathodically protected seawater case. It appears that the brine is 2-5x worse than the CP-SW data with a plateau in growth rates observed at approximately the same point. In comparison to the lab air data, the sour brine crack growth rates were on the order of 5-10x greater.

3.5 Fractography

Macro-images were collected of the fracture surfaces for both the seawater w/CP and the sour brine tested specimens. The images are presented in Figures 3-10 through 3-15. Specimens did not fail during the actual fatigue crack growth test but were subsequently pulled apart for final crack length measurement and to investigate the final fracture surface.

The seawater w/CP specimens are presented in Figures 3-10 through 3-12. Overall, the fracture surfaces are similar in appearance showing a slightly corroded appearance along the region of crack growth. The fresh or non-corroded region shown is a result of the final failure when the specimens were separated into two halves.

The sour brine specimens are shown in Figures 3-13 through 3-15. When comparing the appearance to the seawater, there appears to be slightly more evidence of corrosion but overall no evidence of severe corrosion or attack.

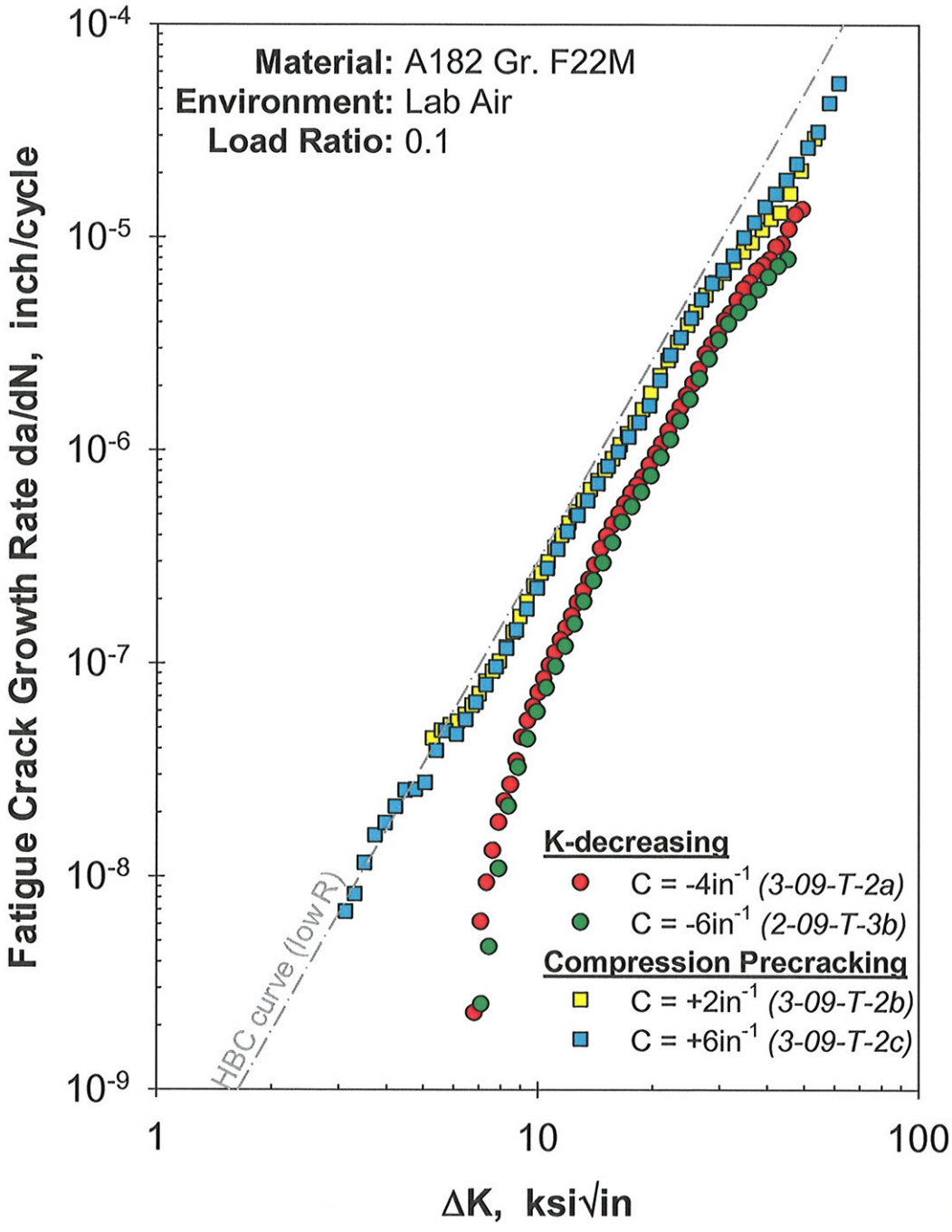

Figure 3-1. FCG results from the preliminary (methods development) phase of testing.

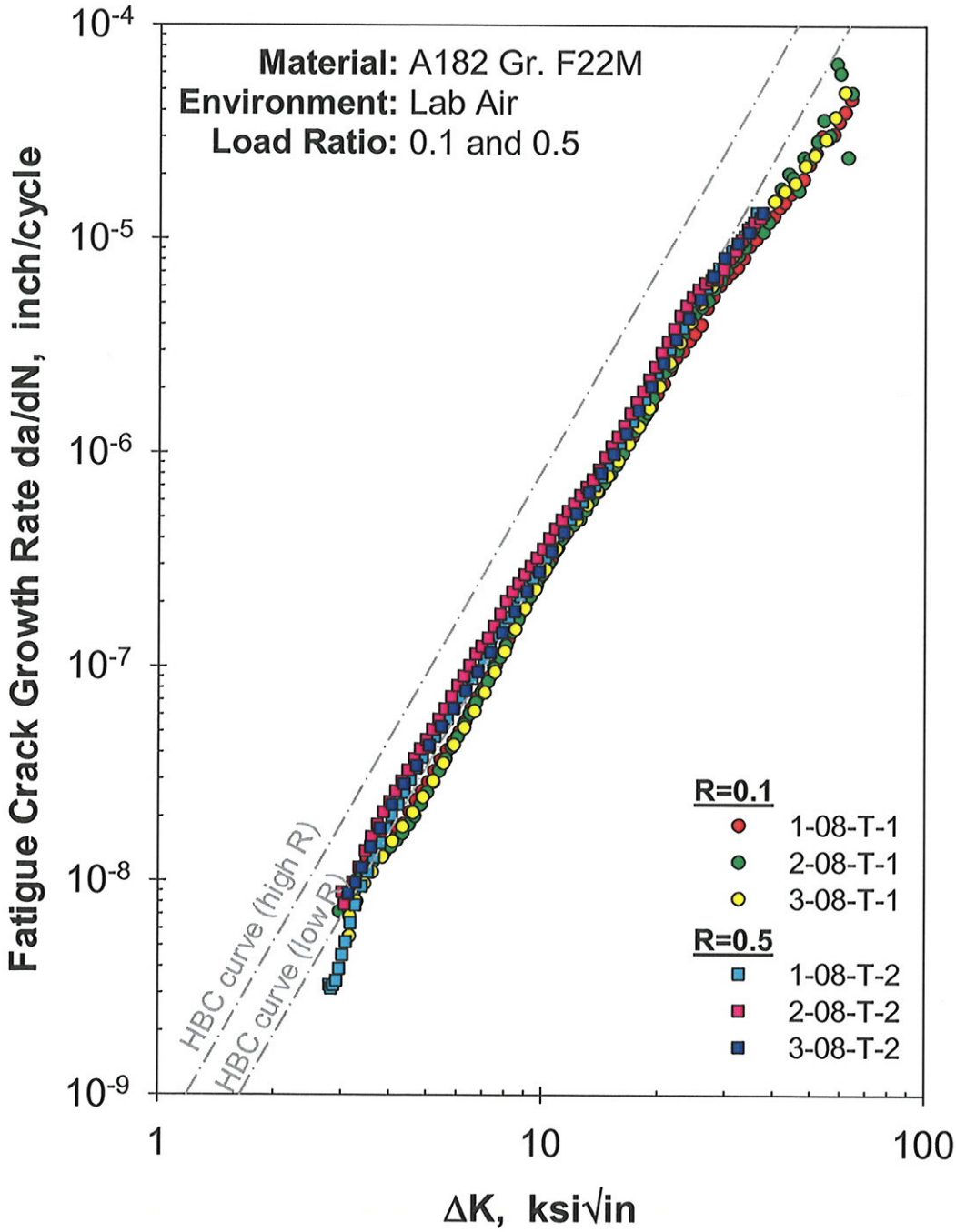

Figure 3-2. Influence of low and high load ratio R on fatigue crack growth rate behavior.

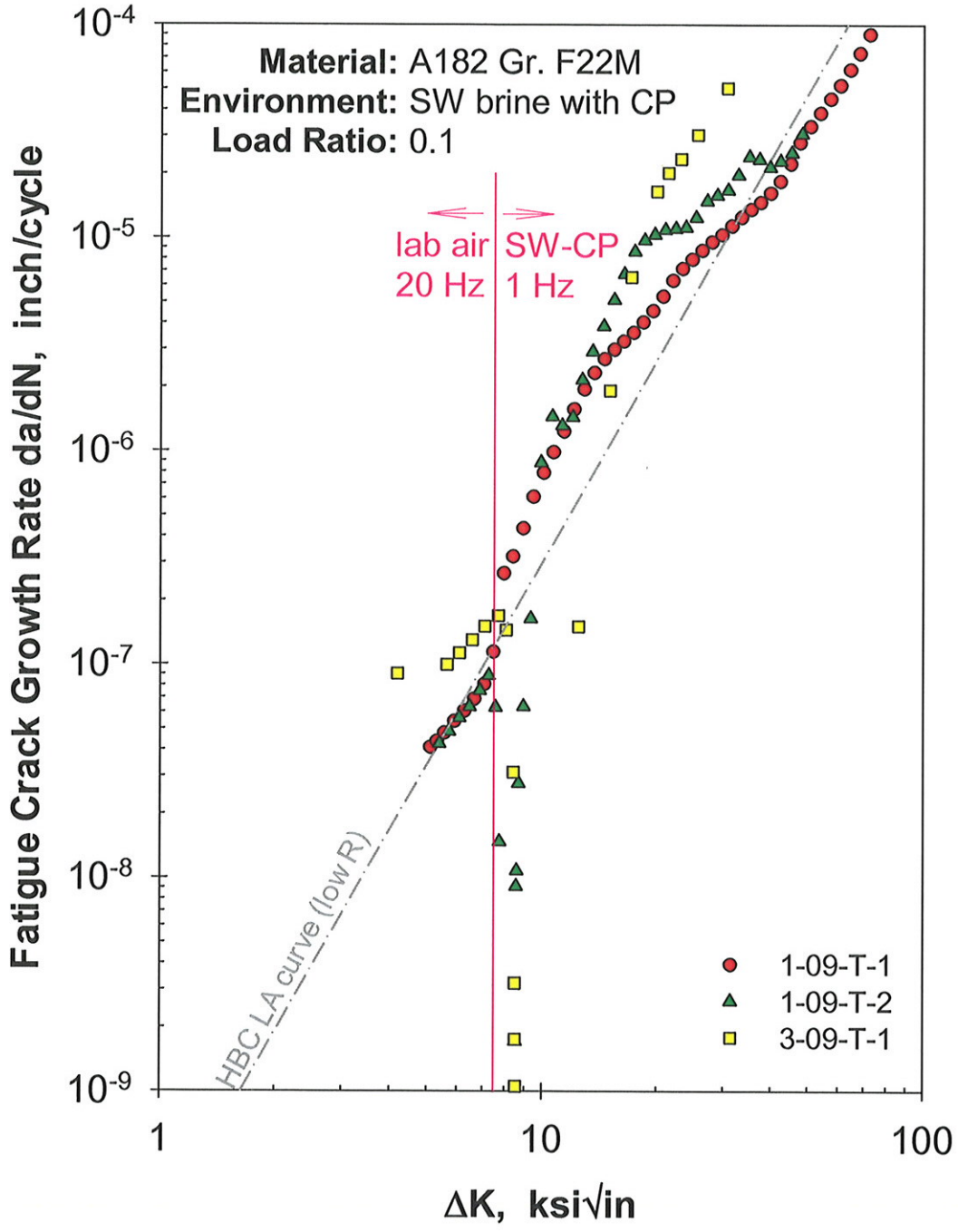

Figure 3-3. Influence of cathodically protected saltwater on fatigue crack growth rate behavior.

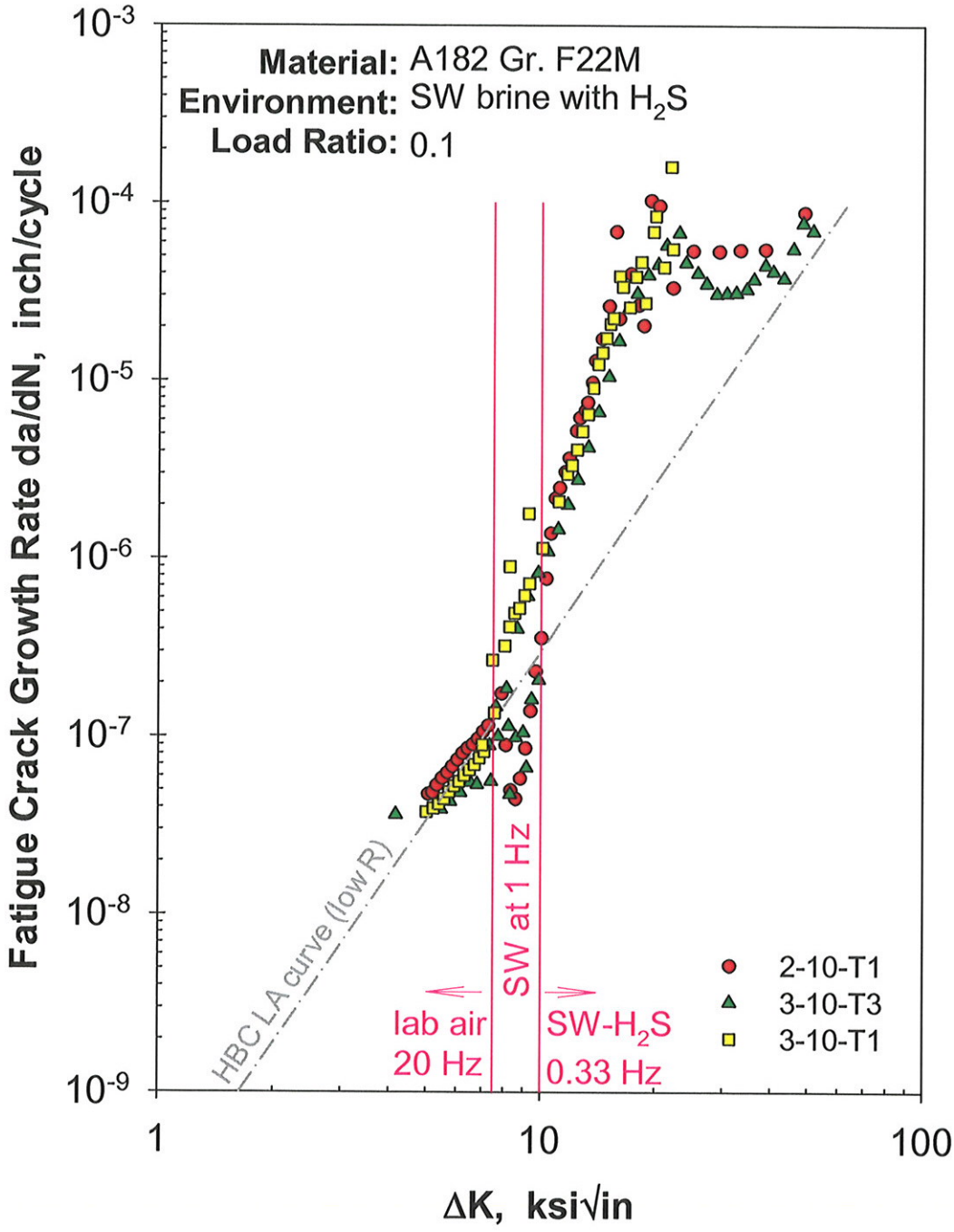

Figure 3-4. Influence of sour saltwater brine on fatigue crack growth rate behavior.

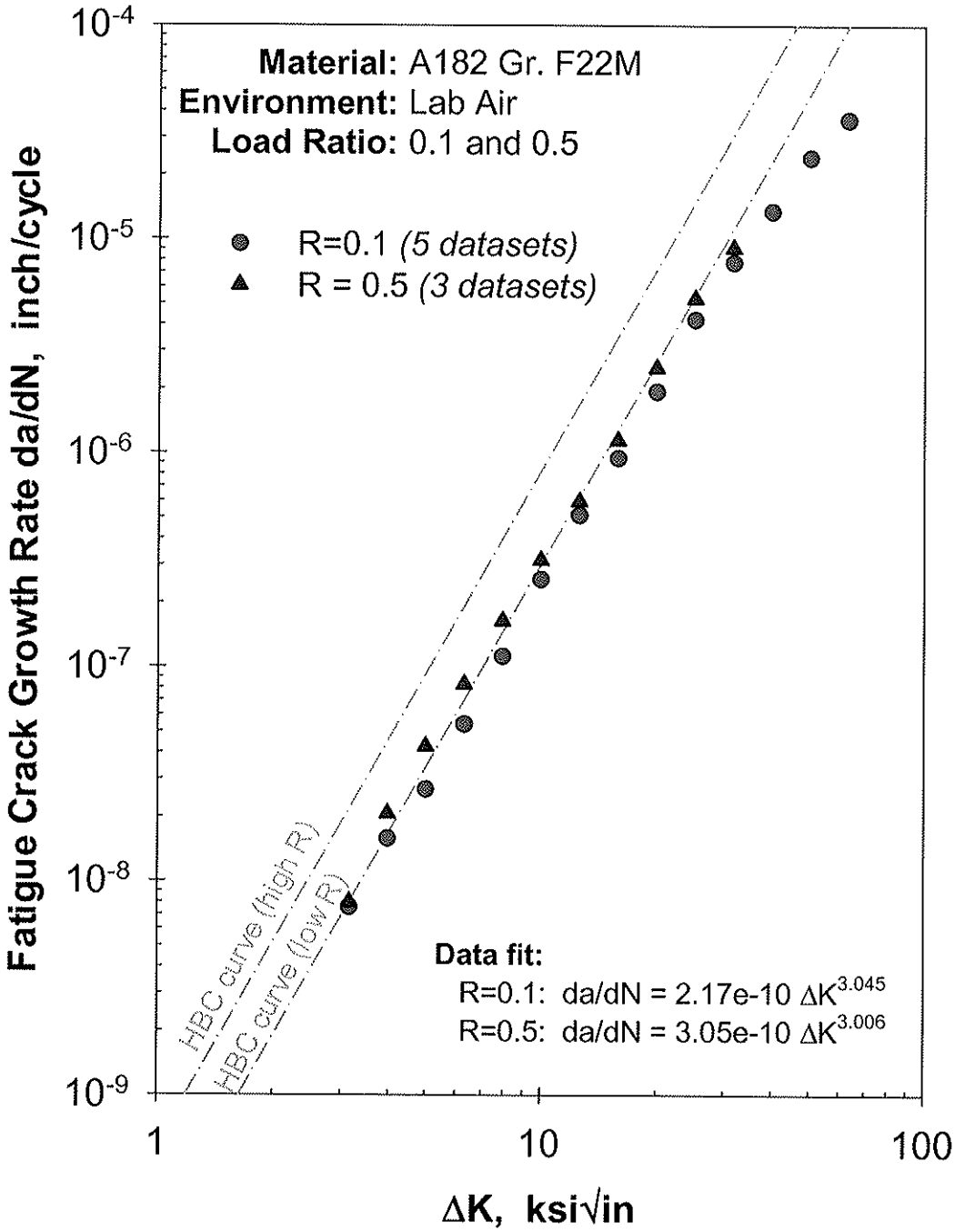

Figure 3-5. Average FCG rate response for the low and high load ratio data.

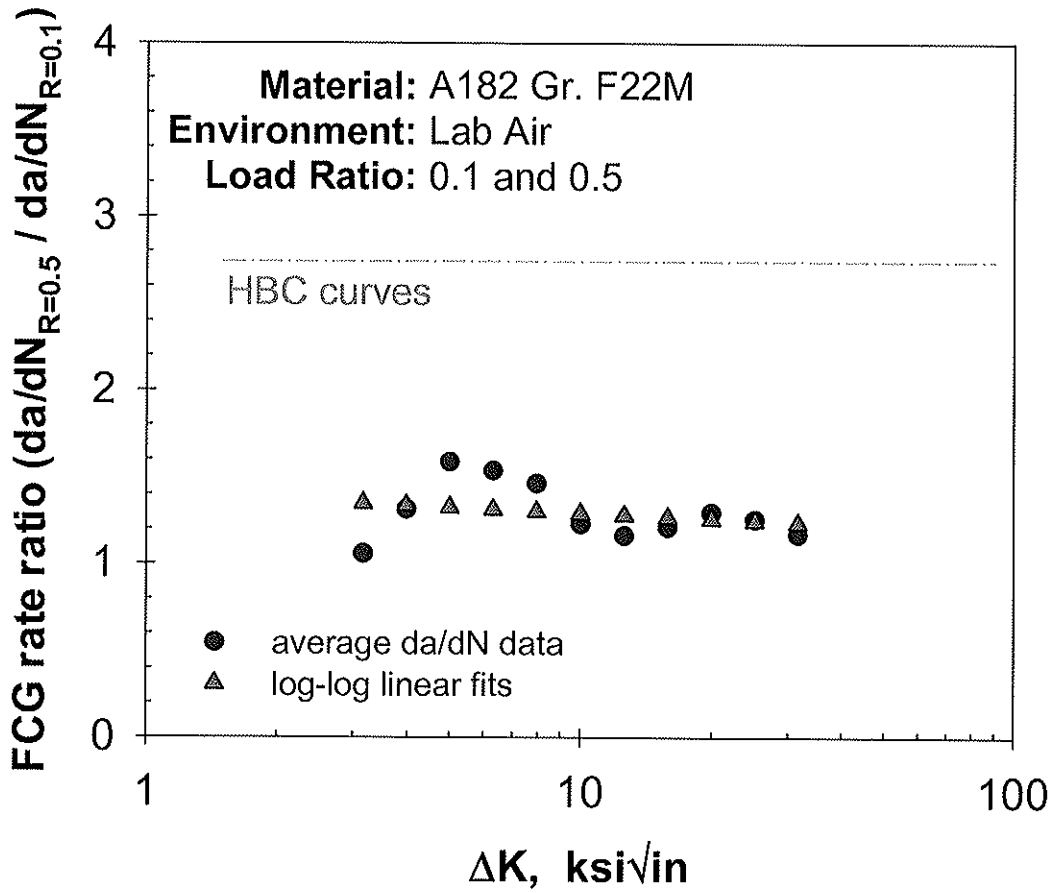

Figure 3-6. Average growth rate increase associated with load ratio.

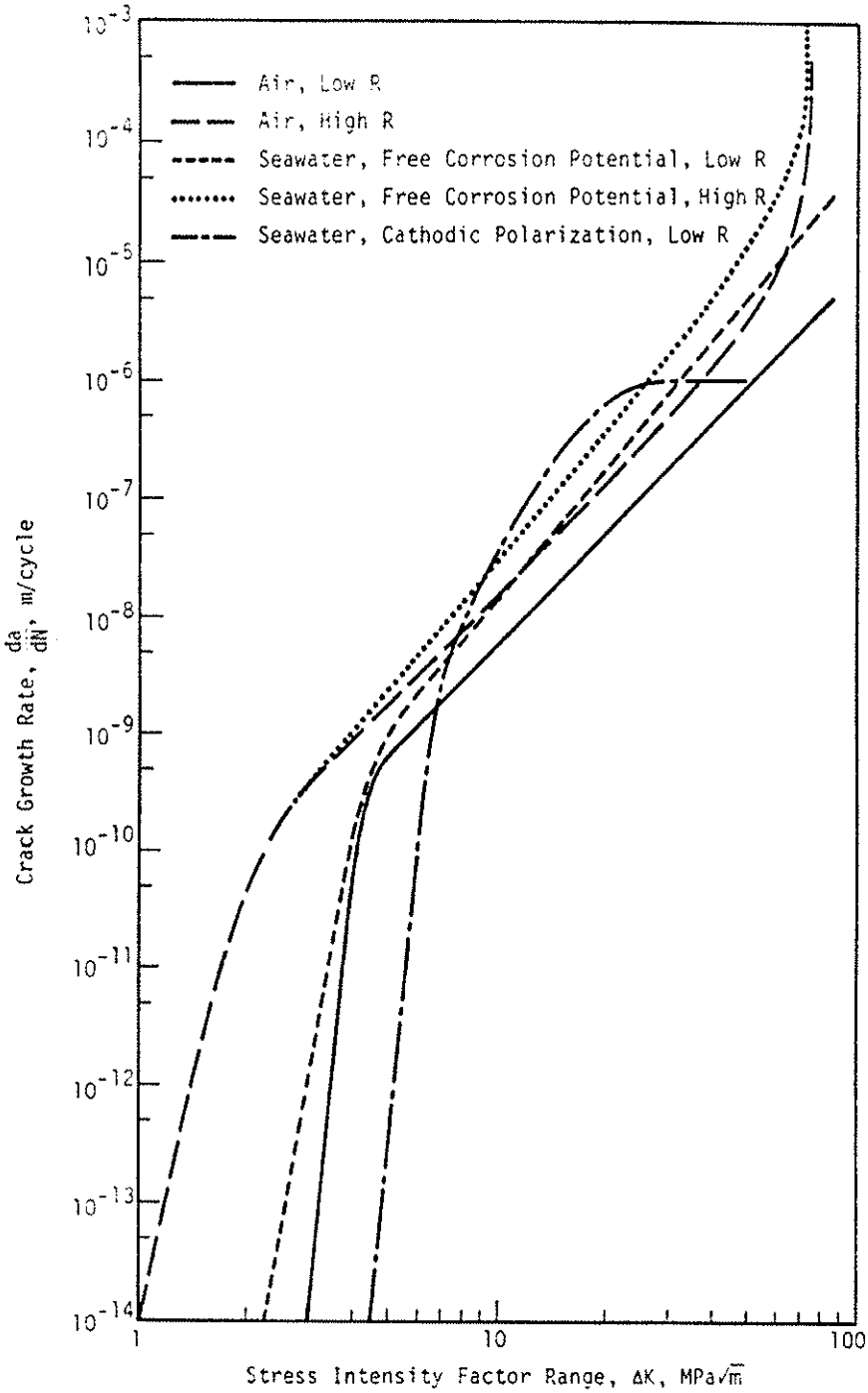

Figure 3-7. Different crack growth rate responses as a function of environment and R (from Reference [5]).

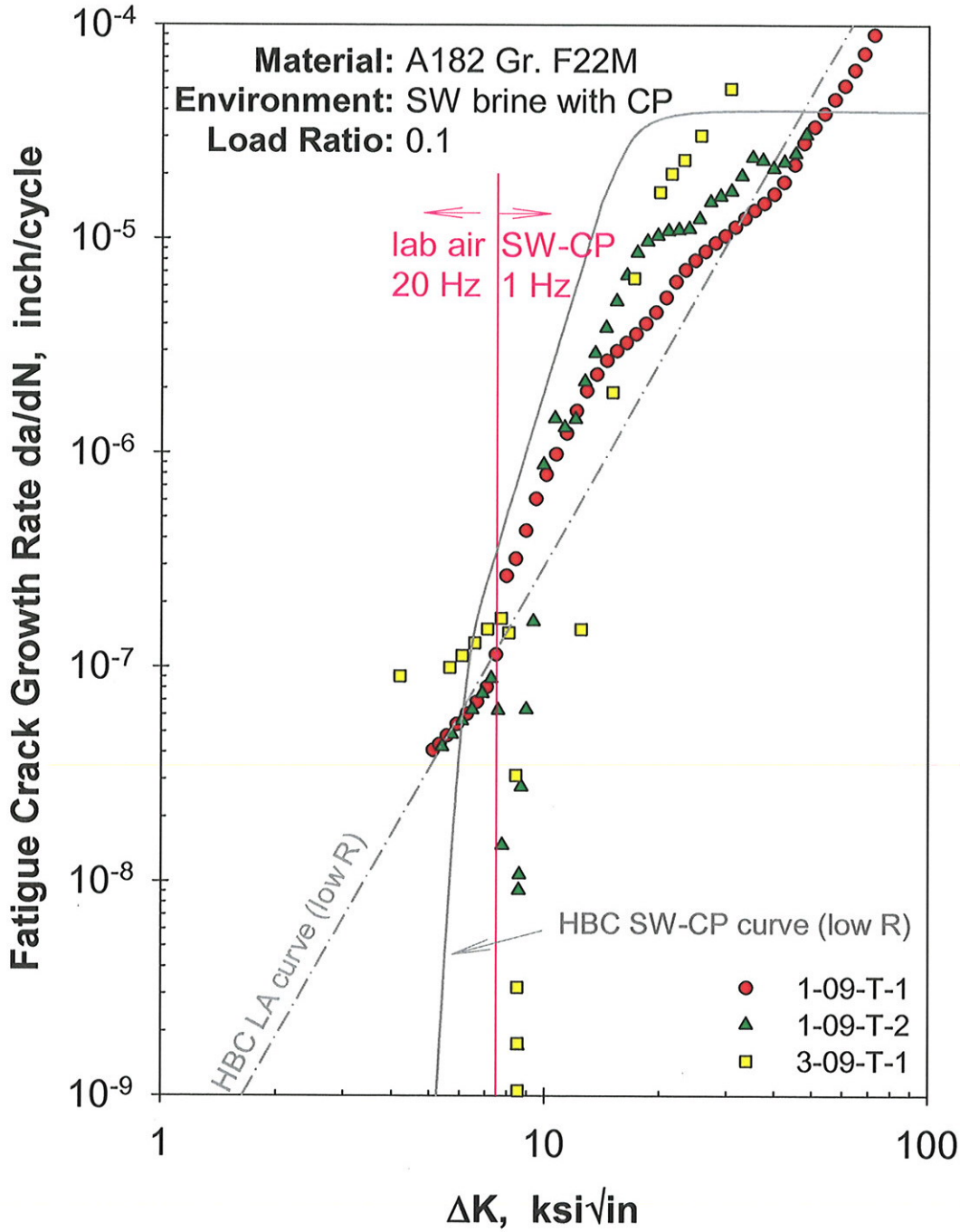

Figure 3-8. Comparison between literature and physically measured cathodically protected seawater FCG data.

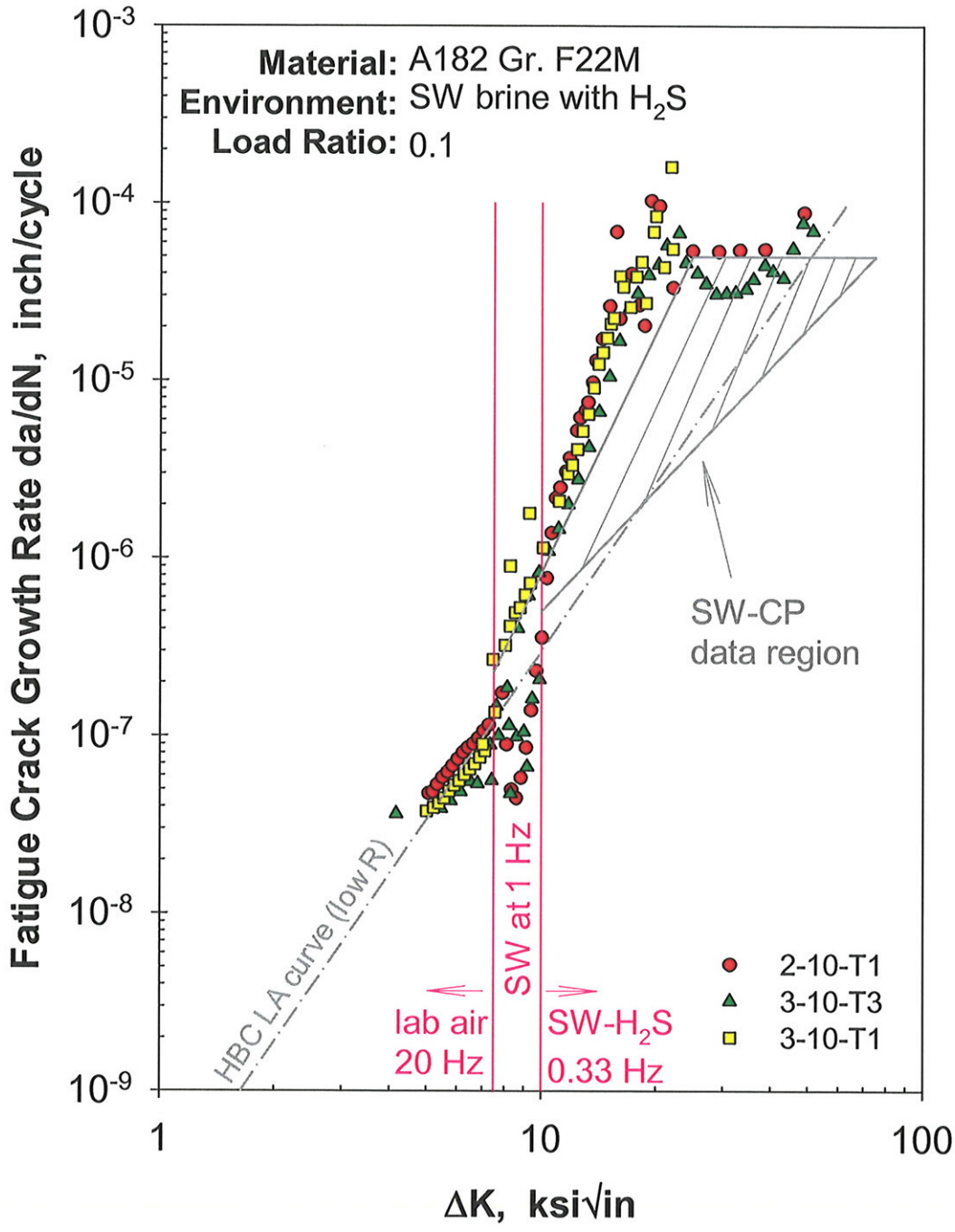

Figure 3-9. Comparison between experimentally measured sour and CP FCG rate data.

Figure 3-10. Fracture surface for specimen 1-09-T-1 (seawater w/CP).

Figure 3-11. Fracture surface for specimen 1-09-T-2 (seawater w/CP).

Figure 3-12. Fracture surface for specimen 3-09-T-1 (seawater w/CP).

Figure 3-13. Fracture surface for specimen 2-10-T-1 (sour brine).

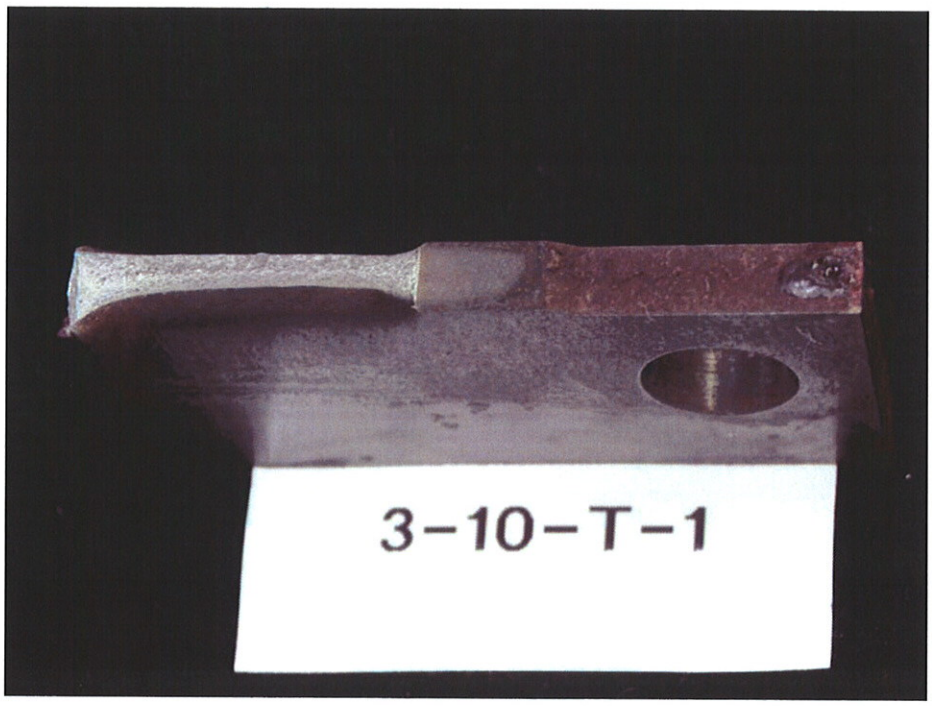

Figure 3-14. Fracture surface for specimen 3-10-T-1 (sour brine).

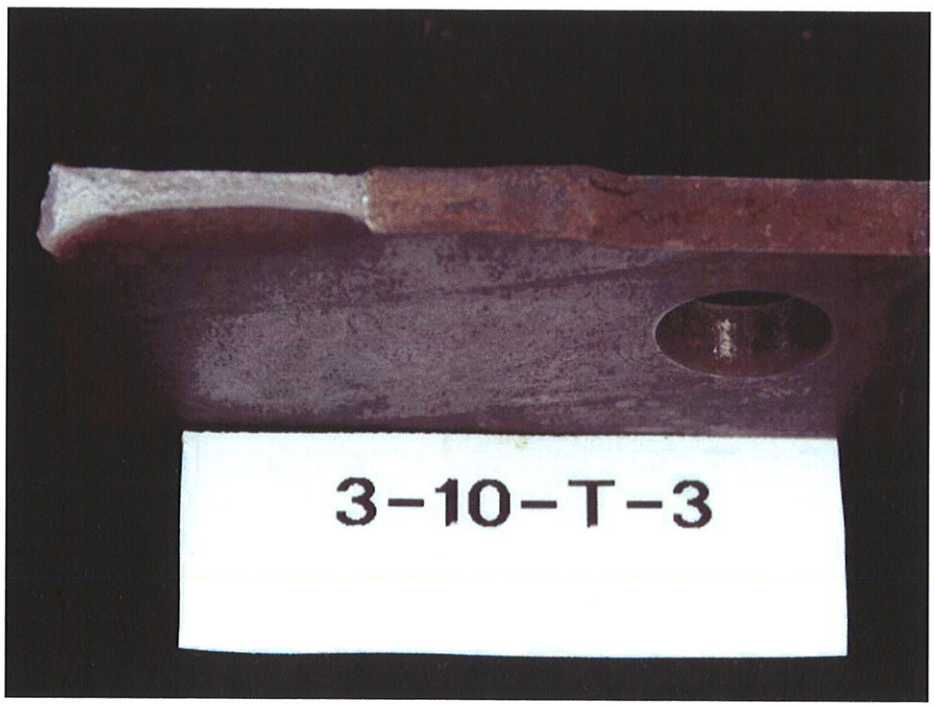

Figure 3-15. Fracture surface for specimen 3-10-T-3 (sour brine).

4.0 SUMMARY

Sixteen fatigue crack growth rate tests were performed on A182 grade F22M steel forgings. Tests were performed in lab air, cathodically protected seawater brine and sour brine environments. The primary results obtained from testing imply the following:

- The A182 material exhibits some sensitivity to K-gradient in a decreasing-K test from high ΔK levels. Testing, performed at C = -4 and -6 in.$^{-1}$, suggests that K-decreasing methods from high ΔK should be avoided.

- Compression-compression precracking has shown to be effective in preconditioning the specimen to starting a fatigue test at very low ΔK level. Using this method resulted in extremely linear FCG data with cycling starting from ΔK = 3 ksi$\sqrt{\text{in}}$.

- The A182 material tested herein exhibits no K-gradient differences in FCG behavior when tested at C = +2 and +6 in.$^{-1}$.

- Lab air testing at R = 0.1 and 0.5 has shown that the A182 material exhibits little discernible load ratio effects. It appears that the difference as a consequence of load ratio (with high R being 1.2-1.6x faster growth rate than low R) is approximately the same as the test-to-test scatter observed.

- The lab air fatigue crack growth behavior of A182 steel appears very similar to the low load ratio HBC relationship. The degree of variability observed was typical for FCG testing of a homogeneous steel (somewhat surprising for the forging).

- Much greater variability in growth rate was observed for the cathodically protected seawater tests, even when compared to the sour brine tests. Continuous crack arrest proved to be a significant problem in one test resulting in it taking approximately one month longer than the other tests where arrest did not occur.

- The A182 data generated herein compared favorably to work performed in the literature, although the fatigue crack growth curve from the literature tended to be slightly more conservative.

- The sour brine FCG data was very consistent, exhibiting growth rates 2-5x higher than the cathodically protected tests in seawater brine. The sour brine crack growth rates were on the order of 5-10x greater than lab air data.

5.0 REFERENCES

[1] "E647-05: Standard Test Method for Measurement of Fatigue Crack Growth Rates," Annual Book of ASTM Standards, Section 3, Volume 3.01, ASTM International, West Conshohocken, PA, 2007.

[2] Newman, J., Jr., Schneider, J., Daniel, A., and McKnight, D, "Compression Precracking to Generate Near Threshold Fatigue-Crack-Growth Rates in Two Aluminum Alloys," *International Journal of Fatigue*, Vol. 27, 2005, pp. 1432-1440.

[3] Hubbard, R. P., "Crack Growth Under Cyclic Compression," *Journal of Basic Engineering,* Vol. 91, 1969, pp. 625-631.

[4] Hudak, S. J., Jr., Burnside, O. H., and Chan, K. S., "Analysis of Corrosion Fatigue Crack Growth in Welded Tubular Joints," *Journal of Energy Resources Technology,* Transactions of the ASME, Vol. 107, June 1985.

[5] Burnside, O. H., Hudak, S. J., Jr., Oelkers, E., Chan, K., and Dexter, R. J., "Long-Term Corrosion Fatigue of Welded Marine Steels," Report for the Ship Structure Committee, Report No. SSC-326, Contract DTCG23-80-C-20028, 1984, pp. 1-420.

[6] Yazdani, N. and Albrecht, P., "Crack Growth Rates of Structural Steel in Air and Aqueous Environments," *Engineering Fracture Mechanics*, Vol. 32, No. 6, 1989, pp. 997-1007.

[7] Eason, E. D., Gilman, J. D., Jones, D. P., and Andrew, S. P., "Technical Basis for a Revised Crack Growth Rate Reference Curve for Ferritic Steels in Air," *Journal of Pressure Vessel Technology, Transactions of the ASME,* Vol. 114, February 1992.

[8] McKeighan, P. C., Feiger, J. H., and McKnight, D. H., "Round Robin Test Program and Results for Fatigue Crack Growth Measurement in Support of ASTM Standard E647," Draft Final Report prepared for ASTM International, Committee E08 on Fatigue and Fracture, Subcommittee E08.06 on Crack Growth Behavior, February 2008.

This page intentionally left blank.

Annex G.2. Crack Growth Rate Data Analysis

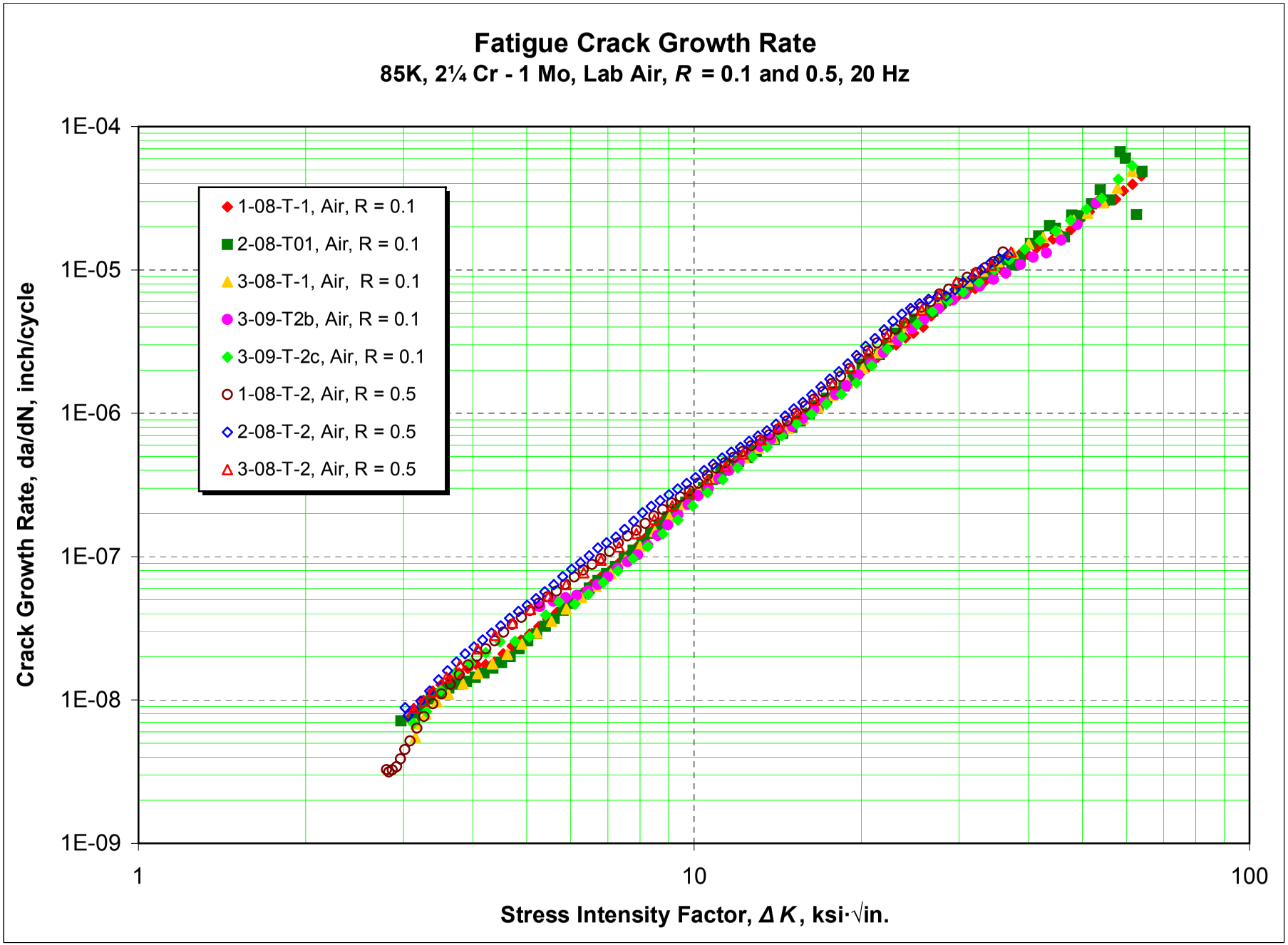

172883 FCGR Data.xls Air-3 2/29/2008

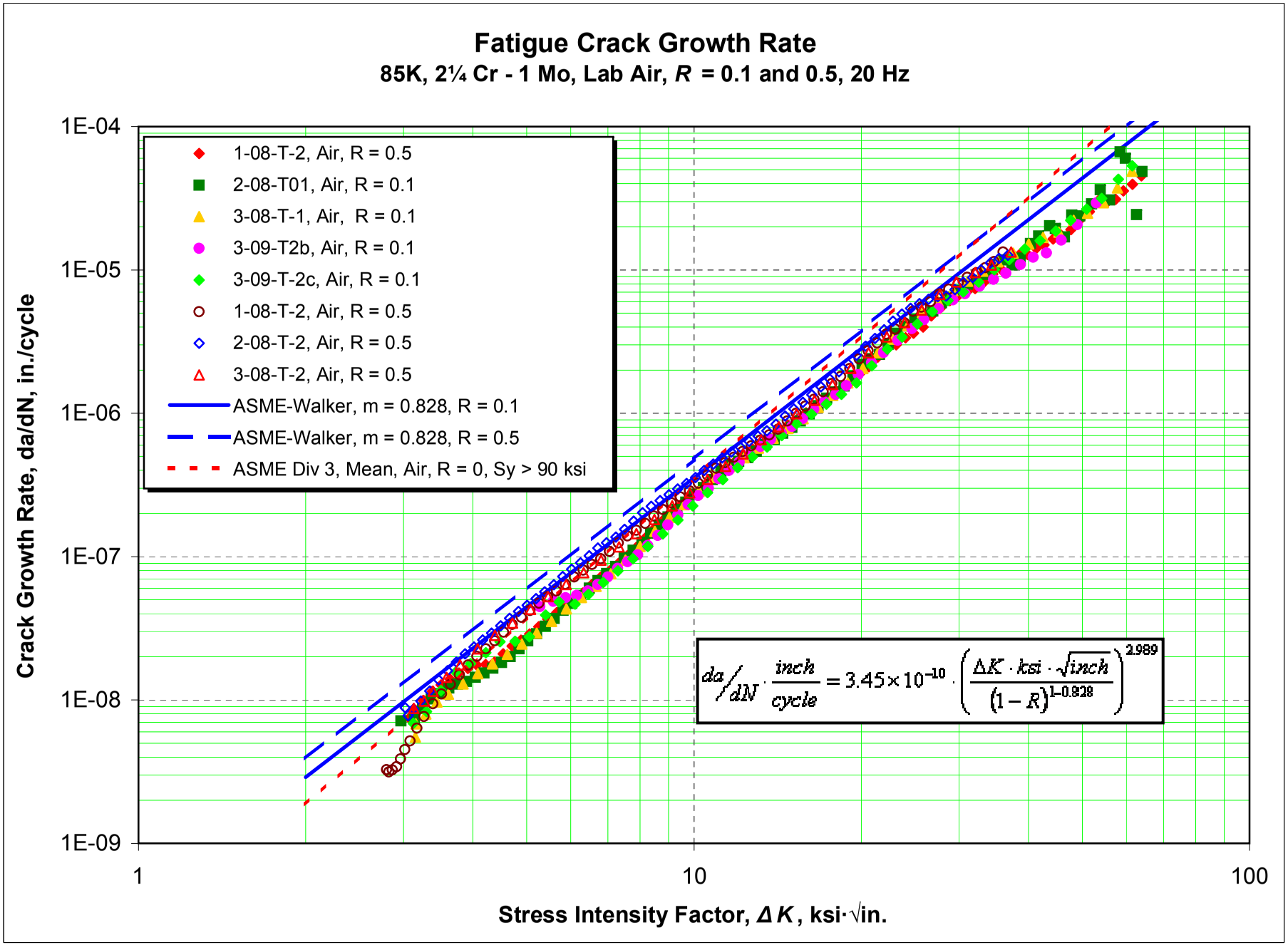

172883 FCGR Data.xls Air-2 2/29/2008

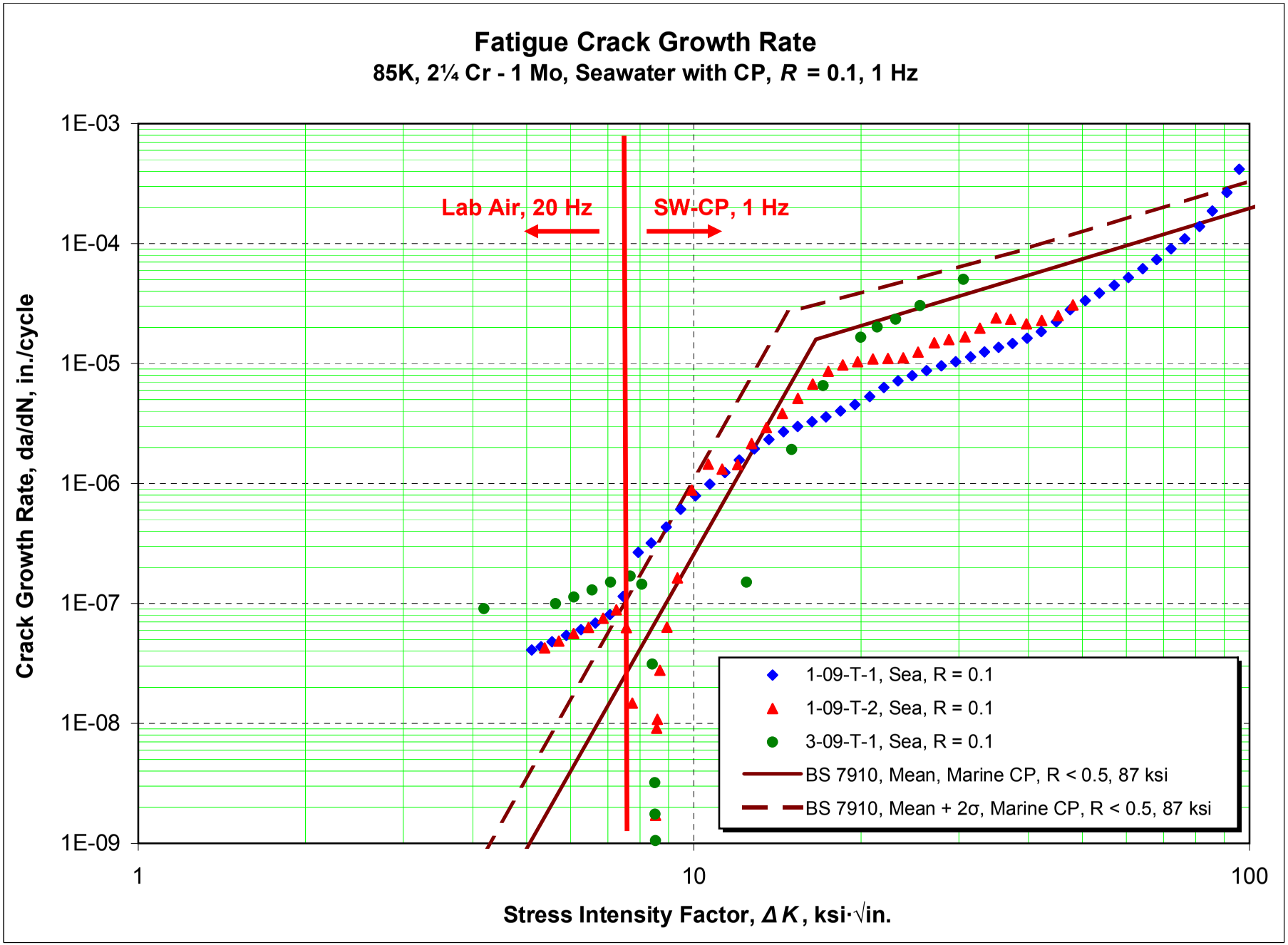

172883 FCGR Data.xls Sea-2 2/29/2008

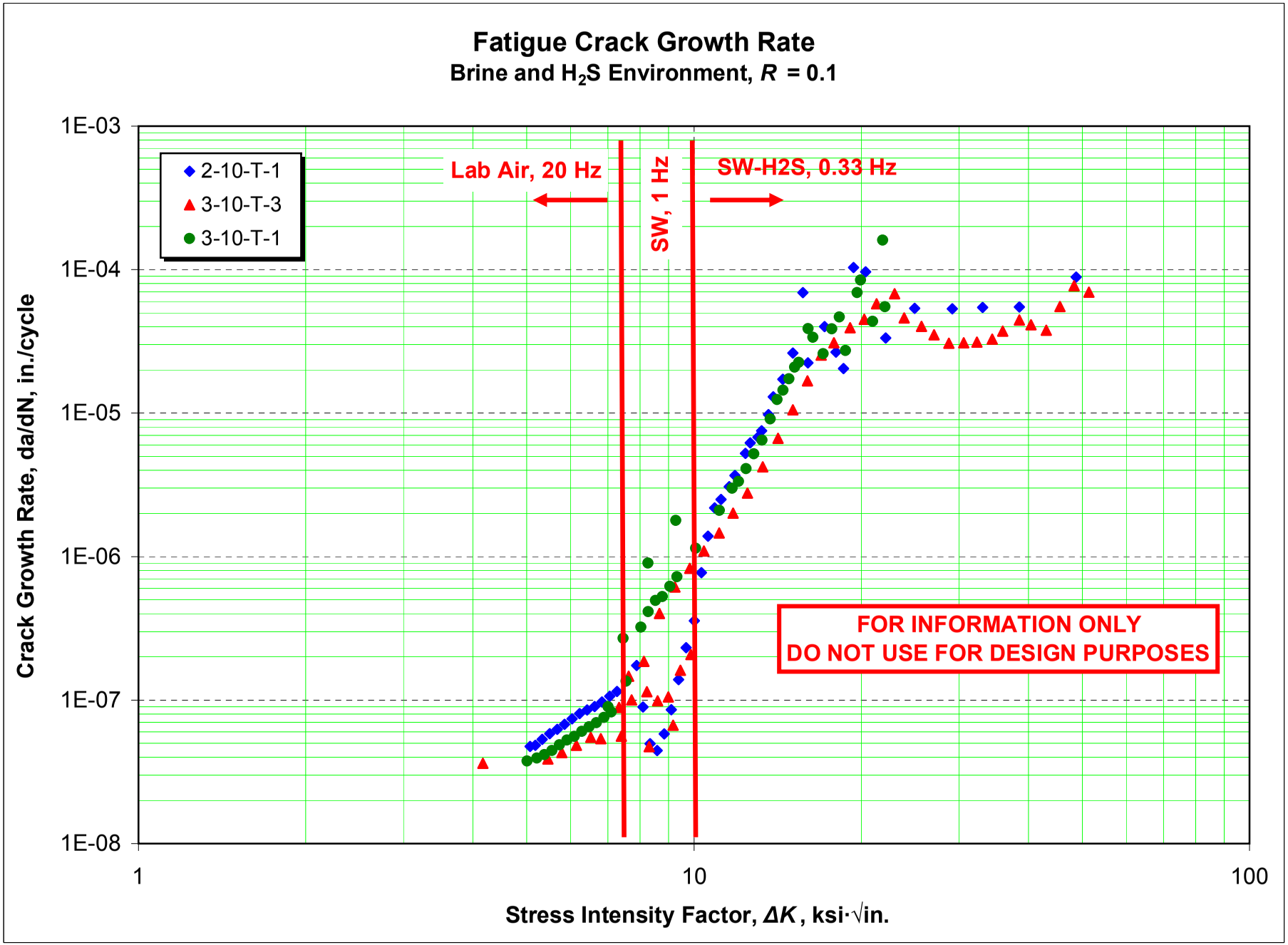

172883 FCGR Data.xls H2S-1 2/29/2008

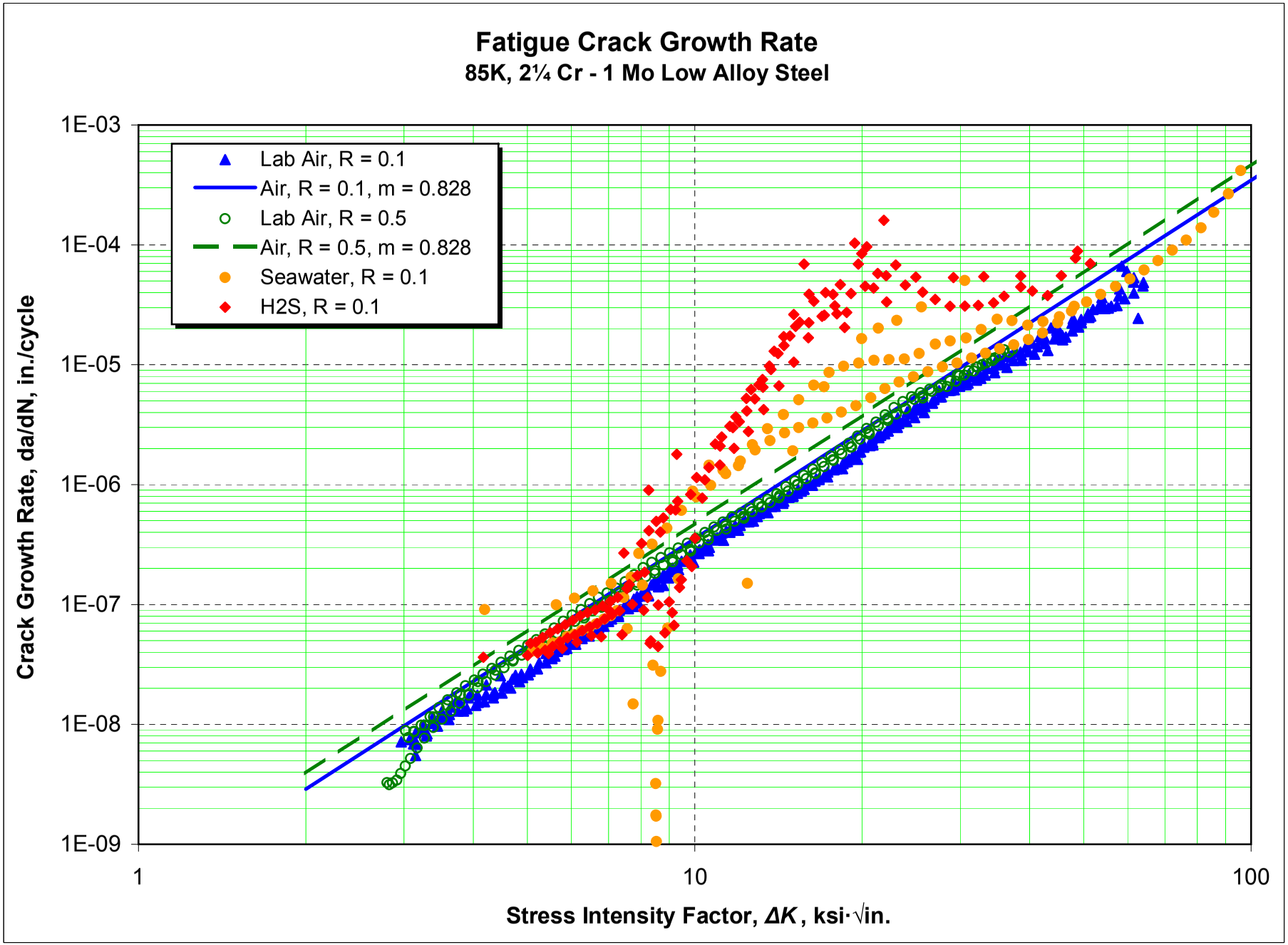

172883 FCGR Data.xls FCGR-1 2/29/2008